Polska Akademia Nauk
Instytut Paleobiologii

ACTA PALAEONTOLOGICA POLONICA

Supplement to Vol. 66 No. 3

Proceedings of the 2nd Palaeontological Virtual Congres

Guest Editors: Vicente D. Crespo and Paolo Citton

Warszawa 2021

ACTA
PALAEONTOLOGICA
POLONICA

Instytut Paleobiologii PAN
ul. Twarda 51/55
PL-00-818 Warszawa, Poland

e-mail: app@twarda.pan.pl; tel.: (+48 22) 697 88 81; fax: (+48 22) 620 62 25

ACTA PALAEONTOLOGICA POLONICA is an international quarterly journal established by Roman Kozłowski in 1956. It publishes papers of general interest from all areas of biologically oriented palaeontology. Papers are judged on the originality of their data, interpretations, and ideas, and on the degree to which their findings can be generalized. All papers are subject to peer reviews. The journal is included in the ISI Science Citation Index Expanded.

Subscriptions for both current and back issues of ACTA PALAEONTOLOGICA POLONICA are available from, the Institute of Paleobiology of the Polish Academy of Sciences. Personal annual subscription price is EUR 68.25, for institutions EUR 78.75. Please add EUR 6 (standard mail) or EUR 12 (priority mail) for mailing per issue. Single and back issues are available; please visit the ordering website of Acta Palaeontologica Polonica at http://www.app.pan.pl/subscription.htm.

Preface

Acta Palaeontologica Polonica 66 (Supplement to 3): S1–S3, 2021

2nd Palaeontological Virtual Congress: Palaeontology in the virtual era

VICENTE D. CRESPO and PAOLO CITTON

Introduction

After the success of the 1st Palaeontological Virtual Congress (Crespo and Manzanares 2019), we decided to try to repeat the success with a new edition. Thus, the 2nd Palaeontological Virtual Congress (2nd PVC; Fig. 1) was born. This second edition of the congress was already conceived in November 2019, prior to the events—sadly known to all—related to the pandemic of COVID-19 disease, and was successfully held during May 2020 (Barral 2020).

Fig. 1. Logo of the 2nd Palaeontological Virtual Congress, designed by Hugo Salais (source: author).

In this way, thanks to the collaboration of different institutions, some of them present in the previous edition such as Universitat de València, Museo Paleontológico de Alpuente, Museu Valencià d'Historia Natural, University of Bristol and, Universidad Nacional a Distancia, plus new incorporations such as Museo de La Plata, Consejo Nacional de Investigaciones Científicas y Técnicas (CONICET), University of Bath, Aristotle University of Thessaloniki, Instituto de Investigaciones en Paleobiología y Geología (IIPG) and Museo Paleontológico Egidio Feruglio, we decided to carry out this adventure again, with a more international character.

The Palaeontological Virtual Congress (PVC) was innovative in the world of palaeontology as it was the first congress developed in an exclusively virtual environment in this science. Three main goals moved us to carry out this second edition, with two main ones, the social and the ecological, to which the pandemic was added later. The new format that we developed for the PVC combines the benefits of traditional meetings with the advantages and simplicity of online platforms. Among the similarities with traditional congresses are the following: providing a forum for discussion, merchandising, guest lectures, "field trips", and an abstract book, etc. Thanks to this format, we reached a high number of palaeontologists around the world. We know the difficulties that researchers from developing countries, independent researchers, or researchers without grants face with travel to different congresses, and this was a good opportunity to strengthen their scientific connections. So, thanks to the volunteer work of the organising committee, we could provide a low registration fee. In addition, these kinds of congresses allow us to reduce the carbon footprint that we humans leave on our planet, as we avoid the pollution associated with a face-to-face meeting (including traveling by plane, car, or train) (Abbott 2019).

Results

Participation.—Thanks in part to the good reception of the 1st PVC, the second edition increased the numbers of the first edition and exceeded our expectations: 398 palaeontologists and palaeontology enthusiasts from 44 different nations and five continents were part of this initiative.

Congress format.—The meeting was organized as any traditional congress: keynotes, general sessions and workshops, and "field trips". In charge of the keynotes were Michael Benton from University of Bristol, Anne Laure Decombeix from Centre National de la Recherche Scientifique-Unité Mixte de Recherche Botany and Modeling of Plant Architecture and Vegetation (CNRS-UMR AMAP), Jesús Lozano Fernández from Institute of Evolutionary Biology, Centro Superior de Investigaciones Científicas-Universidad Pompeu Fabra (CSIC-UPF), and, last but not least, Jim Kirkland and Don DeBlieux from Utah Geological Survey. Participants were able to choose from three forms of presentation: a video presentation with a duration of 10 to 15 minutes; presentation slides (between 10–30 slides); and a poster (up to 5 slides). As in any meeting, all the contributions have been published in the abstract book "2nd Palaeontological Virtual Congress. Book of abstracts. Palaeontology in the virtual era" (Vlachos et al. 2020), that can be downloaded for free on our website, together with the book of abstracts of the 1st PVC (Crespo et al. 2018).

Workshops.—Due to the diversity of topics in palaeontology, it was possible to present a variety of thematic sessions. This idea received a very warm welcome, and five

 https://doi.org/10.4202/app.00938.2021

specific sessions and four general sessions were held on our virtual platform.

Specific sessions.—Evolution and Palaeobiodiversity in Neogene and Quaternary Islands moderated by Carolina Castillo Ruiz, Javier González-Dionis, Elena Cadavid Melero, and Sara Pérez Martín from Universidad de La Laguna (Spain) and Penélope Cruzado-Caballero from Instituto de Investigación en Paleobiología y Geología-CONICET-UNRN (Argentina), and Grupo Aragosaurus-IUCA, Universidad de Zaragoza (Spain).

Fossil insects, their record, ecology and evolution moderated by Jacek Szwedo from Uniwersytet Gdański (Poland).

Palynology as a tool in stratigraphic and paleonvironmental research: advances and perspectives moderated by Adele Bertini, and Gabriele Niccolini from Università degli Studi di Firenze (Italy), and Nathalie Combourieu-Nebout from Histoire Naturelle de l'Homme Prehistorique (France).

PalaeoVC Early Career Session moderated by Bryan Shirley, and Niklas Hohmann from Friedrich-Alexander Universität Erlangen-Nürnberg (Germany), and Danae Thivaiou from Ethnikó ke Kapodistriakó Panepistímio Athinón (Greece).

Paleontology in Education and Society moderated by Rosalía Guerrero-Arenas, and Eduardo Jiménez-Hidalgo from Universidad del Mar (Mexico).

The general sessions are moderated by the organising committee and were divided into Palaeozoic, Mesozoic, Cenozoic, and General Palaeontology, where those papers that could not be classified in the first sessions were placed. The variety of sessions held during the congress provided the participants with a forum for the exchange of ideas and the opportunity to discuss each topic.

Virtual field trips.—After the success and positive feedback of the 1st PVC virtual field trips, we decided to repeat the experience. This time the virtual field trip was a wonderful walk in South Tyrol (North Italy), specifically in the Bletterbach Gorge, which is part of the Dolomites UNESCO World Heritage Site as the Bletterbach Geopark. In this visit we saw the formation from a drone, visited the museum associated with the area, and saw the main fossils found. All these virtual field trips can be visited permanently on our website.

Special issue

As in the first edition, we also wanted to prepare a special volume. On this occasion it is published in *Acta Palaeontologica Polonica*, to be able to continue with the same spirit as a traditional congress. For this reason, we decided to make a special issue, composed of 10 contributions, originating from the expanded abstracts that were presented in the congress.

Abel et al. (2021) discuss a pterodactyloid mandible from the lower Valanginian of Lower Saxony Basin, in Germany. The material represents one of the oldest identifiable member of the Early Cretaceous clade *Anhangueria*, and one of the few known pterosaurs from the Valanginian stage.

Álvarez-Parra et al. (2021) present a new fossiliferous locality of early Miocene age from the Ribesalbes–Alcora Basin in Spain. Here, a quite diverse fauna represented by charophytes, terrestrial plants, arthropods (crustaceans and insects), gastropods, and fish remains, preserved in finely laminated limestone beds and laid down in a lacustrine environment, improve our knowledge about the palaeoecology and palaeoenvironmental evolution of the Basin during the Miocene.

Barasoain et al. (2021) provide the first description of the skull for *Vetelia*, a Miocene genus of armadillos from Argentina and Chile, and emend the diagnosis of the three species included in the genus. Further phylogenetic analysis reveal *Vetelia* to be a member of Priodontini within the subfamily Tolypeutinae, differently from previous hypothesis that included *Vetelia* in the subfamily Euphractinae, thus shedding new light on the evolutionary history of the poorly known Tolypeutinae.

Dankina et al. (2021) study Late Permian chondrichthyans and osteichthyans remains from the North-Sudetic Basin (southwest Poland), identifying an important ecological differentiation within the ichthyofauna dwelling the Zechstein sea.

Davidian et al. (2021) describe the first ichneumonoid aphidiine wasp species from the middle Eocene Sakhalinian amber (Sakhalin Province, Russian Federation). The new taxon represents to date the oldest named species of the genus and bears characters possibly related to an adaptation to parasitize aphids, thus shedding further light on the coevolution between aphids and aphidiine.

Martino et al. (2021) revise hippopotamid remains from the Messinian of Sicily originally used to erect the taxon *Hippopotamus siculus.* By means of morphological and morphometrical analyses, a provisional assignment to the genus *Hexaprotodon* is provided, as well as a discussion of the dispersal pattern across the peri-Mediterranean area.

Núñez-Blasco et al. (2021) describe and compare some specimens of the doedicurin glyptodont *Eleutherocercus solidus.* Cladistic analysis supports Doedicurinae as a monophyletic group of southern South American glyptodonts and the genus *Eleutherocercus* as a sister group of *Doedicurus*, the giant glyptodont of Pleistocene age representing the end member of a trend of latitudinal retraction of the subfamily probably triggered by climate change.

Reyna-Hernández et al. (2021) report hadrosaurid postcranial remains from Coahuila (Mexico) referred to Lambeosaurinae indet. and discuss the significance of the new material in the wider panorama of southern Laramidia during the Campanian–Maastrichtian.

Robledo et al. (2021) describe fossil fruits of the alismataceous plant *Sagittaria montevidensis* from the upper Miocene of Salta province (Argentina), representing the first pre-Quaternary remains of this kind of plants from

South America. The authors also provide a rapid review of the family Alismataceae, suggesting dispersal routes for the genus *Sagittaria* during the Oligocene–Miocene time interval.

Waseem et al. (2021) discuss $\delta^{18}O$ and $\delta^{13}C$ analyses on thirty fossil enamel samples belonging to different middle Miocene mammals from of the Siwalik sub-Group of Pakistan to investigate their palaeodiet and palaeoecology related to dense forests and woodlands.

The future

With this second edition, we are already consolidating our position in the increasingly competitive world of online congresses, as we were the first in the field of palaeontology to organise this type of conference. With the experience gained from these two editions, we are already preparing the third edition for 1–15 December 2021, with new surprises and new forums in which participants can interact in the next congress. Among them, to increase the range and diversity of nationalities and areas of expertise, we have created a social fund for participants from low and lower–middle income countries listed as such on The World Bank's list. In addition, we are introducing the figure of ambassadors, for those participants who wish to advertise us among their colleagues in their country and/or speciality. We also set up a Discord server with multiple text and voice channels so you can give and receive feedback to and from your peers. We look forward to seeing you in the 3rd PVC!

Acknowledgements

Finally, we would like to thank all of the other members of the organising committee (Esther Manzanares, Carlos Martínez-Pérez, José Luis Herráiz, Arturo Gamonal, Fernando Antonio Martín Arnal, Humberto Gracián Ferrón, Francesc Gascó, and Evangelos Vlachos), our colleagues for organizing and coordinating the different thematic sessions, all of the authors for submitting their contributions and to the numerous reviewers that have made this volume and congress possible. We would like also to give special thanks to *Acta Palaeontologica Polonica*, in particular to the Editor in Chief Andrzej Kaim, Museu d'Història Natural de la Universitat de València, Sociedad Geológica de España, Sociedad Española de Paleontología, Paläontologische Gesellschaft, Transmitting Science, PeerJ Life & Environment, Pander Society, and Paleontological Society that have supported this initiative, specially to the University of Valencia (the Department of Botany and Geology) for hosting the space to develop this project. Thanks are also due to the helpful comments on the original manuscript provided by Daniel E. Barta (Oklahoma State University, Tahlequah, USA).

References

Abbott, A. 2020. Low-carbon, virtual science conference tries to recreate social buzz. *Nature* 577: 13.

Abel, P., Hornung, J.J., Kear, B.P., and Sachs, S. 2021. An anhanguerian pterodactyloid mandible from the lower Valanginian of Northern Germany, and the German record of Cretaceous pterosaurs. *Acta Palaeontologica Polonica* 66 (Supplement to 3): S5–S12

Álvarez-Parra, S., Albesa, J., Gouiric-Cavalli, S., Montoya, P., Peñalver, E., Sanjuan, J., and Crespo, V.D. 2021. The early Miocene lake of Foieta la Sarra-A in eastern Iberian Peninsula and its relevance for the reconstruction of the Ribesalbes–Alcora Basin palaeoecology. *Acta Palaeontologica Polonica* 66 (Supplement to 3): S13–S30.

Barasoain, D., González Ruiz, L.R., Tomassini, R.L., Zurita, A.E., Contreras, V.H., and Montalvo, C.I. 2021. First phylogenetic analysis of the Miocene armadillo *Vetelia* reveals novel affinities with Tolypeutinae. *Acta Palaeontologica Polonica* 66 (Supplement to 3): S31–S46.

Barral, A. 2020. Virtual conferences are the future. *Nature Ecology & Evolution* 4: 666–667.

Crespo, V.D. and Manzanares, E. 2019. Palaeontological Virtual Congress: a new way to make science. *Palaeontologia Electronica* 22.3: 1–4.

Crespo, V.D., Manzanares, E., Marquina-Blasco, R., Suñer, M., Herráiz, J.L., Gamonal, A., Arnal, F.A.M., Ferrón, H.G., Gascó, F., and Martínez-Pérez, C. 2018. *1st Palaeontological Virtual Congress. Book of Abstracts. Palaeontology in the Virtual Era*. 212 pp. Universitat de València, Museo de Alpuente and Museu Valencià d'Historia Natural, Valencia.

Dankina, D., Spiridonov, A., Raczyński, P., and Radzevičius, S. 2021. Late Permian ichthyofauna from the North-Sudetic Basin, SW Poland. *Acta Palaeontologica Polonica* 66 (Supplement to 3): S47–S57.

Davidian E.M., Kaliuzhna M.O., and Perkovsky E.E. 2021. First aphidiine wasp from the Sakhalinian amber. *Acta Palaeontologica Polonica* 66 (Supplement to 3): S59–S65.

Martino, R., Pignatti, J., Rook, L., and Pandolfi, L. 2021. Hippopotamid dispersal across the Mediterranean in the latest Miocene: a re-evaluation of the Gravitelli record from Sicily, Italy. *Acta Palaeontologica Polonica* 66 (Supplement to 3): S67–S78.

Núñez-Blasco, A., Zurita, A.E., Miño-Boilini, A.R., Bonini, R.A., and Cuadrelli, F. 2021. The glyptodont *Eleutherocercus solidus* from the late Neogene of North-Western Argentina: Morphology, chronology, and phylogeny. *Acta Palaeontologica Polonica* XX (Supplement to 3): S79–S99.

Reyna-Hernández, R.A., Rivera-Sylva, H.E., Silva-Martínez, L.E., and Guzman-Gutiérrez, J.R. 2021. A large hadrosaurid dinosaur from Presa San Antonio, Cerro del Pueblo Formation, Coahuila, Mexico. *Acta Palaeontologica Polonica* 66 (Supplement to 3): S101–S110.

Robledo, J.M., Contreras, S.A., Baez, J.S., and Galli, C.I. 2021. First Miocene megafossil of arrowhead, alismataceous plant *Sagittaria*, from South America. *Acta Palaeontologica Polonica* 66 (Supplement to 3): S111–S122.

Vlachos, E., Manzanares, E., Crespo, V.D., Martínez-Pérez, C., Ferrón, H.G., Herráiz, J.L., Gamonal, A., Arnal, F.A.M., Gascó, F., and Citton, P. (eds.) 2020. *2nd Palaeontological Virtual Congress Book of Abstracts Palaeontology in the Virtual Era*. 205 pp. Palaeontological Virtual Congress, Valencia.

Waseem, M.T., Khan, A.M., Quade, J., Krupa, A., Dettman, D.L., Rafeh, A., and Ahmad, R.M. 2021. Stable isotope analysis of middle Miocene mammals from the Siwalik sub-Group of Pakistan. *Acta Palaeontologica Polonica* 66 (Supplement to 3): S123–S132.

Vicente D. Crespo [vidacres@gmail.com] (corresponding author), Consejo Nacional de Investigaciones Científicas y Técnicas, División Paleontología Vertebrados, Museo de La Plata, Paseo del Bosque s/n, B1900FWA La Plata, Argentina; Museo Paleontológico de Alpuente, Av. San Blas 17, Alpuente, 46178 Valencia, Spain; Museu Valencià d'Història Natural, L'Hort de Feliu, P.O. Box 8460, Alginet, 46230 Valencia, Spain. Paolo Citton [pcitton@unrn.edu.ar], Instituto de Investigación en Paleobiología y Geología (IIPG), CONICET-Universidad Nacional de Río Negro, Avenida J.A. Roca 1242, CP 8332, General Roca, Río Negro, Argentina.

An anhanguerian pterodactyloid mandible from the lower Valanginian of Northern Germany, and the German record of Cretaceous pterosaurs

PASCAL ABEL, JAHN J. HORNUNG, BENJAMIN P. KEAR, and SVEN SACHS

Abel, P., Hornung, J.J., Kear, B.P., and Sachs, S. 2021. An anhanguerian pterodactyloid mandible from the lower Valanginian of Northern Germany, and the German record of Cretaceous pterosaurs. *Acta Palaeontologica Polonica* 66 (Supplement to 3): S5–S12.

The record of Cretaceous pterosaur remains from Germany is sparse. The material recovered to date includes the fragmentary holotypes of *Targaryendraco wiedenrothi* and *Ctenochasma roemeri*, as well as a few isolated pterodactyloid teeth and some indeterminate skeletal elements, together with a plaster cast of a large *Purbeckopus* manus imprint. Here, we report the discovery of a pterodactyloid pterosaur mandible from lower Valanginian strata of the Stadthagen Formation in the Lower Saxony Basin of Northern Germany. Based on the size and spacing of its alveoli, this fossil is attributable to the cosmopolitan Early Cretaceous pteranodontoid clade Anhangueria. Moreover, it represents the first and only known pterosaur from the Valanginian of Germany and is one of only a handful Valanganian pterosaur occurrences presently recognized worldwide. In addition to the approximately coeval *Coloborhynchus clavirostris* from the Hastings Bed Group of southern England, the Stadthagen Formation pterosaur mandible is among the stratigraphically oldest identifiable anhanguerians.

Key words: Pterosauria, Pterodactyloidea, Anhangueria, Cretaceous, Stadthagen Formation, Lower Saxony.

Pascal Abel [pascal.abel94@web.de], Senckenberg Centre for Human Evolution and Palaeoenvironment, Eberhard-Karls-University Tübingen, Sigwartstraße 28, 72076 Tübingen, Germany.
Jahn J. Hornung [jahn.hornung@yahoo.de], Niedersächsisches Landesmuseum Hannover, Willy-Brandt-Allee 5, 30169 Hannover, Germany.
Benjamin P. Kear [benjamin.kear@em.uu.se], Museum of Evolution, Uppsala University, Norbyvägen 22, 75236 Uppsala, Sweden.
Sven Sachs [sachs.pal@gmail.com], Naturkunde-Museum Bielefeld, Abteilung Geowissenschaften, Adenauerplatz 2, 33602 Bielefeld, Germany.

Received 16 September 2020, accepted 17 May 2021, available online 24 August 2021.

Introduction

Pterosaurs were the first vertebrates to evolve an active volant lifestyle and were globally widespread from the Middle Triassic until their extinction at the end of the Cretaceous (e.g., Butler et al. 2009; Longrich et al. 2018). Among the paraphyletic succession of early pterosaur lineages, only the "short-tailed" pterodactyloids and anurognathids survived beyond the Jurassic–Cretaceous boundary, with pterodactyloids subsequently diverging into the Azhdarchoidea and Pteranodontoidea (Kellner 2003; Hone 2020). One of the most successful of these Cretaceous pterodactyloid clades were the Anhangueria, a cosmopolitan radiation of toothed and often large pteranodontoids, best known from the Aptian–Albian strata of Great Britain and Brazil (Rodrigues and Kellner 2013), but ranging up into the Turonian elsewhere (Rodrigues and Kellner 2013; Pentland et al. 2019, Frey et al. 2020). To date, the stratigraphically oldest known anhanguerian is *Coloborhynchus clavirostris* Owen, 1874 from the upper Berriasian–lower Valanginian of England (Rodrigues and Kellner 2013; Pentland et al. 2019), which suggests possible origination of the group shortly after the Jurassic–Cretaceous transition.

Here we describe a new fragmentary mandible (RE 551.763.120 A 0333/1) of an anhanguerian pterodactyloid from the lower Valanginian of Northern Germany. This specimen was found by fossil collector and preparator Karl-Heinz Hilpert (formerly at the Geologisch-Paläontologisches Museum Münster) in the abandoned Sachsenhagen clay pit in Lower Saxony, and subsequently donated to the Ruhr

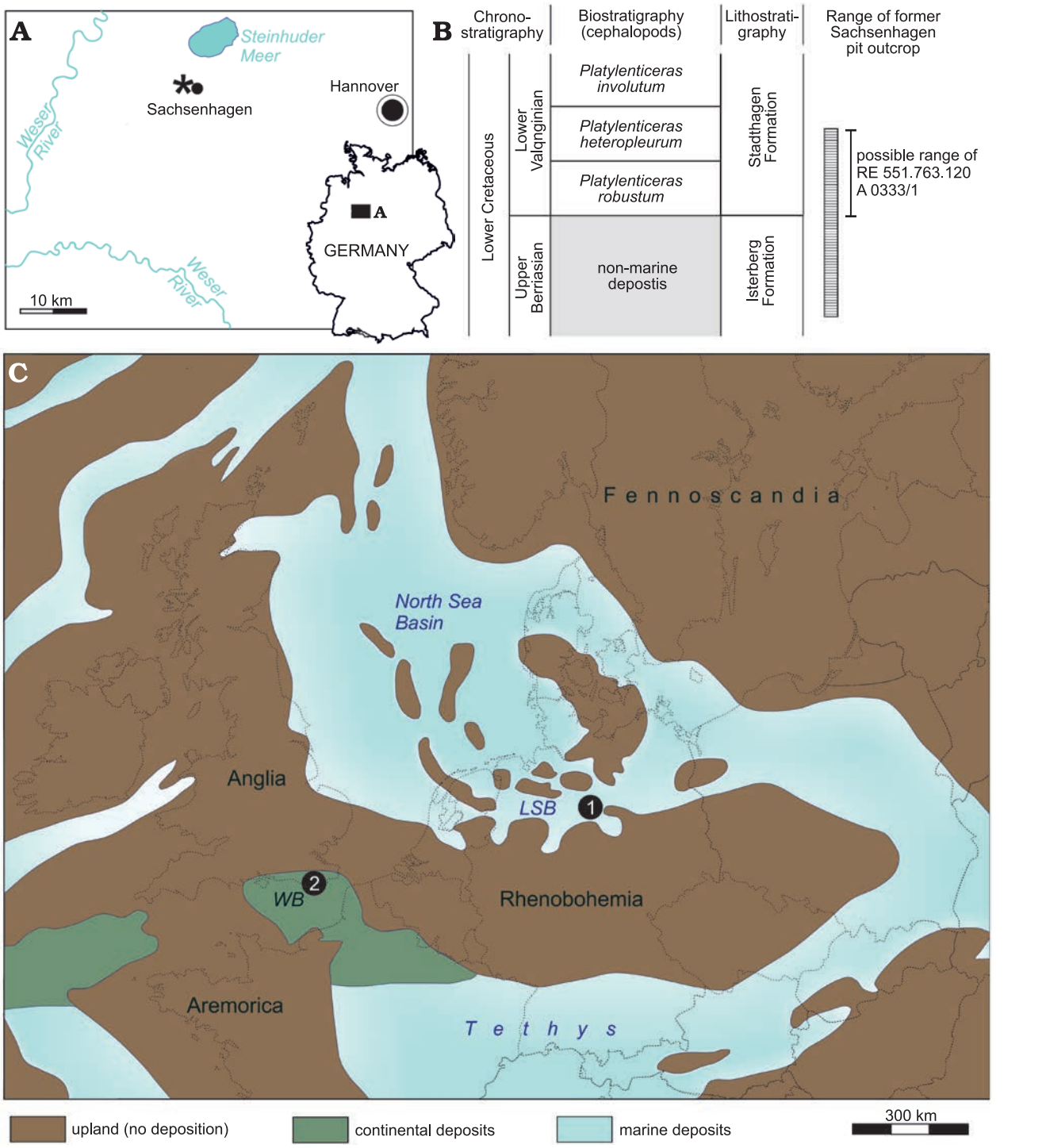

Fig. 1. **A**. Geographic location (asterisk) of the former Sachsenhagen clay-pit. **B**. Stratigraphical framework of the Lower Cretaceous in the former Sachsenhagen clay-pit. Modified after Mutterlose et al. (1997), Mutterlose (2017), and Erbacher et al. (2014a, b). **C**. Palaeogeographic reconstruction of Central Europe during the Valanginian–Hauterivian interval showing the position of Sachsenhagen (1) in the Lower Saxony Basin (LSB) and St. Leonard-on-Sea (2), the locus typicus of the approximately coeval *Coloborhynchus clavirostris*, in the Wessex Basin (WB). Modified after Mutterlose et al. (1997).

Museum Essen in 1998. RE 551.763.120 A 0333/1 is important, because together with *C. clavirostris* it represents one of the oldest known anhanguerian occurrences. In addition, it is one of only very few pterosaur specimens currently identified from the German Cretaceous (von Meyer 1851; Wild 1990; Hornung and Reich 2013; Lanser 2015) and is also the first documented pterosaur fossil found in Germany that is of Valanginian age.

Institutional abbreviations.—GZG.IF, Ichnofossil collection, Geoscience Centre, University of Göttingen, Göttingen, Germany; LWL, LWL-Museum für Naturkunde, Münster, Germany; RE, Ruhr Museum, Essen, Germany; RPMH,

Römer-Pelizaeus-Museum Hildesheim, Hildesheim, Germany; SMNS, Staatliches Museum für Naturkunde Stuttgart, Stuttgart, Germany.

Geological setting

The Sachsenhagen clay pit is located approximately 30 km west of Hannover (Fig. 1A) and was operated as brickworks from 1904 to 1986. Most of the quarry area has since been backfilled and used as a waste dump. The exposed profile spans a lithofacially mostly homogenous, pelitic succession of the upper Berriasian upper Isterberg Formation and lower Valanginian lower Stadthagen Formation (Fig. 1B). The transition between these units correlates with a shift from euryhaline to stenohaline conditions following a marine transgression (Kaufmann et al. 1980; Mutterlose 2017). Paleogeographically, the deposits were formed in a shallow gulf that inundated the Lower Saxony Basin as a southward extension of the North Sea Basin (Fig. 1C; see Mutterlose 2017).

Locality information indicates that RE 551.763.120 A 0333/1 derived from the lower Valanginian lower Stadthagen Formation spanning the *Platylenticeras robustum* and *P. heteropleurum* (Mutterlose 1984, 2017) ammonite zones. Zawischa (1992) and Frerichs and Girod (2017) documented a rich vertebrate fossil assemblage, including actinopterygians (Frerichs 2017a), plesiosaurs (Frerichs 2017b), the thalattosuchian crocodylomorph "*Enaliosuchus schroederi*" Kuhn, 1936 (see Schroeder 1923; Sickenberg 1961; Sachs et al. 2020), and additional indeterminate crocodyliform remains (Frerichs 2017b). Most of the material is currently located in private collections.

Systematic palaeontology

Pterosauria Kaup, 1834

Pterodactyloidea Plieninger, 1901

Pteranodontoidea Kellner, 1996

Anhangueria Rodrigues and Kellner, 2013

Anhangueria indet.

Fig. 2.

Material.—RE 551.763.120 A 0333/1, an incomplete mandible from the abandoned Sachsenhagen clay pit, Sachsenhagen, Lower Saxony, Germany (approximate coordinates 52°23'51" N, 09°15'18" E); *Platylenticeras robustum* or *Platylenticeras heteropleurum* ammonite biozones (NW-European ammonite province of the Sub-Boreal Realm: sensu Kemper et al. 1981, Marek and Shulgina 1996), lower Valanginian, Lower Cretaceous, Stadthagen Formation.

Description.—The preserved mandible includes the posterior section of the symphysis and parts of both dentaries and angulars. The splenials have been disarticulated and are now lost. Thus, the Meckelian groove is exposed on the medial surfaces of both rami (Fig. 2). The mandible has a sub-circular cross-section anterior to the symphyseal contact. There is no evidence of a sagittal crest. The external ventral face of the mandibular rami is shallowly convex. The dorsal side of the symphyseal portion is strongly concave and has an irregular midline suture (Fig. 2A). A conspicuous lateromedial furrow is visible along the length of the rami ventral to the alveolar row. The post-symphyseal space is filled with sediment. However, both rami diverge at an angle of about 23° relative to the longitudinal axis.

The mandible has suffered some diagenetic crushing, resulting in a prominent longitudinal crack on the lateral surface of the left ramus (Fig. 2B). Especially the lateral surface of the right ramus forms two longitudinal bulges, resulting in an undulating surface. The postsymphyseal portions of both rami were previously broken und glued back to the symphysis. Finally, the entire surface area of bone and exposed matrix on RE 551.763.120 A 0333/1 has been varnished and painted at some stage of preparation. This has created a pattern of irregular grooves and ridges along the ventral face of the symphysis. We consider these to be artificial, yet some bulges and rugosities on the median ventral face of the symphysis and posterior parts of the rami could possibly be pathological (Fig. 2C).

Dentary: The dentaries form the mandibular sulcus, alveolar row, and the base of the Meckelian groove. The dorsal trace of the splenial suture is located ventrally adjacent to the alveoli. The ventral suture is not visible. The angular contacts are exposed on the lateral surfaces of the mandibular rami (Fig. 2B, D), however, there is no evidence of the coronoid contacts. On the right ramus, thin ridges extending parallel to the alveolar row and posterodorsally across the lateral surface posterior to the fifth alveolus (Fig. 2D) might border nerve and/or blood vessel channels.

Angular: The angulars form about the ventrolateral third of the external surfaces of the rami, and taper to the level of the posterior-most symphyseal alveoli. Medially, the angu-

Table 1. Linear measurements (in mm) of RE 551.763.120 A 0333/1. Alveoli measured in posterior direction. Asterisks indicate incomplete alveoli and/or alveoli filled with sediment.

Diastemae, ramus	left	14.25	16.84	12.42	12.65		
	right	15.94	16.68	12.76	12.14	13.58	
Alveolar length, ramus	left	4.56*	4.95	4.37*	4.27	4.54	
	right	4.42	4.17	5.20*	4.83	5.31*	5.20
Alveolar width, ramus	left	3.12*	2.99	2.87*	2.70	2.96	
	right	2.86	2.43	2.75	2.58	2.56*	2.81

Maximum preserved length	117.63
Preserved symphysis, dorsal length	28.27
Preserved symphysis, ventral lengt	40.00
Dentary (left), maximum height	18.73
Dentary (left), maximum width	5.86

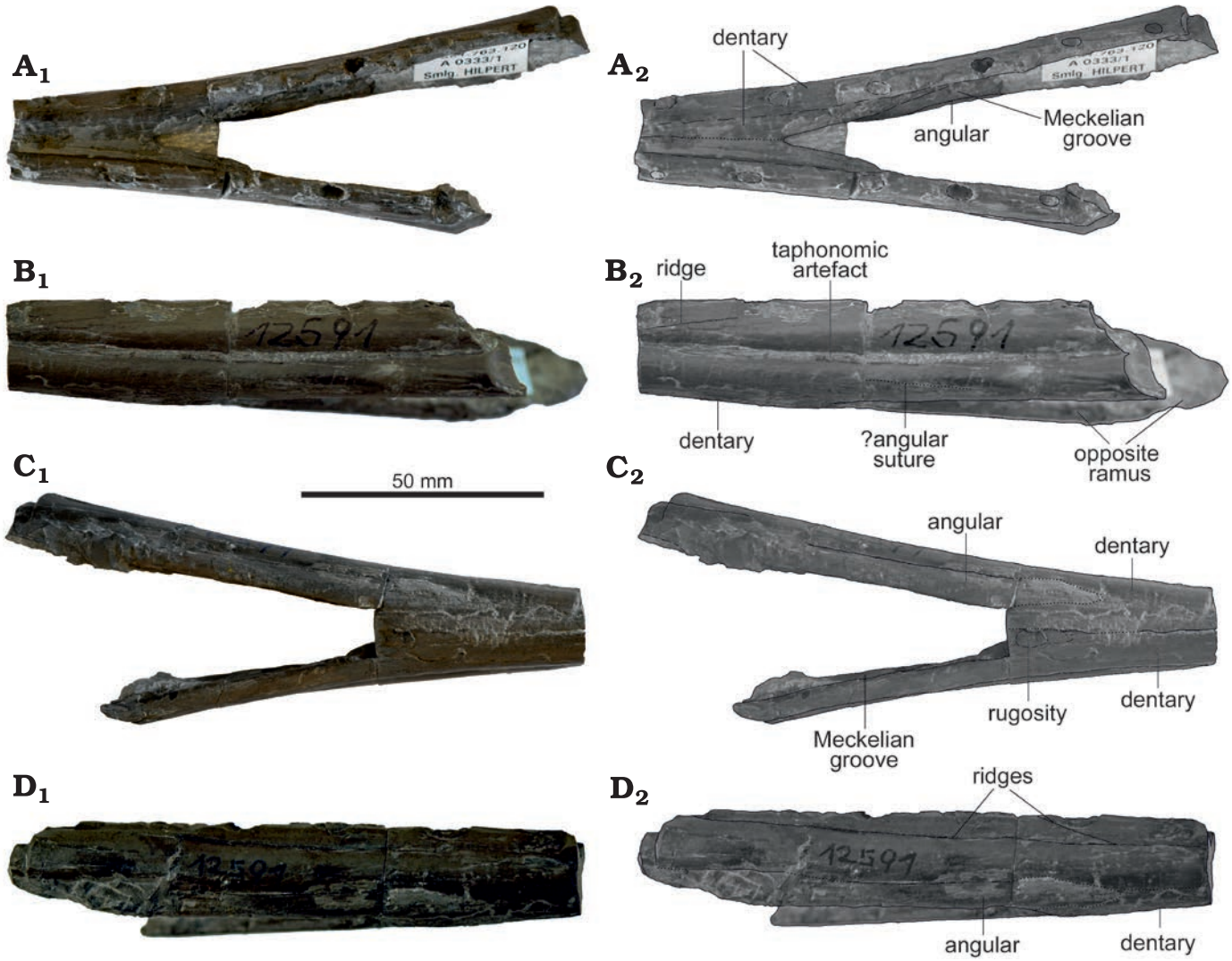

Fig. 2. Mandible of anhanguerian pterosaur RE 551.763.120 A 0333/1 from the lower Valanginian of Sachsenhagen (Northern Germany), in dorsal (**A**), left lateral (**B**), ventral (**C**), and right lateral (**D**) views. Photographs (A_1–D_1), explanatory drawings (A_2–D_2).

lars border the Meckelian groove and presumably sutured to the splenials dorsally.

Alveoli: Five alveoli are preserved on the left ramus, and six on the right; only two alveoli are placed adjacent to the symphysis on either side. They are about 1.5–1.9 times longer than wide, and each alveolus is slightly anteromedially directed (Table 1). The alveolar margins are flush with the surrounding bone. The interalveolar spaces are 2.5–4 times the length of the alveoli and increase in length posteriorly to the second preserved alveolus, but then decreases again further posteriorly (Table 1).

Discussion

Comparisons and classification.—Among Early Cretaceous toothed pterodactyloids, RE 551.763.120 A 0333/1 differs from ctenochasmatids and boreopterids, as these latter possess large numbers of teeth in a "comb-like" arrangement (Kellner 2003; Lü and Ji 2010; Jiang et al. 2014). *Lonchodraco* Rodrigues and Kellner, 2013 and other putative "lonchodectids", such as *Lonchodectes compressirostris* Owen, 1851, *Serradraco sagitirostris* Owen, 1874, *Prejanopterus curvirostris* Vidarte and Calvo, 2010, or *Targaryendraco wiedenrothi* Wild, 1990, are distinguished from the specimen described herein by their "lanceolate" jaw outline, inter-alveolar spacing that is sub-equal to the corresponding alveolar length (Wild 1990; Pereda-Suberbiola et al. 2012; Rodrigues and Kellner 2013; Rigal et al. 2017), and alveolar margins raised to a pedestal (Unwin 2001; Rodrigues and Kellner 2013). Likewise, dsungaripterids have closely spaced alveoli, where the dental bone bulges to envelope the base of the tooth crowns (Martill et al. 2000; Witton 2013; Chen et al. 2020). In istiodactyliforms, the alveoli are even more densely packed (Lü et al. 2008; Witton 2013; Kellner et al. 2019).

By contrast, the alveolar morphology of RE 551.763.120 A 0333/1 is very similar to known anhanguerians, which typically have well-spaced alveoli along the mid- and pos-

terior sections of the mandible (e.g., Wellnhofer 1987; Elgin and Frey 2011; Rodrigues and Kellner 2013). A taxonomic assignment of RE 551.763.120 A 0333/1 within Anhangueria, however, proves to be difficult. Especially the taxa of the specimen-rich Cambridge Greensand and other Lower Cretaceous strata of Great Britain are often only based on anterior rostral fragments, prohibiting a direct comparison with RE 551.763.120 A 0333/1 (Rodrigues and Kellner 2013), where these elements are missing. This includes most notably the roughly coeval *Coloborhynchus clavirostris* from the adjacent British Wealden. But even in more completely known mandibles most diagnostic traits are restricted to the anterior part of the symphysis (e.g., Steel et al. 2005).

Nevertheless, RE 551.763.120 A 0333/1 is distinct from *Anhanguera piscator* Kellner and Tomida, 2000, "*Araripesaurus santanae*" Wellnhofer, 1985, *Mythunga* Molnar and Thulburn, 2007, and "*Tropeognathus robustus*" Wellnhofer, 1987, because it lacks inter-alveolar spaces that decrease in length towards the back of the jaw (Wellnhofer 1985, 1987; Veldmeijer 2003; Pentland and Poropat 2019). RE 551.763.120 A 0333/1 further differs from *Brasileodactylus araripensis* Kellner, 1984, *Ferrodraco lentoni* Pentland, Poropat, Tischler, Sloan, R.A. Elliot, H.A. Elliot, J.A. Elliot, and D.A. Elliot, 2019, *Maaradactylus spielbergi* Veldmeijer, 2003, and *Tropeognathus mesembrinus* Wellnhofer, 1987, because these taxa have inter-alveolar spaces that successively increase in length (Wellnhofer 1987; Veldmeijer 2003; Veldmeijer et al. 2009; Pentland et al. 2019). Lastly, unlike *Anhanguera piscator*, "*Araripesaurus santanae*", and "*Santanadactylus araripensis*" Wellnhofer, 1985, RE 551.763.120 A 0333/1 possesses proportionately large alveoli compared to the transverse width of the mandibular ramus (Wellnhofer 1985; Kellner and Tomida 2000). Besides the alveolar pattern, RE 551.763.120 A 0333/1 differs further from *Maaradactylus spielbergi* by its more pronounced sulcus (Veldmeijer 2003).

The number of symphyseal teeth is variable among anhanguerians, ranging from six in *Cearadactylus atrox* Leonardi and Borgomanero 1985 (Unwin 2002; Vila Nova et al. 2014) or *Tropeognathus mesembrinus* to at least eleven in other far-related species, such as *Maaradactylus spielbergi*, *Brasileodactylus araripensis*, or *Aetodactylus halli* Myers, 2010 (Veldmeijer 2003; Veldmeijer et al. 2009; Myers 2010; Pinheiro and Rodridgues 2017). This makes it impossible to identify the position of the alveoli preserved in our specimen. Nevertheless, in the majority of anhanguerians preserving the mandible, the mandibular rami bear only two to five post-symphyseal teeth (Wellnhofer 1985, 1987; Kellner and Tomida 2000; Veldmeijer 2003; Vila Nova et al. 2014; Pinheiro and Rodrigues 2017), indicating the post-symphyseal alveoli preserved in RE 551.763.120 A 0333/1 may also represent the posterior-most alveoli of the mandible. A notable exception is *Aetodactylus halli*, which has 13 post-symphyseal alveoli (Myers 2010). However, *Aetodactylus halli*, together with the probably closely related *Cimoliopterus cuvieri* Bowerbank, 1851, differ from RE 551.763.120 A 0333/1 and other anhanguerians in their more densely packed teeth (Myers 2010, 2015). Furthermore, they were found to nest outside Anhangueria by some recent phylogenetic studies (Pêgas et al. 2019).

Unlike RE 551.763.120 A 0333/1 and "*Santanadactylus araripensis*" (Wellnhofer 1985), the angulars in *Cearadactylus atrox* and *Anhanguera piscator* do not extend as far as the posterior end of the tooth row (Leonardi and Borgomanero 1985; Kellner and Tomida 2000). The condition of RE 551.763.120 A 0333/1 is closer to "*Santanadactylus araripensis*", where the lateral portion of angular reaches almost the level of the posterior-most alveolus, which is in this taxon the fourth post-symphyseal tooth (Wellnhofer 1985). The same author interpreted the angular in "*Araripesaurus santanae*" to extend distinctly beyond the tooth bearing portion of the mandible, reaching at the least the level of the in anterior direction fifth alveolus. However, Kellner and Tomida (2000) argued that the angular may be significantly shorter in both "*Santanadactylus araripensis*" and "*Araripesaurus santanae*" but based this on the assumption of a congeneric relationship with *Anhanguera piscator*. This cannot be confirmed, because "*Santanadactylus araripensis*" and "*Araripesaurus santanae*" are considered to be nomina dubia (Pinheiro and Rodrigues 2017). Irrespectively, the angular of RE 551.763.120 A 0333/1 is most closely comparable to "*Santanadactylus araripensis*" as described by Wellnhofer (1985), although the anterior extremity is less anteriorly tapered in RE 551.763.120 A 0333/1.

Overall, complete mandibles are only barely known in anhanguerians, and often the mandibular bones are fused beyond distinction, suggesting these specimens may represent adult individuals (Kellner and Tomida 2000; Vila Nova et al. 2014). Evidently, RE 551.763.120 A 0333/1 likely derived from an osteologically immature animal.

Cretaceous pterosaurs from Germany.—Germany is world famous for its record of articulated Upper Jurassic pterosaur remains (e.g., Wellnhofer 1970, 1978; Bennett 2002, 2007; Tischlinger 2010; Hone et al. 2013; Tischlinger and Frey 2013). Conversely, pterosaur fossils of Cretaceous age are extremely rare despite the earliest documented occurrences dating back to the 19th century. This is also in stark contrast to other Cretaceous pterosaur-bearing sites in the world with a rich pterosaur diversity like the northeastern Brazilian Santana Group (e.g., Wellnhofer 1985, 1987; Kellner and Tomida 2000; Unwin 2002), or the British Wealden and Cambridge Greensand (e.g., Unwin 2001; Rodrigues and Kellner 2013; Rigal et al. 2017). The German record is currently restricted to the Lower Cretaceous. However, only the Valanginian and Hauterivian pterosaur specimens derive from strata that were deposited in some distance from the paleo-coastline. All other remains originated from non-marine, lagoonal to fully limnic and fluviatile environments.

The first Cretaceous pterosaur find described from Germany has been the holotype of *Ctenochasma roemeri* (non-catalogued, von Meyer 1851) from the lower Berriasian Münder Formation of the Deister region of Lower Saxony. It

consisted only of a fragmentary mandible, but unfortunately the original specimen in the collection of Clausthal is not traceable (SS personal observation).

Similarly, Hornung and Reich (2013) described a right manus track (GZG.IF.00102), assignable to the large pterosaur ichnotaxon *Purbeckopus* cf. *pentadactylus* Delair, 1963. This positive plaster cast derived from an imprint found in upper Berriasian silicilastics of the Deister Formation near Bückeburg and was made sometime around 1935. However, the original may have never been collected, and the cast was likely produced in situ.

A fragmentary wing phalanx and jaw elements (GZG.STR.50291, GZG.STR.50292, RPMH "Wd. 025") from the upper Berriasian Fuhse Formation near Sehnde in Lower Saxony have yet to be described in detail (Hornung 2013). Additional isolated remains have been recovered from upper Valanginian–lower Hauterivian deposits in the Leine Uplands of Lower Saxony and include what was identified as a metacarpal IV and holotype of "*Ornithocheirus hilsensis*" (Koken, 1883). However, a pterosaurian affinity was disputed (e.g., von Meyer 1884; Williston 1885, 1886; but see also Koken 1885, 1886), and the bone has recently been recognized as the pedal phalanx of a theropod dinosaur (Hornung 2020). Today "*O. hilsensis*" is considered a nomen dubium and the whereabouts of the specimen are unknown (Hornung 2020).

The comparatively best-preserved pterosaur from the Cretaceous of Germany is the holotype of *Targaryendraco wiedenrothi* (SMNS 56628) from the lowermost Hauterivian of the Stadthagen Formation near Hannover in Lower Saxony. Wild (1990) initially named it *Ornithocheirus wiedenrothi*, although its assignment to the "wastebasket" genus *Ornithocheirus* Seeley, 1869, is widely debated (Fletcher and Salisbury 2010; Ford 2013; Rodrigues and Kellner 2013; Abel et al. 2019; Pêgas et al. 2019). Fletcher and Salisbury (2010) grouped it in Ornithocheiridae close to *Aussiedraco molnari* Kellner, Rodrigues, and Costa, 2011, and another indeterminate specimen. Ford (2013) considered the species to be a "lonchodectid" and recombined it as *Lonchodectes wiedenrothi*. However, Rodrigues and Kellner (2013) argued against the validity of *Lonchodectes* and an affinity of the specimen as *Ornithocheirus* to be indeterminable, whereas Abel et al. (2019) reiterated a "lonchodectid" affinity. In a subsequent publication, Pêgas et al. (2019) redescribed the material as *Targaryendraco wiedenrothi* and found it to nest outside of Anhangueria, close to *Aussiedraco molnari* and *Barbosania gracilirostris* Elgin and Frey, 2011.

Lastly, Lanser (2015) reported several isolated teeth of putative ornithocheirids from various middle Barremian–lower Aptian karst-fillings in the Sauerland, North Rhine-Westphalia.

RE 551.763.120 A 0333/1 adds to this sparse record as the currently only recognized Valanginian pterosaur. Furthermore, it is one of only a handful Valanginian pterosaur remains in the world (Barrett et al. 2008; Cadena et al. 2020). Of these, only the probable Valanginian *C. clavirostris* can be confidently assigned to Anhangueria, although, other fragmentary finds may represent anhanguerians as well (Cadena et al. 2020). Finally, RE 551.763.120 A 0333/1 is, next to the teeth described by Lanser (2015), the only clear evidence for anhanguerian pterosaurs found in Germany.

Pterosaurs most frequently occur in limnic, lagoonal, and pelagic paleoenvironments (e.g., Wellnhofer 1970; Wang and Zhonghe 2006; Hone et al. 2018). Given that such depositional settings are typical of the German Cretaceous, the observed scarcity of pterosaur fossils is likely not reflecting their paleoecology, but rather the preservational biases of their fragile bones, and the reduction of Valanginian carbonate platforms in conjunction with a global cooling (Gréselle and Pittet 2010), which might have hindered the formation of Konservatlagerstätten (Butler et al. 2009). This may also explain the globally sparse record of Valanginian pterosaurs. Indeed, sampling is another evident limiting factor relative to other European Early Cretaceous pterosaur assemblages (e.g., the Cambridge Greensand, Unwin 2001; Ford and O'Connor 2004), and suggests that future exploration will likely yield new discoveries.

Conclusions

RE 551.763.120 A 0333/1 is important because it represents the only unambigious pterosaur fossil of Valanginian age recovered from Germany to date.

RE 551.763.120 A 0333/1 is among only a handful of Valanginian pterosaur occurrences yet identified worldwide.

The British *Coloborhynchus clavirostris* is the only other confidently assigned anhanguerian taxon from the respective time interval, representing together with RE 551.763.120 A 0333/1 the oldest known records of this group.

The sparseness of the German Cretaceous pterosaur record may be best explainable by sampling and preservation biases and does not reflect a paleobiological signal.

Acknowledgements

Achim Reisdorf (Ruhr Museum Essen, Germany) and Udo Scheer (previously Ruhr Museum Essen) generously assisted with access to specimen and historical information. We thank the editor Daniel Barta (Tahlequah, USA) and the Editorial Team from *Acta Palaeontologica Polonica* for handling of the manuscript, as well as Eberhard Frey (Staatliches Museum für Naturkunde Karlsruhe, Germany) and a second anonymous reviewer for their constructive comments that helped to enhance our manuscript.

References

Abel, P., Hornung, J., Kear, B., and Sachs, S. 2019. Reassessment of the enigmatic pterosaur '*Ornithocheirus*' *wiedenrothi* from the Lower Cretaceous of Northern Germany. *In*: J.M. Stark and A. Huysseune (eds.), International Congress of Vertebrate Morphology (ICVM) Abstract Issue. *Journal of Morphology* Supplement 280 (S1): S73–S74.

Barrett, P.M., Butler, R.J., Edwards, N.P., and Milner, A.R. 2008. Pterosaur distribution in time and space: an atlas. *Zitteliana* B28: 61–107.

Bennett, S.C. 2002. Soft tissue preservation of the cranial crest of the pterosaur *Germanodactylus* from Solnhofen. *Journal of Vertebrate Paleontology* 22 (1): 43–48.

Bennett, S.C. 2007. A review of the pterosaur *Ctenochasma*: taxonomy and ontogeny. *Neues Jahrbuch für Geologie und Paläontologie Abhandlungen* 245: 23–31.

Bowerbank, J.S. 1851. On the pterodactyles of the Chalk Formation. *Proceedings of the Zoological Society of London* 19: 14–20.

Butler, R.J., Barrett, P.M., Nowbath, S., and Upchurch, P. 2009. Estimating the effects of sampling biases on pterosaur diversity patterns: implications for hypotheses of bird/pterosaur competitive replacement. *Paleobiology* 35: 432–446.

Cadena, E.A., Unwin, D.M., and Martill, D.M. 2020. Lower Cretaceous pterosaurs from Colombia. *Cretaceous Research* 114: 104526.

Chen, H., Jiang, S., Kellner, A.W.A., Cheng, X., Zhang, X., Qiu, R., Li, Y., and Wang, X. 2020. New anatomical information on *Dsungaripterus weii* Young, 1964 with focus on the palatal region. *PeerJ* 8: e8741.

Delair, J.B. 1963. Notes on Purbeck fossil footprints, with description of two hitherto unknown forms from Dorset. *Proceedings of the Dorset Natural History and Archaeological Society* 84: 92–100.

Elgin, R.A. and Frey, E. 2011. A new ornithocheirid, *Barbosania gracilirostris* gen. et sp. nov.(Pterosauria, Pterodactyloidea) from the Santana Formation (Cretaceous) of NE Brazil. *Swiss Journal of Palaeontology* 130: 259–275.

Erbacher, J., Hiss, M., Luppold, F.W., and Mutterlose, J. 2014a. *Minden-Braunschweig-Gruppe*. *Litholex Online Database, Record No. 2008168*. https://litholex.bgr.de/pages/Einheit.aspx?ID=2008168.

Erbacher, J., Hiss, M., Luppold, F.W., and Mutterlose, J. 2014b. *Stadthagen-Formation. Litholex Online Database, Record No.: 2008147*. https://litholex.bgr.de/pages/Einheit.aspx?ID=2008147.

Fletcher, T.L. and Salisbury, S.W. 2010. New pterosaur fossils from the Early Cretaceous (Albian) of Queensland, Australia. *Journal of Vertebrate Paleontology* 30: 1747–1759.

Ford, T.L. 2013. Will the real *Lonchodectes* fly in? *In*: J.M. Sayão, F.R. Costa, R.A.M. Bantim, and A.W.A. Kellner (eds.), *Short Communications/International Symposium on Pterosaurs, Rio Ptero 2013*, 65–67. Taylor & Francis, Rio de Janeiro.

Ford, T.D. and O'Connor, B. 2002. Coprolite mining in England. *Geology Today* 18 (5): 178–181.

Frerichs, U. 2017a. Fische. *Arbeitskreis Paläontologie Hannover* 45: 59–62.

Frerichs, U. 2017b. Reptilien. *Arbeitskreis Paläontologie Hannover* 45: 63–68.

Frerichs, U. and Girod, P. 2017. Überblick über die Fossilien aus der ehemaligen Ziegeleitongrube Sachsenhagen. *Arbeitskreis Paläontologie Hannover* 45: 8–14.

Frey, E.D., Stinnesbeck, W., Martill, D.M., Rivera-Sylva, H.E., and Múzquiz, H.P. 2020. The geologically youngest remains of an ornithocheirid pterosaur from the late Cenomanian (Late Cretaceous) of northeastern Mexico with implications on the paleogeography and extinction of Late Cretaceous ornithocheirids. *Palaeovertebrata* 43: 1–12.

Gréselle, B. and Pittet, B. 2010. Sea-level reconstructions from the Peri-Vocontian Zone (South-east France) point to Valanginian glacio-eustasy. *Sedimentology* 57: 1640–1684.

Hone, D.W. 2020. A review of the taxonomy and palaeoecology of the Anurognathidae (Reptilia, Pterosauria). *Acta Geologica Sinica* 94: 1676–1692.

Hone, D.W., Habib, M.B., and Lamanna, M.C. 2013. An annotated and illustrated catalogue of Solnhofen (Upper Jurassic, Germany) pterosaur specimens at Carnegie Museum of Natural History. *Annals of Carnegie Museum* 82: 165–191.

Hone, D.W., Witton, M.P., and Habib, M.B. 2018. Evidence for the Cretaceous shark *Cretoxyrhina mantelli* feeding on the pterosaur *Pteranodon* from the Niobrara Formation. *PeerJ* 6: e6031.

Hornung, J.J. 2013. *Contributions to the Palaeobiology of the Archosaurs (Reptilia: Diapsida) from the Bückeberg Formation ("Northwest German Wealden"—Berriasian–Valanginian, Lower Cretaceous) of northern Germany*. 400 pp. Unpublished Thesis, Georg August University, Göttingen.

Hornung, J.J. 2020. Comments on "*Ornithocheirus hilsens*" Koken, 1883—one of the earliest dinosaur discoveries in Germany. *PalArch's Journal of Vertebrate Palaeontology* 17: 1–12.

Hornung, J.J. and Reich, M. 2013. The first record of the pterosaur ichnogenus *Purbeckopus* in the late Berriasian (Early Cretaceous) of Northwest Germany. *Ichnos* 20: 164–172.

Jiang, S.-X., Wang, X.-L., Meng, X., and Cheng, X. 2014. A new boreopterid pterosaur from the Lower Cretaceous of western Liaoning, China, with a reassessment of the phylogenetic relationships of the Boreopteridae. *Journal of Paleontology* 88: 823–828.

Kaufmann, R., Opfermann, H.-U., and Petsch, K. 1980. Zur Entwicklungsgeschichte der tiefen Unterkreide (Berrias/Valangin) im Süden des Rehburger Sattels unter besonderer Berücksichtigung der Tongrube Sachsenhagen. *Ballerstedtiana – Beitrag zur naturwissenschaftlichen Erforschung Schaumburg-Lippes und angrenzender Gebiete* 3: 5–27.

Kaup, J.J. 1834. Versuch einer Eintheilung der Säugethiere in 6 Stämme und der Amphibien in 6 Ordnungen. *Isis* 27: 311–315.

Kellner, A.W.A. 1984. Occurrência de uma mandíbula de Pterosauria (*Brasileodactylus araripensis*, nov. gen, nov sp.) na Formação Santana, Cretáceo da Chapada do Araripe, Ceará, Brasil. *In*: *33 Anais Congresso Brasileiro de Geologia 2*, 578–590. Sociedade Brasileira de Geologia, Rio de Janeiro.

Kellner, A.W.A. 1996. Pterosaur phylogeny. *Journal of Vertebrate Paleontology* 16 (3): 45A.

Kellner, A.W.A. 2003. Pterosaur phylogeny and comments on the evolutionary history of the group. *Geological Society, London, Special Publications* 217: 105–137.

Kellner, A.W.A. and Tomida, Y. 2000. Description of a new species of Anhangueridae (Pterodactyloidea) with comments on the pterosaur fauna from the Santana Formation (Aptian–Albian), northeastern Brazil. *National Science Museum Monographs* 17: 9–137.

Kellner, A.W.A., Caldwell, M.W., Holgado, B., Dalla Vecchia, F.M., Nohra, R., Sayão, J.M., and Currie, P.J. 2019. First complete pterosaur from the Afro-Arabian continent: insight into pterodactyloid diversity. *Scientific Reports* 9 (1): 1–9.

Kellner, A.W.A., Rodrigues, T., and Costa, F.R. 2011. Short note on a pteranodontoid pterosaur (Pterodactyloidea) from western Queensland, Australia. *Anais Da Academia Brasileira de Ciências* 83 (1): 301–308.

Kemper, E., Rawson. P.F., and Thieuloy, J.-P. 1981. Ammonites of Tethyan ancestry in the early Lower Cretaceous of north-western Europe. *Palaeontology* 24: 251–311.

Koken, E. 1883. Die Reptilien der norddeutschen unteren Kreide. *Zeitschrift Der Deutschen Geologischen Gesellschaft* 35: 735–827.

Koken, E. 1885. Ueber *Ornithocheirus hilsensis* Koken. *Zeitschrift Der Deutschen Geologischen Gesellschaft* 32: 214–215.

Koken, E. 1886. Über *Ornithocheirus hilsensis* Koken. *Zoologischer Anzeiger* 9: 21–23.

Kuhn, O. 1936. Crocodilia. *In*: W. Quenstedt (ed.). *Fossilium Catalogus I: Animalia*, 75. W. Junk, Berlin.

Lanser, K.P. 2015. Nachweise von Pterosauriern aus einer unterkreidezeitlichen Karstfüllung im nördlichen Sauerland (Rheinisches Schiefergebirge, Deutschland). *Geologie Und Paläontologie in Westfalen* 87: 93–117.

Leonardi, G. and Borgomanero, G. 1985. *Cearadactylus atrox* nov. gen., nov. sp. novo Pterosauria (Pterodactyloidea) da Chapada do Araripe, Ceará, Brasil. *In*: D.A. Campos, C.S. Ferreira, I.M. Brito, and C.F. Viana (eds.), *Trabalhos Apresentados No VIII Congresso Brasileiro De Paleontologia 1983*, 75–80. Ministérios das Minas e Energia, Departamento Nacional da Produção Mineral, Brasília.

Longrich, N.R., Martill, D.M., and Andres, B. 2018. Late Maastrichtian pterosaurs from North Africa and mass extinction of Pterosauria at the Cretaceous–Paleogene boundary. *PLOS Biology* 16 (3): e2001663.

Lü, J. and Ji, Q. 2005. A new ornithocheirid from the Early Cretaceous of Liaoning Province, China. *Acta Geologica Sinica* (English Edition) 79: 157–163.

Marek, S. and Shulgina, N. 1996. Biostratigraphic correlation between

Lower Cretaceous deposits in the central region of East-European Platform and the Polish Lowlands. *Geological Quarterly* 40: 129–140.

Martill, D.M., Frey, E., Diaz, G.C., and Bell, C.M. 2000. Reinterpretation of a Chilean pterosaur and the occurrence of Dsungaripteridae in South America. *Geological Magazine* 137: 19–25.

Meyer, O. von 1884. Ueber *Ornithocheirus hilsensis* Koken und über Zirkonzwillinge. *Zeitschrift Der Deutschen Geologischen Gesellschaft* 36: 411–416.

Meyer, H. von 1851. Ctenochasma Römeri. *Palaeontographica – Beiträge zur Naturgeschichte der Vorwelt* 2 (3): 82–84.

Molnar, R.E. and Thulburn, R.A. 2007. An incomplete pterosaur skull from the Cretaceous of north-central Queensland, Australia. *Arquivos do Museo Nacional, Rio de Janeiro* 65 (4): 461–470.

Mutterlose, J. 1984. Die Unterkreide-Aufschlüsse (Valangin–Alb) im Raum Hannover-Braunschweig. *Mitteilungen aus dem Geologischen Institut der Universität Hannover* 24: 1–61.

Mutterlose, J. 2017. Die ehemalige Tongrube Sachsenhagen. *Arbeitskreis Paläontologie Hannover* 45: 2–7.

Mutterlose, J., Wippich, M., and Geisen, M. 1997. Cretaceous depositional environments of NW Germany. *Bochumer Geologische und Geotechnische Arbeiten* 46: 1–134.

Myers, T.S. 2010. A new ornithocheirid pterosaur from the Upper Cretaceous (Cenomanian–Turonian) Eagle Ford Group of Texas. *Journal of Vertebrate Paleontology* 30: 280–287.

Myers, T.S. 2015. First North American occurrence of the toothed pteranodontoid pterosaur *Cimoliopterus*. *Journal of Vertebrate Paleontology* 35(6): e1014904.

Owen, R. 1851. *A Monograph of the Fossil Reptilia of the Cretaceous Formations. Part 1*, 1–118. The Palaeontographical Society, London.

Owen, R. 1874. The fossil reptilia of the Mesozoic formations. Part 1. Pterosauria. *Palaeontographical Society Monographs* 27: 1–14.

Pêgas, R.V., Holgado, B., and Leal, M.E.C. 2019. On *Targaryendraco wiedenrothi* gen. nov. (Pterodactyloidea, Pteranodontoidea, Lanceodontia) and recognition of a new cosmopolitan lineage of Cretaceous toothed pterodactyloids. *Historical Biology* 33 (8) [available online, https://doi.org/10.1080/08912963.2019.1690482].

Plieninger, F. 1901. Beiträge zur Kenntnis der Flugsaurier. *Palaeontographica* 48: 65–90

Pentland, A.H. and Poropat, S.F. 2019. Reappraisal of *Mythunga camara* Molnar & Thulborn, 2007 (Pterosauria, Pterodactyloidea, Anhangueria) from the upper Albian Toolebuc Formation of Queensland, Australia. *Cretaceous Research* 93: 151–169.

Pentland, A.H., Poropat, S.F., Tischler, T.R., Sloan, T., Elliott, R.A., Elliott, H.A., Elliott, J.A., and Elliott, D.A. 2019. *Ferrodraco lentoni* gen. et sp. nov., a new ornithocheirid pterosaur from the Winton Formation (Cenomanian–lower Turonian) of Queensland, Australia. *Scientific Reports* 9 (1): 13454.

Pereda-Suberbiola, X., Knoll, F., Ruiz-Omeñaca, J.I., Company, J., and Fernández-Baldor, F.T. 2012. Reassessment of *Prejanopterus curvirostris*, a basal pterodactyloid pterosaur from the Early Cretaceous of Spain. *Acta Geologica Sinica* (English Edition) 86: 1389–1401.

Pinheiro, F.L. and Rodrigues, T. 2017. *Anhanguera* taxonomy revisited: Is our understanding of Santana Group pterosaur diversity biased by poor biological and stratigraphic control? *PeerJ* 5: e3285.

Rigal, S., Martill, D.M., and Sweetman, S.C. 2017. A new pterosaur specimen from the Upper Tunbridge Wells Sand Formation (Cretaceous, Valanginian) of southern England and a review of *Lonchodectes sagittirostris* (Owen, 1874). *Geological Society, London, Special Publications* 455: 221–232.

Rodrigues, T. and Kellner, A.W.A. 2013. Taxonomic review of the *Ornithocheirus* complex (Pterosauria) from the Cretaceous of England. *ZooKeys* 308: 1–112.

Sachs, S., Young, M.T., and Hornung, J.J. 2020. Reassessment of *Enaliosuchus schroederi*, a metriorhynchid crocodylomorph from the Lower Cretaceous of Northern Germany *In*: E. Vlachos, E. Manzanares, V.D. Crespo, C. Martínez-Pérez, H.G. Ferrón, J.L. Herráiz, A. Gamonal, F.A.M. Arnal, F. Gascó, and P. Citton (eds.), *2nd Palaeontological Virtual Congress, May 1–15th, 2020—Book of Abstracts*, 141.

Schroeder, H. 1923. Ein Meereskrokodilier aus der Unteren Kreide Norddeutschlands. *Jahrbuch Der Preußischen Geologischen Landesanstalt Zu Berlin* 42: 352–364.

Seeley, H.G. 1869. *Index to the Fossil Remains of Aves, Ornithosauria, and Reptilia, from the Secondary System of Strata, Arranged in the Woodwardian Museum of the University of Cambridge*. 143 pp. Deighton, Bell, and Co., Cambridge.

Sickenberg, O. 1961. Das wiedergefundene Typusexemplar vom Meereskrokodil aus Sachsenhagen. *Bericht Der Naturhistorischen Gesellschaft Hannover* 105: 5–6.

Steel, L., Martill, D.M., Unwin, D.M., and Winch, J.D. 2005. A new pterodactyloid pterosaur from the Wessex Formation (Lower Cretaceous) of the Isle of Wight, England. *Cretaceous Research* 26: 686–698.

Tischlinger, H. 2010. Pterosaurs of the "Solnhofen" Limestone: new discoveries and the impact of changing quarrying practices. *Acta Geoscientica Sinica* 31: 62–63.

Tischlinger, H. and Frey, E. 2013. A new pterosaur with mosaic characters of basal and pterodactyloid Pterosauria from the upper Kimmeridgian of Painten (Upper Palatinate, Germany). *Archaeopteryx* 31: 1–13.

Unwin, D.M. 2001. An overview of the pterosaur assemblage from the Cambridge Greensand (Cretaceous) of Eastern England. *Fossil Record* 4: 189–221.

Unwin, D.M. 2002. On the systematic relationships of *Cearadactylus atrox*, an enigmatic Early Cretaceous pterosaur from the Santana Formation of Brazil. *Fossil Record* 5: 239–263.

Veldmeijer, A.J. 2003. Description of *Coloborhynchus spielbergi* sp. nov. (Pterodactyloidea) from the Albian (Lower Cretaceous) of Brazil. *Scripta Geologica* 125 (35): e139.

Veldmeijer, A.J., Meijer, H.J., and Signore, M. 2009. Description of pterosaurian (Pterodactyloidea: Anhangueridae, Brasileodactylus) remains from the Lower Cretaceous of Brazil. *Deinsea* 13: 9–40.

Vidarte, C.F. and Calvo, M.M. 2010. Un nuevo pterosaurio (Pterodactyloidea) en el Cretácico Inferior de La Rioja (España). *Boletín Geológico y Minero* 121: 311–328.

Vila Nova, B.C., Sayão, J.M., Neumann, V.H., and Kellner, A.W.A. 2014. Redescription of *Cearadactylus atrox* (Pterosauria, Pterodactyloidea) from the Early Cretaceous Romualdo Formation (Santana Group) of the Araripe Basin, Brazil. *Journal of Vertebrate Paleontology* 34: 126–134.

Wang, X. and Zhonghe, Z. 2006. Pterosaur assemblages of the Jehol Biota and their implication for the Early Cretaceous pterosaur radiation. *Geological Journal* 41: 405–418.

Wellnhofer, P. 1970. Die Pterodactyloidea (Pterosauria) der Oberjura-Plattenkalke Süddeutschlands. *Bayerische Akademie der Wissenschaften, Mathematisch-Wissenschaftliche Klasse, Abhandlungen* 141: 1–133.

Wellnhofer, P. 1978. *Pterosauria. Handbuch der Palaeoherpetologie, Teil 19*. 82 pp. Gustav-Fischer Verlag, Lutherstadt Wittenberg.

Wellnhofer, P. 1985. Neue Pterosaurier aus der Santana-Formation (Apt) der Chapada do Araripe, Brasilien. *Palaeontographica. Abteilung A, Paläozoologie, Stratigraphie* 187: 105–182.

Wellnhofer, P. 1987. New crested pterosaurs from the Lower Cretaceous of Brazil. *Mitteilungen der Bayerischen Staatssammlung für Paläontologie und Historische Geologie* 27: 175–186.

Wild, R. 1990. Ein Flugsaurierrest (Reptilia, Pterosauria) aus der Unterkreide (Hauterive) von Hannover (Niedersachsen). *Neues Jahrbuch für Geologie und Paläontologie Abhandlungen* 181: 241–254.

Williston, S.W. 1885. Über *Ornithocheirus hilsensis* Koken. *Zoologischer Anzeiger* 8: 628–629.

Williston, S.W. 1886. Über *Ornithocheirus hilsensis* Koken. *Zoologischer Anzeiger* 9: 282–283.

Witton, M.P. 2013. *Pterosaurs: Natural History, Evolution, Anatomy*. 304 pp. Princeton University Press, Oxfordshire.

Zawischa, D. 1992. Fossilien aus der Tongrube Sachsenhagen. *Arbeitskreis Paläontologie Hannover* 20 (2): 33–50.

The early Miocene lake of Foieta la Sarra-A in eastern Iberian Peninsula and its relevance for the reconstruction of the Ribesalbes–Alcora Basin palaeoecology

SERGIO ÁLVAREZ-PARRA, JOAQUÍN ALBESA, SOLEDAD GOUIRIC-CAVALLI, PLINI MONTOYA, ENRIQUE PEÑALVER, JOSEP SANJUAN, and VICENTE D. CRESPO

Álvarez-Parra, S., Albesa, J., Gouiric-Cavalli, S., Montoya, P., Peñalver, E., Sanjuan, J., and Crespo, V.D. 2021. The early Miocene lake of Foieta la Sarra-A in eastern Iberian Peninsula and its relevance for the reconstruction of the Ribesalbes–Alcora Basin palaeoecology. *Acta Palaeontologica Polonica* 66 (Supplement to 3): S13–S30.

The Ribesalbes–Alcora Basin (Castelló Province, Spain) contains two lower Miocene units that are rich in fossils. The Unit B contains oil-shale and laminated bituminous dolomicrite related to a palaeolake, whereas the Unit C is composed of sandstone and mudstone beds from distal deltaic and shallow lacustrine environments. The La Rinconada and San Chils localities from the Unit B have yielded a fossil assemblage of plants, molluscs, arthropods, and vertebrates, while the localities from the Unit C in the Campisano ravine (Araia/Mas d'Antolino outcrop) are rich in mammalian record. Here we study a new palaeolake deposit of laminated lacustrine limestone beds in the Unit C named Foieta la Sarra-A. This new locality has provided an assemblage of charophytes, terrestrial plants, molluscs, arthropods, and teleosteans. The latter represent the only known fish record from the Ribesalbes–Alcora Basin to date. Although the specimens are generally poorly preserved, the presence of soft-body preservation due to the action of microbial mats at the lake bottom allows considering the Foieta la Sarra-A locality as a Konservat-Lagerstätte. The Foieta la Sarra-A palaeolake had a different water chemistry compared to that represented in the Unit B. Its depth was about a few metres and the water level suffered periodic fluctuations. This new locality sheds light on the palaeoenvironmental dynamics of the Ribesalbes–Alcora Basin during the early Miocene and provides a new approach to the palaeoecological reconstruction of the basin.

Key words: Characeae, Poales, Gastropoda, Cladocera, Insecta, Teleostei, palaeoenvironment, taphonomy, palaeoecology, lacustrine basin, Neogene, Konservat-Lagerstätte, Spain.

Sergio Álvarez-Parra [sergio.alvarez-parra@ub.edu], Departament de Dinàmica de la Terra i de l'Oceà and Institut de Recerca de la Biodiversitat (IRBio), Facultat de Ciències de la Terra, Universitat de Barcelona, c/ Martí i Franquès s/n, 08028, Barcelona, Spain.
Joaquín Albesa [joaquin.albesa@uv.es], Departament de Botànica i Geologia, Universitat de València, Dr. Moliner 50, 46100, Burjassot, Valencia, Spain; Museu Valencià d'Història Natural, L'Hort de Feliu, P.O. Box 8460, Alginet, 46230 Valencia, Spain.
Soledad Gouiric-Cavalli [sgouiric@fcnym.unlp.edu.ar], Consejo Nacional de Investigaciones Científicas y Técnicas, División Paleontología Vertebrados, Museo de La Plata, Paseo del Bosque s/n, B1900FWA La Plata, Argentina.
Plini Montoya [p.montoya@uv.es], Departament de Botànica i Geologia, Universitat de València, Dr. Moliner 50, 46100, Burjassot, Valencia, Spain.
Enrique Peñalver [e.penalver@igme.es], Instituto Geológico y Minero de España (Museo Geominero), c/ Cirilo Amorós 42, 46004, Valencia, Spain.
Josep Sanjuan [js76@aub.edu.lb], Department of Geology, American University of Beirut-AUB, 11-0236 Beirut, Lebanon; Departament de Dinàmica de la Terra i de l'Oceà, Facultat de Ciències de la Terra, Universitat de Barcelona, c/ Martí i Franquès s/n, 08028, Barcelona, Spain.
Vicente D. Crespo [vidacres@gmail.com] (corresponding author), Consejo Nacional de Investigaciones Científicas y Técnicas, División Paleontología Vertebrados, Museo de La Plata, Paseo del Bosque s/n, B1900FWA La Plata, Argentina; Museo Paleontológico de Alpuente, Av. San Blas 17, Alpuente, 46178 Valencia, Spain; Museu Valencià d'Història Natural, L'Hort de Feliu, P.O. Box 8460, Alginet, 46230 Valencia, Spain.

Received 15 October 2020, accepted 6 April 2021, available online 19 August 2021.

Introduction

Lakes are remarkable ecological archives due to their high sensitivity to climatic changes, a characteristic that can also be used in deep time (Cohen 2003). Indeed, the fossil content and sedimentary record of palaeolakes provide valuable information, such as palaeoclimatic, chemical, and temperature conditions (Talbot and Allen 1996). During the Miocene, a large portion of the European continent was covered by lakes (e.g., Neubauer et al. 2015a, b; Mandic et al. 2019; Vasilyan 2020). Those which developed in the Iberian Peninsula produced exceptionally well-preserved fossil assemblages with Konservat-Lagerstätte characteristics (e.g., McNamara et al. 2012; Peñalver et al. 2016). Remarkable Iberian Konservat-Lagerstätten in Miocene lacustrine deposits are the fossil localities of Rubielos de Mora (Teruel Province), Bicorb (Valencia Province), La Rinconada and San Chils (the latter two in Castelló Province). These well-preserved and diverse fossil assemblages originated under anoxic conditions at the lake bottom with presence of microbial mats (Peñalver 2002; Peñalver and Gaudant 2010).

The Ribesalbes–Alcora Basin is a Neogene complex graben covering around 150 km^2 located in SE Iberian Range (Anadón et al. 1989; Fig. 1A). This basin is well-known for the mining activities leading to oil-shale extraction in the La Rinconada (Ribesalbes) and San Chils (l'Alcora) mines until the early 20th century and clay extraction in the Campisano ravine (Araia/Mas d'Antolino area) which continues nowadays (Peñalver et al. 2016; Crespo 2017). The Campisano ravine contains seven sections with mammalian fossil record that have been proposed as a Site of Geological Interest (Costa-Pérez et al. 2019), i.e., Mas dels Coixos, Mas de Torner, Araia Cantera Sud, Barranc de Campisano, Foieta la Sarra, Mas d'Antolino B and Corral de Brisca (Fig. 1A). La Rinconada is a well-known locality that has provided an outstanding record of plants, molluscs, ostracods, arachnids, insects, amphibians, bird feathers and coprolites (Peñalver et al. 2016). Furthermore, a fossil assemblage from the San Chils locality has been recently described showing a strong similarity to the assemblage of La Rinconada (Álvarez-Parra and Peñalver 2019). Both localities have been interpreted as different areas of the same meromictic palaeolake, mostly contemporaneous, that occupied the basin during the early Miocene (Álvarez-Parra and Peñalver 2019). The exceptional preservation of their fossil record is related to the presence of microbial mats at the lake bottom (Peñalver et al. 2016). Interestingly, these fossil localities lack fish record, which might be related to an endorheic origin of the lake or an inappropriate water chemistry for the species that could reach the lake (Peñalver et al. 2016).

Forty-five fossiliferous levels rich in mammal remains have been recently described by Crespo et al. (2019c), in addition to the ones previously studied by Agustí et al. (1988), in the seven Campisano ravine sections. Their general features, together with the geological and preliminary biostratigraphic framework, were published by Crespo et al. (2019c), who described the geology of the area and placed the sections under study a stratigraphic context. In addition, many of the small mammal groups found in these sections have already been studied, including two new species of bat and dimylid (Furió et al. 2012; Crespo 2017; Crespo et al. 2019a, b, 2020a, b, 2021a, b). Among the different studied sections from these localities, the Foieta la Sarra section includes the Foieta la Sarra-1 locality, which yields a rich record of vertebrate remains (Crespo et al. 2019c). The faunal assemblage of the Foieta la Sarra-1 locality listed by Crespo et al. (2019c) is: *Amphiperatherium frequens erkertshofense* (Koenigswald, 1970), *Heteroxerus rubricati* Crusafont, Villalta, and Truyols, 1955, *Megacricetodon primitivus* (Freudenthal, 1963), *Democricetodon decipiens* (Freudenthal and Daams, 1988), *Eumyarion weinfurteri* (Schaub and Zapfe, 1953), *Microdyromys koenigswaldi* De Bruijn, 1966, *Peridyromys murinus* (Pomel, 1853), *Pseudodryomys ibericus* De Bruijn, 1966, *Simplomys julii* (Daams, 1989), *Glirudinus undosus* Mayr, 1979, *Ligerimys ellipticus* Daams, 1976, *Galerix symeonidisi* Doukas, 1986, Talpidae sp. indet., and cf. *Soricella discrepans* Doben-Florin, 1964. The preliminary study of the palaeoecology of this mammalian assemblage by Crespo (2017) indicated an increase of the open forest, as well as higher humidity and temperature than the oldest localities from the Campisano ravine.

Here, we describe the fossil record and the palaeoecology of a new lower Miocene locality we name Foieta la Sarra-A, which namely consists of laminated lacustrine limestone beds located at the base of the Foieta la Sarra section. Our main goal is to infer the taphonomic and palaeoecological conditions of this outcrop. Together with the current data from La Rinconada and San Chils localities, our new findings shed light on the palaeoenvironmental dynamics of the Ribesalbes–Alcora Basin during the early Miocene.

Abbreviations.—EDX, X-ray energy microanalysis.

Geological setting

The deposits of the Ribesalbes–Alcora Basin are composed of detrital and carbonatic materials deposited in alluvial and lacustrine environments overlying a Mesozoic basement (Anadón et al. 1989) and divided into the Ribesalbes sequence (early to middle Miocene in age) and the Alcora sequence (late Miocene in age). The Ribesalbes sequence includes five depositional units (A to E from the base to the top) defined by Anadón et al. (1989). The Unit A consists of a 300 m interval of breccia of Mesozoic limestone clasts with minor interbedded red sandstone and mudstone. The Unit B is characterised by oil-shales and laminated bituminous dolomicrite of the La Rinconada and San Chils localities, which yield a rich and diverse lacustrine fossil record. The Unit C crops out in the Campisano ravine, where the mammalian fossiliferous sites are located. This unit is composed of sandstone beds ranging in thickness between 15

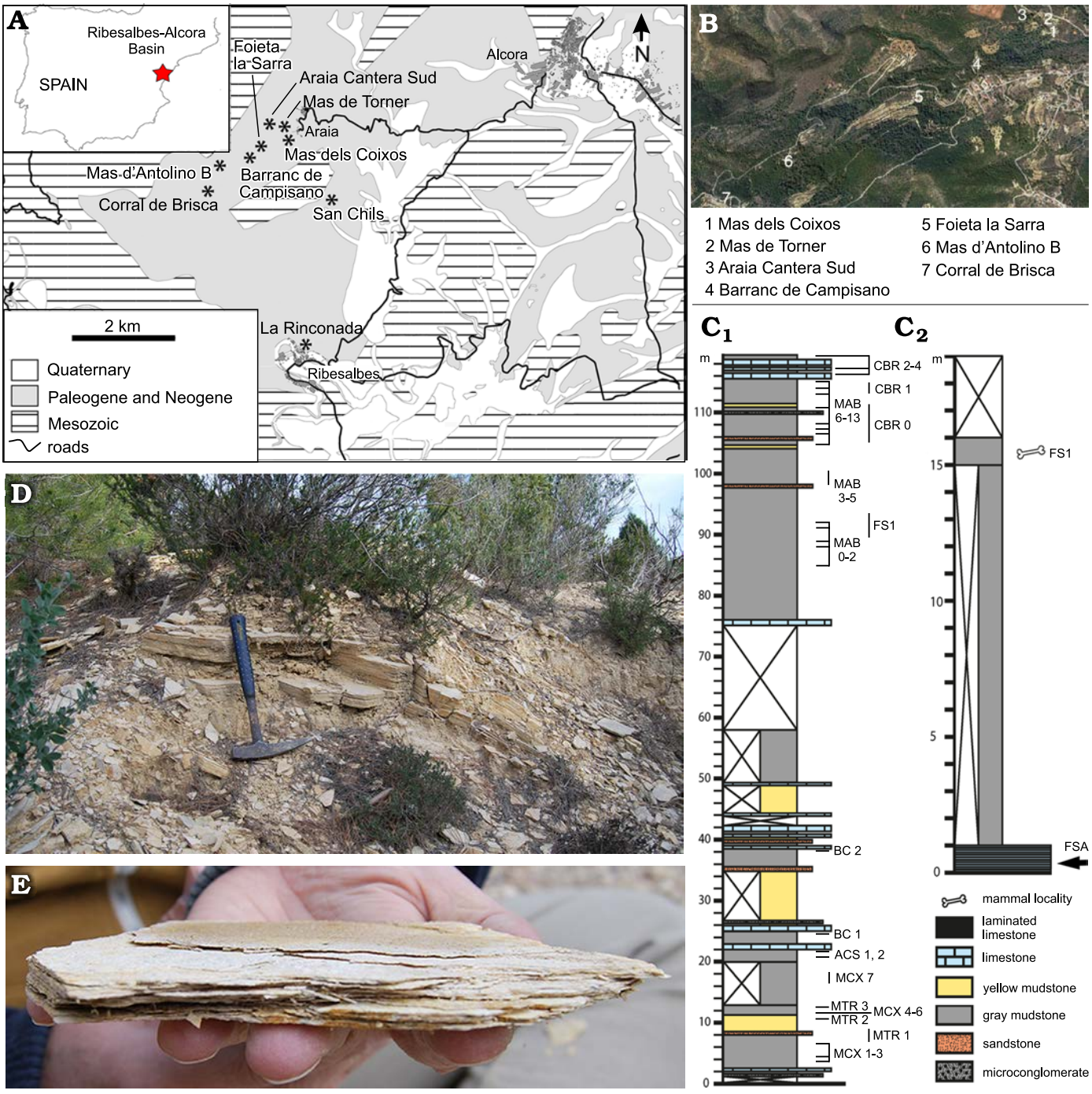

Fig. 1. **A**, **B**. Geographic and geological location of the Ribesalbes–Alcora Basin (Castelló Province, Valencian Community, Spain) with indication of the Campisano ravine (1–7), San Chils, and La Rinconada localities. **C**. Synthetic stratigraphic column of the Campisano ravine (C_1), and Foieta la Sarra section (C_2), showing the location of the Foieta la Sarra-1 (FS1) and the studied Foieta la Sarra-A (FSA) mammalian fossiliferous localities. **D**. Fossiliferous laminated slabs of laminated lacustrine limestone at the lower Miocene Foieta la Sarra-A locality. **E**. Detail of the fine lamination of the Foieta la Sarra-A of the Foieta la Sarra-A laminated limestone rocks. Abbreviations: ACS, Araia Cantera Sud; CBR, Corral de Brisca; BC, Barranc de Campisano; MAB, Mas d'Antolino B; MCX, Mas dels Coixos; MTR, Mas de Torner. A, B modified from Crespo (2017), Crespo et al. (2019c).

cm and 1.5 m, and which show cross and laminated bedding that alternates with thick massive mudstone strata interbedded with a few dolomitic and calcareous layers. These facies were interpreted by Anadón et al. (1989) as distal deltaic and shallow lacustrine environments. The Unit D represents an olistostrome of Cretaceous rocks, reflecting tectonic activity. Lastly, the Unit E is composed of thin bedded limestone strata rich in ostracods and charophytes, with interbedded mudstone horizons. On the other hand, the upper Alcora sequence consists of conglomerate beds related to alluvial deposits up to 200 m thick. This sequence displays a continuous transition without unconformities over the Ribesalbes sequence in the Campisano ravine (Anadón et al. 1989).

A synthetic stratigraphic column (Fig. 1C_1) and a geolo-

gical study of the Campisano ravine was presented by Crespo et al. (2019c). The stratigraphic section is 120 m thick and it is chiefly formed by mudstone and limestone beds, including some sandstone and microconglomerate layers. In the Campisano ravine, the Foieta la Sarra section is correlated to the lower part of the Mas d'Antolino B section (Fig. $1C_2$). The Foieta la Sarra stratigraphic section is 19 m thick and it consists of grey mudstone. A 1 m thick laminated lacustrine limestone bed, which corresponds to the Foieta la Sarra-A locality, can be distinguished at the base of the Foieta la Sarra section. The mammalian fossil site is located at the top of the Foieta la Sarra section, 16 m above the base, within grey sandy mudstone beds.

According to Crespo et al. (2019b), the presence of the genera *Megacricetodon*, *Ligerimys*, and *Democricetodon* in the Foieta la Sarra-1 locality is correlated with the Biozone C of the MN4 (early Aragonian, early Miocene, 16.49–15.94 Ma), based on the comparison with the Aragonian type area in the Calatayud–Montalbán Basin (García-Paredes et al. 2016). The Biozone C of the MN4 is divided in two sub-biozones, i.e., Ca and Cb, with the limit between them at approx. 16.20 Ma after Van der Meulen et al. (2012). The limit between these sub-biozones is present at the Campisano ravine (Crespo et al. 2019c). Specifically, the Foieta la Sarra-1 locality has provided the oldest record of *Eumyarion weinfurteri* and *Ligerimys ellipticus* within the biostratigraphy of the Campisano ravine localities and in the basin (Crespo et al. 2019c). Considering lower and upper stratigraphic levels, Foieta la Sarra-1 is older than the level Mas d'Antolino B-3 due to the high abundance of *Megacricetodon* and the scarcity of *Democricetodon*, which are probably correlated with the sub-biozone Ca from the Calatayud–Montalbán Basin. Foieta la Sarra-1 is younger than the level Mas d'Antolino B-0B because of the presence of both the genus *Eumyarion* and the species *L. ellipticus*, which are probably correlated with the sub-biozone Cb from the Calatayud–Montalbán Basin (Crespo et al. 2019, 2021b). Considering this information and the stratigraphic position of Foieta la Sarra-A locality studied here, its age could be approximately 16.20 Ma (early Miocene), and thus located at the base of the Cb sub-biozone.

Material and methods

The material studied herein includes compressed fossils of plants, molluscs, arthropods, and fish recorded in 45 laminated slabs excavated from the Foieta la Sarra-A locality at the Foieta la Sarra section near Araia d'Alcora (l'Alcora, Castelló Province, Spain; Fig. 1). The fossil specimens from Foieta la Sarra-A are housed at the Museu de la Universitat de València de Historia Natural (MUVHN) in Burjassot (Valencian Community, Spain). The sedimentary rock exposed at Foieta la Sarra-A does not show significant signals of weathering, although several Recent small roots and fungal mycelia were removed from the slabs. The rock slabs were observed with a Leica MS5 stereomicroscope. To enhance visibility of some microfossils, slabs were submerged in ethanol. Specimens were photographed using a Leica DMS1000 stereomicroscope with an attached digital camera, and the drawings were made using a camera lucida attached to the Leica MS5 stereomicroscope. All of these methods took place at the Department of Botany and Geology of the Universitat de València.

The micromorphology of the samples was imaged using a FEI INSPECT (5350 NE Dawson Creek Drive Hillsboro, Oregon 97124, USA) Scanning Electron Microscope (SEM) at the Museo Nacional de Ciencias Naturales (MNCN) in Madrid (Spain). The SEM microscope in low vacuum mode allows hydrated samples to be studied in their original state using the large field detector (LFD), since it is close to the sample in order to avoid electron losses. In addition, the samples were observed with the Backscattering Electron Detector (BSED), which were conductive in high vacuum mode. The SEM resolution at low vacuum was 4.0 nm at 30 kV (BSED); the accelerating voltage was 20 kV, low vacuum 0.50 torr, and 10 mm of working distance. The X-ray energy microanalysis (EDX) of the ephippial microsculpture, chironomid larval galleries and fish remains were conducted with an energy-dispersive X-ray spectrometer (INCA Energy 200 energy dispersive system, Oxford Instruments) at the MNCN (Madrid, Spain).

Anatomic terminology for fish remains follows Lagler (1947), Daniels (1996), Schultze (2015) and Bräger and Moritz (2016).

Foieta la Sarra-A fossil assemblage

The Foieta la Sarra-A locality has yielded a diverse record of plants (including charophytes and embryophytes), molluscs, arthropods (including crustaceans and insects) and vertebrates represented by fish. The botanical and faunal taxa of Foieta la Sarra-A are available in Table 1.

Plants.—Three grey-yellowish limestone intervals containing abundant charophyte remains have been distinguished in the Foieta la Sarra-A (Fig. 2A, B). These intervals are exclusively composed of compressed vegetative (thallus) fragments and poorly preserved gyrogonites (calcified fructifications of Characeae) forming a type of calcareous sedimentary rocks defined as characeite by Soulié-Märsche et al. (2010). The flattened charophyte stems studied herein consist of isostichous corticated thalli. Considering that living charophyte genera have not changed their vegetative structure since the Miocene, these charophyte thalli can be attributed to the genus *Chara* since among the living charophytes only this genus develops corticated stems (Soulié-Märsche et al. 2010). Complete articulated thalli would be required for a species-level attribution. Few poorly preserved gyrogonites occur among charophyte stems (Fig. 2B). The absence of complete gyrogonites and their poor preservation

Table 1. Botanical and faunal record from the lower Miocene Foieta la Sarra-A locality (Ribesalbes–Alcora Basin, Castelló Province, Spain).

Charophyta	
Charophyceae	
Charales	
Characeae	*Chara* sp.
Embryophyta	
Monocotyledoneae	
Poales	Poaceae, Cyperaceae, Sparganiaceae or Juncaceae indet.
Dicotyledoneae	
Incertae sedis	*Dicotylophyllum* sp.
Malpighiales	
Salicaceae	*Salix*? sp.
Mollusca	
Gastropoda	
Littorinimorpha	Hydrobiidae? indet.
Hygrophila	Lymnaeidae indet.
Planorbidae	*Ferrissia* sp.
	Gyraulus sp.
Arthropoda	
Branchiopoda	Ostracoda indet.
Cladocera	
Daphniidae	*Daphnia* (*Ctenodaphnia*) sp.
Insecta	
Coleoptera	Coleoptera indet.
Hemiptera	Pentatomidae? indet.
Diptera	Psychodidae? indet.
Vertebrata	
Actinopterygii	
Teleostei	Teleostei indet.
Cyprinodontiformes	
Cyprinodontidae	cf. *Aphanius* sp.

hinder a detailed taxonomic attribution. Several molds and casts of planorbid gastropods (*Gyraulu*s sp.) also occur associated to these characeite intervals.

Several microlevels of Foieta la Sarra-A show accumulations of burned plant remains or fusinite (Fig. 2C) as described from La Rinconada and San Chils localities (Peñalver et al. 2016; Álvarez-Parra and Peñalver 2019), possibly resulting from wildfires near the palaeolake. Undetermined seeds with slightly bilobate apex have been found, although their preservation is poor. The Foieta la Sarra-A plant record also includes leaves, but their taxonomic affinities are challenging to determine. A large leaf remain and scarce small fragments with straight margins and parallel veins (Fig. 2D) are similar to specimens of *Typha latissima* A. Braun, 1851 in Heer, 1855 (Typhaceae) found in the Miocene Rubielos de Mora locality (Barrón and Diéguez 2001); this type of plant remain is also found in La Rinconada and San Chils localities. However, they are usually poorly preserved and their morphotype could correspond to Poaceae, Cyperaceae, Sparganiaceae or Juncaceae belonging to the order Poales (Peñalver et al. 2016; Álvarez-Parra and Peñalver 2019). Two slender leaves with distal areas partly preserved, 11.6 mm long and 2.9 mm maximum wide and 14.3 mm long and 2.12 mm maximum wide, respectively (Fig. 2E, F), seem to be similar to the morphotypes of *Dicotylophyllum* sp. present in La Rinconada (Barrón and Postigo-Mijarra 2011). Two poorly preserved leaf remains with around 6 mm maximum width have been tentatively determined as *Salix*? sp. (Salicaceae) based on the straight, slightly parallel margins and their similarity to the specimens of *Salix lavateri* A. Braun emend. Hantke, 1851 from La Rinconada (Barrón and Postigo-Mijarra 2011; Fig. 2G, H).

Molluscs.—The gastropod assemblage recorded in the studied samples is poorly preserved. Almost all specimens consist of moulds and impressions, which hinder accurate taxonomic attributions. The assemblage consists of at least four freshwater morphotypes, one of which belongs to the superfamily Truncatelloidea and the rest to the superfamily Lymnaeoidea. The Truncatelloidea superfamily is represented in Foieta la Sarra-A, with 15 recognised specimens in seven of the examined samples, by a single morphotype (Fig. 3A–C). Due to the incompleteness of the specimens and their poor preservation, they may belong to Hydrobiidae or Bithyniidae. However, the general ovate-conical morphology of the specimens, with convex spiral whorls and, above all, their small size, suggest the attribution to the family Hydrobiidae.

Regarding the three morphotypes of the superfamily Lymnaeoidea, 120 specimens belonging to the families Lymnaeidae and Planorbidae have been studied. Lymnaeidae is represented by one morphotype, from which eight specimens have been identified (Fig. 3D–G). Seven correspond to fragments of adult specimens (Fig. 3D, E) and one to a juvenile (Fig. 3F, G). The fragments of the adults are very incomplete but show elongate morphology, a last round of rapid growth, and ornamentation of growth constrictions in the vicinity of the aperture. The juvenile specimen, with dimensions of up to 6.7 mm long and 3.7 mm wide, is compressed and deteriorated. Nevertheless, an elongate-ovate shell with three whorls is visible, its spire being short and conical, with a last whorl enlarging rapidly. The assignment at the genus level is challenging, but the characteristics observed match those of the genera *Stagnicola* and *Radix*. Vilanova y Piera (1859) cited the presence of "Lymnaeas" in several areas of the Castelló Province, including the "Balsa de Fanzara" (the classical name for the Cenozoic sediments of the Ribesalbes–Alcora Basin), although this author did not provide further information. In any case, we prefer to keep the determination of the lymnaeid morphotype at the family level.

Two species of the family Planorbidae have been identified in Foieta la Sarra-A, i.e., *Ferrissia* sp. (Fig. 3H–L), with 41 specimens present in 16 of the studied laminated slabs, and *Gyraulus* sp. (Fig. 3M–R), with 71 specimens in 21 of the slabs. The specimens of *Ferrissia*, the largest with 5.90 mm long and 3.89 mm wide, have a limpet-like morphology with an elliptical basal outline. The anterior shell portion is

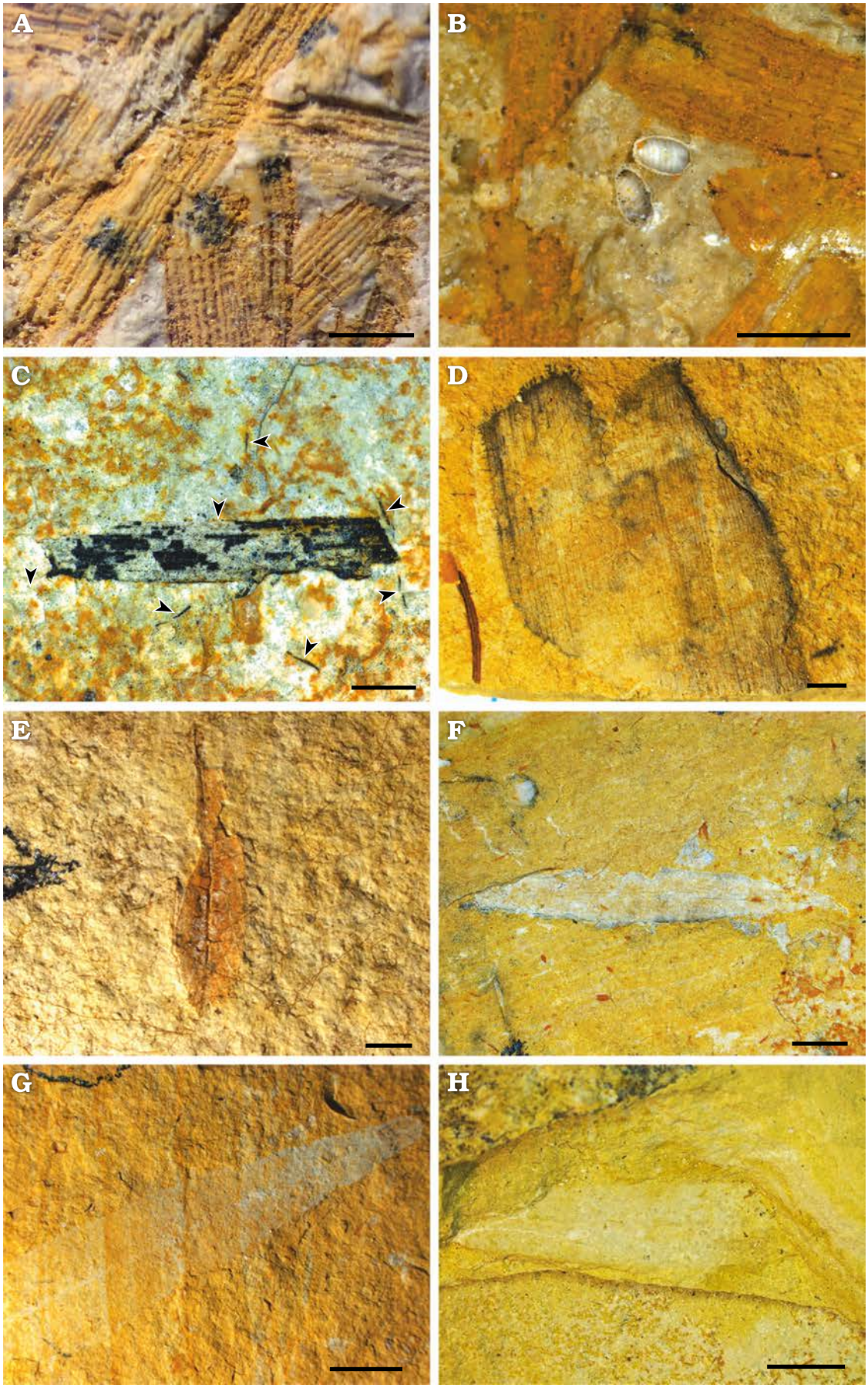
A
B
C
D
E
F
G
H

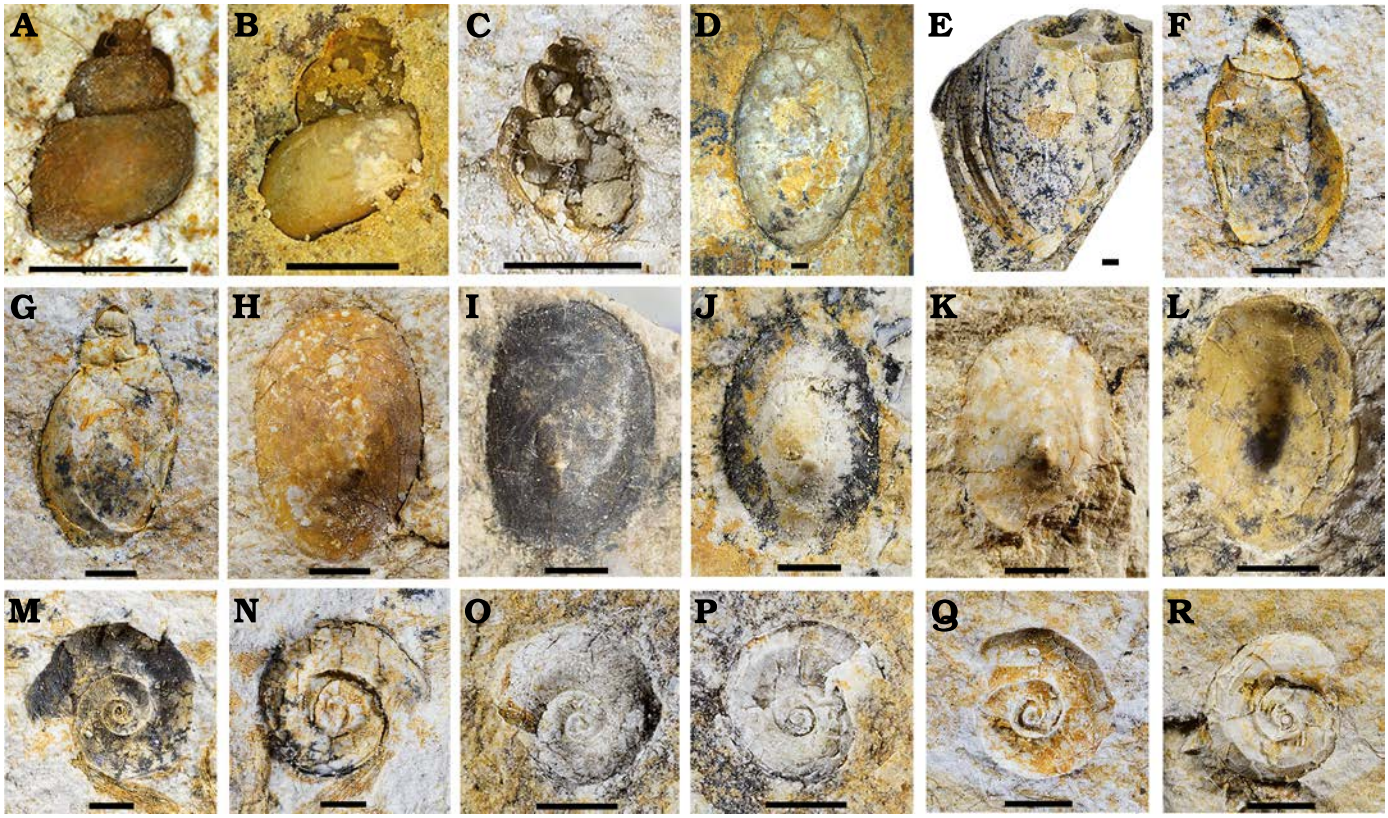

Fig. 3. Molluscs from the lower Miocene Foieta la Sarra-A locality (Ribesalbes–Alcora Basin, Castelló Province, Spain). **A**–**C**. Hydrobiidae? indet. specimens (A, FS-9A-1; B, FS-44C-2; C, FS-15-1). **D**–**G**. Lymnaeidae indet. specimens (D, FS-10-1; E, FS-39-1; F, FS-28B-2; G, FS-28A-2). **H**–**L**. *Ferrissia* sp. specimens (H, FS-16-1; I, FS-16-3; J, FS-13A-1; K, FS-31C-3; L, FS-39-2). **M**–**R**. *Gyraulus* sp. specimens (M, FS-42A-1; N, FS-42B-1; O, FS-35B-1; P, FS-35A-1; Q, FS-7B-1; R, FS-7A-1). Scale bars 1 mm.

slightly broader and convex, the flanks are nearly straight or slightly convex, and the posterior part is convex. The shell apex is slightly deflected to the right, its posterior portion is slightly concave, and its anterior portion is weakly convex in lateral view. The ornamentation is poorly preserved. These specimens of *Ferrissia* from Foieta la Sarra-A locality differ from the middle Miocene *Ferrissia illyrica* (Neumayr, 1880) from the Dinaride Lake System (Neubauer et al. 2011, 2013, 2015c) by its narrower contour. The early–middle Miocene *Ferrissia wittmanni* (Schlickum, 1964) from Southern Germany and Austria (Harzhauser and Kowalke 2002; Kowalke and Reichenbacher 2005; Harzhauser et al. 2014) also has a narrower profile, as well as concave flanks and a cup-shaped apex. Moreover, the late Miocene *Ferrissia truci* Wautier, 1975, from France (Wautier 1975) differs from the Foieta la Sarra-A specimens by its more elongate contour, as well as the elongate apical region with a rounded apex located far back and strongly inclined to the right. The shape of the shell of the studied specimens is particularly similar to that of *Ferrissia deperdita* (Desmarest, 1814), a common species in the middle Miocene of Central Europe. However, the general degree of preservation and particularly the ornamentation prevent us from assigning our specimens to the latter species. On the other hand, *Gyraulus* sp. is the most abundant gastropod species in the studied samples. However, all fossils attributed to this taxon correspond to incomplete moulds and impressions, which hinders the determination to species level. However, the characteristics of this morphotype, whose shell reaches four whorls among the largest specimens, are consistent with those of *Gyraulus* based on the growth pattern (with whorls moderately increasing in diameter), the estimated dimensions among the studied specimens (with a maximum diameter of 5.18 mm), and the ornamentation of growth lines, i.e., prosocline in umbilical view and prosocyrt in apical view.

Arthropods.—Crustaceans and insects represent the hitherto recovered arthropod record from the Foieta la Sarra-A locality. Crustaceans include Ostracoda and Cladocera. Ostracod shells 1–2 mm long, 0.5–1 mm wide without apparent ornamentation have been found (Fig. 4A); they have been recorded both as isolated specimens and as mass records (blooms) in the laminated slabs. The poor preservation

← Fig. 2. Plant remains from the lower Miocene Foieta la Sarra-A locality (Ribesalbes–Alcora Basin, Castelló Province, Spain). **A**, **B**. *Chara* sp. corticated isostichous thalli (FS-3A) and two gyrogonites surrounded by thalli (FS-3B). **C**. Burned plant remains or fusinite of diverse size (arrowheads) (FS-8A-1). **D**. Poorly preserved Poaceae, Cyperaceae, Sparganiaceae or Juncaceae leaf remain (FS-21B-1). **E**, **F**. *Dicotylophyllum* sp. leaf remains (E, FS-22A-1; F, FS-24B-1). **G**, **H**. *Salix*? sp. leaf remains (G, FS-19B-2; H, FS-40-1). Scale bars A–C, 1 mm; D–F, 2 mm; G, H, 4 mm.

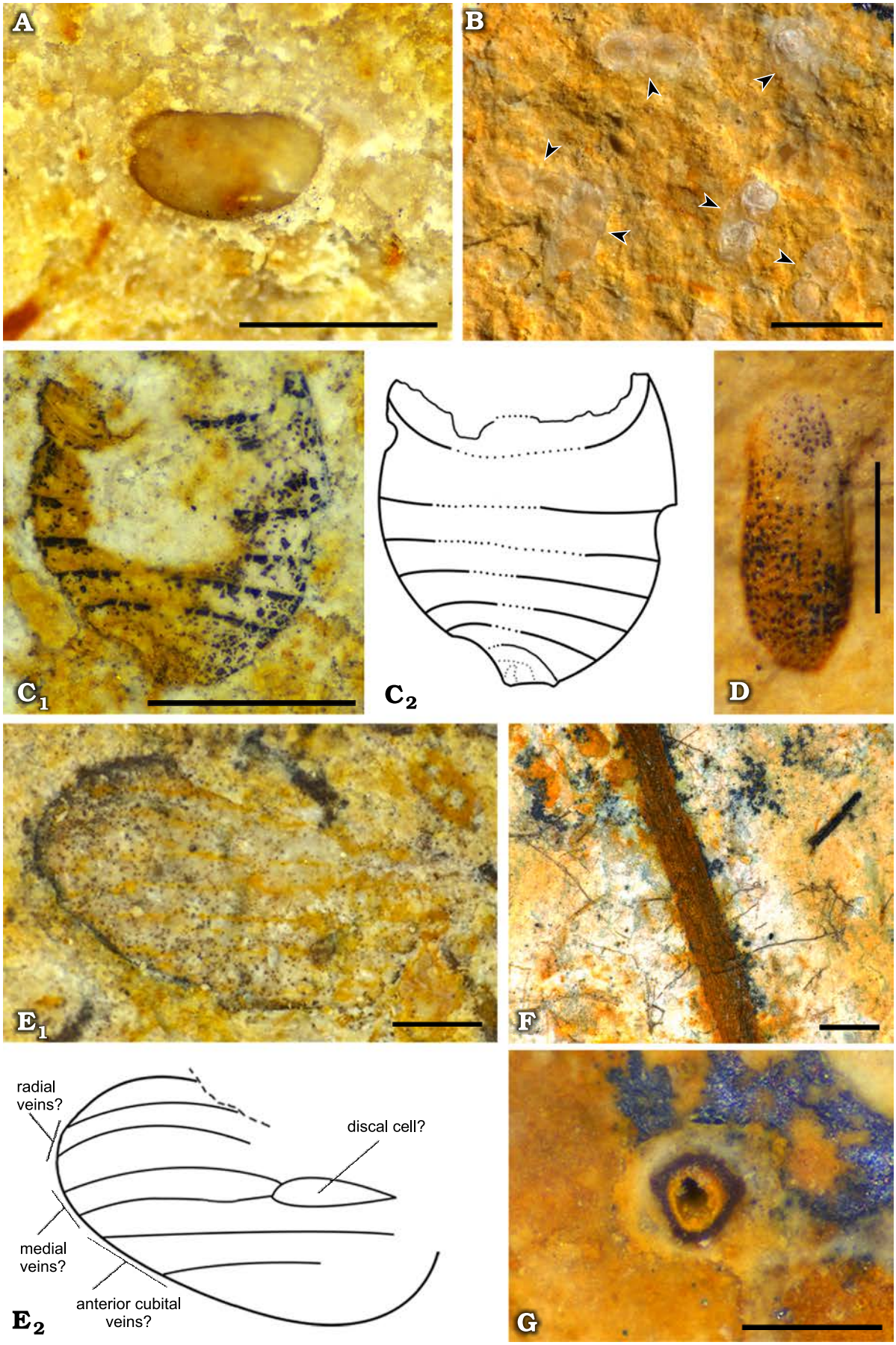
A
B
C1
C2
D
E1
F
radial veins?
discal cell?
medial veins?
anterior cubital veins?
E2
G

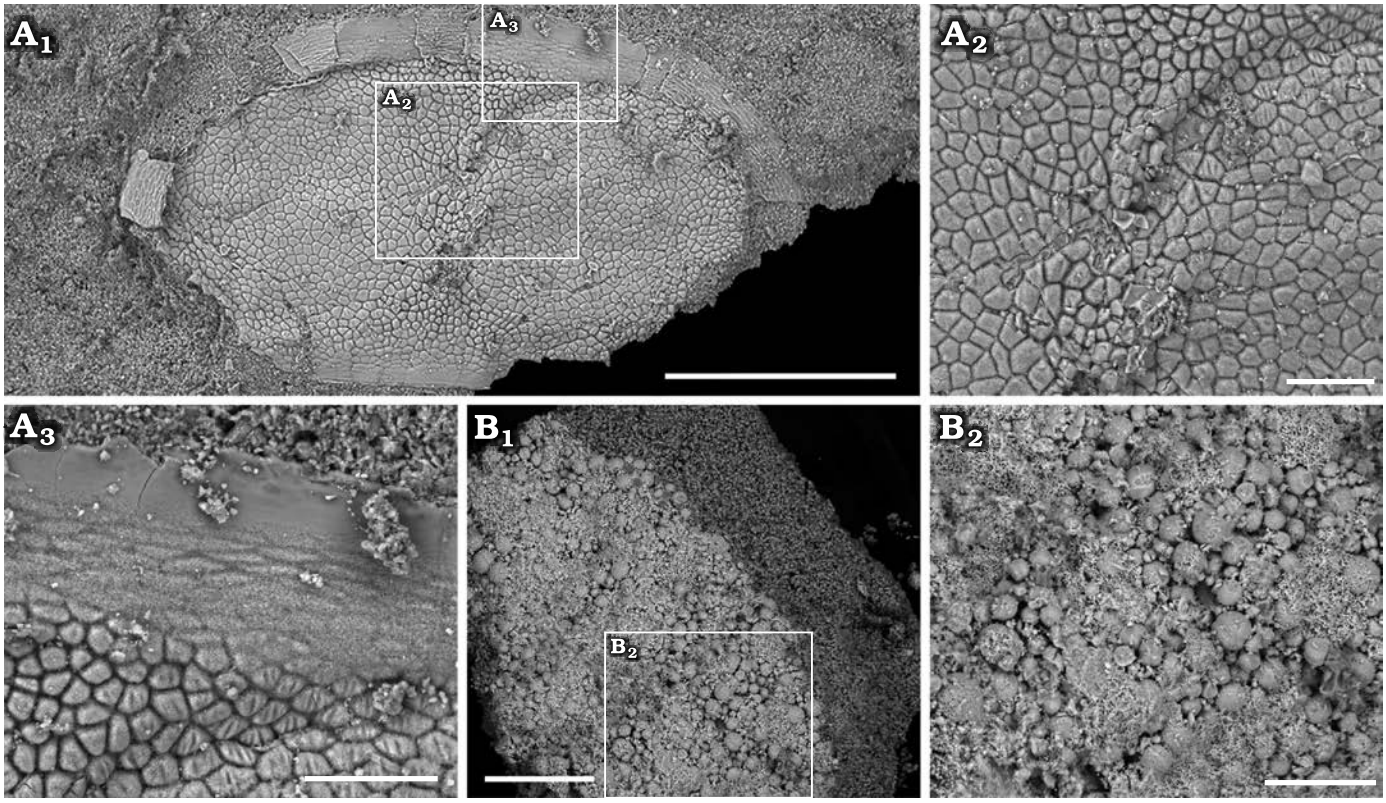

Fig. 5. SEM images of arthropod remains from the lower Miocene Foieta la Sarra-A locality (Ribesalbes–Alcora Basin, Castelló Province, Spain). **A**. Complete *Daphnia* (*Ctenodaphnia*) sp. (Cladocera) ephippium (A_1) showing an exceptionally well-preserved reticulated microsculpture (FS-43B-4); detail showing the limit between the paired egg chambers (A_2), and the dorsal ridge with variation in microsculpture in the top of the image (A_3). **B**. Chironomid larval gallery (B_1) and its filling material (B_2) resulting from oxidation of the original framboidal pyrite (FS-34A-1). Scale bars: A_1, 0.3 mm; A_2, A_3, B_2, 0.05 mm; B_1, 0.1 mm.

of the Foieta la Sarra-A ostracod shells prevents a proper determination. On the other hand, mass records of cladoceran ephippia occur in the Foieta la Sarra-A slabs (Fig. 4B). Specimens are around 0.8–1 mm long and 0.4–0.5 mm wide with an ovoid or sub-rectangular shape. Although the ephippia are poorly preserved, the margins of the valve (originally highly sclerotised) and the paired egg chambers can be distinguished. The dorsal margin lacks spinules. The ephippia show their typical reticular microsculpture (Fig. 5A) with high value of Ca element (Fig. 6A). The ephippial accumulations do not show uniform orientations in the slabs (see Peñalver et al. 1996). The morphotype of the Foieta la Sarra-A ephippia corresponds to the subgenus *Daphnia* (*Ctenodaphnia*) based on the sub-rectangular shape and the axes of the eggs being sub-parallel to the dorsal margin (Kotov and Taylor 2011), as in two specimens recorded from the San Chils locality (Álvarez-Parra and Peñalver 2019). Miocene cladoceran ephippia have been found in several lacustrine deposits from the Iberian Peninsula, such as Rubielos de Mora (Peñalver et al. 1996), Bellver de Cerdanya in Lleida (Martín-Closas and Delclòs 2007), and Tresjuncos in Cuenca (Bustillo et al. 2017).

Regarding insects, specimens belonging to the orders Hemiptera, Coleoptera, and Diptera have been found. First, a partly preserved abdomen divided in at least seven sclerites of 1.32 mm in length and 1.46 mm in maximum width has been found (Fig. 4C); its distal area is deformed, and the genitalia are not visible. Its morphology could correspond to a pentatomid hemipteran (Hemiptera: Pentatomidae). This group is represented in the San Chils locality by a *Sciocoris*? sp. specimen (Álvarez-Parra and Peñalver 2019). Moreover, beetles (Coleoptera) are represented among the Foieta la Sarra-A material by a poorly preserved isolated elytron, 0.91 mm in length with rounded apex and ornamentation constituted by ten or 11 rows of hollows (Fig. 4D). Beetles had been previously reported from the Ribesalbes–Alcora Basin (Peñalver et al. 2016; Álvarez-Parra and Peñalver 2019). Lastly, an isolated wing with a rounded apex, six longitudinal veins and a fusiform (discal?) cell likely belongs to a psychodid fly (Diptera: Psychodidae) (Quate and Vockeroth 1981). In

← Fig. 4. Arthropods from the lower Miocene Foieta la Sarra-A locality (Ribesalbes–Alcora Basin, Castelló Province, Spain). **A**. Undetermined ostracod shell, FS-38A-1. **B**. Mass record of *Daphnia* (*Ctenodaphnia*) sp. (Cladocera) ephippia, FS-21A; each specimen is indicated with an arrowhead. **C**. Photograph (C_1) and drawing (C_2) of a Pentatomidae? (Hemiptera) abdomen, FS-41-1. **D**. Isolated beetle (Coleoptera) elytron, FS-19B-1. **E**. Photograph (E_1) and drawing (E_2) of a Psychodidae? (Diptera) wing, FS-44D-1. **F**, **G**. Chironomid larval galleries in longitudinal (FS-45-1) and transversal (FS-29) views, respectively. Scale bars: A, B, C, E, F, 1 mm; D, G, 0.5 mm.

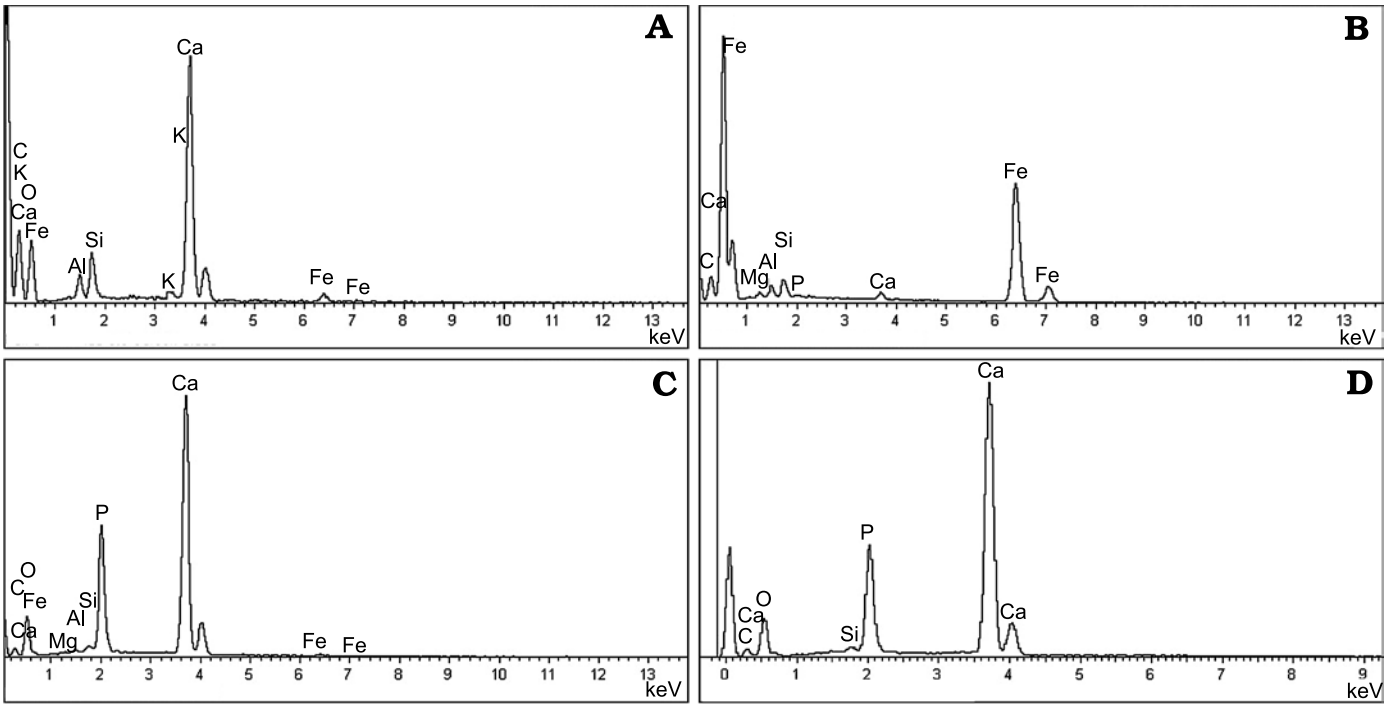

Fig. 6. EDX microanalyses of specimens from the lower Miocene Foieta la Sarra-A locality (Ribesalbes–Alcora Basin, Castelló Province, Spain). **A**. Ephippial microsculpture of *Daphnia* (*Ctenodaphnia*) sp. (FS-43B-4). **B**. Filling material of a chironomid larval gallery (FS-34A-1). **C**. Morphotype 2 fish scale (FS-21C-9). **D**. Isolated fish bone (FS-21).

any case, this determination should remain tentative as the wing margin is not clearly defined and the veins obscured due to preservation (Fig. 4E). This would be the first report of the family Psychodidae in the Ribesalbes–Alcora Basin. In addition, U-shaped and rather straight galleries of around 0.2–1 mm in diameter and different lengths have been found in the slabs from Foieta la Sarra-A (Fig. 4F); their sections are circular (Fig. 4G). This type of ichnofossils of around 1 mm in diameter is commonly related to bioturbation produced by chironomid (Diptera) larvae and are usually found in lacustrine deposits (Walshe 1951). Similar ichnofossils attributed to chironomid larval galleries have been found in other Cenozoic outcrops from the Iberian Peninsula (e.g., Rodríguez-Aranda and Calvo 1998). The galleries show an orange-brown colour resulted of the oxidation process of the original framboidal pyrite (Fig. 5B), as EDX microanalysis indicates (Fig. 6B).

Fishes.—A poorly preserved and incomplete teleostean specimen, abundant clumps of scales and bones, isolated scales, and other scattered remains comprise the fish record from Foieta la Sarra-A. The incomplete teleostean specimen, preserved as a part and a counterpart, preserved its anterior part. It is comprised by a crushed skull, scales of the abdominal region and the dorsal and pectoral fins (Fig. 7A). The skull is crushed and only the dentary bone and some bones of the opercular apparatus are recognisable, although distinctive features of the fish skull are obscured by dissolution and/or enzymatic attack, which hinder both a detailed anatomic description and an accurate taxonomic assignment. As far as it can be described, the dorsal fin appears to be triangular; no scutes, basal or fringing fulcra are observed. The dorsal fin base length is about 30 mm and dorsal pterygiophores are badly preserved. There are ca. 15 dorsal fin rays with long bases, in the preserved part of which segmentation and branching are not evident. It is unclear if only the first dorsal fin ray forms the leading margin of the fin. The distal portion of the fin is obscured by sediment. The vertebral column and its associated elements are not apparent. Although, one badly preserved vertebral centrum is observed near the base of the skull, it is not clear whether it belongs to this specimen or not. The squamation is composed by small, thin sub-squarish elasmoid scales of the cycloid type (morphotype 1, see below). Scales are imbricated, most of them completely preserved. Some isolated scales show their anterior field exposed; the posterior field, which is inserted below the epidermis, appears to be large. No lateral line scales have been recognised, nor ctenoid or spinoid scales are observed in the specimen. Circulii are present as concentric crests surrounding the focus area of the scales; the focus seems to be displaced from the central area. Circulii of the posterior and lateral fields are smooth and seems to be regularly spaced. The so-called first circulii are also smooth. The scales are composed by two layers: the superficial layer and the basal bony plate (Fig. 8B). The basal bony plate is the main part of the scale; its structure or size of collagen fibres is not evident in the available material.

The clumps of scale and bones are well-sorted (Fig. 7B, C). Among the bones, some fin rays and ribs have been identified. The scales in the clumps are represented by at least

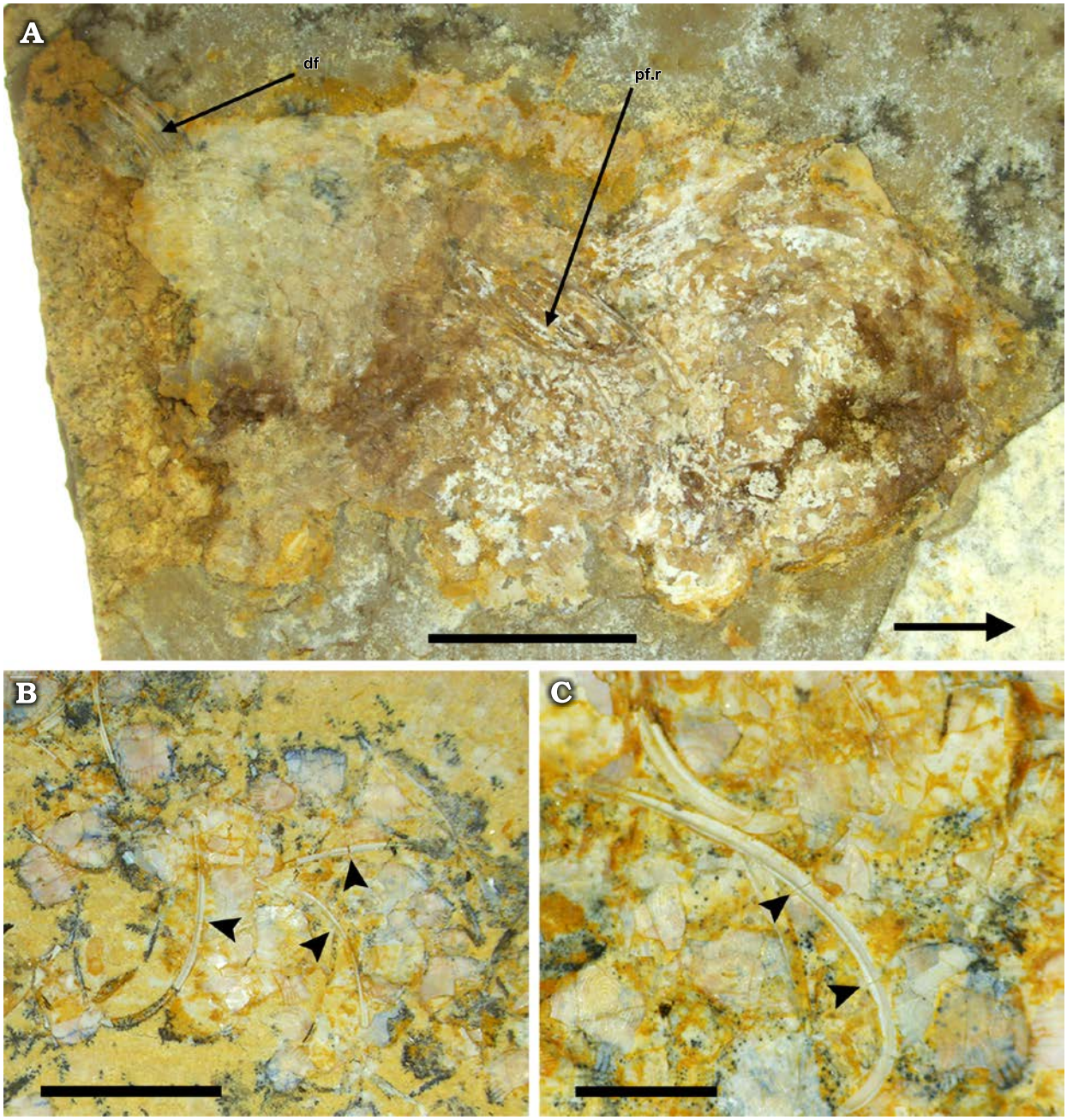

Fig. 7. Fish remains from the lower Miocene Foieta la Sarra-A locality (Ribesalbes–Alcora Basin, Castelló Province, Spain). **A**. Poorly preserved teleostean specimen (FS-23A-1); df: dorsal fin, pf.r: pectoral fin rays; the arrow indicates the anterior region of the specimen. **B**, **C**. Clump of scales and bones (FS-38A-2); arrowheads indicate diagenetic fractures. Scale bars: A, B, 5 mm; C, 2 mm.

the two morphotypes described below. It is unclear if these two morphotypes of scales belong to the same individual. Moreover, it is also unclear if some of these clumps represent bromalites (i.e., coprolites, cololites, and regurgitalites; see Hunt and Lucas 2012). Some fin rays and ribs (i.e., fractures perpendicular to the major axis of the bone; Fig. 7B, C), as well as most of the scales, exhibit diagenetic fractures.

Fish scales from Foieta la Sarra-A are represented by at least two morphotypes that are described below. The morphotype 1 is well-represented in the incomplete specimen covered with articulated scales (see above), as well as in the clumps of scales and bones. EDX analysis of fish scales of morphotype 2 (Fig. 6C) and an isolated bone (Fig. 6D) confirm that the scale and bone are composed namely of Ca, P, and O, indicating the prevalence of apatite.

Morphotype 1: Thin sub squarish elasmoid scales of the cycloid type. These scales measure ca. 1.5 mm long (measured antero-posteriorly) and 1.6 mm wide (measured in the widest portion) (Fig. 8A, B). They have a relatively small focus that is antero-posteriorly elongate. Circulii are well-developed. The anterior field is striated (see Bräger and Moritz 2016: fig. 3B) and bears 13 to 17 radii (= ridges). The so-called first circulii are concave to straight. Lepidonts (= small tooth-like structures anchored to circulii) are not observed.

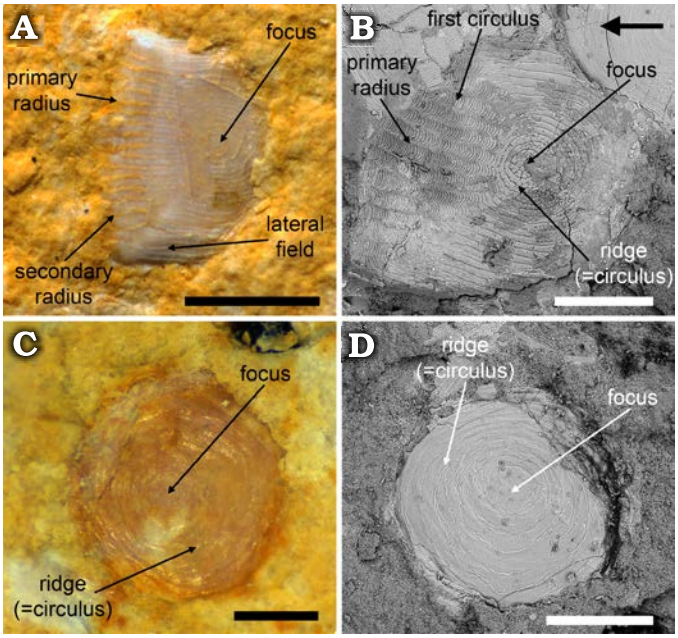

Fig. 8. Fish scale morphotypes from the lower Miocene Foieta la Sarra-A locality (Ribesalbes–Alcora Basin, Castelló Province, Spain). **A**, **B**. General view and SEM image of the morphotype 1 (FS-21B-2 and FS-21A-10, respectively); the arrow indicates de anterior field of the scale. **C**. General view (C_1) and SEM image (C_2) of the morphotype 2 (FS-21C-9). Scale bars: A, 1 mm; B, C, D, 0.5 mm.

The posterior field seems to be convex and smooth. Two generations (principal and secondary) of radius (=ridges) are easily recognised. The posterior field of the scales does not show tubercles, but its absence cannot be fully ascertained due to the preservation of the available material.

This scale morphotype is commonly found in many freshwater fishes (e.g., Cyprinodontiformes and Atheriniformes), and it is most similar to the scales present in some killifish species of the genus *Aphanius* (e.g., Gholami et al. 2013; Teimori et al. 2017).

It is important to highlight that scales might vary in type (ctenoid and cycloid) and morphology (rounded, squarish, etc.) in the same individual relative to the different body sections of an individual. Scales are plastic structures; their general morphology is highly (intra- and interspecifically) variable; also, microstructure seems to show a high degree of intraspecific variation, at least in some cyprinodontiforms such as *Aphanius* (e.g., Gholami et al. 2013) and clupeiforms (e.g., Patterson et al. 2002). Because taxonomy based on isolated scales appears to be problematic (e.g., Bräger et al. 2017), we prefer to leave them unassigned.

Morphotype 2: Elasmoid scale of the cycloid type, thin, rounded or circular in shape, diameter about 1 mm (Fig. 8C, D). The scale has a large focus located in the middle and concentric circulii. Radii and spines or ctenii are lacking. The number of circulii (seven to ten) is almost equal across the entire field. Circulii are almost equally spaced and concentric. This scale resembles those present in the freshwater gadid teleostean *Lota lota* Linnaeus, 1758, which is the only freshwater member of the family Gadidae and is adapted to cold waters (Lagler 1947; Oates et al. 1993; Daniels 1996). Note that some members of Salmoniformes have similar scale morphology (Patterson et al. 2002).

Discussion

Taphonomy.—The laminated limestone beds from Foieta la Sarra-A are interpreted as lacustrine deposits; the recorded taxa correspond to a typical assemblage of a perennial palaeolake, characterised by the presence of lymnaeid and planorbid molluscs, ostracods, and charophytes (Freytet and Verrecchia 2002). The Foieta la Sarra-A record fulfils the requirements to be considered a Konservat-Lagerstätte based on the preservation of soft-bodied specimens, such as the well-preserved reticulated microsculpture of the *Daphnia* (*Ctenodaphnia*) ephippia (Fig. 5A) and insect remains (Fig. 4C–E), which is explained by the presence of microbial mats in the palaeolake (Wilby et al. 1996). The incomplete fish specimen with articulated bones, fins, and scales in original position (Fig. 7A) could have reached the bottom of the lake articulated in conditions of low water energy (see below). The carcass lacks evidence of flotation, as well as of predation and/or scavenging. Aside from this singular specimen, bacterial decay and flotation appear to be evident in the remaining fish carcasses, as most of the specimens are disarticulated and forming clumps (Fig. 7B, C), perhaps due to scavengers since no clear orientation of the elements is apparent. In any case, at least some of the clumps could be bromalites; thus, their preservation resulted from rapid burial after production. The well-developed diagenetic fractures on bones and scales evidence the fossil diagenesis (Fig. 7B, C). There appears to be no directional scatter of *Daphnia* (*Ctenodaphnia*) sp. ephippia, fish scales, and/or lepidotrichia. Thus, the palaeolake was apparently quiet, lacking currents that could have affected the distribution of fish carcasses. Characeite rocks and the slabs with chironomid larval galleries correspond to the in situ record of marginal areas of the lake, while the rest of the specimens were deposited at the lake bottom covered by microbial mats.

The presence of charophytes, mass records of cladoceran ephippia, ostracods, and fish remains in Foieta la Sarra-A indicates that the water chemistry was dissimilar to that of the palaeolake of the Unit B which is apparently lacking these taxa (Peñalver et al. 2016). The laminated slabs from La Rinconada and San Chils resulted from the sedimentation of fine-grained particles on microbial mats at the anoxic bottom from a meromictic lake (Anadón et al. 1989; Peñalver et al. 2016; Álvarez-Parra and Peñalver 2019). The environmental conditions related to the presence of microbial mats in Foieta la Sarra-A could also be different. As noted above, it is unclear if the clumps of fish scales and bones resulted from scavenging or they are bromalites. Therefore, we propose two hypotheses for the presence of microbial mats at the lake bottom: (i) as finding potentially scavenged fish is incompatible with an anoxic lake bottom, the microbial mats were related

to a lake bottom that was at least slightly saline (Bauld 1981; Peñalver and Gaudant 2010); this contradicts the molluscan assemblage found, which indicates freshwater conditions in the palaeolake; (ii) if the fish remains were bromalites, the lake bottom could have been anoxic. The preservation of the Foieta la Sarra-A materials is worse than other Miocene palaeolakes such as Bicorb and La Rinconada (Peñalver and Gaudant 2010; Peñalver et al. 2016), so it is plausible that the microbial mats of Foieta la Sarra-A were thin veils rather than thick mats. A detailed taphonomic study of the Foieta la Sarra-A palaeolake is beyond the aims of this contribution, and future studies will have to address that matter.

Palaeoecological reconstruction of the Foieta la Sarra-A palaeolake and its surroundings.—The botanical and faunal composition of the Foieta la Sarra-A record (Table 1) represents the community that inhabited a lacustrine environment and contiguous areas during the early Miocene.

Charophyte accumulations of *Chara* sp. recorded as characeite are related to the presence of charophyte meadows at the lower marginal areas of the lake, which was well-oxygenated and well-illuminated based on the finding of thalli and gyrogonites (Soulié-Märsche et al. 2010). Charophyte stems are well-preserved and somewhat fragmented, suggesting that the environment was relatively quiet, without the action of strong currents nor waves. The charophyte meadows corresponded to one of the primary producers in the palaeolake.

The assemblage of molluscs is composed of 127 poorly preserved specimens of four freshwater gastropod taxa. The 93.3% are pulmonate species (Lymnaeidae indet., *Ferrissia* sp., and *Gyraulus* sp.) which, as a whole, indicate aquatic environments that are shallow, stagnant or with weak currents and abundant aquatic vegetation (Glöer 2002). *Ferrissia* would also indicate the existence of probable reed-belts on the shore while Lymnaeidae and *Gyraulus* point out the possibility of temporary desiccation (Fetcher and Falkner 1993; Glöer 2002). Many extant individuals studied in Europe, determined as *Ferrissia wautieri* (Mirolli, 1960) but according to Vecchioni et al. (2017) corresponding to the allochthonous species of cosmopolitan distribution *Ferrissia californica* (Rowell, 1863), inhabit stagnant to lentic waters, living among the leaves of aquatic vegetation and underneath the leaves of reeds-belts on the upper littoral zone and showing little sensitivity to water quality (Glöer 2002). Some authors also indicate that the same species is thermophilous and lives in eutrophicated waters (Van der Velde 1991). Extant species of Lymnaeidae preferably inhabit shallow, permanently stagnant or weakly flowing waters, with salinities ranging from freshwater to oligohaline in the case of *Stagnicola* and up to mesohaline in *Radix*; lymnaeids typically live on macrophyte vegetation feeding on epiphytes (Adam 1960; Okland 1990; Glöer 2002). Some lymnaeid species withstand periods of desiccation and inhabit temporary water bodies, even those being located on flood plains (Fetcher and Falkner 1993). Extant species of *Gyraulus* live in a variety of conditions, preferably in shallow waters, including water bodies that are ephemeral, stagnant, or slowly running and abundant in vegetation (Glöer 2002; Welter-Schultes 2012). The fourth taxon (Hydrobiidae? indet.), which represents 6.7% of the specimens studied, suggests permanent waters, at least at the time of deposition. Extant species of Hydrobiidae thrive in permanently flooded freshwater to brackish water environments (Arconada and Ramos 2003).

Lymnaeids feed namely by scraping algae and diatoms from rocks or macrophytes (Pyron and Brown 2015), although they often consume filamentous algae (Kesler et al. 1986). Extant Holarctic species of *Ferrissia* show a preference for periphytic algae, especially diatoms (Burky 1971). Concerning the genus *Gyraulus*, the analysis of stomach content indicates a primarily detritivorous diet (Dudgeon and Yipp 1985), although other studies also show algal consumption (e.g., Hann et al. 2001). The species of Hydrobiidae have a widely diverse diet, including detritus, bacteria, filamentous algae, and diatoms, among others. Studies on the feeding habits of some freshwater hydrobiid species (Radea et al. 2017), as well as species from other related families such as Amnicolidae (Kesler 1981), show a diet suggesting the importance of periphyton diatom grazing. In sum, the combination of the four gastropod taxa found in Foieta la Sarra-A suggest that the palaeolake was shallow, perennial, and quiet (absence of strong currents). Moreover, this molluscan assemblage indicates that the aquatic macrophytes were abundant in the shallow areas of the lake such as the littoral zone, and the shores were also covered with helophytic vegetation. This vegetation was important in maintaining molluscan populations, as constituted the main substrate for the epiphytes on which molluscs fed on, particularly in the case of Lymnaeidae. Moreover, this vegetation would contribute to the formation of detritus which could support the *Gyraulus* sp. populations. These characteristics are compatible with a vegetated shore of the lake whose waters were oligohaline at the most.

Daphnia cladocerans are filter-feeding crustaceans of freshwater habitats (Ebert 2005). The specimens from Foieta la Sarra-A correspond to the subgenus *Daphnia* (*Ctenodaphnia*), which is related to shallow, temporary water bodies (Popova et al. 2016). *Daphnia* (*Ctenodaphnia*) ephippia from Foieta la Sarra-A have been found as mass records in the rock slabs, suggesting environmentally stressful conditions, such as temporary desiccation or lack of food resources, that caused the change in their reproductive cycle from parthenogenetic to ephippial females (Peñalver et al. 1996; Ebert 2005). The finding of these records is interesting, as it appears to contradict the permanent water condition inferred by charophytes, some of the molluscs and fish. Nonetheless, *Daphnia* (*Ctenodaphnia*) individuals could have occupied lake margins that desiccated during dry periods in a lake with a fluctuating extension. Predators of *Daphnia* (*Ctenodaphnia*) could have been other arthropods as well as vertebrates, although their presence did not affect the emergence of massive *Daphnia* populations. Although cladoceran ephippia have not been found in the extensive

fossil record of La Rinconada (Peñalver et al. 2016), and they are represented in San Chils only by two specimens in a slab (Álvarez-Parra and Peñalver 2019), similar ephippial mass occurrences were found in Rubielos de Mora (Peñalver et al. 1996). Moreover, the occurrence of mass records of *Daphnia* (*Ctenodaphnia*) in Foieta la Sarra-A indicates that the water chemistry of this palaeolake was different in comparison to the lacustrine deposits from the Unit B. Furthermore, ephippia from Foieta la Sarra-A do not show a preferential orientation in the slabs, suggesting a low energy environment. Lastly, they are found associated to mass occurrences of ostracods, like the ones from Rubielos de Mora and Bellver de Cerdanya Miocene outcrops (Peñalver et al. 1996).

The absence of dipteran pupal exuviae in Foieta la Sarra-A is noteworthy, as they are abundant in La Rinconada and San Chils, where they indicate stagnant water and lack of predators (Peñalver et al. 2016; Álvarez-Parra and Peñalver 2019). The presence of fish predators matches such absence of dipteran exuviae, although the record of the latter would require a higher grade of exceptional preservation than that observed in Foieta la Sarra-A. Nonetheless, the finding of Chironomidae larval galleries occurring at the lake bottom suggests that populations of this group of flies were present in this lacustrine environment; chironomid larvae are found in ecosystems of different characteristics, although their presence in Foieta la Sarra-A could be related to shallow waters of a lentic environment and were microphagic, i.e., feeding on detritus and small plants or animals (Oliver 1981).

The teleostean fish scale morphotype 1 resembles the scales present in some killifish (Cyprinodontiformes), a large group of secondarily freshwater fishes with a wide geographical distribution. More specifically, the scale morphotype 1 resembles the scales present in species *Aphanius*, including small omnivorous eurythermic and eurhyhaline species that inhabit brackish and salt marshes, coastal lagoons, river mouths and freshwater environments (Gaudant 1993; Nelson et al. 2016). Therefore, *Aphanius* species are highly ecologically flexible fishes that tolerate a wide range of temperature and salinities, and so they may occur in a wide range of habitats (Teimori et al. 2014). Despite their omnivory, the diet of some *Aphanius* species has a high degree of seasonal variation and, in general terms, includes several small invertebrates and their eggs, as well as diatoms (Leonardos 2008). Also, some species of *Aphanius* display some differences in habitat preference related to their age (Alcaraz and García-Berthou 2007).

Although the palaeoichtyofauna can be useful to understand the palaeoenvironment, it is important to highlight that "deducing a type of environment from only a single taxon′s autoecology risks falling into a circular reasoning but this analysis is, however valuable if its incorporates a set of signals that point to the same environment" (Cavin 2017: 4). Moreover, due to the high diversity of fishes' lifestyles and their ability to live in environments with changes in salinity, using them to determine or define types of freshwater environments is challenging.

The palaeovegetation of Foieta la Sarra-A corresponds to a typical riparian assemblage, similar to the La Rinconada and San Chils assemblages related to a lacustrine palaeoenvironment (Barrón and Postigo-Mijarra 2011; Postigo-Mijarra and Barrón 2013; Álvarez-Parra and Peñalver 2019), based on the presence of specimens of Poales, *Dicotylophyllum* sp., and *Salix*? sp. Palaeofires could be recurrent based on the accumulations of fusinite in the Foieta la Sarra-A rock. The scarcity of insects in the fossil record of Foieta la Sarra-A might be explained by the presence of vertebrates such as fishes, which fed on the former when they were washed to the lake. Abundant amphibian, crocodilian (and other reptilian), and mammalian record has been found in the other levels of the Foieta la Sarra section and Campisano ravine localities (Crespo 2017; Crespo et al. 2019c; VDC unpublished data), whereas amphibians and bird (only feathers) remains have appeared in La Rinconada and San Chils (Peñalver et al. 2016; Álvarez-Parra and Peñalver 2019). Therefore, although these vertebrates could have inhabited the riparian environment or that contiguous the palaeolake of Foieta la Sarra-A, there is a gap of such faunal record to date.

Palaeoenvironmental dynamics during the early Miocene in the Ribesalbes–Alcora Basin.—The deposits of the Ribesalbes–Alcora Basin show a dynamic environmental evolution of the water body during the early Miocene. The oil-shale and laminated bituminous dolomicrite of La Rinconada and San Chils localities, belonging to the Unit B, correspond to the record of a meromictic palaeolake (Peñalver et al. 2016). On the contrary, the stratigraphically higher fine grain facies of the Campisano ravine, belonging to the Unit C, represent the distal deposits of an alluvial fan or a muddy floodplain (Crespo et al. 2019c), indicating an environmental change during the early Miocene in the basin. The laminated slabs found in Foieta la Sarra-A hitherto represent the only record of a well-developed palaeolake in the stratigraphy of the Campisano ravine (Crespo et al. 2019c), showing that the palaeoenvironments inferred for the facies of the Unit C are more diverse than previously assumed.

The palaeolake corresponding to the deposits of the Unit B, which outcrops in La Rinconada and San Chils, had a permanent water stratification, with an anoxic lake bottom were microbial mats developed (De las Heras et al. 2003). This water stratification was probably influenced by the inferred subtropical climate that prevailed in the area (Peñalver et al. 2016). Water depth could be several tens of metres in areas away from the shore (De las Heras et al. 2003). The water was basic in character, oligo- or mesosaline and with high sulphate content (De las Heras et al. 2003). The slight salinity could have also contributed to the stratification of the water column (Peñalver et al. 2016).

The Foieta la Sarra-A palaeolake shows taphonomic and palaeoecological similarities to the lacustrine record of the Unit B, such as the fine lamination due to the presence of microbial mats at the lake bottom (which enabled the fossil preservation and is characteristic of Konservat-

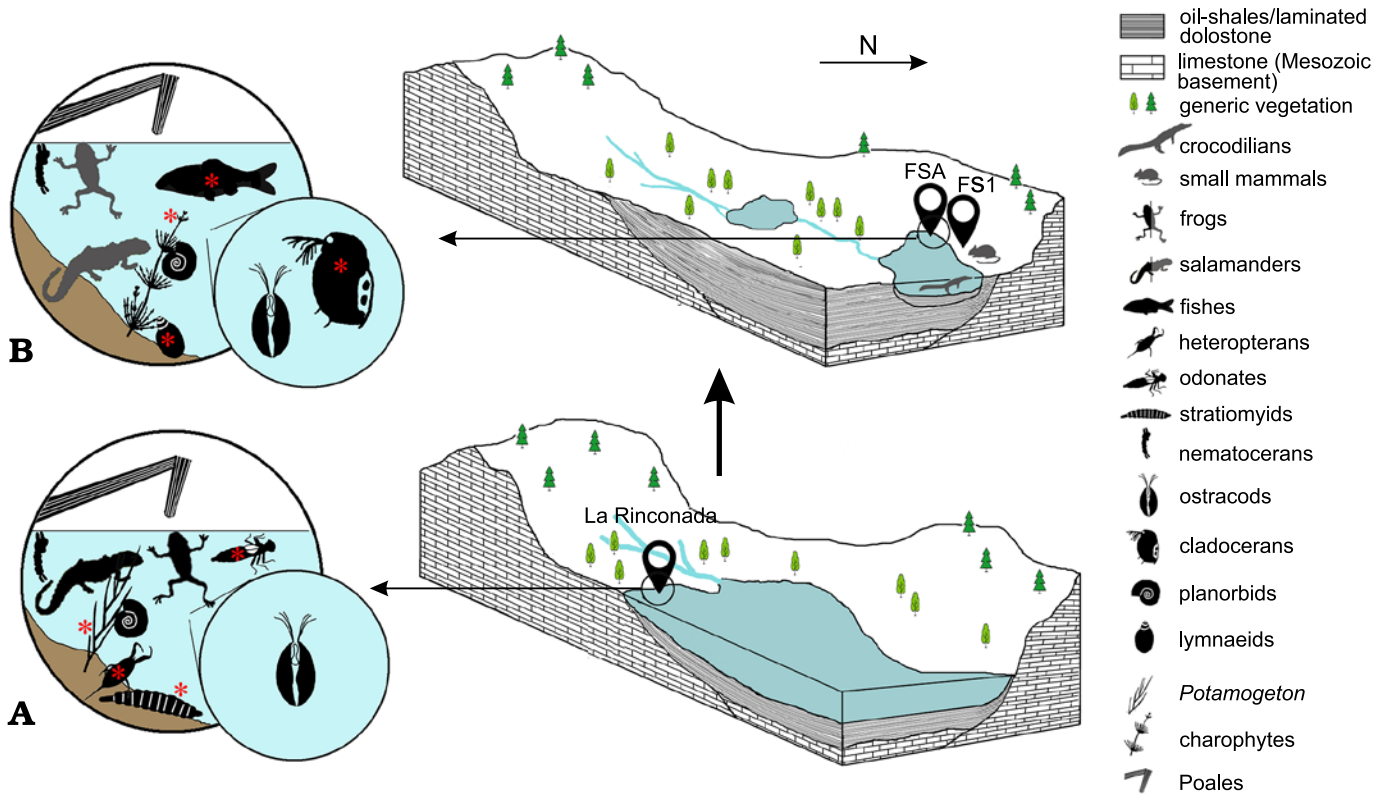

Fig. 9. Synthetic 3D representation of the aquatic environment evolution in the Ribesalbes–Alcora Basin (Castelló Province, Spain) during the early Miocene, mostly based on the La Rinconada (ca. 19 Ma, belonging to the Unit B) and Foieta la Sarra-A (ca. 16.20 Ma, belonging to the Unit C) deposits, which nowadays are separated by around 4 km. Rock deposits have been strongly simplified (e.g., breccia and sandstone are not represented). The significant differences in the aquatic biota are marked with red asterisks. Animals represented in grey correspond to the fossil record of the Foieta la Sarra-1 (FS1) mammalian locality, which are not recorded in the slabs of Foieta la Sarra-A Foieta la Sarra-A (FSA). In La Rinconada (**A**), heteropterans are represented by the families Nepidae and Notonectidae, odonates by the infraorders Zygoptera and Anysoptera, and nematocerans by the families Chironomidae and Chaoboridae. In Foieta la Sarra-A (**B**), planorbids are represented by the genera *Ferrissia* and *Gyraulus*, and nematocerans have been inferred based on chironomid larval galleries in the Foieta la Sarra-A slabs. Silhouettes not to scale.

Lagerstätten) and the finding of plant remains and fossil insects (Peñalver et al. 2016). Interestingly, Foieta la Sarra-A shares with San Chils, but not with the widely studied La Rinconada, the presence of *Daphnia* (*Ctenodaphnia*) sp. ephippia, although only represented by two specimens in San Chils (Álvarez-Parra and Peñalver 2019), in contrast to the mass records from Foieta la Sarra-A. La Rinconada has yielded fossil record of amphibians (Peñalver et al. 2016), which have not been found in Foieta la Sarra-A. Despite that, Foieta la Sarra-A has provided charophytes and lymnaeids, not recorded in the Unit B, and the only fish remains of the Ribesalbes–Alcora Basin to date. Considering the overall data from the palaeolakes of the Unit B and Foieta la Sarra-A, the palaeoenvironment and the palaeoecology were clearly different (Fig. 9). Their palaeoenvironments differ due to a change of the water chemistry. The three main mechanisms controlling the water chemistry of lakes are atmospheric precipitation, rock dominance of the basin and evaporation-crystallisation processes (Gibbs 1970), and these three could explain the environmental dynamics of the palaeolake records of the basin. The rock dominance of the basin corresponds to the basement that crops out in the marginal areas of the basin and is eroded by the lotic waters, which arrive to the lakes formed in the central areas and set the chemistry of their waters (Gibbs 1970). The deposits of the Unit B have been tentatively dated as slightly older than the deposits of the Unit C (Peñalver et al. 2016), but it is unlikely that the rock dominance of the basin could change enough to modify the water chemistry in such a short time. Therefore, the factors that influenced a change of the water chemistry in the palaeolakes of the basin need to be further studied based on sedimentological works and geochemical analyses of the Foieta la Sarra-A rock. An increase of the humidity in the second local biozone of the Campisano ravine was proposed after the preliminary studies of the mammalian palaeoecology and isotopes in the fossiliferous localities (Ríos 2013; Crespo 2017). The faunal assemblage in the second local biozone (after Crespo et al. 2019c) apparently shows more humid preferences than in the first one (Crespo 2017; Crespo et al. 2019c). The Foieta la Sarra-A assemblage and palaeoecology confirm an increase of the humidity in the second local biozone. Indeed, there was a stable water body at least during the beginning of the second biozone, with no lacustrine sediment apparent during the first biozone. A tropical climate has been inferred for the

early Miocene forest of the Campisano ravine surrounding the palaeolake (Crespo et al. 2020b).

The seven sections of the Campisano ravine, corresponding to the Unit C, include facies that represent different palaeoenvironments (Crespo 2017; Crespo et al. 2019c). Most of the deposits are mudstone beds with variegated colours, suggesting that sediments were exposed to subaerial conditions. Sandstone and microconglomerate channels are interpreted as the fluvial contribution to the distal parts of alluvial fans in a low-energy environment. These channels correspond, for instance, to specific high energy episodes related to large floods caused by storms. Thinner tabulate sandstone layers that cover a larger lateral surface, were probably deposited in the floodplains (Crespo 2017; Crespo et al. 2019c). Massive limestone beds were probably deposited in shallow lacustrine and marshy environments subjected to the fluctuation of the water level. Furthermore, several levels of the sections from the Campisano ravine indicate particular environments. These include: (i) dark lenticular beds with black-lignitiferous mudstone probably related to a palustrine environment (in the levels Mas dels Coixos-3 and Mas d'Antolino B-11), (ii) palaeosols associated with longer intervals of subaerial exposure (in the level Mas dels Coixos-4-6), (iii) fine ferruginous and red-coloured levels probably associated to low sedimentation rate episodes and combined with abundant iron supplies (in the level Araia Cantera Sud-2), (iv) evaporitic deposits in the form of gypsum layers formed on the edge of a lake (in the levels Mas d'Antolino B-0A and Mas d'Antolino B-0B), and (v) laminated limestone beds as those from Foieta la Sarra-A (Crespo 2017; Crespo et al. 2019c). Particularly, an increase of the energy in the environment is observed in the Foieta la Sarra section (Fig. 1B), as the laminated limestone beds are at the bottom of the deposit (Foieta la Sarra-A) and sandy mudstone is present at the top (Foieta la Sarra-1). Accordingly, the Campisano ravine deposits reflect the complexity of the palaeoenvironments of a palaeolake and its surroundings. The Foieta la Sarra-A locality in particular shows the environmental evolution of a palaeolake that occurred in the basin in comparison with the record of the Unit B.

Conclusions

Foieta la Sarra-A corresponds to the record of a different palaeolake to that of the Unit B, or a later phase of the same, providing evidence of the palaeoenvironmental dynamics of the Ribesalbes–Alcora Basin during the early Miocene. The Foieta la Sarra-A palaeolake had a different water chemistry in comparison to that of the Unit B. Such factor explains the presence of mass occurrences of ostracods and *Daphnia* (*Ctenodaphnia*) sp. ephippia. The occurrence of characeite beds indicates that the palaeolake depth was not significant (i.e., a few metres). Moreover, the water level underwent periodic fluctuations, favouring the mass production of *Daphnia* (*Ctenodaphnia*) sp. ephippia in the most marginal palaeolake areas under stress conditions. The scarcity of insects could be related to the abundance of fishes as predators, to preservation, and/or to sampling biases.

A new palaeontological work is planned in the near future in order to increase the known fossil assemblage from Foieta la Sarra-A. Furthermore, a sedimentological and geochemical approach would shed further light on the palaeolake environment. The search of new lacustrine limestone levels in the stratigraphy of the Campisano ravine, as well as new palaeontological excavations in La Rinconada and San Chils would provide new data on the complex palaeoecology of the Ribesalbes–Alcora Basin during the early Miocene.

Acknowledgements

We would like to thank Esther Bueno (Universitat de València, Spain), Óscar Caballero (Museo Nacional de Ciencias Naturales-Consejo Superior de Investigaciones Científicas, Madrid, Spain), Mireia Costa-Pérez (Universitat de València, Spain), María Victoria Paredes-Aliaga (Institut Cavanilles de Biodiversitat y Biologia Evolutiva, Burjassot, Spain) and Andreu Vilaplana-Climent (Universitat de València, Spain) for their participation during the prospection work. María Victoria Paredes-Aliaga provided the photographs for Fig. 1C, D. We are grateful to Eduardo Barrón (Instituto Geológico y Minero de España, Madrid, Spain) for his observations about the palaeobotanical record. We thank Thomas A. Neubauer (Justus-Liebig-Universität Gießen, Gießen, Germany) for his observations about the molluscan record, which enabled to refine the reconstructions and improved the original manuscript. SG-C wants to thank Mauricio Bigurrarena Ojeda (Universidad Nacional de La Plata, La Plata, Argentina) for valuable discussions on fish taphonomy. We are indebted to Ricardo Pérez-de la Fuente (Oxford University Museum of Natural History, UK) for the proofreading of the manuscript. SÁ-P thanks the support from the Secretary of Universities and Research of the Government of Catalonia (Spain) and the European Social Fund. PM acknowledges the Spanish Research Project PGC2018-094122-B100 (AEI/ FEDER, UE). VDC is the beneficiary of a postdoctoral fellowship from the Argentinian Consejo Nacional de Investigaciones Científicas y Técnicas (CONICET). We are grateful to the corrections and suggestions from the editors, Nevena Andrić-Tomašević (Universität Tübingen, Germany), and an anonymous reviewer, which have significantly improved the manuscript. This study was presented as an abstract at the 2nd Palaeontological Virtual Congress, to whose organisers we are grateful for their initiative and thank for their invitation to participate in this Special Volume.

References

Adam, W. 1960. *Faune de Belgique. Mollusques. Tome I. Mollusques terrestres et dulcicoles*. 402 pp. Patrimoine de l'Institut royal des Sciences naturelles de Belgique, Brussels.

Agustí, J., Anadón, P., Ginsburg, L., Mein, P., and Moissenet, E. 1988. Araya et Mira: nouveaux gisements de mammifères dans le Miocène Inférieur-Moyen des Chaînes Ibériques orientales et méditerranéennes. Conséquences stratigraphiques et structurales. *Paleontologia i Evolució* 22: 83–101.

Alcaraz, C. and García-Berthou, E. 2007. Food of an endangered cyprinodont (*Aphanius iberus*): ontogenetic diet shift and prey electivity. *Environmental Biology of Fishes* 78: 193–207.

Álvarez-Parra, S. and Peñalver, E. 2019. Palaeoentomological study of the lacustrine oil-shales of the lower Miocene San Chils locality (Ribe-

salbes–Alcora Basin, Castellón province, Spain). *Spanish Journal of Palaeontology* 34: 187–203.

Anadón, P., Cabrera, L., Julià, R., Roca, E., and Rosell, L. 1989. Lacustrine oil-shale basins in Tertiary grabens from NE Spain (Western European rift system). *Palaeogeography, Palaeoclimatology, Palaeoecology* 70: 7–28.

Arconada, B. and Ramos, M.A. 2003. The Ibero-Balearic region: one of the areas of highest Hydrobiidae (Gastropoda, Prosobranchia, Rissooidea) diversity in Europe. *Graellsia* 59: 91–104.

Barrón, E. and Diéguez, C. 2001. Estudio macroflorístico del Mioceno Inferior lacustre de la Cuenca de Rubielos de Mora (Teruel, España). *Boletín Geológico y Minero* 112: 13–56.

Barrón, E. and Postigo-Mijarra, J.M. 2011. Early Miocene fluvial-lacustrine and swamp vegetation of La Rinconada mine (Ribesalbes–Alcora Basin, Eastern Spain). *Review of Palaeobotany and Palynology* 165: 11–26.

Bauld, J. 1981. Occurrence of benthic microbial mats in saline lakes. *Hydrobiologia* 81: 87–111.

Bräger, Z. and Moritz, T. 2016. A scale atlas for common Mediterranean teleost fishes. *Vertebrate Zoology* 66: 275–386.

Bräger, Z., Staszny, Á., Mertzen, M., Moritz, T., and Horváth, G. 2017. Fish scale identification: from individual to species-specific shape variability. *Acta Ichthyologica et Piscatoria* 47: 331–338.

Burky, A. 1971. Biomass turnover, respiration, and interpopulation variation in the stream limpet *Ferrissia rivularis* (Say). *Ecological Monographs* 41: 235–251.

Bustillo, M.Á., Díaz-Molina, M., López-García, M.J., Delclòs, X., Peláez-Campomanes, P., Peñalver, E., Rodríguez-Talavera, R., and Sanchiz, B. 2017. Geology and paleontology of Tresjuncos (Cuenca, Spain), a new diatomaceous deposit with Konservat-Lagerstätte characteristics from the European late Miocene. *Journal of Iberian Geology* 43: 395–411.

Cavin, L. 2017. *Freshwater Fishes: 250 Millon Years of Evolutionary History*. 199 pp. ISTE Press, Elsevier, London.

Cohen, A.S. 2003. *Paleolimnology: The History and Evolution of Lake Systems*. 528 pp. Oxford University Press, New York.

Costa-Pérez, M., Álvarez-Parra, S., Paredes-Aliaga, M.V., Caballero, Ó., Bueno, E., Vilaplana-Climent, A., and Crespo, V.D. 2019. Valoración patrimonial de los yacimientos del Mioceno inferior del Barranco de Campisano de la Cuenca de Ribesalbes–Alcora (Araia d'Alcora, Castelló, España). *Spanish Journal of Palaeontology* 34: 125–130.

Crespo, V.D. 2017. *Los mamíferos del Mioceno Inferior de la Cuenca de Ribesalbes–Alcora (Castelló, España)*. 695 pp. Unpublished Ph.D. Thesis, Universitat de València, Valencia.

Crespo, V.D., Fagoaga, A., Montoya, P., and Ruiz-Sánchez, F.J. 2019a. Oldtimers and newcomers: the shrews and heterosoricids from the Ribesalbes–Alcora Basin (east of Spain). *Palaeontologia Electronica* 22.3.64: 1–22.

Crespo, V.D., Fagoaga, A., Ruiz-Sánchez, F.J., and Montoya, P. 2021a. Diggers, gliders and runners: the squirrels from the Ribesalbes–Alcora Basin (East of Spain). *Bulletin of Geosciences* 96: 83–97.

Crespo V.D., Gamonal, A., Montoya, P., and Ruiz-Sánchez, F.J. 2021b. Eomyids from the Ribesalbes-Alcora Basin (Early Miocene, Iberian Peninsula) and their biostratigraphic and paleoecologic implications. *Rivista Italiana di Paleontologia e Stratigrafia* 127: 497–514.

Crespo, V.D., Goin, F.J., Montoya, P., and Ruiz-Sánchez, F.J. 2020a. Early Miocene marsupialiforms, gymnures, and hedgehogs from Ribesalbes–Alcora Basin (Spain). *Journal of Paleontology* 94: 1213–1227.

Crespo, V.D., Marquina-Blasco, R., Ruiz-Sánchez, F.J., and Montoya, P. 2019b. An unusual insectivore assemblage from the early Miocene of southwestern Europe: the talpids and dimylids from the Ribesalbes–Alcora Basin (Spain). *Comptes Rendus Palevol* 18: 407–416.

Crespo, V.D., Sevilla, P., Montoya, P., and Ruiz-Sánchez, F.J. 2020b. A relict tropical forest bat assemblage from the early Miocene of the Ribesalbes–Alcora Basin (Castelló, Spain). *Earth and Environmental Science Transactions of the Royal Society of Edinburgh* 111 (4): 247–258.

Crespo, V.D., Suárez-Hernando, O., Murelaga, X., Ruiz-Sánchez, F.J., and Montoya, P. 2019c. Early Miocene mammal assemblages from the Campisano ravine in the Ribesalbes–Alcora Basin (E Spain). *Journal of Iberian Geology* 45: 181–194.

Daniels, R. 1996. Guide to the identification of scales of inland fishes of Northeastern North America. *New York State Museum Bulletin* 488: 1–105.

De las Heras, F.X.C., Anadón, P., and Cabrera, L. 2003. Biomarker record variations in lacustrine coals and oil shales: contribution from Tertiary basins in NE Spain. *In*: B.L. Valero-Garcés (ed.), *Limnogeology in Spain: a Tribute to Kerry R. Kelts*, 187–228. Consejo Superior de Investigaciones Científicas, Madrid.

Dudgeon, D. and Yipp, M. 1985. The diets of Hong Kong freshwater gastropods. *In*: B. Morton and D. Dudgeon (eds.), *Proceedings of Second International Workshop on the Malacofauna of Hong Kong and Southern China*, 491–509. Hong Kong University Press, Hong Kong.

Ebert, D. 2005. *Ecology, Epidemiology and Evolution of Parasitism in* Daphnia. 98 pp. National Center for Biotechnology Information, Bethesda.

Fetcher, R. and Falkner, G. 1993. *Moluscos*. 287 pp. Blume, Barcelona.

Freytet, P. and Verrecchia, E.P. 2002. Lacustrine and palustrine carbonate petrography: an overview. *Journal of Paleolimnology* 27: 221–237.

Furió, M., Ruiz-Sánchez, F.J., Crespo, V.D., Freudenthal, M., and Montoya, P. 2012. The southernmost Miocene occurrence of the last European herpetotheriid *Amphiperatherium frequens* (Metatheria, Mammalia). *Comptes Rendus Palevol* 11: 371–377.

García-Paredes, I., Álvarez-Sierra, M.Á., Van den Hoek Ostende, L.W., Hernández-Ballarín, V., Hordijk, K., López-Guerrero, P., Oliver, A., and Peláez-Campomanes, P. 2016. The Aragonian and Vallesian high-resolution micromammal succession from the Calatayud-Montalbán Basin (Aragón, Spain). *Comptes Rendus Palevol* 15: 781–789.

Gaudant, J. 1993. Un exemple de "régression évolutive" chez des poisons cyprinodontidae du miocène supérieur d'Espagne: *Apanius illunensis* nov. sp. *Geobios* 26: 449–454.

Gholami, Z., Teimori, A., Esmaili, H.R., Schultz-Mirbach, T., and Reichenbacher, B. 2013. Scale surface microstructure and scale size in the tooth-carp genus *Aphanius* (Teleostei: Cyprinodontiformes) from endorheic basins in Southwest Iran. *Zootaxa* 3619: 467–490.

Gibbs, R.J. 1970. Mechanisms controlling world water chemistry. *Science* 170: 1088–1090.

Glöer, P. 2002. *Die Tierwelt Deutschlands, 73. Teil: Die Süßwassergastropoden Nord- und Mitteleuropas. Bestimmungsschlüssel, Lebensweise, Verbreitung*. 327 pp. ConchBooks, Hackenheim.

Hann, B.J., Mundy, C.J., and Goldsborough, L.G. 2001. Snail-periphyton interactions in a prairie lacustrine wetland. *Hydrobiologia* 457: 167–175.

Harzhauser, M. and Kowalke, T. 2002. Sarmatian (late middle Miocene) gastropod assemblages of the Central Paratethys. *Facies* 46: 57–82.

Harzhauser, M., Neubauer, T.A., Gross, M., and Binder, H. 2014. The early middle Miocene mollusc fauna of Lake Rein (Eastern Alps, Austria). *Palaeontographica, Abteilung A: Palaeozoology—Stratigraphy* 302 (1–6): 1–71.

Hunt, A.P. and Lucas, S.G. 2012. Classification of vertebrate coprolites and related trace fossils. *New Mexico Museum of Natural History and Science* 57: 137–146.

Kesler, D.H. 1981. Periphyton grazing by *Amnicola limosa*: an enclosure-exclosure experiment. *Journal of Freshwater Ecology* 1: 51–59.

Kesler, D.H., Jokinen, E.H., and Munns, W.R. 1986. Trophic preferences and feeding morphology of two pulmonate snail species from a small New England pond, U.S.A. *Canadian Journal of Zoology* 64: 2570–2575.

Kotov, A.A. and Taylor, D.J. 2011. Mesozoic fossils (>145 Mya) suggest the antiquity of the subgenera of *Daphnia* and their coevolution with chaoborid predators. *BMC Evolutionary Biology* 11: 129.

Kowalke, T. and Reichenbacher, B. 2005. Early Miocene (Ottnangian) Mollusca of the Western Paratethys—ontogenetic strategies and palaeoenvironments. *Geobios* 38: 609–635.

Lagler, K.F. 1947. Lepidological Studies 1. Scale Characters of the Families of Great Lakes Fishes. *Transactions of the American Microscopical Society* 66: 149–171.

Leonardos, I. 2008. The feeding ecology of *Aphanius fasciatus* (Valenciennes, 1821) in the lagoonal system of Messolongi (western Greece). *Scientia Marina* 72: 393–401.

Mandic, O., Hajek-Tadesse, V., Bakrač, K., Reichenbacher, B., Grizelj, A., and Miknić, M. 2019. Multiproxy reconstruction of the middle Miocene Požega palaeolake in the Southern Pannonian Basin (NE Croatia) prior to the Badenian transgression of the Central Paratethys Sea. *Palaeogeography, Palaeoclimatology, Palaeoecology* 516: 203–219.

Martín-Closas, C. and Delclòs, X. 2007. The Miocene paleolake of La Cerdanya (Eastern Pyrenees). *Geo-Guías* 3: 181–205.

McNamara, M.E., Orr, P J., Alcalá, L., Anadón, P., and Peñalver, E. 2012. What controls the taphonomy of exceptionally preserved taxa—environment or biology? A case study using frogs from the Miocene Libros Konservat-Lagerstätte (Teruel, Spain). *Palaios* 27: 63–77.

Nelson, J.S., Grande, T., and Wilson, M.V.H. 2016. *Fishes of the World*. Fifth edition. 707 pp. Wiley, New Jersey.

Neubauer, T.A., Mandic, O., and Harzhauser, M. 2011. Middle Miocene freshwater mollusks from Lake Sinj (Dinaride Lake System, SE Croatia; Langhian). *Archiv für Molluskenkunde: International Journal of Malacology* 140: 201–237.

Neubauer, T.A., Mandic, O., and Harzhauser, M. 2013. The Middle Miocene freshwater mollusk fauna of Lake Gacko (SE Bosnia and Herzegovina): taxonomic revision and paleoenvironmental analysis. *Fossil Record* 16: 77–96.

Neubauer, T.A., Harzhauser, M., Georgopoulou, E., Kroh, A., and Mandic, O. 2015a. Tectonics, climate, and the rise and demise of continental aquatic species richness hotspots. *Proceedings of the National Academy of Sciences* 112: 11478–11483.

Neubauer, T.A., Harzhauser, M., Kroh, A., Georgopoulou, E., and Mandic, O. 2015b. A gastropod-based biogeographic scheme for the European Neogene freshwater systems. *Earth-Science Reviews* 143: 98–116.

Neubauer, T.A., Mandic, O., and Harzhauser, M. 2015c. The freshwater mollusk fauna of the middle Miocene Lake Drniš (Dinaride Lake System, Croatia): a taxonomic and systematic revision. *Austrian Journal of Earth Sciences* 108: 15–67.

Oates, D.W., Krings, L.M., and Ditz, K.L. 1993. *Field Manual for the Identification of Selected North American Freshwater Fish by Fillets and Scales*. 181 pp. University of Nebraska, Lincoln.

Okland, J. 1990. *Lakes and Snails. Environment and Gastropoda in 1500 Norwegian Lakes*. 515 pp. Universal Book Service/Dr. W. Backbuys, Oegstgeest.

Oliver, D.R. 1981. Chironomidae. *In*: J.F. McAlpine, B.V. Peterson, G.E. Shewell, H.J. Teskey, J.R. Vockeroth, and D.M. Wood (eds.), *Manual of Nearctic Diptera, Vol. 1, 27 (29)*, 423–458. Research Branch Agriculture Canada, Ottawa.

Patterson, R.T., Wright, C., Chang, A.S., Taylor, L.A., Lyons, P.D., Dallimore, A., and Kumar, A. 2002. Atlas of common squamatological (fish scale) material in coastal British Columbia and an assessment of the utility of various scale types in paleofisheries reconstruction. *Palaeontologia Electronica* 4: 1–88.

Peñalver, E. 2002. *Los insectos dípteros del Mioceno del Este de la Península Ibérica; Rubielos de Mora, Ribesalbes y Bicorp. Tafonomía y sistemática*. 548 pp. PhD Thesis. Universitat de València, Valencia.

Peñalver, E. and Gaudant, J. 2010. Limnic food web and salinity of the upper Miocene Bicorb palaeolake (eastern Spain). *Palaeogeography, Palaeoclimatology, Palaeoecology* 297: 683–696.

Peñalver, E., Barrón, E., Postigo Mijarra, J.M., García Vives, J.A., and Saura Vilar, M. 2016. *El paleolago de Ribesalbes. Un ecosistema de hace 19 millones de años*. 201 pp. Servicio de Publicaciones, Diputació de Castelló and Instituto Geológico y Minero de España, Ministerio de Economía y Competitividad, Castellón de la Plana.

Peñalver, E., Martínez-Delclòs, X., and De Renzi, M. 1996. Registro de pulgas de agua [Cladocera: Daphniidae: *Daphnia* (*Ctenodaphnia*)] en el Mioceno de Rubielos de Mora (Teruel, España). *Comunicaciones de la II Reunión de Tafonomía y Fosilización* 1: 311–317.

Popova, E.V., Petrusek, A., Kořínek, V., Mergeay, J., Bekker, E.I., Karabanov, D.P., Galimov, Y.R., Neretina, T.V., Taylor, D.J., and Kotov, A.A. 2016. Revision of the Old World *Daphnia* (*Ctenodaphnia*) *similis* group (Cladocera: Daphniidae). *Zootaxa* 4161: 1–40.

Postigo-Mijarra, J.M. and Barrón, E. 2013. Zonal plant communities of the Ribesalbes–Alcora Basin (La Rinconada mine, eastern Spain) during the early Miocene. *Botanical Journal of the Linnean Society* 173: 153–174.

Pyron, M. and Brown, K.M. 2015. Introduction to Mollusca and the Class Gastropoda. *In*: J.H. Thorp and D.C. Rogers (eds.), *Thorp and Covich's Freshwater Invertebrates, Ecology and General Biology*, *Fourth Edition, 18*, 383–421. Academic Press, London.

Quate, L.W. and Vockeroth, J.R. 1981. Psychodidae. *In*: J.F. McAlpine, B.V. Peterson, G.E. Shewell, H.J. Teskey, J.R. Vockeroth, and D.M. Wood (eds.), *Manual of Nearctic Diptera*, *Vol. 1, 27 (17)*, 293–300. Research Branch Agriculture Canada, Ottawa.

Radea, C., Louvrou, I., Konstantinos Bakolitsas, K., and Economou-Amilli, A. 2017. Local endemic and threatened freshwater hydrobiids of Western Greece: elucidation of anatomy and new records. *Folia Malacologica* 25: 3–13.

Ríos, M. 2013. *Estudio multi-isotópico de la paleoecología y la paleoclimatología de la Cuenca de Ribesalbes–Alcora (Castellón, España) durante el Óptimo Climático del Mioceno*. 76 pp. Unpublished MSc Thesis, Universitat de València, Valencia.

Rodríguez-Aranda, J.P. and Calvo, J.P. 1998. Trace fossils and rhizoliths as a tool for sedimentological and palaeoenvironmental analysis of ancient continental evaporite successions. *Palaeogeography, Palaeoclimatology, Palaeoecology* 140: 383–399.

Schultze, H.-P. 2015. Scales, enamel, cosmine, ganoine, and early osteichthyans. *Comptes Rendus Palevol* 15: 83–102.

Soulié-Märsche, I., Bieda, S., Lafond, R., Maley, J., Baitoudji, M., Vincent, P.M., and Faure, H. 2010. Charophytes as bio-indicators for lake level high stand at "Trou au Natron", Tibesti, Chad, during the Late Pleistocene. *Global Planetary Change* 72: 334–340.

Talbot, M.R. and Allen, P.A. 1996. Lakes. *In*: H.G. Reading (ed.), *Sedimentary Environments: Processes, Facies and Stratigraphy*, 5–36. Blackwell Publishing, Oxford.

Teimori, A., Esmaeli, H.R., Erpenbeck, D., and Reichenbacher, B. 2014. A new and unique species of the genus *Aphanius* Nardo, 1827 (Teleostei: Cyprinodontidae) from Southern Iran: a case of regressive evolution. *Zoologischer Anzeiger* 253: 327–337.

Teimori, A., Motamedi, M., and Manizadeh, N. 2017. Microstructural characterization of the body key scale morphology in six Iranian endemic *Aphanius* species (Cyprinodontidae): their taxonomic and evolutionary significance. *Journal of Ichthyology* 57: 533–546.

Van der Meulen, A.J., Paredes, I.G., Sierra, M.Á., van den Hoek Ostende, L.W., and Hordijk, K. 2012. Updated Aragonian biostratigraphy: small mammal distribution and its implications for the Miocene European Chronology. *Geologica Acta* 10: 159–179.

Van der Velde, G. 1991. Population dynamics and population structure of *Ferrissia wautieri* (Mirolli, 1960) (Gastropoda, Ancylidae) in a pond near Nijmegen (The Netherlands). *Hydrobiological Bulletin* 24: 141–144.

Vasilyan, D. 2020. Fish, amphibian and reptilian assemblage from the middle Miocene locality Gračanica—Bugojno palaeolake, Bosnia and Herzegovina. *Palaeobiodiversity and Palaeoenvironments* 100: 437–455.

Vecchioni, L., Marrone, F., Aculeo, M., and Arizza, V. 2017. Are there autochthonous *Ferrissia* (Mollusca: Planorbidae) in the Palaearctic? Molecular evidence of a widespread North American invasion of the Old World. *The European Zoological Journal* 84: 411–419.

Vilanova y Piera, J. 1859. Memoria geognóstico-agrícola sobre la provincia de Castellón. *Memorias de la Real Academia de Ciencias de Madrid* 4: 577–803.

Walshe, B.M. 1951. The feeding habits of certain chironomid larvae (subfamily Tendipedinae). *Proceedings of the Zoological Society of London* 121: 63–79.

Wautier, J. 1975. Présence d'Espèces du genre *Ferrissia* Walker, 1903 (Gastropoda, Basommatophora) dans le Néogène du bassin rhodanien (France). *Geobios* 8: 423–433.

Welter-Schultes, F. 2012. *European Non-marine Molluscs, A Guide For Species Identification*. 760 pp. Planet Poster Editions, Göttingen.

Wilby, P.R., Briggs, D.E., Bernier, P., and Gaillard, C. 1996. Role of microbial mats in the fossilization of soft tissues. *Geology* 24: 787–790.

First phylogenetic analysis of the Miocene armadillo *Vetelia* reveals novel affinities with Tolypeutinae

DANIEL BARASOAIN, LAUREANO R. GONZÁLEZ RUIZ, RODRIGO L. TOMASSINI, AFREDO E. ZURITA, VÍCTOR H. CONTRERAS, and CLAUDIA I. MONTALVO

Barasoain, D., González Ruiz, L.R., Tomassini, R.L., Zurita, A.E., Contreras, V.H., and Montalvo, C.I. 2021. First phylogenetic analysis of the Miocene armadillo *Vetelia* reveals novel affinities with Tolypeutinae. *Acta Palaeontologica Polonica* 66 (Supplement to 3): S31–S46.

Vetelia is a Miocene genus of armadillos from Argentina and Chile, traditionally included within the subfamily Euphractinae (Chlamyphoridae, Cingulata, Xenarthra). It includes the species *Vetelia puncta* (early–middle Miocene), *Vetelia perforata* (middle–late Miocene), and *Vetelia gandhii* (late Miocene), mostly known by isolated osteoderms. In this contribution, we provide the first description of the skull for this genus, based on new materials (PVSJ-289 and PVSJ-154) here assigned to *V. gandhii*. A detailed characterization allows us to amend the diagnosis of the three known species, and to include, for the first time, the genus *Vetelia* into a morphological phylogenetic analysis. Phylogenetic results reveal a closer affinity to the Tolypeutinae, including the extant genera *Priodontes* (giant armadillos), *Cabassous* (naked-tailed armadillos), and *Tolypeutes* (three banded armadillos), and the fossil genera *Pedrolypeutes* and *Kuntinaru*, than to the Euphractinae. More specifically, *Vetelia* is included within the Priodontini, as sister group of the clade composed by *Cabassous* + *Priodontes*. Taking into account the scarce record of fossil Tolypeutinae, this new proposal fills an important temporal gap in the evolutionary history of this linage. Finally, we also provide new information on the diagnostic morphological characters of the Priodontini and Tolypeutini.

Key words: Mammalia, Euphractinae, Tolypeutinae, phylogeny, Neogene, South America.

Daniel Barasoain [danielbarasoain@gmail.com] and Afredo E. Zurita [aezurita74@yahoo.com.ar], Laboratorio de Evolución de Vertebrados y Ambientes Cenozoicos, Centro de Ecología Aplicada del Litoral (UNNE-CONICET) y Cátedra de Paleontología, Facultad de Ciencias Exactas, Naturales y Agrimensura, Universidad Nacional del Nordeste, RP5 3400 Corrientes, Argentina.
Laureano R. González Ruiz [gonzalezlaureano@yahoo.com.ar], Laboratorio de Investigaciones en Evolución y Biodiversidad (LIEB-FCNyCS sede Esquel, UNPSJB) y Centro de Investigaciones Esquel de Montaña y Estepa Patagónica (CIEMEP), CONICET, Universidad Nacional de La Patagonia San Juan Bosco (UNPSJB), Roca 780, 9200 Esquel, Chubut, Argentina.
Rodrigo L. Tomassini [rodrigo.tomassini@yahoo.com.ar], INGEOSUR, Departamento de Geología, Universidad Nacional del Sur-CONICET, Avenida Alem 1253, 8000 Bahía Blanca, Argentina.
Víctor H. Contreras [vcontre@unsj-cuim.edu.ar], Instituto de Geología Dr. Emiliano P. Aparicio, departamentos Geología y Biología, Facultad de Ciencias Exactas, Físicas y Naturales, Universidad Nacional de San Juan, Avenida Ignacio de La Rosa y calle Meglioli, Rivadavia, 5400, San Juan, Argentina.
Claudia I. Montalvo [cmontalvolp@yahoo.com.ar], Facultad de Ciencias Exactas y Naturales, Universidad Nacional de La Pampa, Avenida Uruguay 151, 6300 Santa Rosa, Argentina.

Received 28 September 2020, accepted 4 December 2020, available online 2 June 2021.

Introduction

Xenarthra (early Eocene–Recent) constitutes one of the main clades, and possibly the most basal, among placental mammals (Gelfo et al. 2009; O'Leary et al. 2013). This peculiar group is the result of a long process of endemic evolution during the isolation of South America, which lasted for most of the Cenozoic (Cione et al. 2015). There is general consensus that the origin of Xenarthra is an event posterior to the separation of South America and Africa (see Vizcaíno and Bargo 2014), while molecular evidence suggests that the clade could have arisen ca. 100 Ma (Delsuc et al. 2004).

Xenarthrans encompass both fossil and extant representatives of two different ecologic and morphological mono-

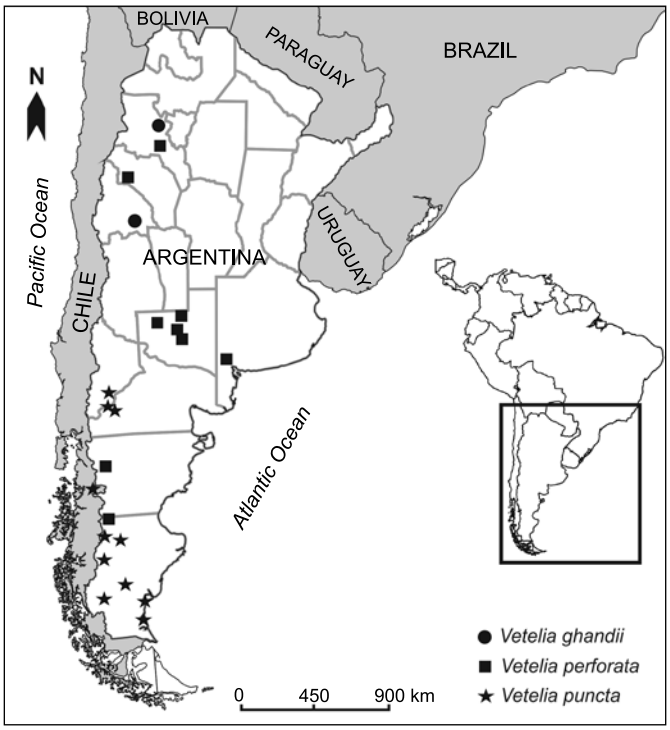

Fig. 1. Map showing the geographic distribution of *Vetelia* species in Argentina and Chile.

phyletic groups: on the one hand Pilosa, which includes sloths and anteaters, and on the other hand, Cingulata, which includes armadillos, glyptodonts, pampatheres, and pachyarmaterids (Engelmann 1985; O'Leary et al. 2013; Gaudin and Croft 2015; Fernicola et al. 2017). Cingulata ("armored" xenarthrans) is the most ancient (early Eocene; Bergqvist et al. 2004; Gelfo et al. 2009; Woodburne et al. 2014) and diverse clade, with a complex evolutionary history that led to the development of very diverse sizes and morphologies, with distinct taxa occupying very different ecological niches.

Molecular data suggest that living armadillos can be gathered in two families, Dasypodidae and Chlamyphoridae. Among chlamyphorids, three subfamilies are recognized: Chlamyphorinae (fairy armadillos), Euphractinae (yellow and hairy armadillos), and Tolypeutinae (naked-tailed, giant, and three banded armadillos) (Möller-Krull et al. 2007; Delsuc et al. 2012, 2016; Gibb et al. 2016; Mitchell et al. 2016).

Extant tolypeutines are represented by *Tolypeutes* Illiger, 1811 [*T. matacus* (Desmarest, 1804) and *T. tricinctus* (Linnaeus, 1758)], included in the tribe Tolypeutini, and *Cabassous* McMurtrie, 1831 [*C. tatouay* (Desmarest, 1804), *C. unicinctus* (Linnaeus, 1758), *C. chacoensis* Wetzel, 1980, and *C. centralis* (Miller, 1899)] and *Priodontes* Cuvier, 1825 [*P. maximus* (Kerr, 1792)], included in the tribe Priodontini (Wetzel 1985; McKenna and Bell 1997; Gibb et al. 2016).

Although Tolypeutinae actually presents the highest diversity among living armadillos, the fossil representatives of this subfamily are very scarce and its evolutionary history still remains largely unknown (Billet et al. 2011). *Kuntinaru boliviensis* Billet, Hautier, Muizon, and Valentin, 2011, from the late Oligocene (~26 Ma; MacFadden et al. 1994) of Bolivia is the oldest record of the subfamily. The age of this taxon is consistent with the results provided by molecular analyses, which suggest that the divergence of tolypeutines occurred before 29 Ma, during the early Oligocene (Delsuc et al. 2004). *Pedrolypeutes praecursor* Carlini, Vizcaíno, and Scillato-Yané, 1997, from the middle Miocene (~14–12 Ma) of Colombia, is interpreted as a possible ancestor of the extant *Tolypeutes*, based on similarities observed at the level of the dorsal carapace osteoderms (Carlini et al. 1997). Finally, more modern representatives of Tolypeutinae are *Tolypeutes* sp. from the late Pliocene of Argentina, *T. matacus* from the Pleistocene–Holocene of Argentina and Bolivia, *T. tricinctus* from the Pleistocene–Holocene of Brazil (e.g., Scillato-Yané 1980, 1982; Carlini et al. 1997; McKenna and Bell 1997; Oliveira and Pereira 2009), and *Cabassus* sp. from the late Pleistocene–early Holocene of Brazil (Oliveira et al. 2014, and references therein).

According to the known findings, tolypeutine armadillos are absent from the fossil record during two long periods, between the late Oligocene and middle Miocene, and between the middle Miocene and late Pliocene/Quaternary transition. With respect to this situation, Billet et al. (2011) considered the tolypeutines as a clear example of a "ghost lineage", and suggested that it could be related with a historical misidentification of the diagnostic characters of the representatives of this subfamily.

Vetelia Ameghino, 1891, is an armadillo mainly restricted to the Miocene of Argentina and Chile (Fig. 1), represented by the type species *Vetelia puncta* Ameghino, 1891 (early–middle Miocene) and the referred species *Vetelia perforata* Scillato-Yané, 1977 (middle–late Miocene) and *Vetelia gandhii* Esteban and Nasif, 1996 (late Miocene), all of them mostly know by isolated osteoderms of the dorsal carapace (Scillato-Yané 1977, 1982; González Ruiz 2010). This genus has been traditionally included within the subfamily Euphractinae (Scillato-Yané 1982; Esteban and Nasif 1996; Urrutia et al. 2008; González Ruiz 2010). However, Hofstetter (1958) suggested a possible relationship with the Tolypeutinae Priodontini, based on the similarity of dorsal carapace osteoderms between *V. puncta* and the extant *Cabassous* and *Priodontes*. Despite this observation, no studies were performed in order to test this hypothesis.

In this contribution, we describe the most complete specimen of *Vetelia* (i.e., PVSJ-289) from the late Miocene of San Juan Province (Argentina), which allows the first detailed anatomical description of the skull and mandible of this genus. In addition, the diagnosis of the three known species is revised and a morphological phylogenetic analysis is performed to test their relationships with other Euphractinae and Tolypeutinae armadillos. The higher affinity observed with tolypeutines, particularly with the Priodontini *Priodontes* and *Cabassus*, provides novel information on the poorly known evolutionary his-

tory of this lineage, filling an important temporal gap in the fossil record.

Institutional abbreviations.—AMNH, American Museum of Natural History, New York, USA; CD-UNNE, Colección Didáctica de la Universidad Nacional del Nordeste, Corrientes, Argentina; CML, Colección Mamíferos, Facultad de Ciencias Naturales e Instituto Miguel Lillo, San Miguel de Tucumán, Argentina; FMNH, Field Museum of Natural History, Chicago, USA; INGEO-PV, Instituto de Geología "Dr. Emiliano P. Aparicio", Universidad Nacional de San Juan, San Juan, Argentina; LEVAC-CO, Colección Laboratorio de Evolución de Vertebrados y Ambientes Cenozoicos, Corrientes, Argentina; MACN, Museo Argentino de Ciencias Naturales "Bernardino Rivadavia", Buenos Aires, Argentina; MD-CH, Colección Arroyo Chasicó, Museo Municipal de Ciencias Naturales "Carlos Darwin", Punta Alta, Argentina; MLP, Museo de La Plata, La Plata, Argentina; MMH-CH, Colección Arroyo Chasicó, Museo Municipal de Ciencias Naturales "Vicente Di Martino", Monte Hermoso, Argentina; PVL, Colección de Paleontología de Vertebrados, Facultad de Ciencias Naturales e Instituto Miguel Lillo, San Miguel de Tucumán, Argentina; PVSJ, Instituto y Museo de Ciencias Naturales, Universidad Nacional de San Juan, San Juan, Argentina.

Other abbreviations.—SALMA, South American Land Mammal Age. We follow standard convention in abbreviating tooth families as I, C, P, and M, with upper and lower case letters referring to upper and lower teeth, respectively.

Material and methods

This study includes the description and comparison of specimens referred to the three known species of *Vetelia* (*V. puncta*, *V. perforata*, and *V. ghandii*). We also consider specimens of the extant tolypeutines *Priodontes*, *Cabassous*, and *Tolypeutes* (see SOM 1, Supplementary Online Material available at http://app.pan.pl/SOM/app66-Barasoain_etal_SOM.pdf). Bibliographic information is also considered for the species *Kuntinaru boliviensis* and *Pedrolypeutes praecursor* (Billet et al. 2011; Carlini et al. 1997, respectively). The biostratigraphic schemes (e.g., SALMA, regional stages/ages, international stages) considered for the different records vary according to the age and geographical provenance (see below). Skull, mandible, molariforms, and osteoderms measurements (Tables 1–3) were obtained by using a 0.02 mm resolution digital calliper.

Phylogenetic analysis

We carried out a cladistic analysis, based on morphological characters, in order to determine the phylogenetic affinities of *Vetelia*. Representatives of this genus are included for the first time in a cladistic analysis. In this case, we used *V. gandhii* and *V. perforata*. We opted to exclude *V. puncta* of this analysis because the scarce known specimens (represented only by isolated osteoderms) do not allow the codification of most characters here considered.

The matrix includes 24 taxa and 148 morphological characters (see SOM 2), including both cranial (skull, mandible, and teeth; 1–125) and carapace (dorsal carapace and osteoderms; 126–148) features. All characters were treated as unordered and given the same weight (1.0), according to Gaudin's (2004) criterion. The matrix (see SOM 3) was created through the software Mesquite 3.04 (Maddison and Maddison 2008). A total of 96 characters were codified as binary, while 52 were multistate (non-additive). Characters that were not preserved or could not be observed were coded as "?", while non-codifiable characters or characters states were coded as "–".

The out-group includes three xenarthran taxa: the sloth *Bradypus* Linnaeus, 1758, the anteater *Tamandua* Rafinesque, 1815, and the peltephilid armadillo *Peltephilus* Ameghino, 1887, which were used to root the phylogenetic trees, as they represent all main groups within Xenarthra. The in-group includes 20 genera of both extinct and extant dasypodid and chlamyphorid armadillos, selected to reflect as best as possible their past and present diversity: (i) the Dasypodidae *Dasypus* Linnaeus, 1758, and †(extinct) *Stegotherium* Ameghino, 1887 (subfamily Dasypodinae); (ii) the Chlamyphoridae euphractines: †*Prozaedyus*, Ameghino 1891, †*Proeutatus* Ameghino, 1891, †*Eutatus* Gervais, 1867, *Zaedyus* Ameghino, 1889, *Euphractus* Wagler, 1830, *Chaetophractus* Fitzinger, 1871, †*Paleuphractus* Kraglievich, 1934, †*Proeuphractus* Ameghino, 1886, and †*Macroeuphractus* Ameghino, 1887; (iii) the Chlamyphoridae chlamyphorines †*Chlamydophractus* (Barasoain, Tomassini, Zurita, Montalvo, and Superina, 2020c), *Chlamyphorus* Harlan, 1825, and *Calyptophractus* Fitzinger, 1871; and (iv) the Chlamyphoridae tolypeutines †*Pedrolypeutes* Carlini, Vizcaíno, and Scillato-Yané, 1997, *Tolypeutes* Illiger, 1811, *Priodontes* Cuvier, 1825, *Cabassous* McMurtrie, 1831, and †*Kuntinaru* Billet, Hautier, Muizon, and Valentin, 2011. Additionally, the in-group also includes the genus here analyzed, *Vetelia*, including the species *V. gandhii* and *V. perforata.*

The character-taxon matrix was evaluated using the software "TNT", with an "Implicit Enumeration" analysis carried out under the maximum parsimony criteria (Goloboff et al. 2008). For the resulting Most Parsimonious Trees (MPT), the following values were calculated: tree length (TL), Consistency Index (CI), and Retention Index (RI). Additionally, several clade support values for each node were obtained through both absolute and relative Bremer support, and a 1000 replicates "traditional search" Standard Bootstrap analysis and Jacknife resampling (Felsenstein 1985; Bremer 1994; Farris et al. 1996; Goloboff and Farris 2001).

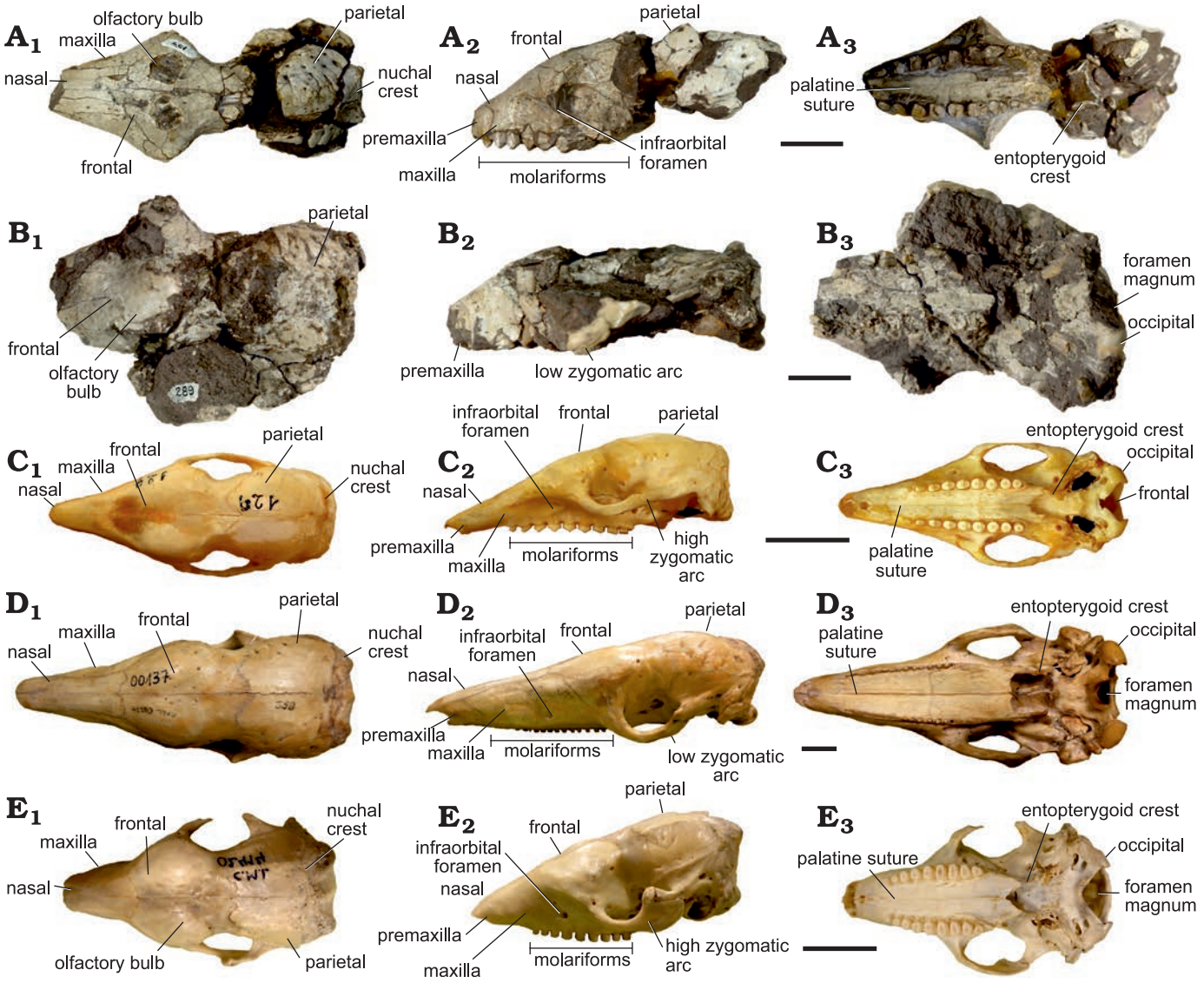

Fig. 2. Skulls of *Vetelia ghandii* Esteban and Nasiff, 1996, from the late Miocene, Loma de Las Tapias, Argentina (A, B) and extant tolypeutine species (C–E). **A**. PVSJ-154. **B**. PVSJ-289. **C**. *Tolypeutes matacus* (Desmarest, 1804), CD-UNNE-129. **D**. *Priodontes maximus* (Kerr, 1792), CML-00137. **E**. *Cabassus chacoensis* Wetzel, 1980, CML-02414. In dorsal (A_1–E_1), lateral (A_2–E_2), and ventral (A_3–E_3) views. Scale bars 20 mm.

Systematic palaeontology

Xenarthra Cope, 1889

Cingulata Illiger, 1811

Chlamyphoridae Pocock, 1924

Tolypeutinae Gray, 1865

Priodontini Gray, 1873

Genus *Vetelia* Ameghino, 1891

Figs. 2–5.

Type species: *Vetelia puncta* Ameghino, 1891, Santa Cruz Formation, mid-early Miocene, Karaiken, Santa Cruz Province, Argentina.

Included species: *Vetelia puncta*, *Vetelia perforata* Scillato-Yané, 1977, and *Vetelia ghandii* Esteban and Nasif, 1996.

Emended diagnosis (after Ameghino 1891).—Large armadillo, comparable in size to *Priodontes maximus*. Fixed osteoderms with a wide and slightly convex central figure, which does not reach the posterior margin; lateral peripheral figures becoming fused with central figure towards the posterior margin; one to four anterior figures. Fixed osteoderms of the scapular shield more elongated than those of the pelvic shield. Mobile osteoderms with a wide and slightly convex central figure, which starts at the transitional zone and reaches the posterior margin of the osteoderm; undivided and elongated lateral peripheral figures. Mobile osteoderms with similar width to that of fixed osteoderms, but twice longer. Both fixed and mobile osteoderms with piliferous foramina of the posterior margin arranged in a single row. Skull with very wide and low zygomatic arches, and developed olfactory bulbs. Flat cranial case, without sagittal crest, and a strong w-shaped nuchal crest. Wide and broad snout, and presence of premaxillary teeth (observed

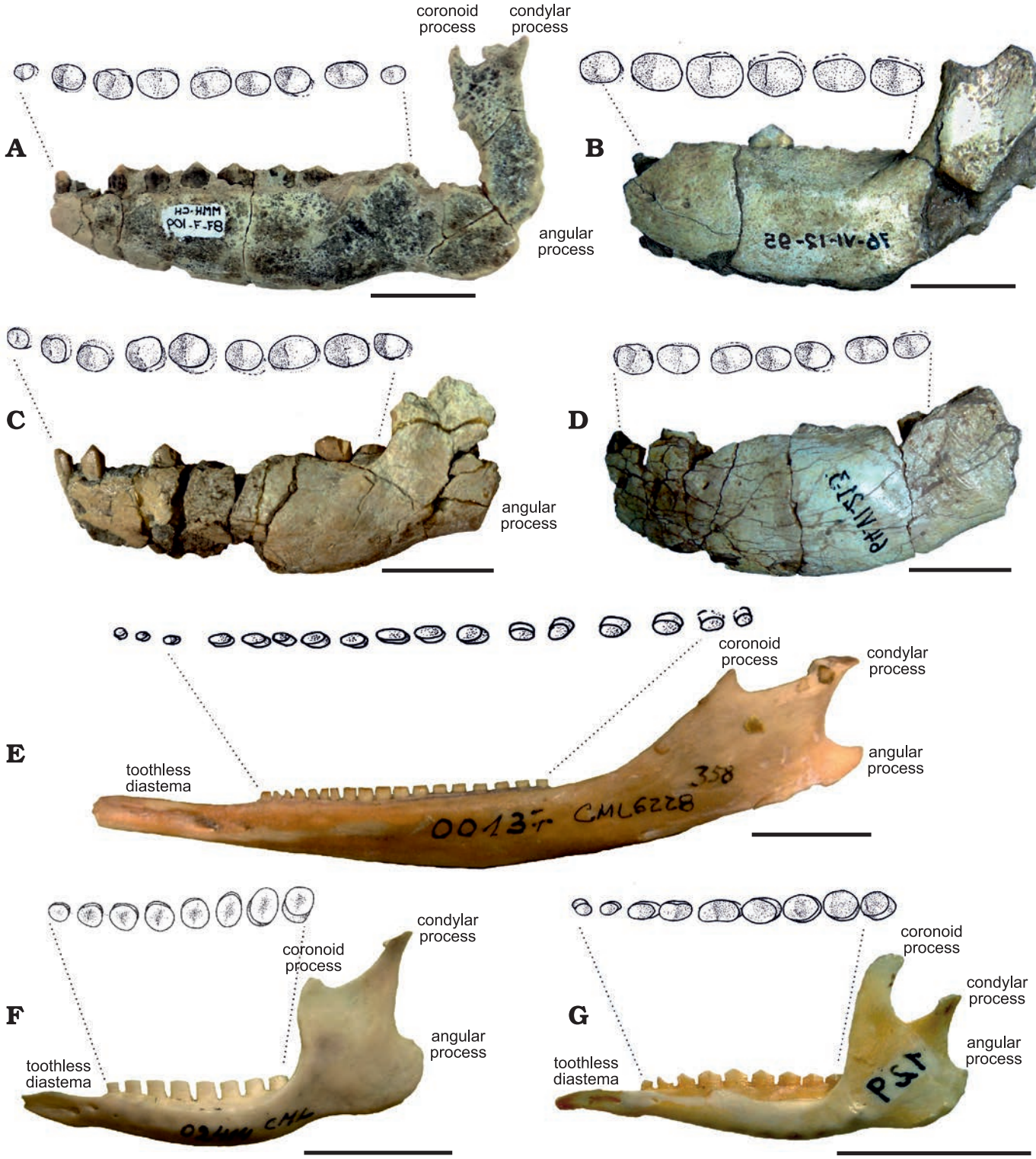

Fig. 3. Hemimandibles (labial views) of *Vetelia* spp. (A–D) and extant tolypeutine species (E–G), with detail of the molariform occlusal surface. **A**, **B**. *Vetelia perforata* Scillato-Yané, 1977, late Miocene, Arroyo Chasicó, Argentina. **A**. MMH-CH-87-7-109. **B**. MLP-76-VI-12-95. **C**, **D**. *Vetelia ghandii* Esteban and Nasiff, 1996. **C**. PVSJ-289; late Miocene, Loma de Las Tapias, Argentina. **D**. MLP-64-V1-21-3; late Miocene, Los Berros, Argentina. **E**. *Priodontes maximus* (Kerr, 1792), CML-00137; Recent, without provenance data. **F**. *Cabassus chacoensis* Wetzel, 1980, CML-02414; Recent, Chaco Province, Argentina. **G**. *Tolypeutes matacus* (Desmarest, 1804), CD-UNNE-129; Recent, without provenance data. Scale bars 20 mm.

in *V. ghandii*). Very robust and massive mandible, with nine ovate and chisel-shaped molariforms. Tooth row extended to the most proximal end of the horizontal ramus, without anterior dental diastema. Condylar process taller than coronoid process; angular process located at the occlusal surface level. Low vertical ramus, with its height equivalent to one

third of the horizontal ramus length (observed in *V. perforata* and *V. ghandii*).

Stratigraphic and geographic range.—Early Miocene–late Miocene. Pinturas Formation (early Miocene), "Pinturan" (SALMA); Santa Cruz and Boleadoras formations (early Miocene), Santacrucian SALMA; Río Frías Formation (early–middle Miocene), Friasian SALMA; Collón Curá Formation (middle Miocene), Colloncuran SALMA; Río Mayo Formation (middle–late Miocene), Mayoan SALMA; Arroyo Chasicó, Huachipampa and Loma de Las Tapias formations (late Miocene), Chasicoan stage/age; Cerro Azul and Chiquimil formations (late Miocene), Chasicoan/Huayquerian stages/ages; Desencuentro and El Morterito formations (late Miocene), Huayquerian stage/age; and Playa del Zorro Aloformation (late Miocene), Tortonian–Messinian. Santa Cruz, Chubut, Neuquén, Río Negro, Buenos Aires, La Pampa, La Rioja, San Juan, and Catamarca provinces, Argentina; Región Aysén, Chile (Fig. 1).

Vetelia puncta Ameghino, 1891

Fig. 4.

Holotype: MACN-A-2139, fixed and mobile osteoderms.

Type horizon: Santa Cruz Formation, mid-early Miocene.

Type locality: Karaiken, Santa Cruz Province, Argentina.

Material.—Other referred material (see SOM 1).

Emended diagnosis.—Species with similar osteoderm size and ornamentation pattern than *V. perforata* and *V. ghandii*, but differing from them by the presence, in both fixed and mobile osteoderms, of numerous piliferous foramina along a main sulcus that delimitate the central figure. Small foramina in the anterior and lateral margins of the osteoderms. Piliferous foramina of the posterior margin similar to the condition in *V. ghandii*, but larger and less numerous than in *V. perforata*.

Stratigraphic and geographic range.—Early–middle Miocene. Pinturas Formation (early Miocene), "Pinturan" SALMA; Santa Cruz and Boleadoras formations (early Miocene), Santacrucian SALMA; Río Frías Formation (early–middle Miocene), Friasian SALMA. Santa Cruz Province, Argentina and Región Aysén, Chile (Fig. 1).

Vetelia perforata Scillato-Yané, 1977

Figs. 3, 4.

Holotype: MLP 28-X-11-45, fixed, semimobile, and mobile osteoderms.

Type horizon: Arroyo Chasicó Formation, late Miocene.

Type locality: Arroyo Chasicó, Buenos Aires Province, Argentina.

Material.—Other referred material (see SOM 1).

Emended diagnosis.—Species with similar size and osteoderm ornamentation pattern than *V. puncta* and *V. ghandii*, but differing from them by the presence, in both fixed and mobile osteoderms, of smaller and very numerous piliferous foramina located in the posterior margin. Also differs from *V. puncta* by the absence of foramina in the anterior and lateral margins of the osteoderms, and from *V. ghandii* by the presence of rounded borders along the entire dorsal carapace margins. Very robust and massive mandible, with nine ovate and chisel-shaped molariforms. Tooth row extended to the most proximal ending of the horizontal ramus, without anterior diastema. Condylar process taller than coronoid process; angular process located at the occlusal surface level. Low vertical ramus, being its height equivalent to one third of the horizontal ramus length. Contact between horizontal and vertical ramus in an obtuse angle (~110º) in contrast to the straight angle (~90º) in *V. ghandii*.

Stratigraphic and geographic range.—Middle–late Miocene; Río Mayo Formation (middle–late Miocene), Mayoan SALMA; Arroyo Chasicó Formation (late Miocene), Chasicoan stage/age; Cerro Azul and Chiquimil formations (late Miocene), Chasicoan/Huayquerian stages/ages; Desencuentro Formation (late Miocene), Huayquerian stage/age. Santa Cruz, Chubut, Buenos Aires, La Pampa, La Rioja, and Catamarca provinces, Argentina (Fig. 1).

Vetelia gandhii Esteban and Nasif, 1996

Figs. 2–5.

Holotype: PVL 4800, fixed and mobile osteoderms.

Type horizon: Playa del Zorro Alloformation, late Miocene.

Type locality: Santa María, Catamarca Province, Argentina.

Material.—Other referred material (see SOM 1).

Emended diagnosis.—Species with similar size and osteoderm ornamentation pattern to *V. puncta* and *V. perforata*. It differs from *V. puncta* by the absence of foramina in the anterior and lateral margins of the osteoderms, and from *V. perforata* by the presence of larger and less numerous foramina in the posterior margin of the osteoderms. Dorsal carapace with a reduced scapular shield, including just two

Fig. 4. Osteoderms from Argentina of *Vetelia* spp. (A–D) and extant Priodontini species (E–L), with detail of the horny scale and bony surface ornamentation pattern (A_3, E_3, D_3, I_3, K_3). **A**. A drawing of *Vetelia* spp. osteoderms: fixed (A_1) and mobile (A_2). **B**. *Vetelia puncta* Ameghino, 1891, MACN-A-2139; middle–early Miocene, Karaiken: fixed (B_1) and mobile (B_2). **C**. *Vetelia perforata* Scillato-Yané, 1977, MD-CH-125; late Miocene, Arroyo Chasicó: fixed (C_1) and mobile (C_2). **D**. *Vetelia ghandii* Esteban and Nasiff, 1996, PVSJ-151; late Miocene, Loma de Las Tapias: fixed (D_1) and mobile (D_2) . **E**. A drawing of *Cabassous* spp. fixed osteoderms: horny scale (E_1) and bony surface (E_2). **F**. *Cabassous tatouay* (Desmarest, 1804), CML-03066, fixed osteoderms of the pelvic shield; Recent, Chaco Province. **G**. A drawing of *Cabassous* spp. mobile osteoderms: horny scale (G_1) and bony surface (G_2). **H**. *Cabassous tatouay* (Desmarest, 1804), CML-03066, mobile osteoderms; Recent, Chaco Province. **I**. A drawing of *Priodontes* sp. fixed osteoderms: horny scale (I_1) and bony surface (I_2). **J**. *Priodontes maximus* (Kerr, 1792), AMNH-147493, fixed osteoderms of the pelvic shield; Recent, Chaco Province. **K**. A drawing of *Priodontes* spp. mobile osteoderms: horny scale (K_1) and bony surface (K_2). **L**. *Priodontes maximus* (Kerr, 1792), AMNH-147493, mobile osteoderms; Recent, Chaco Province. Scale bars 20 mm. A, E, G, I, and K, not to scale. →

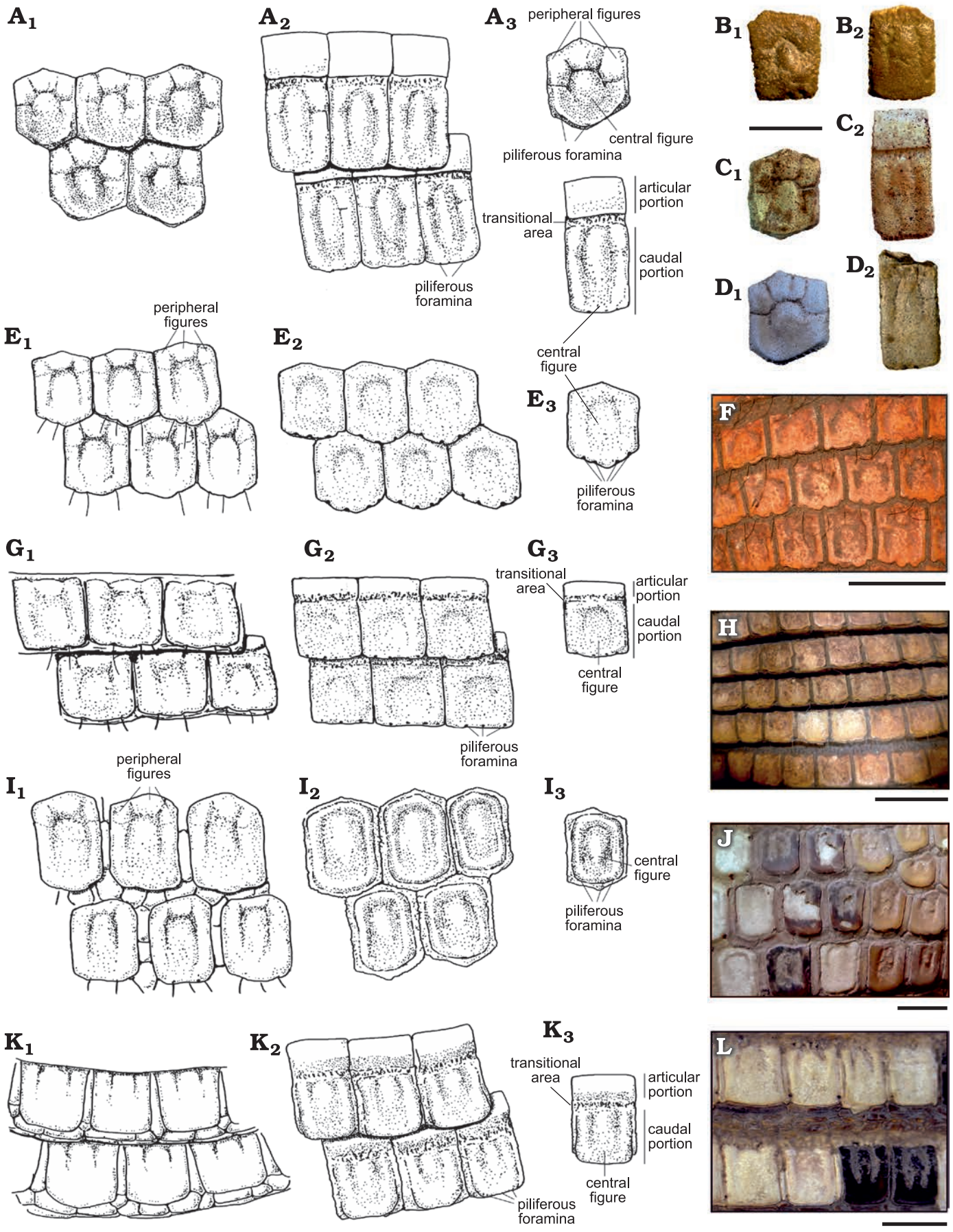
A1
A2
A3
peripheral figures
central figure
piliferous foramina
articular portion
transitional area
caudal portion
piliferous foramina
central figure
B1
B2
C2
C1
D2
D1
E1
peripheral figures
E2
E3
piliferous foramina
F
G1
G2
G3
transitional area
articular portion
caudal portion
central figure
piliferous foramina
H
I1
peripheral figures
I2
I3
central figure
piliferous foramina
J
K1
K2
K3
transitional area
articular portion
caudal portion
central figure
piliferous foramina
L

rows of fixed osteoderms, and mobile bands composed of at least five rows of osteoderms. Differs from *V. perforata* in having serrated dorsal carapace edges towards the posterior margin of the pelvic shield. Skull with very wide and low zygomatic arches, and developed olfactory bulbs. Flat cranial case with absence of sagittal crest, and a strong relief w-shaped nuchal crest. Wide and broad snout, and presence of premaxillary teeth. Nine ovate and chisel-shaped molariforms, both in upper and lower dental series. Toothrows anteriorly extended, with absence of both upper and lower anterior diastema, and flat palatines. Contact between horizontal and vertical ramus forms at a straight angle (~90º), differing from the obtuse angle (~110º) in *V. perforata*.

Remarks.—PVSJ-289, from Loma de Las Tapias Formation, San Juan Province (see SOM 1), described here for the first time, represents the most complete specimen known for the genus.

Stratigraphic and geographic range.—Late Miocene; Loma de Las Tapias Formation (late Miocene), Chasicoan stage/age; El Morterito Formation (late Miocene), Huayquerian stage/age; Playa del Zorro Aloformation (late Miocene), Tortonian–Messinian stages. San Juan and Catamarca provinces, Argentina (Fig. 1).

Results

Skull of *Vetelia gandhii*.—Descriptions are based on two almost complete skulls (PVSJ-154 and PVSJ-289) here assigned to *Vetelia gandhii* (Fig. $2A_1$–A_3, B_1–B_3). These are the first skulls referred to the genus *Vetelia*. They are large (Table 1), with a similar cranial width to that of *Priodontes*, but ~33% shorter. This is due to a strong rostral shortening, which differs to that observed in some mainly insectivorous armadillos such as *Dasypus*, *Priodontes*, and some species of *Prozaedyus* (i.e., *P. proximus* [Ameghino, 1887] and *P. exilis* [Ameghino, 1887]) (see Smith and Redford 1990; Vizcaíno and Fariña 1994; Barasoain et al. 2020a).

In dorsal view (Fig. $2A_1$, B_1), frontal bones are barely anteriorly projected between the maxillary bones and the suture between frontal and nasal bones is straight as in *Tolypeutes* (Fig. $2C_1$–C_3), *Priodontes* (Fig. $2D_1$–D_3), and *Cabassous* (Fig. $2E_1$–E_3). Contrasting with this condition, in *Euphractus*, *Chaetophractus*, and *Zaedyus*, this suture has an arrow-point morphology towards the beginning of the nasal bones. At the start of the anterior zygomatic process, the frontal bones bear a pair of developed olfactory bulbs, very similar to some species of *Cabassous* (i.e., *C. tatouay* [Desmarest, 1804]). Past the anterior zygomatic process, the skull greatly narrows to its minimum width at the level of the orbit. Damaged areas do not allow observing the suture between frontal and parietal bones. The zygomatic arch traces a very broad lateral curve, giving place to a very large orbit area when compared with most armadillos, only similar to that of *Macroeuphractus*. The cranial case is mainly flattened and does not develop a sagittal crest. The nuchal crest has a marked anteriorly oriented relief, with a w-shaped profile, similar to that of *Priodontes* and some species of *Cabassous* (i.e., *C. centralis* [Miller, 1899]). On the contrary, extant euphractine armadillos and the genera *Tolypeutes* and *Kuntinaru* display a nuchal crest with a less pronounced relief and a c-shaped profile.

In lateral view (Fig. $2A_2$, B_2), premaxillary bones are strongly reduced, resulting in a high, wide, and robust rostrum. This morphology generates a less sigmoid dorsal profile of the skull, due to a smaller difference between anterior and posterior cranial heights, than that of most armadillos. The infraorbital foramen is located at the basis of the anterior zygomatic root, a position that is shared with extant euphractine armadillos and *Tolypeutes*. In *Priodontes* and *Cabassous*, this foramen is located more anteriorly. The zygomatic arch is laterally compressed and the curve generated by the jugal bone reaches a low position at the midpoint, reaching the level of the tooth occlusal surface. A similar condition is present in *Cabassous* and *Tolypeutes*, while in *Priodontes* the zygomatic arch reaches an even lower position, its lowest point being at a much lower level than the tooth occlusal level. In extant euphractine armadillos, the zygomatic arch is higher and located at a more dorsal position, with its lowest point at the alveolar level. Towards the posterior half of the zygomatic arch, the jugal bone maintains an approximately uniform width, as in *Tolypeutes* and *Priodontes*, and does not develop the mediolaterally compressed process that is observed in *Cabassous* and euphractines.

In ventral view (Fig. $2A_3$, B_3), the anterior zygomatic processes start to laterally expand at the level of the Mf4, different to extant euphractines, in which the suture between both palatine bones generates a small crest. The whole palatine surface is flat, as occurs in most tolypeutines, with exception of *Tolypeutes* and some species of *Cabassous* (i.e., *C. unicinctus* [Linnaeus, 1758]). The choanae and basicranial areas are damaged in both skulls. However, PVSJ-154

Table 1. Cranial measurements (in mm) of *Vetelia ghandii* specimens.

Measurements	PVSJ-154	PVSJ-289
maximum skull length	110.71	97.85
maximum skull width at the olfactory bulbs level	46.42	57.14
minimum interorbitary width	25.85	32.14
cranial height at Mf1 level	14.61	19.48
cranial height at Mf4 level	21.53	31.16
cranial height at Mf9 level	38.46	35.06
maximum length of the palatine	62.54	64.34
palatine width at Mf1 level	8.33	12.23
palatine width at Mf4 level	16.66	20.12
palatine width at Mf9 level	16.67	21.32
orbital length	28.57	32.14
maximum length of the dental series	58.33	54.14
molariform length	4.8–8.33	5–11
molariform width	2.77–6.25	3.54–6.43

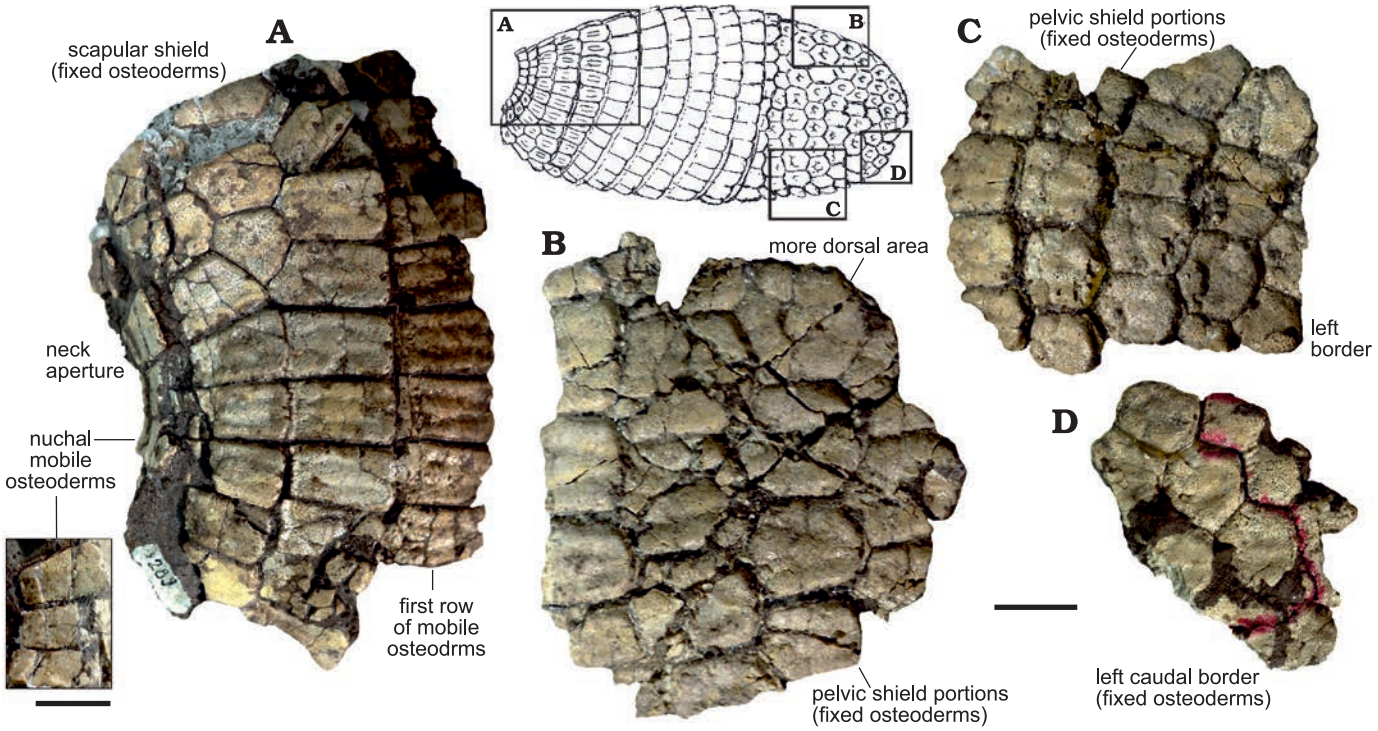

Fig. 5. Features of the different portions of the dorsal carapace of the *Vetelia ghandii* Esteban and Nasiff, 1996, PVSJ-289 (most complete specimen) from the late Miocene of Loma de Las Tapias, San Juan Province, Argentina. **A**. Anterior fragment, with detail on the nuchal band. **B**. Dorsal fragment of the pelvic shield. **C**. Lateral fragment of the pelvic shield. **D**. Caudal fragment. Scale bars 20 mm.

shows the entopterygoid crests sub-parallel and aligned with the dental series; in PVSJ-289, the occipital condyles have a strong ventral development.

Upper dental series are composed of nine massive and robust molariforms (Mf1–Mf9), which are sub-cylindrical, with an anteroposterior main axis. Size increases from Mf1 to Mf6, and then decreases to Mf9 (Table 1). It is noteworthy that the largest molariforms (Mf5–Mf7) are slightly bilobulated. Occlusal surface develops a chisel-shaped morphology, as it is common in armadillo molariforms with little wear. The Mf1 is located in the premaxillary bone. The presence of premaxillary teeth is common in euphractines, but not in tolypeutine armadillos (González Ruiz and MacPhee 2014; González Ruiz et al. 2014, 2017). Tooth rows represent more than half of the length of the skull; they are sub-parallel and extended anteriorly, almost reaching the premaxillary tip. Indeed, armadillos generally develop toothless anterior diastemas (see Thenius 1989). The last two molariforms (Mf8–Mf9) are located posteriorly to the level of the anterior zygomatic root.

Mandibles of *Vetelia perforata* and *Vetelia gandhii*.— Descriptions are based on mandibular remains of *Vetelia perforata* (Fig. 3A, B) (MMH-CH-87-7-109 and MLP-76-VI-12-95) and *V. gandhii* (Fig. 3C, D) (PVSJ-289 and MLP-64-V1-21-3). MMH-CH-87-7-109 and PVSJ-289 present smaller dimensions than MLP-76-VI-12-95 and MLP-64-V1-21-3 (Table 2), reflecting clear individual variation. Dentary is massive and robust, with a similar morphology in both species. The angle between horizontal and vertical ramus is nearly straight (~90º) in *V. ghandii* and obtuse (~120º) in *V. perforata*.

Horizontal ramus is proportionally much wider than in most armadillos (see Scillato-Yané 1982). *Chaetophractus* is the extant armadillo with the widest mandible (Squarcia et al. 2009; Sidorkewicj and Casanave 2013), which is approximately a third thinner than in *Vetelia*. Towards the rostrum, the horizontal ramus becomes slightly thinner, but does not develop the sharpened and narrowed morphology observed in extant armadillos, due to the enlargement of the rostrum. The maximum width of the horizontal ramus is located at the level of the mf8 (Table 2), passing to an abrupt constriction at the level of the mf9. The largest specimens (MLP-76-VI-12-95 and MLP-64-V1-21-3; Fig. 3E, G) show a proportionally wider and thicker horizontal ramus than the smaller specimens. However, to evaluate the significance of this character, a larger sample is necessary to determine possible intraspecific variability (including ontogenetic variability).

The outer surface of the hemimandible is mostly smooth. Two to four mental foramina are located between the mf2 and mf5.

Vertical ramus is robust and its height is equivalent to one third of the total length of the horizontal ramus. The vertical ramus is lower in *Priodontes* (Fig. 3E) and *Cabassous* (Fig. 3F) compared to *Tolypeutes* (Fig. 3G) and euphractine armadillos, in which it is equivalent to more than half the total length of the horizontal ramus. Both the coronoid and the condylar processes are located above the level of the occlusal dental surface, while the angular process is

Table 2. Mandibular measurements (in mm) of *Vetelia ghandii* and *Vetelia perforata* specimens.

Measurements	*Vetelia ghandii*		*Vetelia perforata*	
	PVSJ-289	MLP-64-V1-21-3	MMH-CH-87-7-109	MLP-76-VI-12-95
horizontal ramus maximum length	78.56	–	94.54	–
vertical ramus maximum length	–	–	49.45	–
mandibular height at Mf1 level	11.5	–	6.54	–
mandibular height at Mf4 level	16	18.23	15.27	17
mandibular height at Mf9 level	21.21	20.58	23.27	21
maximum length of the dental series	57.5	–	66.66	–
molariform length	3–6.32	7.05–8.82	3.33–8	8.43
molariform width	3.5–5.57	4.70–5.88	4–6.22	5

approximately at the same level, as it occurs in all extant tolypeutines. In euphractine armadillos, the three processes are located above the occlusal surface level. The presence of a condylar process taller than the coronoid process is shared by *Vetelia*, *Priodontes maximus*, and the four species of *Cabassous*. The angular process is well developed, surpassing the level of the condylear process towards the caudal area, although it is more ventrally expanded in *V. perforata*. In the internal side of the angular process, a large scarred depression indicates the insertion area of a well-developed masseter muscle. In the internal side of the vertical ramus, the mandibular foramen is located at the level of the alveolar surface of the toothrow.

The lower dental series of both *V. perforata* and *V. ghandii* are composed of nine sub-cylindrical, chisel-shaped molariforms. General characteristics are similar to those described for the upper series of *V. ghandii*. The size increases from mf1 to mf6, and then decreases from mf7 to mf9. The toothrow occupies almost the total length of the horizontal ramus and is anteriorly extended to the most proximal extreme. In fact, the mf1 is anteriorly projected, protruding from the anterior end of the hemimandible. This condition, observed in both *V. perforata* and *V. ghandii*, suggests a feature that is unique among armadillos, which generally develop anterior toothless mandibular spouts (see Thenius 1989).

Carapace of *Vetelia* spp.—*Fixed osteoderms*: *Vetelia* (Fig. 4A_1, A_2, B–D) has osteoderms comparable in size to those of *Priodontes*, but thicker. They are sub-hexagonal, as in *Cabassous* (Fig. 4B_1–B_3, C_1–C_3) and *Priodontes* (Fig. 4I_1, I_2, J–D_3, K_1–K_2, L), in contrast to the typical sub-rectangular osteoderms of euphractine armadillos. *Tolypeutes* has the most regular hexagonal and isodiametric osteoderms.

All species of *Vetelia* share a common ornamentation pattern. It includes a wide and slightly convex central figure, surrounded by two lateral peripheral figures and a variable number of anterior minor peripheral figures. The central figure is anteriorly and laterally delimited by a main sulcus that disappears towards the posterior half of the osteoderm, generating a fusion between central and lateral figures. Minor sulci delimit lateral and anterior peripheral figures. *Vetelia puncta* (Fig. 4B) shows well-developed foramina both in the main and minor sulci, while *V. perforata* (Fig. 4C) and *V. ghandii* (Fig. 4D) lack these foramina.

Anterior peripheral figures vary from one to four, though the most common ornamentation pattern is the presence of three figures. Osteoderms with only one figure, as in the holotype of *V. puncta* (MACN-A-2139), seem to belong to the posterodorsal region of the pelvic shield. In many armadillos, osteoderms of this region are highly modified due to the presence of odoriferous glands (Scillato-Yané 1982).

A similar ornamentation pattern is observable in *Priodontes* and *Cabassous*. However, in many cases, this ornamentation is only preserved in the horny scales that cover the osteoderms during the armadillo's lifetime, and becomes diffuse or even absent on the bony surface (Fig. 4H, J, L). This is a peculiar phenomenon also recognized in other groups of armadillos, such as the extant representatives of Chlamyphorinae (Barasoain et al. 2020b, c).

The posterior margin of the osteoderm has a single row of piliferous foramina. In *V. perforata* these foramina are small and numerous (6–14), while in *V. puncta* and *V. ghandii* they are larger and less abundant (2–4). *Vetelia puncta* also develops small foramina in the anterior and lateral margins.

The most complete specimen of *V. ghandii* (PVSJ-289) shows a very reduced scapular shield, composed of only two rows of fixed osteoderms, located between the nuchal osteoderms and the first row of mobile osteoderms (Fig. 5A). Scapular fixed osteoderms (Fig. 5A) seem to be more elongated than those of the pelvic shield (Fig. 5B–D). *Cabassous*, *Priodontes*, and *Tolypeutes* do not show significant differences between scapular and pelvic fixed osteoderms. In the specimen PVSJ-289, the shape of the fixed osteoderms of the pelvic shield slightly changes towards the lateral margins of the dorsal carapace, becoming subsquare, as occur in *Priodontes*. *Vetelia ghandii* has serrated borders in the posterior portion of the pelvic shield, while *V. perforata* has rounded borders (see Scillato-Yané 1982).

Mobile osteoderms: These osteoderms are sub-rectangular, similar in width to fixed osteoderms, but approximately twice as long (Table 3, Fig. 4A_2). They are divided into an articular and a caudal portion, separated from each other by a very rugose transitional area. The articular portion has a smooth unornamented surface whose length is equivalent to half the caudal portion. The caudal portion shows a similar ornamentation pattern in all the species of *Vetelia*. It includes a wide and slightly convex central figure, which begins in the limit with the transitional area and reaches the posterior mar-

gin, where it becomes slightly narrower. The central figure is delimited by a shallow and wide main sulcus. Along this sulcus, *V. puncta* has several piliferous foramina (Fig. 4B), while *V. perforata* (Fig. 4C) and *V. ghandii* (Fig. 4D) lack foramina. The central figure is surrounded by two undivided and elongated peripheral lateral figures. The latter widen at the most anterior part of the osteoderms, resulting in minor peripheral figures that are not completely delimitated by sulci. Some osteoderms show well-developed anterior peripheral figures, while these figures are very diffuse in others.

Similar ornamentation pattern is observable in *Priodontes* and *Cabassous* species. However, as it occurs in fixed osteoderms, the ornamentation in both extant taxa is generally preserved only in the horny scales that cover the osteoderms, while it is diffuse or absent in the bony surface (Fig. 4H, J, L).

The posterior margin of the osteoderm has a single row of piliferous foramina. In *V. perforata*, these foramina are smaller and more numerous (5–14) than in *V. puncta* (2–5) and *V. ghandii* (2–5). *V. puncta* also has small foramina in the lateral margins.

Phylogeny and affinities of *Vetelia* with Tolypeutinae

The general topology of the obtained most parsimonious tree (Fig. 6) is consistent with previous results of morphological phylogenetic analyses including armadillos (e.g., Gaudin and Wible 2006; Billet et al. 2011; Herrera et al. 2017). Some differences are related to the taxa considered in each analysis.

In our analysis, the armadillos compose a monophyletic group, with the genus *Peltephilus* as the sister-group of the remaining taxa. The latter are gathered in a large clade that is, in turn, divided in two well-differentiated clades, one formed by Dasypodidae (*Dasypus* + *Stegotherium*) and another by Chlamyphoridae (all the remaining taxa). This main division agrees with the latest phylogenetic analyses based on molecular data of extant armadillos (e.g., Delsuc et al. 2002, 2012; Möller-Krull et al. 2007).

The family Chlamyphoridae is divided into two main clades. One of them is composed of representatives of the subfamilies Euphractinae and Chlamyphorinae, while the other gathers the genera of Tolypeutinae.

The extinct euphractine *Prozaedyus* is recovered as the sister-taxon of the remaining Euphractinae and Chlamyphorinae, which is congruent with previous interpretations (Engelmann 1985; Gaudin and Wible 2006; Billet et al. 2011; Barasoain et al. 2020a–c). The representatives of the tribe Eutatini (i.e., *Proeutatus* and *Eutatus*) appear as the sister-group of a clade that clusters the Chlamyphorinae and the representatives of the tribe Euphractini. Though molecular data suggest a close relationship between Chlamyphorinae and Tolypeutinae, results from morphological analyses seem to be disturbed due to the particular and highly derived morphology of the fairy armadillos (see also Barasoain et al. 2020a, b).

Table 3. Osteoderm measurements (in mm) of different *Vetelia* species.

Taxa	Fixed osteoderms		Mobile osteoderms	
	length	width	length	width
V. puncta	15.32–20.21	13.75–16.87	19.23–28.12	9.3–17
V. perforata	19.46–21.75	13.91–20.36	20.08–32.75	10.03–16.04
V. ghandii	15.50–22.14	13.32–20.55	20.04–27.50	11.04–15.34

Tolypeutinae constitutes a monophyletic group, supported by nine synapomorphies: 16[1], 37[3], 45[0], 48[1], 58[1], 87[1], 112[1], 132[1], and 142[0] (see SOM 2), and is divided in two main clades. One of them clusters *Tolypeutes* + *Pedrolypeutes*, and is supported by three synapomorphies: 128[1], 129[0], and 148[1] (see SOM 2, 4); this clade is here recognized as tribe Tolypeutini. The other clade includes *Kuntinaru* as sister group of the clade composed by the remaining taxa. The latter is here recognized as tribe Priodontini. It clusters the species of *Vetelia*, *Cabassous*, and *Priodontes*, and is supported by 15 synapomorphies: 14[1], 15[1], 35[1], 43[1], 44[0], 51[1], 69[1], 71[2], 96[2], 129[1], 133[1], 136[1], 143[0], 144[1], and 145[0] (see SOM 2 and 4). Within Priodontini, the species of *Vetelia* (*V. ghandii* and *V. perforata*) form the sister group of the clade composed of *Cabassous* and *Priodontes*.

Discussion

The subfamily Tolypeutinae is represented by the extant genera *Tolypeutes*, *Priodontes*, and *Cabassous*, plus the extinct *Kuntinaru* (Billet et al. 2011), *Pedrolypeutes* (Carlini et al. 1997), and *Vetelia* (this work). However, the identification and characterization of this clade is relatively recent and its status was not confirmed until molecular analyses were carried out on living armadillos (Delsuc et al. 2002, 2003). Historically, and according to the old systematic schemes, extant tolypeutines were grouped into two different tribes: Tolypeutini, including the two species of *Tolypeutes* (*T. matacus* and *T. tricinctus*), and Priodontini, with *Priodontes maximus* and the four species of *Cabassous* (*C. tatouay*, *C. unicinctus*, *C. chacoensis*, and *C. centralis*).

The most plesiomorphic clade within Tolypeutinae, here assigned to Tolypeutini, is composed of *Pedrolypeutes* and *Tolypeutes*. Considering that both genera share two synapomorphic characters (e.g., hexagonal isodiametric osteoderms and presence of small tubercles on the dorsal surface of the osteoderms), the middle Miocene taxon *Pedrolypeutes* can be proposed as the possible ancestor of *Tolypeutes* (see Carlini et al. 1997). According to our phylogenetic analysis, Tolypeutini retains a high number of plesiomorphic characters, being morphologically closer to the Euphractinae.

Molecular phylogenetic analysis performed by Delsuc et al. (2002) placed the Tolypeutini *Tolypeutes* and the Prio-

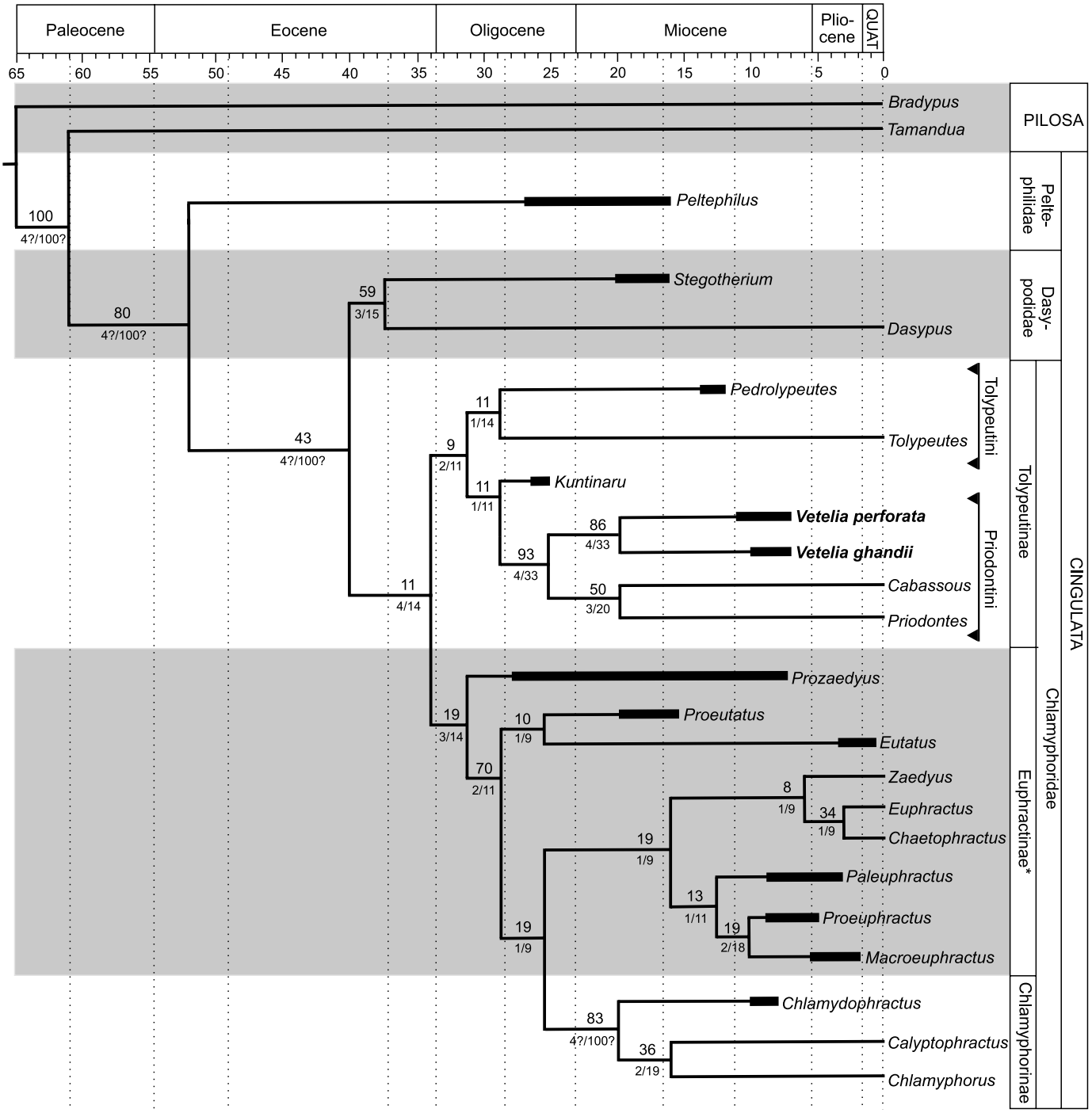

Fig. 6. Most parsimonious tree resulting from the phylogenetic analysis and support values. Numbers above each branch indicate Bootstrap support. Numbers below each branch indicate absolute and relative Bremer support, respectively. Black rectangles are showing the temporal distribution of extinct taxa. *Euphractinae is here recovered as a paraphyletic group.

dontini *Cabassous* in a sister-group relationship. However, several other phylogenetic analyses have supported a closer relationship between *Cabassous* and *Priodontes*, based on their similar external features (Engelmann 1985; Wetzel 1985; Gaudin and Wibble 2006) and spermatozoa morphology (Cetica et al. 1998). According to Delsuc et al. (2002: 12), information obtained from molecular data could be related to a "rapid cladogenesis event that left only short time intervals for molecular synapomorphies to accumulate in these two groups", which in some cases can lead to an unclear result when using this technique.

Based on a detailed morphological analysis, Gaudin and Wible (2006: 172) considered that "*Tolypeutes* is more closely allied with euphractan armadillos than with any other dasypodid armadillos". Many other authors (e.g., Simpson 1945; Hoffstetter 1958; Paula Couto 1979; Scillato-Yané 1982; Wetzel 1985) have previously included *Tolypeutes* in a distinct subfamily or tribe. Our study supports these

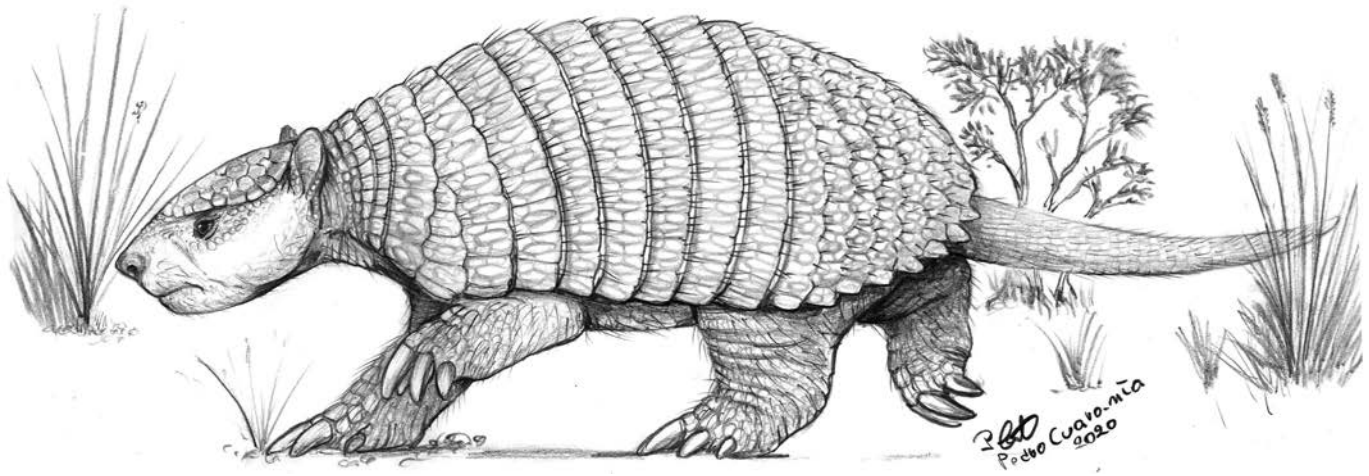

Fig. 7. Reconstruction (by Pedro Cuaranta, CECOAL (UNNE-CONICET), Corrientes, Argentina) of *Vetelia ghandii* Esteban and Nasiff, 1996, based on the most complete known specimens of the genus (PVSJ-154 and PVSJ-289; late Miocene, Loma de Las Tapias, San Juan Province, Argentina). Not to scale.

previous proposals of a close relationship beteween the Tolypeutini and the Euphractinae. The obtained results reflect several plesiomorphic characters shared between the Tolypeutini (*Tolypeutes* + *Pedrolypeutes*) and Euphractinae armadillos: (i) development of a crest along the suture bone on the posterior half palatine suture; (ii) higher central position of the zygomatic arc; (iii) taller mandibular vertical ramus; and (iv) coronoid process taller than condylar process.

The other well-differentiated clade within Tolypeutinae, assigned here to Priodontini, is composed of *Vetelia*, *Cabassous*, and *Priodontes*. This clade includes several autopomorphic characters with respect to the Tolypeutini, and is well supported by diverse cranio-mandibular and carapace (dorsal carapace and osteoderms) synapomorphic characters: (i) absence of a crest along the bone suture on the posterior half palatine; (ii) lower central position of the zygomatic arc; (iii) w-shaped nuchal crest with strong relief; (iv) lower vertical mandibular ramus; (v) condylar process taller than coronoid process; (vi) angular process located at the molariforms occlusal surface level; (vii) common ornamentation pattern of both fixed and mobile osteoderms; and (viii) development of rounded borders in all or almost all the dorsal carapace.

In the clade Priodontini (Fig. 7), *Vetelia* probably branched before the clade composed of *Cabassous* and *Priodontes*. This result is supported by the retention of some plesiomorphic characters in *Vetelia*, shared with the Tolypeutini and *Kuntinaru*: (i) proportionally reduced nasal bone (<25% of the total skull length); (ii) infraorbital foramen placed in a most posterior position; and (iii) less posterior extent of the palatines after the tooth row ending.

Previous systematic studies (e.g., Scillato-Yané 1982; Urrutia et al. 2008; González Ruiz 2010) considered *Vetelia* as an Euphractinae, based on a few fragmentary specimens, mainly represented by isolated osteoderms. The detailed anatomical descriptions provided herein, based on new cranial and mandibular remains and more complete portions of dorsal carapaces, suggest a very close relationship between *Vetelia* and previously described Tolypeutinae, which is supported by the phylogenetic analysis. This relationship is particularly close with the tribe Priodontini, as previously suggested by Hoffstetter (1958). In fact, all the analyzed characters related to the osteoderms and most of the cranio-mandibular characters reflect the close affinity of *Vetelia* with *Cabassous* and *Priodontes*, which form together the clade Priodontini.

On the other hand, most of the characters shared by *Vetelia* and the Euphractinae armadillos are related to the dentition: (i) development of premaxillary teeth; (ii) toothrow length; and (iii) position of last lower tooth in relation to the vertical ramus of the mandible. In this sense, the most relevant character is the presence of premaxillary teeth, which is characteristic of the euphractines. However, it is important to note that not all euphractines have premaxillary teeth, as it occurs in two species of *Prozaedyus*, *P. proximus* and *P. exilis*, both interpreted as insectivores (Vizcaíno and Fariña 1994; Barasoain et al. 2020a) and in taxa with very reduced toothrows, such as *Stegotherium*, with possible myrmecophageal habits (Vizcaíno 1994; Vizcaíno et al. 2006). The presence or absence of premaxillary teeth could be related to feeding habit adaptations rather than to phylogenetic constraints. Among Tolypeutinae, the presence of premaxillary teeth in *T. matacus* is considered as a rare dental anomaly (González Ruiz and MacPhee 2014).

In the cranio-dental phylogenetic analysis carried out by Billet et al. (2011), *Kuntinaru* is the sister taxon of the clade composed of all the remaining tolypeutines. In contrast, in our phylogenetic analysis, *Kuntinaru* is the sister taxon of Priodontini (*Vetelia* + *Cabassous* + *Priodontes*). This result is due to the incorporation of both dorsal carapace characters (unknown for *Kuntinaru*) and new fossil taxa (*Vetelia* and *Pedrolypeutes*). Some cranial features of *Kuntinaru* (e.g., posterior position of the infraorbital foramen, posterior extent of the palatines, and c-shaped nuchal crest) suggest higher affinities with the Tolypeutini (*Pedrolypeutes* +

Tolypeutes), but the lack of osteoderm and dorsal carapace materials in this taxon prevent more detailed interpretations.

Finally, the inclusion of the Miocene genus *Vetelia* within Tolypeutinae increases the diversity of this subfamily in the Neogene of southern South America, filling an important temporal gap in its fossil record. Moreover, it also extends the paleobiogeographical distribution of tolypeutines to the Patagonian Argentina and Chile during part of the Miocene. This novel approach to the Tolypeutinae phylogenetic scheme reflects the need for further research focused on this group of armadillos, including a more comprehensive systematic review of known fossil taxa and an improvement of the lists of diagnostic morphological characters for tolypeutine genera and species.

Conclusions

We report the most complete remains belonging to the Miocene armadillo genus *Vetelia* and provide, for the first time, a detailed anatomical description of the cranial skeletal elements. This study allows a better morphological characterization of the genus, revealing some diagnostic characters among armadillos, such as a shortened rostrum, a very robust dentary with a short vertical ramus, and the absence of an anterior toothless diastema in both upper and lower dental series.

These new anatomical data lead to the proposal of an amended diagnosis for the three known species of *Vetelia* (*V. ghandii*, *V. perforata*, and *V. puncta*), and the inclusion of this genus, for the first time, into a phylogenetic analysis. A close phylogenetic relationship is determined between *Vetelia* and the extant Tolypeutinae, more specifically with the representatives of the tribe Priodontini, *Cabassous* and *Priodontes*. Several synapomorphic characters support the inclusion of *Vetelia* within the Tolypeutinae Priodontini rather than within the subfamily Euphractinae, such as the morphology of the condylar and angular processes of the mandible and the development of a common ornamentation pattern of both fixed and mobile osteoderms of the dorsal carapace.

This new proposal fills a temporal gap into the evolutionary history of tolypeutine armadillos, which are very scarce in the fossil record. Both molecular and morphological data show two well characterized natural groups clustered within Tolypeutinae. In this respect, this work also leads to a redefinition and reconceptualization of the old Priodontini and Tolypeutini tribes, which is useful to address the systematics of Tolypeutinae. Finally, we provide new information on the diagnostic morphological characters of the Priodontini and Tolypeutini tribes (see SOM 4).

Acknowledgements

We thank the curators Ricardo Martínez (Museo de Ciencias Naturales, San Juan, Argentina), Ricardo Caputo (MD), Natalia Sánchez (MMH), Marcelo Reguero (MLP), and Laura Chornogubsky (MACN) for the access to the studied specimens. Reconstruction of *Vetelia ghandii* and drawings were made by Pedro Cuaranta (Centro de Ecología Aplicada del Litoral, Corrientes, Argentina). Romina Mauriño (Universidad Nacional del Nordeste, Corrientes, Argentina) contributed with photography editing. We also thank the editor Olivier Lambert (Institut Royal des Sciences Naturelles de Belgique, Belgium) and both reviewers François Pujos (Instituto Argentino de Nivología, Glaciología y Ciencias Ambientales, Mendoza, Argentina) and Martín Zamorano (Universidad Nacional de La Plata-CONICET, La Plata, Argentina), whose comments greatly improved the manuscript. Esperanza Cerdeño (Instituto Argentino de Nivología, Glaciología y Ciencias Ambientales, Mendoza, Argentina) made a critical review of the manuscript and helped with the English. This research was partially funded by grant PICT 2017 0765, PI QOO2/17, Secretaría General de Ciencia y Tecnología, Universidad Nacional del Sur (PGI 24/H154), project 06-G, Facultad de Ciencias Exactas y Naturales of the Universidad Nacional de La Pampa and CICITCA-UNSJ, E 1151, Universidad Nacional de San Juan, Argentina.

References

Ameghino, F. 1886. Contribución al conocimiento de los mamíferos fósiles de los terrenos terciarios antiguos de Paraná. *Boletín de la Academia Nacional de Ciencias de Córdoba* 9: 3–226.

Ameghino, F. 1887. Enumeración sistemática de las especies de mamíferos fósiles coleccionados por Carlos Ameghino en los terrenos eocenos de la Patagonia austral y depositados en el Museo de La Plata. *Boletín del Museo de la Plata* 1: 1–26.

Ameghino, F. 1889. Contribución al conocimiento de los mamiferos fósiles de la Republica Argentina. *Actas de la Academia Nacional de Ciencias de Cordoba* 6: 1–1027.

Ameghino, F. 1891. Mamíferos y aves fósiles argentinas. *Revista Argentina de Historia Natural* 1: 240–288.

Barasoain, D., Contreras, V.H., Tomassini, R.L., and Zurita, A.E. 2020a. A new pygmy armadillo (Cingulata, Euphractinae) from the late Miocene of Andean Argentina reveals an unexpected evolutionary history of the singular *Prozaedyus* lineage. *Journal of South American Earth Sciences* 100: 102589.

Barasoain, D., Tomassini, R.L., Zurita, A.E., Montalvo, C.I., and Superina, M. 2020b. A new fairy armadillo (Cingulata, Chlamyphorinae) from the upper Miocene of Argentina: first fossil record of the most enigmatic Xenarthra. *Journal of Vertebrate Paleontology* 39 (5): e1716778.

Barasoain, D., Tomassini, R.L., Zurita, A.E., Montalvo, C.I., and Superina, M. 2020c. *Chlamydophractus*, new name for *Chlamyphractus* Barasoain et al., 2020 (Xenarthra, Chlamyphorinae), non *Chlamyphractus* Castellanos, 1940 (Xenarthra, Glyptodontidae). *Journal of Vertebrate Paleontology* 40 (2): e1774890.

Bergqvist, L.P., Abrantes, E.A.L., and Avilla L.S. 2004. The Xenarthra (Mammalia) of São José de Itaboraí Basin (upper Paleocene, Itaboraian), Rio de Janeiro, Brazil. *Geodiversitas* 26: 326−337.

Billet, G., Hautier, L., De Muizon, C., and Valentin, X. 2011. Oldest cingulate skulls provide congruence between morphological and molecular scenarios of armadillo evolution. *Proceedings of the Royal Society B: Biological Sciences* 278: 2791–2797.

Bremer, K.R. 1994. Branch support and tree stability. *Cladistics* 10: 295−304.

Carlini, A.A., Vizcaíno, S.F., and Scillato-Yané, G.J. 1997. Armored xenarthrans: a unique taxonomic and ecologic assemblage. *In*: R.D. Madden, R.L. Cifelli, and J.J Flynn (eds.), *Vertebrate Paleontology in the Neotropics. The Miocene Fauna of La Venta, Colombia*, 13–226. Smithsonian Institution Press, Washington, DC.

Cetica, P.D., Solari, A.J., Merani, M.S., De Rosas, J.C., and Burgos, M.H. 1998. Evolutionary sperm morphology and morphometry in armadillos. *Journal of Submicroscopic Cytology and Pathology* 30: 309–314.

Cione, A.L., Gasparini, G.M., Soibelzon, E., Soibelzon, L.H., and Tonni, E.P. 2015 *The Great American Biotic Interchange. A South American Perspective*. 106 pp. Springer, Dordrecht.

Cope, E.D. 1889. The Edentata of North America. *The American Naturalist* 23: 657–664.

Cuvier, F. 1825. *Des dents de mammifères, considérées comme caractères zoologiques*. 258 pp. F.G. Levrault, Le Norman, Paris.

Delsuc, F., Scally, M., Madsen, O., Stanhope, M.J., De Jong, W.W., Catzeflis, F.M., Springer, M.S., and Douzery, E.J.P. 2002. Molecular phylogeny of living xenarthrans and the impact of character and taxon sampling on the placental tree rooting. *Molecular Biology and Evolution* 19: 1656–1671.

Delsuc, F., Stanhope, M.J., and Douzery, E.J. 2003. Molecular systematics of armadillos (Xenarthra, Dasypodidae): contribution of maximum likelihood and Bayesian analyses of mitochondrial and nuclear genes. *Molecular Phylogenetics and Evolution* 28: 261–275.

Delsuc, F., Vizcaíno, S.F., and Douzery, E.J. 2004. Influence of Tertiary paleoenvironmental changes on the diversification of South American mammals: a relaxed molecular clock study within xenarthrans. *BMC Evolutionary Biology* 4: 11.

Delsuc, F., Gibb, G.C., Kuch, M., Billet, G., Hautier, L., Southon, J., Rouillard, J.M., Fernicola, J.C., Vizcaíno, S.F., MacPhee, R.D.E., and Poinar, H.N. 2016. The phylogenetic affinities of the extinct glyptodonts. *Current Biology* 26: 155−156.

Delsuc, F., Superina, M., Tilak, M.K., Douzery, E.J., and Hassanin, A. 2012. Molecular phylogenetics unveils the ancient evolutionary origins of the enigmatic fairy armadillos. *Molecular Phylogenetics and Evolution* 62: 673–680.

Desmarest, A.G. 1804. Tableau methodique des mammifères. *In*: J.-F.-P. Deterville (ed.), *Nouveau dictionnaire d'histoire naturelle, appliquée aux arts, à l'agriculture, à l'économie rurale et domestique, à la médecine, etc., par une société de naturalistes et d'agriculteurs: avec des figures tirées des trois règnes de la nature. Tome 24*, 5–38 pp. Chez Deterville, Paris.

Engelmann, G. 1985. The phylogeny of the Xenarthra. *In*: G.G. Montgomery (ed.), *The Ecology and Evolution of Armadillos, Sloths, and Vermilinguas*, 51–64. Smithsonian Institution Press, Washington, DC.

Esteban, G.I., and Nasif, N.L. 1996. Nuevos Dasypodidae (Mammalia, Xenarthra) del Mioceno tardío del Valle del Cajón, Catamarca, Argentina. *Ameghiniana* 33: 327–334.

Farris, J.S., Albert, V.A., Källersjö, M., Lipscomb, D., and Kluge, A.G. 1996. Parsimony jackknifing outperforms neighbor-joining. *Cladistics* 12: 99–124.

Felsenstein, J. 1985. Confidence limits on phylogenies: an approach using the bootstrap. *Evolution* 39: 783–791.

Fernicola, J.C., Rinderknecht, A., Jones, W., Vizcaíno, S.F., and Porpino, K. 2017. A new species of *Neoglyptatelus* (Mammalia, Xenarthra, Cingulata) from the late Miocene of Uruguay provides new insights on the evolution of the dorsal armor in cingulates. *Ameghiniana* 55: 233–253.

Fitzinger, L.J. 1871. Die naturliche Familie der Gurtelthiere (Dasypodes). *Akademie der Wissenschaften in Wien, Sitzungsberichte, Mathematisch-naturwissenschaftliche Klasse, Abteilung* 64: 209–276.

Gaudin, T.J. 2004. Phylogenetic relationships among sloths (Mammalia, Xenarthra, Tardigrada): the craniodental evidence. *Zoological Journal of the Linnean Society* 140: 255–305.

Gaudin, T.J. and Croft, D.A. 2015. Paleogene Xenarthra and the evolution of South American mammals. *Journal of Mammalogy* 96: 622–634.

Gaudin, T.J. and Wible, J.R. 2006. The phylogeny of living and extinct armadillos (Mammalia, Xenarthra, Cingulata): a craniodental analysis. *In*: M.T. Carrano, T.J. Gaudin, R.W. Blob, and J.R. Wible (eds.), *Amniote Paleobiology: Perspectives on the Evolution of Mammals, Birds and Reptiles*, 153–198. University of Chicago Press, Chicago.

Gelfo, J.N., Goin, F.J., Woodburne, M.O., and Muizon, C.D. 2009. Biochronological relationships of the earliest South American Paleogene mammalian faunas. *Palaeontology* 52: 251–269.

Gervais, P. 1867. Sur une nouvelle collection d'ossementes fossiles de Mammifères recueillé par M. Fr. Seguin dans la Confédération Argentine. *Comptes rendus des séances de l'Académie des Sciences* 65: 279–282.

Gibb, G.C., Condamine, F.L., Kuch, M., Enk, J., Moraes-Barros, N., Superina, M., Poinar, H.N., and Delsuc, F. 2016. Shotgun mitogenomics provides a reference phylogenetic framework and timescale for living xenarthrans. *Molecular Biology and Evolution* 33: 621−42.

Goloboff, P.A. and Farris J.S. 2001. Methods for quick consensus estimation. *Cladistics* 17: 26–34.

Goloboff, P.A., Farris, J.S., and Nixon, K.C. 2008. TNT, a free program for phylogenetic analysis. *Cladistics* 24: 774−786.

González Ruiz, L.R. 2010. *Los Cingulata (Mammalia, Xenarthra) del Mioceno temprano y medio de Patagonia (edades Santacrucense y "Friasense"). Revisión sistemática y consideraciones bioestratigráficas* 471 pp. Ph.D. Thesis, Facultad de Ciencias Naturales y Museo, Universidad Nacional de La Plata, La Plata.

González Ruiz, L.R. and MacPhee, R.D. 2014. Dental anomalies in *Tolypeutes matacus* (Desmarest, 1804) (Mammalia, Xenarthra, Cingulata). *XXVII Jornadas Argentinas de Mastozoología, Libro de Resúmenes*, 94, Esquel, Chubut.

González Ruiz, L.R. and Scillato-Yané, G.J. 2007. El género Vetelia Ameghino (Xenarthra, Dasypodidae). Distribución cronológica y geográfica durante el Mioceno de Patagonia, Argentina. XXIII Jornadas Argentinas de Paleontología de Vertebrados. 21 al 23 de Mayo, Trelew (Chubut), Argentina. *Ameghiniana* 44 (4): 21R.

González Ruiz, L.R., Aya-Cuero, C.A., and Martin, G.M. 2017. La dentición de *Priodontes maximus* (Kerr, 1792): fórmula, morfología y anomalías. *XXX Jornadas Argentinas de Mastozoología, Libro de Resúmenes*, 135. Bahía Blanca, Buenos Aires.

González Ruiz, L.R., Góis, F., Scillato-Yané. G.J., Oliva, C., Contreras, V., and Esteban, G. 2014. New records of Vetelia Ameghino (Mammalia, Xenarthra, Dasypodidae) in the Miocene of Argentina: anatomical and paleobiogeographic implications. *74th International Palaeontological Congress September 28–October 3, Abstract Volume*, 722. CCT-CONICET, Mendoza.

González Ruiz, L.R., Ladevèze, S., and MacPhee, R.D. 2014. Dental anomalies in *Euphractus sexcinctus* Wagler (Mammalia: Xenarthra: Dasypodidae). *In*: *94 Annual Meeting of the American Society of Mammalogists, Abstract Book*, 59–60. Oklahoma City, Oklahoma.

Gray, J.E. 1865. Revision on the genera and species of entomophagus Edentata, founded on examination of the specimens in the British Museum. *Proceedings of the Zoological Society of London* 33: 359–386.

Gray, J.E. 1873. *Hand-list on the Edentata, Pachydermata and Ruminantia in the British Museum*. 174 pp. British Museum (Natural History), London.

Harlan, R. 1825. Description of a new genus of mammiferous quadrupeds, of the order Edentata. *Annals of the Lyceum Museum of Natural History* 1: 235–245.

Herrera, C.M., Powell, J.E., Esteban, G.I., and del Papa, C. 2017. A new Eocene dasypodid with caniniforms (Mammalia, Xenarthra, Cingulata) from northwest Argentina. *Journal of Mammalian Evolution* 24: 275–288.

Hoffstetter, R. 1958. Xenarthra. *In*: P. Piveteau (ed.), *Traité de Paléontologie, Vol.2 no.6, Mammifères Evolution*, 535–636. Masson et Cie, Paris.

Illiger, C.D. 1811. *Prodromus systematis mammalium et avium additis terminis zoographicis uttriusque classis*. 301 pp. Salfeld, Berlin.

Kerr, R. 1792. *The Animal Kingdom or Zoological System, of the Celebrated Sir Charles Linnaeus. Class I. Mammalia: Contain a Complete Systematic Description, Arrangement, and Nomenclature, of all the Known Species and Varieties of Mammalia, or Animals Which Give Suck To Their Young; Being a Translation of That Part of the Systema Naturae, As Lately Published, With Great Improvements, By Professor Gmelin of Goettingen, Together With Numerous Additions From More Recent Zoological Writers, and Illustrated With Copperplates*. 400 pp. A. Strahan, T. Cadell, and W. Creech, Edinburgh.

Kraglievich, L. 1934. *La antigüedad pliocena de las faunas de Monte Hermoso y Chapadmalal, deducidas de su comparación con las que*

le precedieron y sucedieron. 306 pp. Imprenta "El Siglo Ilustrado", Montevideo.

Linnaeus, C. 1758. *Systema naturæ: per regna tria naturaæ, secundum classes, ordines, genera, species, cum characteribus, differentiis, synonymis, locis*. Tome 1. Editio Decima Reformata. 824 pp. Impensis Direct Laurentii Salvii, Holmiæ.

MacFadden, B.J., Wang, Y., Cerling, T.E., and Anaya, F. 1994. South American fossil mammals and carbon isotopes: a 25 million-year sequence from the Bolivian Andes. *Palaeogeography, Palaeoclimatology, Palaeoecology* 107: 257–268.

Maddison, W.P. and Maddison, D.R. 2008. Mesquite: a modular system for evolutionary analysis. Version 3.04. Available at http://mesquiteproject.org

McKenna, M.C. and Bell, S.K. 1997. *Classification of Mammals Above the Species Level*. 631 pp. Columbia University Press, New York.

McMurtrie, H. 1831. *The Animal Kingdom Arranged in Conformity With its Organization, by the Baron Cuvier. The Crustacea, Arachnides and Insecta, by P.A. Latreille. Translated from the French with Notes and Additions by H. M'Murtrie*. 448 pp. G. & C. & H. Carvill, New York.

Miller, G.S. 1899. Notes on the naked-tailed armadillos. *Proceedings of the Biological Society of Washington* 13: l–8.

Mitchell, K.J., Scanferla, A., Soibelzon, E., Bonini, R., Ochoa, J., and Cooper, A. 2016. Ancient DNA from the extinct South American giant glyptodont *Doedicurus* sp. (Xenarthra: Glyptodontidae) reveals that glyptodonts evolved from Eocene armadillos. *Molecular Ecology* 25: 3499–3508.

Möller-Krull, M., Delsuc, F., Churakov, G., Marker, C., Superina, M., Brosius, J., Douzery, E.J.P., and Schmitz, J. 2007. Retroposed elements and their flanking regions resolve the evolutionary history of xenarthran mammals (armadillos, anteaters, and sloths*). Molecular Biology and Evolution* 24: 2573−2582.

O'Leary, M.A., Bloch, J.I., Flynn, J.J., Gaudin, T.J., Giallombardo, A., Giannini, N.P., Goldberg, S.L., Kraatz, B.P., Luo, Z.X., Meng, J., Ni, X., Novacek, M.J., Perini, F.A., Randall, Z.S., Rougier, G.W., Sargis, E.J., Silcox, M.T., Simmons, N., Spaulding, M., Velazco, P.M., Weksler, M., Wible, J.R., and Cirranello, A. 2013. The placental mammal ancestor and the post-K-Pg radiation of placentals. *Science* 339: 662–667.

Oliveira, E.V. and Pereira, J.C. 2009. Intertropical cingulates (Mammalia, Xenarthra) from the Quaternary of Southern Brazil: Systematics and paleobiogeographical aspects. *Revista Brasileira de Paleontologia* 12: 167–178.

Oliveira, P.V., Ribeiro, A.M., Oliveira, E.V., and Viana, M.S.S. 2014. The dasypodidae (mammalia, xenarthra) from the urso fóssil cave (quaternary), parque nacional de ubajara, state of ceará, brazil: paleoecological and taxonomic aspects. *Anais da Academia Brasileira de Ciências* 86: 147–158.

Paula-Couto, C. 1979. Tratado de paleomastozoologia. *Academia Brasileira de Ciências* 15 (1): 1–590.

Pocock, R.I. 1924. The external characters of the South American edentates. *Proceedings of the Zoological Society of London* 2: 983–1031.

Rafinesque, C.S.S. 1815. *Analyse de la nature, ou tableau de l'univers et des corps organisés*, 224. L'Imprimerie de Jean Barravecchia, Palermo.

Scillato-Yané, G.J. 1977. Notas sobre los Dasypodidae (Mammalia, Edentata) del Plioceno del territorio argentino I. Los restos de edad Chasiquense (Plioceno inferior) del sur de la Provincia de Buenos Aires. *Ameghiniana* 14: 133–144.

Scillato-Yané, G.J. 1980. Catálogo de los Dasypodidae fósiles (Mammalia, Edentata) de lal República Argentina. *Actas II Congreso Argentino de Paleontología y Bioestratigrafía y I Congreso Latinoamericano de Paleontología. Buenos Aires 1978* 3: 7–36.

Scillato-Yané, G.J. 1982. *Los Dasypodidae (Mammalia: Edentata) del Plioceno y Pleistoceno de Argentina.* 127 pp. Ph.D. Thesis, Facultad de Ciencias Naturales y Museo,Universidad Nacional de La Plata, La Plata.

Sidorkewicj, N.S. and Casanave, E.B. 2013. Morphological characterization and sex-related differences of the mandible of the armadillos *Chaetophractus vellerosus* and *Zaedyus pichiy* (Xenarthra, Dasypodidae), with consideration of dietary aspects. *Iheringia. Série Zoologia* 103: 153–162.

Simpson, G.G. 1945. The principles of classification and a classification of mammals. *Bulletin of the American Museum of Natural History* 85: 1–367.

Smith, K. and Redford, K.H. 1990. The anatomy and function of the feeding apparatus in two armadillos (Dasypoda): anatomy is not destiny. *Journal of Zoology* 222: 27–47.

Squarcia, S.M., Sidorkewicj, N.S., Camina, R., and Casanave, E.B. 2009. Sexual dimorphism in the mandible of the armadillo *Chaetophractus villosus* (Desmarest, 1804) (Dasypodidae) from northern Patagonia, Argentina. *Brazilian Journal of Biology* 69: 347–352.

Thenius, E. 1989. Zähne und Gebiß der Säugetiere. *In*: J. Niethammer, H. Schliemann, and D. Starck (eds.), *Handbuch der Zoologie. Band VIII Mammalia*, 513. Verlag Walter de Gruyter, Berlin.

Urrutia, J., Montalvo, C., and Scillato-Yané, G. 2008. Dasypodidae (Xenarthra, Cingulata) de la Formación Cerro Azul (Mioceno tardío) de la provincia de La Pampa, Argentina. *Ameghiniana* 45 (2): 289–302.

Vizcaino, S.F. 1994. Mecánica masticatoria de *Stegotherium tessellatum* Ameghino (Mammalia, Xenarthra) del Mioceno de Santa Cruz (Argentina). Algunos aspectos paleoecológicos relacionados. *Ameghiniana* 31: 283–290.

Vizcaíno, S.F. and Bargo, M.S. 2014. Loss of ancient diversity of xenarthrans and the value of protecting extant armadillos, sloths and anteaters. *Edentata* 15: 27–38.

Vizcaíno, S.F. and Fariña, R.F. 1994. Caracterización trófica de los armadillos (Mammalia, Xenarthra, Dasypodidae) de Edad Santacrucense (Mioceno temprano) de Patagonia (Argentina). *Acta Geologica Leopoldensia* 39: 191–200.

Vizcaíno, S.F., Bargo, M.S., Kay, R.F., and Milne, N. 2006. The armadillos (Mammalia, Xenarthra, Dasypodidae) of the Santa Cruz Formation (early–middle Miocene): An approach to their paleobiology. *Palaeogeography, Palaeoclimatology, Palaeoecology* 237: 255–269.

Wagler, J. 1830. *Naturliches System der Amphibien, mit vorangehender Classification der Saugethiere und Vogel*, 354. J.G. Cotta'sche Buchhandlung, München.

Wetzel, R.M. 1980. Revision of the naked-tailed armadillos, genus *Cabassous* McMurtrie. *Annals of the Carnegie Museum* 49: 323–357.

Wetzel, R.M. 1985. The identification and distribution of recent Xenarthra (= Edentata). *In*: G.G. Montgomery (ed.), *The Evolution and Ecology of Armadillos, Sloths, and Vermilinguas*, 5–21. Smithsonian Institution Press, Washington, DC.

Woodburne, M.O., Goin, F.J., Raigemborn, M.S., Heizler, M., Gelfo, J.N., and Oliveira, E.V. 2014. Revised timing of the South American early Paleogene land mammal ages. *Journal of South American Earth Sciences* 54: 109–119.

Late Permian ichthyofauna from the North-Sudetic Basin, SW Poland

DARJA DANKINA, ANDREJ SPIRIDONOV, PAWEŁ RACZYŃSKI, and SIGITAS RADZEVIČIUS

Dankina, D., Spiridonov, A., Raczyński, P., and Radzevičius, S. 2021. Late Permian ichthyofauna from the North-Sudetic Basin, SW Poland. *Acta Palaeontologica Polonica* 66 (Supplement to 3): S47–S57.

The late Permian time was a transformative period before the most severe mass extinction known. Even though fishes constitute a key component of marine ecosystems since the Silurian, their biogeographic patterns during the late Permian are currently insufficiently known. The new ichthyofaunal material described here comes from the southeastern part of the Zechstein Basin, from the calcareous storm sediments alternating with marls, which were deposited in less energetic conditions. Chondrichthyans and osteichthyans are reported here for the first time from the Nowy Kościół quarry in the SW Poland. The assemblage consists of various euselachian dermal denticles, actinopterygian scales and teeth, and isolated hybodontoid tooth putatively assigned as extremely rare ?*Gansuselache* sp. from the Permian. The diverse actinopterygian tooth shapes show significant ecological differentiation of fishes exploring sclerophagous, durophagous, and herbivory modes of feeding in the given part of the Zechstein Basin suggesting the presence of complex ecosystems even in hyper-saline conditions of an epicontinental sea.

Key words: Euselachii, Actinopterygii, teeth, scales, trophic groups, Permian, Zechstein, Poland.

Darja Dankina [darja.dankina@gmail.com], Andrej Spiridonov [s.andrej@gmail.com], and Sigitas Radzevičius [sigitas.radzevicius@gf.vu.lt], Department of Geology and Mineralogy, Vilnius University, M.K. Čiurlionio st. 21/27, LT03101, Vilnius, Lithuania.
Paweł Raczyński [pawel.raczynski@uwr.edu.pl], Department of Physical Geology, Institute of Geological Sciences, University of Wrocław, Pl. Maksa Borna 9, 50-205 Wrocław, Poland.

Received 14 October 2020, accepted 5 December 2020, available online 2 June 2021.

Introduction

Ever since the Carboniferous, Osteichthyes and Chondrichthyes have been the most successful marine vertebrates (Near et al. 2012; Pindakiewicz et al. 2020). Late Permian fish fossils are widely distributed in the marine and freshwater ecosystems around Pangea (Koot 2013; Romano et al. 2016) including saline, semi-enclosed, lagoon or the playa-like Zechstein Sea in NW Europe. Fish fossils from this basin are known from Germany (Diedrich 2009), England (King 1850), East Greenland (Nielsen 1952), Latvia (Dankina et al. 2020) and Lithuania (Dankina et al. 2017).

Until now only very rare and taxonomically low diversity occurrences of the fish remains were found in the southeastern part of the Zechstein successions. Kaźmierczak (1967) putatively assigned some teeth and scales as Palaeoniscidae in the Zechstein sequences at the Kajetanów quarry in the Holy Cross Mountains, central Poland. Incomplete *Platysomus* sp. trunks were also found from the copper-bearing Zechstein layers and *Palaeoniscus* sp. trunks from the Lubin mine in SW Poland, which are stored at the University of Wroclaw.

The current study represents the first record of the ichthyofaunal assemblage from a new paleoichthyological locality—the Nowy Kościół quarry in the SW Poland. The paleoenvironmental and ecological changes in the eastern Zechstein Sea ecosystems are discussed in connection to the ecomorphological features of described teeth assemblages. The described ichthyofaunal assemblage patterns from the SW Poland shed new light on the dispersal patterns and palaeobiogeography of fishes in the Zechstein Sea.

Institutional abbreviations.—VU-ICH-NK, Geological Museum at the Institute of Geosciences of Vilnius University, Vilnius, Lithuania.

Geological setting

The Zechstein Basin in Poland is a result of widespread cyclic carbonate and evaporite sediments (Poszytek and

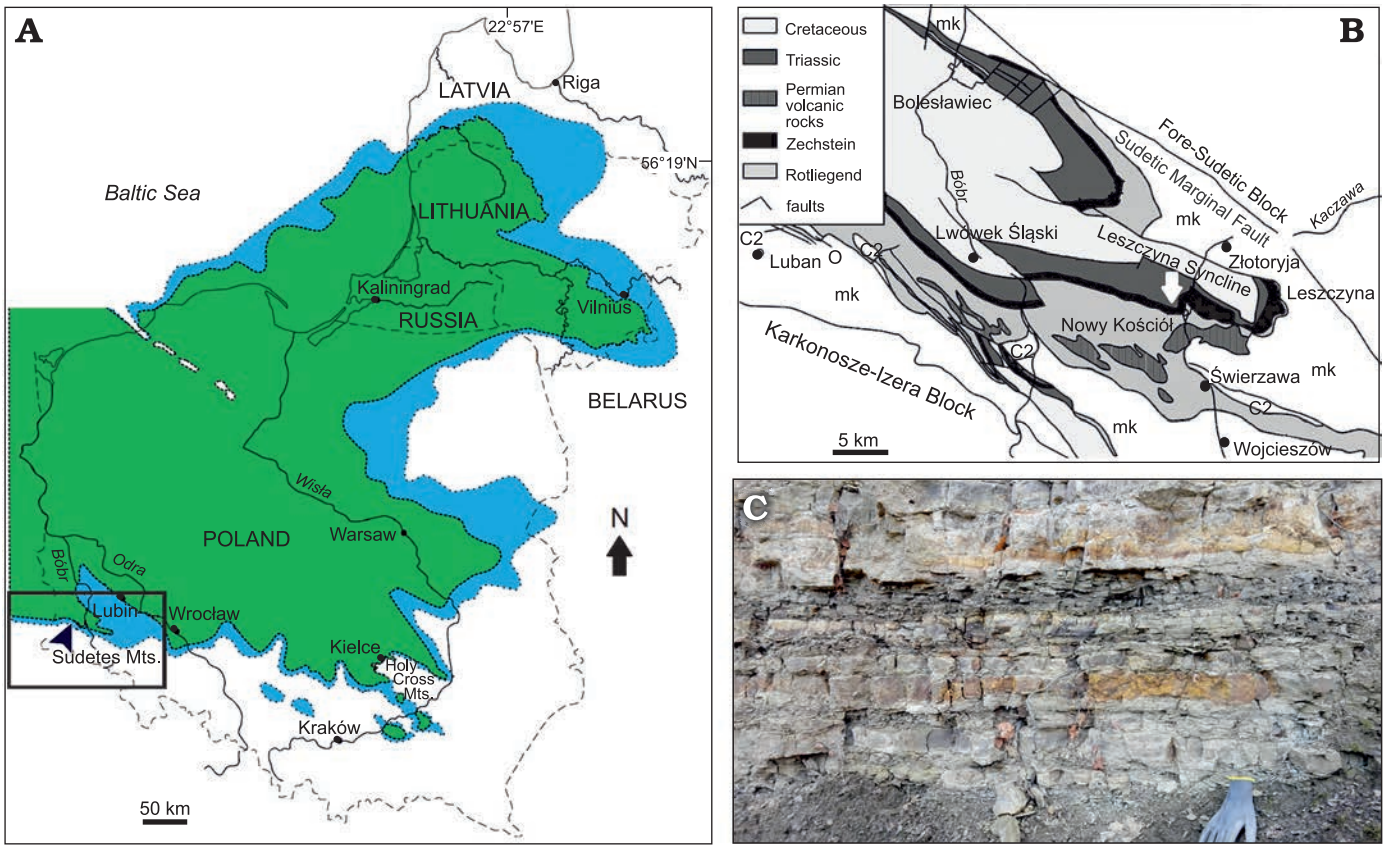

Fig. 1. Location of the late Permian fish-bearing site in SW Poland. **A**. Map of the Eastern Europe with position of Nowy Kościół (blue, the original distribution of the eastern margin of Zechstein Limestone; green, current distribution of Zechstein sediments in Poland, Russia, Lithuania, and Latvia; Raczyński and Biernacka 2014). **B**. The geological map of the North-Sudetic Basin showing location of studied site (white arrow) (after Biernacka et al. 2005). **C**. Photograph of the middle Zechstein limestone sequences of the Nowy Kościół section from 2016. mk, Kaczawa metamorphic rock; C2, Upper Carboniferous.

Suchan 2016). The studied sites of the first Zechstein cycle in SW Polish suggested an existence of a narrow zone of upper Permian sediments in the outer part of the North-Sudetic Basin (Gunia and Milewicz 1962; Raczyński 1997; Biernacka et al. 2005; Fig. 1A). The Nowy Kościół area is located in the Leszczyna Syncline in the southeastern, marginal part of the Zechstein Basin (Biernacka et al. 2005; Fig. 1B). Scupin (1933) proposed lithostratigraphic division of the upper Permian association in this part of the Zechstein Basin. According to Scupin's (1933) division, the limestone-marl association is subdivided into three main units: spotted marl, copper-bearing marl, and lead-bearing marl (Biernacka et al. 2005).

The limestone-marl sequence with the underlying Basal Limestone (micritic limestone) and overlying middle Zechstein (micro-oncolitic limestone) are equivalent to the carbonate rocks of the first evaporitic cyclothem assigned as Zechstein Limestone (Ca1) (Peryt 1978; Raczyński 1997; Biernacka et al. 2005). The duration of sedimentation of the entire first evaporitic cyclothem did not exceed two million years (Menning 1995; Biernacka et al. 2005). The upper Permian limestone-marl association was deposited in the ~20–30 km width and ~100 km length zone along the WNW-ESE stretching lagoon (Biernacka et al. 2005; Fig. 1B).

Material and methods

The studied material was collected in the Nowy Kościół quarry in SW Poland (51°5'19.654''N, 15°52'43.613''E) (Fig. 1). Sediments are mostly carbonates consisting of marl and limestone layers. In total eleven samples were collected. Two samples were taken from the Basal Limestone; three samples from copper-bearing marl; three samples from lead-bearing marl; three samples from Middle Zechstein Limestone (Fig. 2). The total weight of the collected samples reached ~128.4 kg. The average mass of each sample was ~14 kg.

The fossil-bearing samples were chemically prepared using standard chemical dissolution technique in buffered formic acid described by Jeppsson et al. (1999). The residues were dried at room temperature and sieved from 0.2 to 0.063 mm sieves in order to more effectively optically spot and pick microremains under the binocular microscope under fixed magnification. Scanning electron microscope (SEM) imaging of the selected fish remains was conducted at the Nature Research Centre (Vilnius, Lithuania).

The collected samples yielded 112 isolated chondrichthyan and osteichthyan fish microremains. The collection is housed in the Geological Museum at the Institute of Geosciences of Vilnius University (VU-ICH-NK).

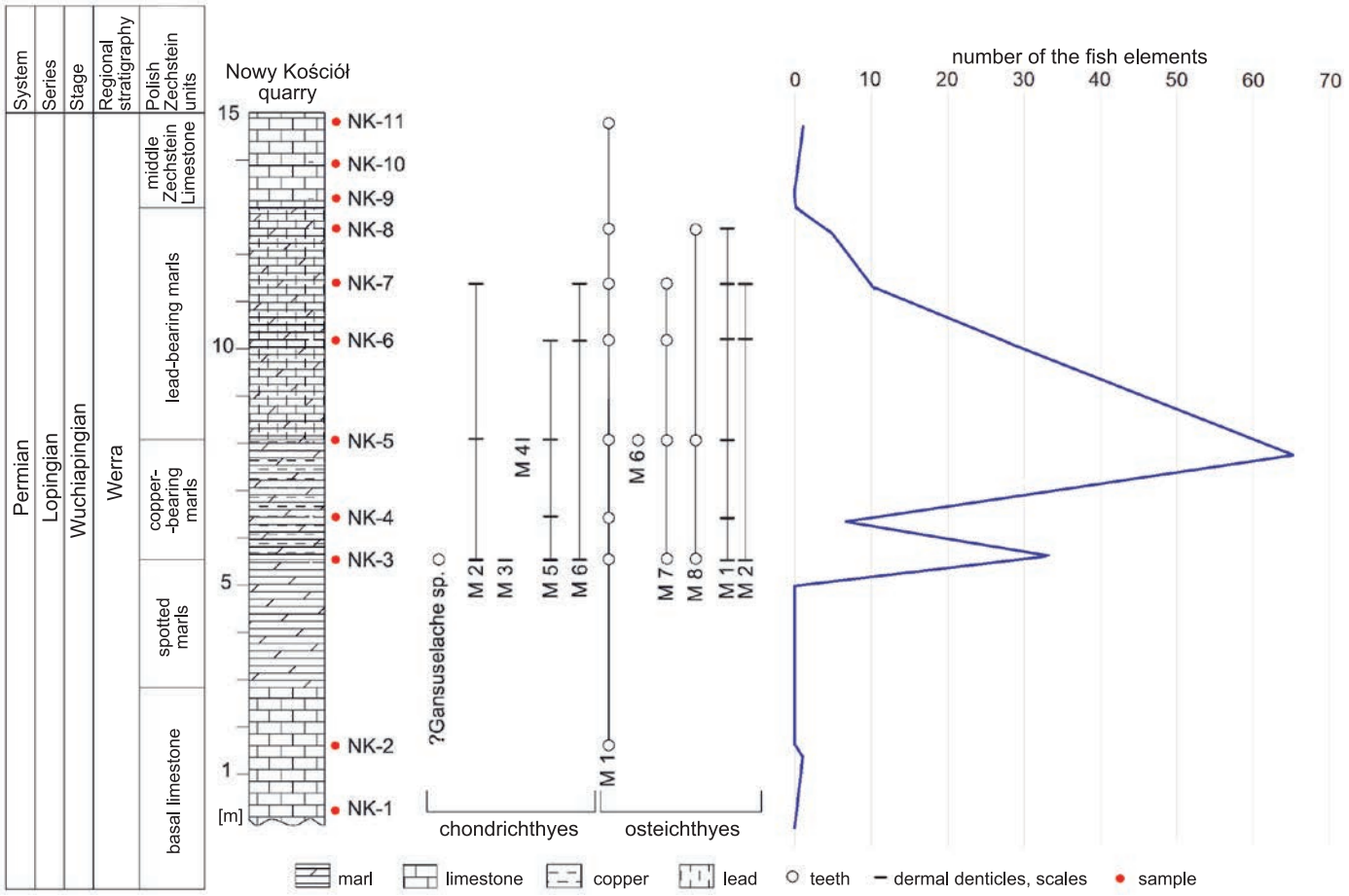

Fig. 2. Stratigraphical profile of the Nowy Kościół quarry with an indication of the late Permian fish assemblage, stratigraphic repartition of the chondrichthyan and osteichthyan taxa based on isolated teeth, dermal denticles and scales; and its vertical distribution. M, morphotype.

Systematic palaeontology

Class Chondrichthyes Huxley, 1880

Subclass Elasmobranchii Bonaparte, 1838

Order Hybodontiformes Patterson, 1966

Superfamily Hybodontoidea Owen, 1846

Family Lonchidiidae Herman, 1977

Genus *Gansuselache* Wang, Zhang, Zhu, and Zhao, 2009

Type species: *Gansuselache tungshengi* Wang, Zhang, Zhu, and Zhao, 2009; Mazongshan Mountain, Gansu Province, north-western China; Fangshankou Formation, late Permian.

?*Gansuselache* sp.

Fig. 3A.

Material.—Single isolated tooth (VU-ICH-NK-001) from the upper Permian of the Nowy Kościół Quarry, Leszczyna Syncline, SW Poland.

Description.—The tooth is mesiodistally elongate (slightly less than 3 mm in length), labiolingually compressed, low-crowned, slightly inclined lingually and near-symmetrical. The tooth crown is multicuspid; its central cusp is higher and wider than two pairs of low lateral cusplets. The cusplets are ornamented separately with two or three vertical strong ridges that continue to the root in labial and lingual face of the tooth. The tooth root is massive, higher in labial face than in the lingual one. It has some enlarged and irregular foramina on both lingual and lateral faces, which are filled by sediments. The tooth base is oval and deeply concave.

Remarks.—The teeth of ?*Ganunselache* sp. are rare in late Permian material. However, the analysed tooth here is assigned to ?*Gansuselache* sp. as it matches the following diagnosed characters: multicuspid crown, with central high cusp and lower two pairs of cusplets which are covered by vertical strong ridges. Similar teeth were found in the late Permian material of the Fangshankou Formation in north-western China (Wang et al. 2009: fig.7C).

Cohort Euselachii Hay, 1902

Euselachii indet.

Fig. 3B–R.

Material.—44 isolated dermal denticles were found from the upper Permian of the Nowy Kościół Quarry, Leszczyna Syncline, SW Poland. The dermal denticles are represented

Table 1. The different morphotypes distribution of late Permian fish remains in Latvia, Lithuania, and Poland.

	Morpho-type	Poland (Nowy Kościół)	Lithuania (Karpėnai)	Latvia (Kūmas)
Euselachii dermal denticle	M1	–	–	+
	M2	+	+	+
	M3	+	+	+
	M4	+	+	+
	M5	+	+	+
	M6	+	+	+
Actinopterygii teeth	M1	+	+	+
	M2	–	–	+
	M3	–	+	+
	M4	–	+	+
	M5	–	–	+
	M6	–	+	+
	M7	+	–	–
	M8	+	–	–
Actinopterygii scales	M1	+	+	+
	M2	+	–	+
	M3	–	–	+
	M4	–	+	+
	M5	–	–	+
	M6	–	–	+

Table 2. The main characteristics of the different morphotypes of Euselachii dermal denticles. M1–6, morphotype 1–6.

Morphotype	Crown ridges	Crown symmetry	Horizontal crown	Visible neck	Roots foramina
M1	no	yes	yes	yes	yes
M2	yes	yes	yes	yes	no
M3	partly	yes	partly	yes	yes
M4	yes	no	yes	partly	no
M5	partly	partly	no	no	no
M6	yes	partly	no	no	no

here by SEM microphotographs of microremains VU-ICH-NK-002–018.

Description.—The microremains are identified as euselachian-type dermal denticles based on resembling material from the middle Permian of the Apache Mountains in West Texas, USA (Ivanov et al. 2013); Permian of the Kanin Peninsula in Russia (Ivanov and Lebedev 2014); Lower Triassic of Oman (Koot et al. 2015); Carboniferous of Oklahoma, USA (Ivanov et al. 2017); upper Permian of Lithuania (Dankina et al. 2017), and Latvia (Dankina et al. 2020); and are divided into morphotypes based on the morphological differences between their crown, neck, and base.

The morphotype numeration and description in this study is taken from previous studies of late Permian euselachian material from southern Latvia (Dankina et al. 2020; Tables 1, 2).

Morphotype 2: Seven dermal denticles from this morphotype were found in the Nowy Kościół quarry (Fig. 3B–D). The denticles have a trident or nearly trident crown with a high, slender, and narrow neck (Fig. 3B), hidden under the crown in apical view (Fig. 3C, D). The crown sits horizontally or slightly obliquely up on the neck. The exterior of the crown is sculptured with numerous gentle convex ridges and furrows originating at the longitudinal crest and reaching 0.1–0.4 mm length. The base has a rhomboid surface and one roundish canal opening in proximal view. The denticle reaches 0.3–0.4 mm height, and 0.4–0.5 mm crowns length and width.

Morphotype 3: Four dermal denticles from this morphotype were found in the Nowy Kościół quarry (Fig. 3E–G). The roundish crown is smooth, thick, without ornamentation (Fig. 3E, F). The crown sits horizontally on the neck and reaches around 0.4–0.8 mm in diameter. The neck is wide and massive. The wide base is slightly curved, multipetaloid in shape, and with concave canal opening in the proximal view (Fig. 3G).

Morphotype 4: Two dermal denticles from this morphotype were found in the Nowy Kościół quarry (Fig. 3H, I). The denticle has a curved outline of the crown; strongly convex, with three continuous ridges joined on the top of the surface (Fig. 3H). Sometimes, the crown is flat, thick, without ornament, has a serrated margin (Fig. 3I_1). The crown is placed horizontally on the slender neck. The neck is short and narrow. The base has an indeterminate sinuous shape with deep vertical grooves along base outline. Dermal denticles reach 0.3–0.6 mm in length and 0.5–0.6 mm in width.

Morphotype 5: 21 dermal denticles from this morphotype were found in the Nowy Kościół quarry (Fig. 3J–L). The denticles have an anteriorly-inclined crown ornamented by some short ridges (4–5 ridges) on the anterior side (Fig. 3J, L). This type of denticles have a smooth, drop-like crown margin surface, which sits evidently obliquely up on the wide low neck (Fig. 3K). The crown reaches 0.4–0.5 mm length. The neck and crown widths are almost identical and approximately equal 0.3–0.4 mm (Fig. 3J). The base is flat, sinuous, multipetaloid in shape (Fig. 3L) with concave canal openings in the proximal view.

Morphotype 6: 10 dermal denticles from this morphotype were found in the Nowy Kościół quarry (Fig. 3M–

Fig. 3. Euselachian dermal denticles and hybodontoid tooth from the upper Permian of the Nowy Kościół quarry, Poland. **A**. ?*Gansuselache* sp. tooth VU-ICH-NK-001, labial (A_1) and lingual (A_2) views. **B**–**D**. Euselachian-type dermal denticles of morphotype 1. **B**. VU-ICH-NK-002, crown view. **C**. VU-ICH-NK-003, crown view. **D**. VU-ICH-NK-004, lateral view. **E**–**G**. Euselachian-type dermal denticles of morphotype 2. **E**. VU-ICH-NK-005, crown view. **F**. VU-ICH-NK-006, crown view. **G**. VU-ICH-NK-007, basal view. **H**, **I**. Euselachian-type dermal denticles of morphotype 3. **H**. VU-ICH-NK-008, apex crown view. **I**. VU-ICH-NK-008, apex crown (I_1) and basal (I_2) views. **J**–**L**. Euselachian-type dermal denticles of morphotype 4. **J**. VU-ICH-NK-010, crown view. **K**. VU-ICH-NK-011, lateral view. **L**. VU-ICH-NK-012, apex crown. **M**–**R**. Euselachian-type dermal denticles of morphotype 5. **M**. VU-ICH-NK-013, lateral crown (M_1) and lateral basal (M_2) views. **N**. VU-ICH-NK-014, apex crown (N_1) and basal (N_2) views. **O**. VU-ICH-NK-015, lateral crown view. **P**. VU-ICH-NK-016, crown view. **Q**. VU-ICH-NK-017, lateral crown view. **R**. VU-ICH-NK-018, lateral basal view. →

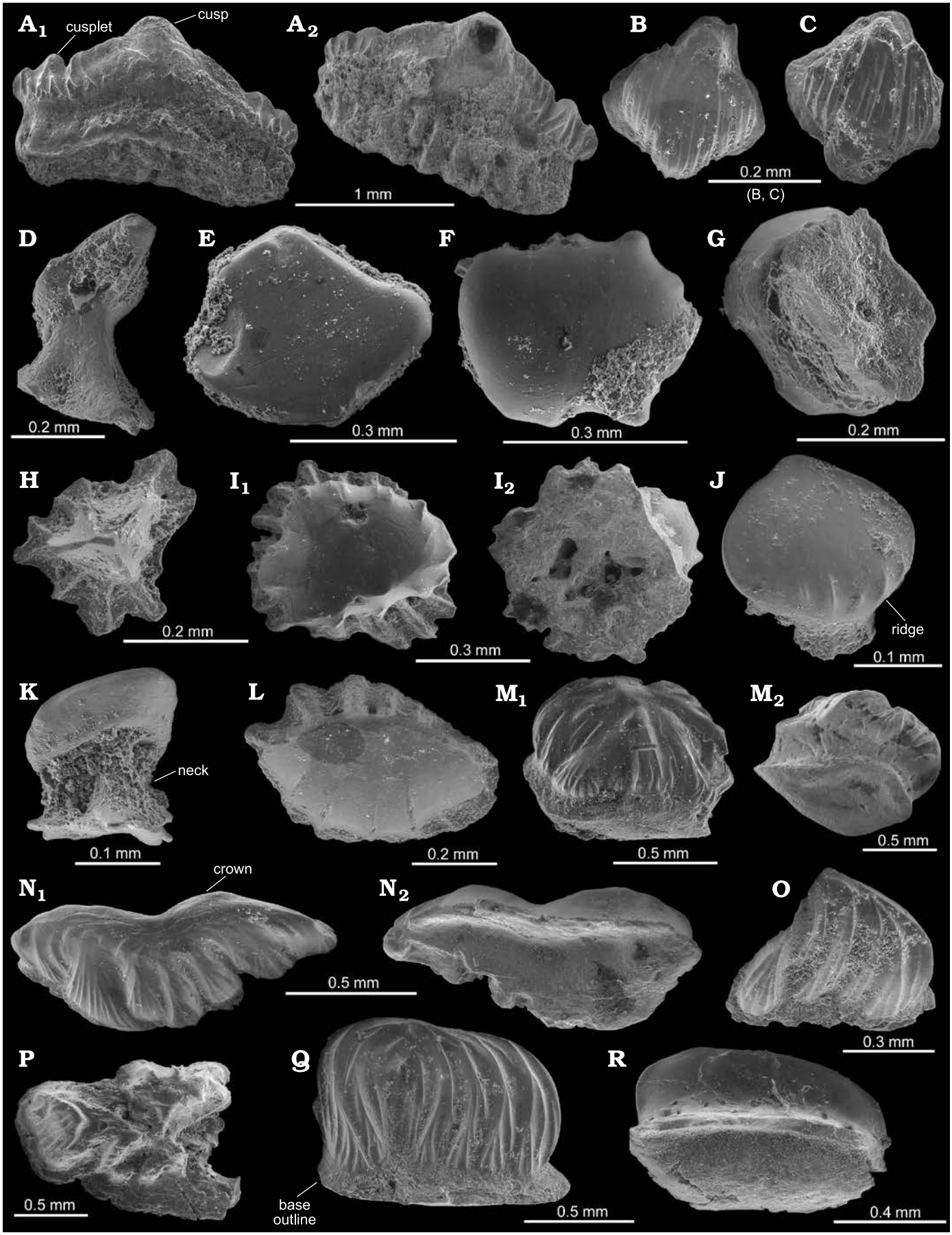
A1
cusplet
cusp
A2
1 mm
B
C
0.2 mm
(B, C)
D
0.2 mm
E
0.3 mm
F
0.3 mm
G
0.2 mm
H
0.2 mm
I1
I2
0.3 mm
J
ridge
0.1 mm
K
neck
0.1 mm
L
0.2 mm
M1
0.5 mm
M2
0.5 mm
N1
crown
N2
0.5 mm
O
0.3 mm
P
0.5 mm
Q
base
outline
0.5 mm
R
0.4 mm

R). The denticles have a complex crown shape, from very narrow, subparallel with straight ridges (Fig. 3O, Q) to wide triangular being striated by curved, branched ridges (Fig. 3P). The neck is poorly developed. The base is low and flat. Its profile has a rhomboid (Fig. $3M_2$) or polygonal outline (Fig. $3N_2$), with a slightly convex basal surface (Fig. $3M_2$) and without any foramina (Fig. 3R). These dermal denticles could reach 0.7–2.0 mm in length and 0.5–0.8 mm in height.

Remarks.—Complex shape of the morphotype 2 denticles is morphologically similar to Carboniferous chondrichthyan scales of Oklahoma, USA (Ivanov et al. 2017). Also, this morphotype is similar to Devonian–early Carboniferous ctenacanthid scales in Belarus (Ivanov and Plax 2018); Carboniferous in Lublin area, SE Poland (Ginter and Skompski 2019); and Devonian of the Holy Cross Mountains (Liszkowski and Racki 1992). The identical dermal denticles of morphotype 3 have been found and described as late Permian euselachian-type dermal denticles from Naujoji Akmenė Formation in Lithuania (Dankina et al. 2017) and Latvia (Dankina et al. 2020). A roundish denticle of morphotype 4 was interpreted as being a ?hybodont/synechodontiform scale from the Lower Triassic in Oman (Koot et al. 2015). Similar denticles but with different neck have been found and described as late Permian euselachian-type denticles from the Naujoji Akmenė Formation in Lithuania (Dankina et al. 2017) and Latvia (Dankina et al. 2020). The morphological similarities of the morphotype 5 dermal denticles (shape of the crown, roots, slender neck) have been found and described as Triassic Hybodontidae dermal denticles in Spitsbergen (Reif 1978) and as late Permian euselachian-type denticles from the Naujoji Akmenė Formation in Lithuania (Dankina et al. 2017) and Latvia (Dankina et al. 2020). The morphotype 6 denticles with similar features (shape of the crown, ornament, base) were identified as hybodontiform scales from the Upper Triassic in Germany (Reif 1978) and Middle Triassic in Spain (Manzanares et al. 2014). Also, the denticles with morphological similarities (size, trident crown, ornament) have been found and described as late Permian euselachian-type dermal denticles from the Naujoji Akmenė Formation in Lithuania (Dankina et al. 2017) and Latvia (Dankina et al. 2020).

Table 3. The main characteristics of the different morphotypes of Actinopterygii teeth. M1–8, morphotype 1–8.

Morpho-type	Surface ornament	Flat crown top	Visible roots	Tooth symmetry	Micro-tubercles
M1	no	no	partly	yes	yes
M2	yes	yes	partly	yes	yes
M3	yes	partly	no	partly	yes
M4	no	partly	partly	yes	yes
M5	no	yes	no	yes	yes
M6	yes	partly	no	partly	yes
M7	no	partly	no	partly	partly
M8	no	no	partly	yes	partly

Superclass Osteichthyes Huxley, 1880

Class Actinopterygii Cope, 1887

Actinopterygii indet. (teeth)

Fig. 4A–L.

Material.—38 isolated teeth (Fig. 4A–L) from the upper Permian of the Nowy Kościół Quarry, Leszczyna Syncline, SW Poland. The teeth are represented here by SEM microphotographs of microremains VU-ICH-NK-019–030.

Description.—The teeth divided into three morphotypes based on their different shape and enameloid microstructure. The morphotype numeration and description in this study is continued on from previous studies of the late Permian actinopterygian material from southern Latvia (Dankina et al. 2020; Tables 1, 3).

Morphotype 1: 26 teeth from this morphotype were found in the Nowy Kościół quarry (Fig. 4A–E). The canine-like teeth are conical, straight (Fig. 4A, B) or curved characterised by the "horn-like" shape (Fig. 4C), thin (Fig. 4A) or wide and convex in the central part (Fig. 4E), with an acrodin cap. Tooth surface is smooth, with no distinct visible ornament, although the microtubercles are well-developed (Fig. $4D_2$). The microtubercles are proximo-distally elongated, narrow and blend together in oblique rows (Fig. $4D_2$). Morphotype 1 teeth reach 0.4–1.2 mm in width and 0.6–1.9 mm in length.

Morphotype 7: Five teeth from this morphotype were found in the Nowy Kościół quarry (Fig. 4F–I). The molar teeth are roundish (Fig. 4F), short, slightly depressed in labial-lingual face (Fig. 4G), cylindrical in shape (Fig. 4H), and with convex outline in lateral view (Fig. 4I). The surface of these teeth is smooth with a slightly concave central part (Fig. $4F_1$, I_1). Some teeth have well-developed, vertically elongated, narrow microtubercles (Fig. $4G_1$). These teeth reach a maximum of 0.2–0.6 mm in width, 0.6–1.2 mm in length and 0.4–1.0 mm in height.

Morphotype 8: Five teeth from this morphotype were found in the Nowy Kościół quarry (Fig. 4J–L). The teeth are straight, wide, and narrow (depressed in labial-lingual face) and with well-developed, vertically elongated, narrow

Fig. 4. Actinopterygian remains from the upper Permian of the Nowy Kościół quarry, Poland. **A**–**E**. Actinopterygian teeth of morphotype 1. **A**. VU-ICH-NK-019, lateral view. **B**. VU-ICH-NK-02-20, lateral view. **C**. VU-ICH-NK-021, lateral view. **D**. VU-ICH-NK-022, lateral view (D_1), microtubercles structure (D_2). **E**. VU-ICH-NK-023, lateral view. **F**–**I**. Actinopterygian teeth of morphotype 3. **F**. VU-ICH-NK-024, externo-lateral (F_1) and basal (F_2) views, detailed tissue pattern (F_3). **G**. VU-ICH-NK-025, lateral (G_1) and external (G_2) views. **H**. VU-ICH-NK-026, lateral view. **I**. VU-ICH-NK-027, lateral (I_1) and externo-lateral (I_2) views. **J**–**L**. Actinopterygian teeth of morphotype 4. **J**. VU-ICH-NK-028, lingo-lateral (J_1) and labio-lateral (J_2) views. **K**. VU-ICH-NK-029, lingual (K_1) and labial (K_2) views. **L**. VU-ICH-NK-030, lateral view. **M**–**P**. Actinopterygian scales of morphotype 1, VU-ICH-NK-031–034, all external view. **Q**. Actinopterygian scale of morphotype 2, VU-ICH-NK-035, external view. →

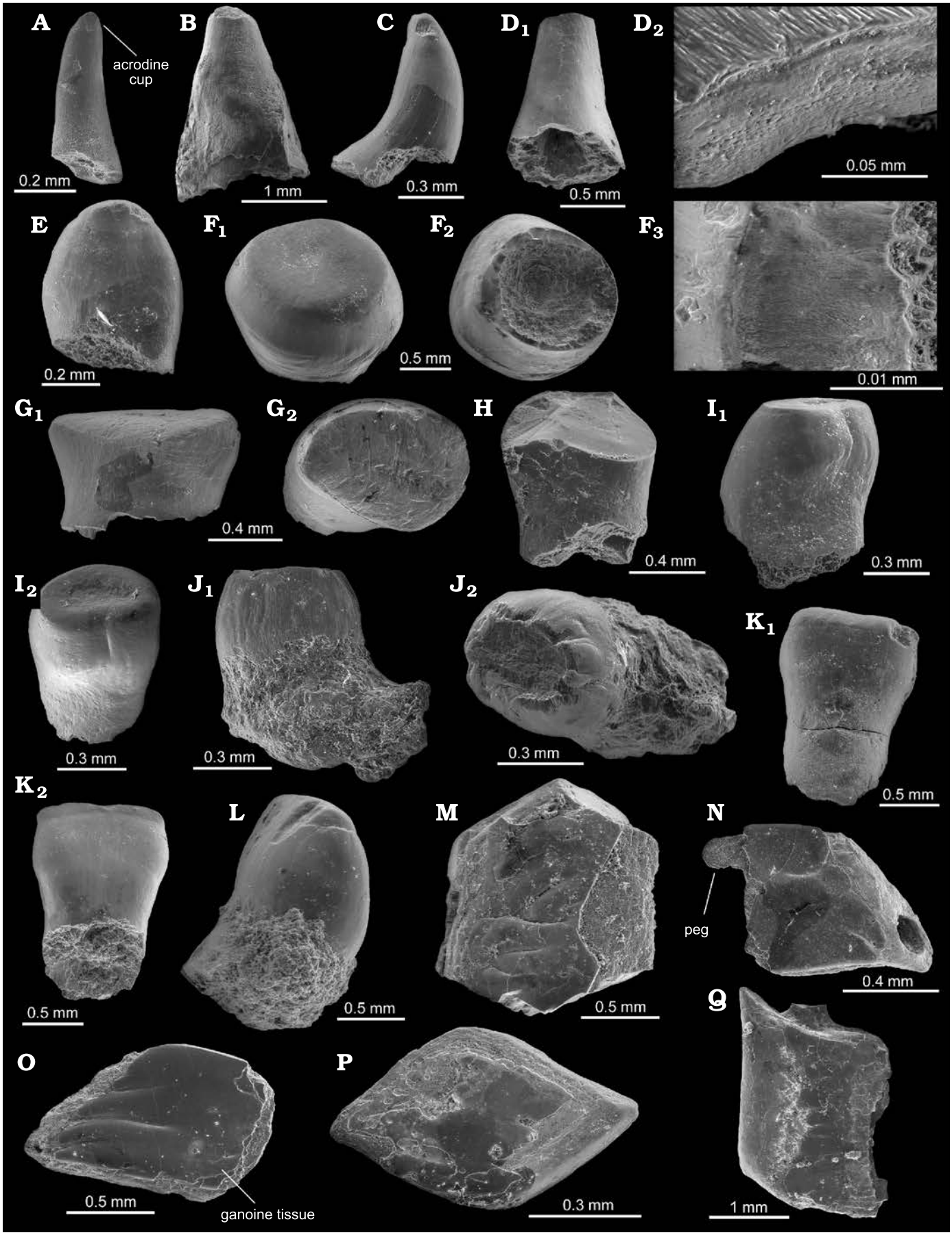
A
acrodine cup
0.2 mm
B
1 mm
C
0.3 mm
D1
0.5 mm
D2
0.05 mm
E
0.2 mm
F1
F2
0.5 mm
F3
0.01 mm
G1
G2
0.4 mm
H
0.4 mm
I1
0.3 mm
I2
0.3 mm
J1
0.3 mm
J2
0.3 mm
K1
0.5 mm
K2
0.5 mm
L
0.5 mm
M
0.5 mm
N
peg
0.4 mm
Q
1 mm
O
0.5 mm
ganoine tissue
P
0.3 mm

microtubercles (Fig. 4J). Some teeth consist of the three layers: upper layer is dark grey; middle, light grey; lower, medium grey; according to the SEM picture (Fig. 4K, L) while under microscope the tooth's upper part has the light amber acrodin (almost white); middle part is dark brown; and lower part—mid-amber colour. Rarely the tooth has concave top of the central part (Fig. 4K$_2$, L). The surface is smooth, without any ornament (Fig. 4K, L), sometimes with preserved sediments in the lower part of the tooth (Fig. 4L). These teeth reach 0.7 mm in width and 1.2 mm in height.

Remarks.—Similar Actinopterygii teeth of the morphotype 1 are known from Permian fish assemblages in Argentina (Cione et al. 2010), Latvia (Dankina et al. 2020) and Lithuania (Dankina et al. 2017). Moreover, the *Gyrolepis albertii* conical teeth with transparent acrodin cup are known from the Upper Triassic of the Westbury Formation in southwest Britain (Landon et al. 2017: fig.6A).

Actinopterygii indet. (scales)

Fig. 4M–Q.

Material.—29 scales (Fig. 4M–Q) from the upper Permian of the Nowy Kościół Quarry, Leszczyna Syncline, SW Poland. The scales are represented here by SEM microphotographs of microremains VU-ICH-NK-031–035.

Description.—The scales divided into two morphotypes relatively based on their different shape and ganoine layer characteristics. The morphotype numeration and description in this study is taken from previous studies of late Permian euselachian material from southern Latvia (Dankina et al. 2020; Tables 1, 4).

Morphotype 1: 26 scales from this morphotype were found in the Nowy Kościół quarry (Fig. 4M–P). The scales are rhombic-shaped, thick, massive and gently convex in their central part. Scales have numerous small, roundish-shaped microtubercles in the outer ganoine-covered field part (Fig. 4M–P). The surface is covered by smooth ganoine tissue (Fig. 4P), with some fine, slightly diagonally oriented, short ridges, which are separated by narrow grooves (Fig. 4O). In rare cases, scales have a well-preserved peg articulation and significantly wide anterior entry of the lateral line canal (Fig. 4N). Scales reach 0.6–1.0 mm in length and 0.4–0.6 mm in width.

Morphotype 2: Three scales from this morphotype were found in the Nowy Kościół quarry (Fig. 4Q). Elongated rhombic-shaped scale with almost right-angled (~90°) all four corners. The base is thick and convex in the central part. The scale has preserved a fragment of the peg articulation. The ganoine-covered field is smooth without any ornament. The scale reaches 2.3 mm length and 1.4 mm width.

Remarks.—The scales collection of morphotype 1 with similar morphological characteristics (rhombic shape and ganoine pattern) was found in late Permian actinopterygian scales from Lithuania (Dankina et al. 2017) and Latvia (Dankina et al. 2020). Also, rhomboidal scales are known from the middle Permian of the Apache Mountains in West Texas, USA (Ivanov et al. 2013); Permian in England (King 1850); and Permian in Argentina (Cione et al. 2010). The morphotype 2 scale seems to be similar to the Middle Triassic *Gyrolepis* sp. rhomboidal scales from the North-Sudetic Basin in Poland (Chrząstek 2013).

Table 4. The main characteristics of the different morphotypes of Actinopterygii scales. M1–6, morphotype 1–6.

Morpho-type	Ganoine top	Scale symmetry	Surface ridges	Surface grooves	Micro-tubercles	Canal openings
M1	yes	yes	no	partly	yes	yes
M2	yes	partly	no	yes	no	no
M3	yes	no	no	partly	yes	yes
M4	yes	no	yes	no	yes	no
M5	yes	no	no	no	yes	yes
M6	yes	partly	no	partly	yes	yes

Discussion

The hybodontoids are one of the best-known groups of fossil sharks and their teeth, spines and scales are common fossils in several Mesozoic rock formations (Wang et al. 2009). The new material (isolated chondrichthyan tooth) described herein is attributed to the family Lonchidiidae. This tooth has the most morphological similarities (elongate shape, low-crowned, higher central cusp and two pairs of low lateral cusplets, ornament, deep root, with irregular, numerous foramina) to the teeth of *Gansuselache* from the upper Permian of north-western China (Wang et al. 2009). Although *Lissodus* teeth are similarly shaped (Ginter et al. 2010), the main differences between them and the described tooth are blunt cusps and an absence of the coarse vertical ridge ornamentation, which descends from the tip of the cusp downwards. Additionally, no obvious labial peg was observed, which is typical for *Lissodus*. On the other hand, the geographic distribution of the genus *Gansuselache* Wang et al. (2009) first described from the late Permian deposits in north-western China, is poorly known. However, the Lonchidiidae remains are more widely distributed and known from the Permian of the Kanin Peninsula, Arkhangelsk Region in Russia (Ivanov and Lebedev 2014); lower Permian of Germany (Hampe 1996); and middle Permian of central Japan (Yamagishi and Fujimoto 2011).

Herein, actinopterygian teeth are divided into three different morphotypes based on the various shapes. The tooth form is mainly determined by the different types of food ray-finned fishes consume. Every trophic group is characterised by a certain mode of feeding, suited type of diet, and specific morphofunctional adaptations of jaws and teeth (Esin 1997). According to Esin (1997) who described major trophic groups of fish, "morphotype 1" with a small canine-like shape suggests "specialised sclerophagous"

and "small predator" diets. The small predatory teeth are conical with acute terminations (Fig. 4A, B). Sometimes this morphotype of teeth are high, conic, slightly turned back into the mouth (Fig. 4C) and high-conic with blunt top shapes (Fig. 4E). Smaller teeth (presumably of juvenile individuals) of this type are covered with numerous acute microtubercles (Fig. 4D). Fishes with similar teeth shape mostly fed on crustaceans with hard shells and also on aquatic insects (Esin 1997). The earliest aquatic insects are known from the early Permian (Sinitshenkova 2003). This type of feeding could be compared to that of modern chubs or perch, which diets include arthropods, small fishes and vegetation (Esin 1997). The Permian genera, such as *Acropholis*, *Acrolepsis*, *Palaeoniscum*, *Elonichthys*, *Varialepis* are characterised by this tooth ecomophotype (Esin 1997). *Acropholis* remains are known from the Permian of Greenland (Aldinger 1937) and Russia (Nurgaliev et al. 2015); *Acrolepsis* was found in Permian sequences of Germany (Diedrich 2009), the United Kingdom (King 1850) and Russia (Nurgaliev et al. 2015); Permian *Palaeoniscum* was found in United Kingdom (King 1850); Germany (Diedrich 2009), Russia (Nurgaliev et al. 2015), Turkey (Hoşgör and Štamberg 2014); Permian *Elonichthys* are known from Greenland (Aldinger 1937) and Russia (Nurgaliev et al. 2015); while Permian *Varialepis* was found in Russia (Tverdokhlebov et al. 2005; Nurgaliev et al. 2015), and USA (Ivanov et al. 2013).

Morphotype 7 teeth suggest durophagous-type mode of feeding. These teeth are rod-shaped or slightly depressed cylinders with rounded and almost rounded flat or concave apex (Fig. 4F–I). These teeth most likely were used for crushing and grinding of hard external skeletons, such as shells (Purnell and Darras 2015) of molluscs or brachiopods as well as possibly soft-bodied invertebrates (polychaetes) (Esin 1997). Productid brachiopods, and many species of bivalves were common in the Zechstein strata and are known from the Holy Cross Mountains, Poland (Kaźmierczak 1967), England (Ramsay 1878), and Lithuania (Suveizdis 1975). Also, polychaetes are known from the upper Permian of Poland (Szaniawski 1968). This type of teeth can be compared to the modern breams in their mode of life (Esin 1997). Morphotype 8 teeth are interpreted here to represent a "grazing" trophic mode (Fig. 4J–L). These teeth come in a variety of different shapes, others are characterised by the saw-edge or even are fused into the "beak", like in modern parrotfishes. The wide and thin teeth are adapted for feeding on water vegetation, apparently used for cutting thin threadlike algae (Esin 1997). This morphotype of teeth is characterised by the herbivorous diet, which is very similar to Recent freshwater teleosts, such as characiforms and cichlids (Pindakiewicz et al. 2020).

The morphotype diversity of fish teeth from the upper Permian in the SW Poland indicates that ray-finned fishes already started wide exploration of different feeding modes before the onset of the Mesozoic.

Conclusions

The micropaleontological study of the late Permian fish assemblages from the distal storm deposits of the Nowy Kościół quarry revealed assemblages that are composed of non-abundant but relatively diverse isolated microremains of different fish taxa, including euselachian dermal denticles, diverse actinopterygians scales and teeth, and ?*Gansuselache* sp. tooth. The finding of the later taxon significantly extends the known geographic distribution of this hybodontiform genus (or closely related forms), which was previously known only from China.

The stratigraphic distribution of fish remains and in particular their abundance in Nowy Kościół site shows high congruence with the Werra marine transgression. This transgression created the favourable conditions for flourishing of fish fauna in the Zechstein Basin. The highest abundance of fish microremains and their diversity was found at the boundary between copper-bearing and lead-bearing marl sequences in Nowy Kościół quarry. The association of transgression with higher abundance of ichtyofauna could be explained by two-fold effect. Transgression should have positively affected abundance by increasing runoff of nutrients from surrounding terrain in a warmer climate, and diluting hyper-saline waters. On other hand warmer climates, which accompany transgressions, should have promoted effectiveness of biomass transfer to the higher trophic levels occupied by fishes by physiologically reinvigorating predation efficiency (Britten and Sibert 2020).

The diverse morphology of actinopterygian denticulation demonstrates the prevalence of three trophic groups in the eastern Zechstein Sea margin. Those groups are inferred based on the three ecomorphotypes, which dominate the assemblages: (i) morphotype 1, teeth of specialised sclerophagous and small predators; (ii) morphotype 7, the crushing and grinding teeth of durophagous-type; (iii) morphotype 8, peg-like teeth adapted for herbivory or general grazing. The actinopterygian teeth material indicates that small generalized predators dominated among the recorded ichthyofauna. The diversity of different types of teeth indicates an onset of active ecomorphological specialization among the fish taxa, which further strengthens the case that the roots of Mesozoic Marine Revolution were set in Palaeozoic.

Acknowledgements

The authors would like to thank Michał Ginter (University of Warsaw, Poland) and anonymous reviewer for significantly improving the manuscript. Also, we would like to express our thanks to Vaida Kirkliauskaitė (Vilnius University, Lithuania), who helped safely transport samples. Many thanks to Laurynas Šiliauskas (Nature Research Centre, Lithuania) for the SEM micrographs. This research was carried out by the Open Access to the research infrastructure of the Nature Research Centre (Vilnius) under the Lithuanian open access network initiative. The field work in Poland was financed by Sepkoski Grant 2018 of Paleontological Society (PaISIRP).

References

Aldinger, H. 1937. Permische ganoidfische aus Ostgrönland. *Meddelelser om Grønland* 102 (3): 1–392.

Biernacka, J., Borysiuk, K., and Raczyński, P. 2005. Zechstein (Ca1) limestone-marl alternations from the North-Sudetic Basin, Poland: depositional or diagenetic rhythms? *Geological Quarterly* 49: 1–14.

Bonaparte, C.L.J.L. 1838. Selachorum tabula analytica. *Nuovi Annali delle Scienze Naturali* 1: 195–214.

Britten, G.L. and Sibert, E.C. 2020. Enhanced fish production during a period of extreme global warmth. *Nature communications* 11: 1–6.

Chrząstek, A. 2013. Trace fossils from the Lower Muschelkalk of Raciborowice Górne (North Sudetic Synclinorium, SW Poland) and their palaeoenvironmental interpretation. *Acta Geologica Polonica* 63: 315–353.

Cione, A.L., Gouiric-Cavalli, S., Mennucci, J.A., Cabrera, D.A. and Freije, R.H. 2010. First vertebrate body remains from the Permian of Argentina (Elasmobranchii and Actinopterygii). *Proceedings of the Geologists' Association* 121: 301–312.

Cope, E.D. (1887). Zittel's manual of paleontology. *American Naturalist* 17: 1014–1019.

Dankina, D., Chahud, A., Radzevičius, S., and Spiridonov, A. 2017. The first microfossil record of ichthyofauna from the Naujoji Akmenė Formation (Lopingian), Karpėnai Quarry, North Lithuania. *Geological Quarterly* 61: 602–610.

Dankina, D., Spiridonov, A., Stinkulis, Ģ., Manzanares, E., and Radzevičius, S. 2020. A late Permian ichthyofauna from the Zechstein Basin, Lithuanian-Latvian Region. *Journal of Iberian Geology* 46: 1–21.

Diedrich, C.G. 2009. A coelacanthid-rich site at Hasbergen (NW Germany): taphonomy and palaeoenvironment of a first systematic excavation in the Kupferschiefer (upper Permian, Lopingian). *Palaeobiodiversity and Palaeoenvironments* 89: 67–94.

Esin, D.N. 1997. Peculiarities of trophic orientation changes in palaeoniscoid assemblages from the upper Permian of the European part of Russia. *Modern Geology* 21: 185–196.

Ginter, M. and Skompski, S. 2019. The squamation of "*Ctenacanthus*" *costellatus* (Chondrichthyes: Ctenacanthiformes) from the Carboniferous of Lublin area, south-eastern Poland. *Acta Geologica Polonica* 69: 571–582.

Ginter, M., Hampe, O., Duffin, C.J., and Schultze, H.-P. 2010. *Handbook of Paleoichthyology. Volume 3D. Chondrichthyes. Paleozoic Elasmobranchii: Teeth*. 168 pp. Verlag Dr. Friedrich Pfeil, München.

Gunia, T. and Milewicz, J. 1962. Development of the Zechstein in the North-Sudetic Basin. *Biuletyn Państwowego Instytutu Geologicznego* 173: 115–126.

Hampe, O. 1996. Dermale Skelettreste von *Lissodus* (Chondrichthyes: Hybodontoidea) aus dem Unterperm des Saar-Nahe-Beckens. *Paläontologische Zeitschrift* 70: 225–243.

Hay, O.P. 1902. Bibliography and catalogue of the fossil vertebrata of North America. *Bulletin of the United States Geological Survey* 179: 1–868.

Herman, J. 1977. Les Sélaciens des terrains néocrétacés & paléocènes de Belgique & des contrées limitrophes. Eléments d'une biostratigraphie intercontinentale. *Mémoires pour servir à l'explication des Cartes géologiques et minières de la Belgique* 15: 1–450.

Hoşgör, I. and Štamberg, S. 2014. A first record of late middle Permian actinopterygian fish from Anatolia, Turkey. *Acta Geologica Polonica* 64: 147–159.

Huxley, T.H. 1880. On the application of the laws of evolution to the arrangement of the Vertebrata and more particularly of the Mammalia. *Proceedings of the Zoological Society of London* 43: 649–662.

Ivanov, A.O. and Lebedev, O.A. 2014. Permian chondrichthyans of the Kanin Peninsula, Russia. *Paleontological Journal* 48: 1030–1043.

Ivanov, A.O. and Plax, D.P. 2018. Chondrichthyans from the Devonian–Early Carboniferous of Belarus. *Estonian Journal of Earth Sciences* 67: 43–58.

Ivanov, A.O., Nestell, G.P., and Nestell, M.K. 2013. Fish assemblage from the Capitanian (middle Permian) of the Apache Mountains, West Texas, USA. *The Carboniferous–Permian Transition: Bulletin* 60: 152–160.

Ivanov, A.O., Seuss, B., and Nützel, A. 2017. The fish assemblage from the Pennsylvanian Buckhorn Asphalt Quarry Lagerstätte (Oklahoma, USA). *Paläontologische Zeitschrift* 91: 565–576.

Jeppsson, L., Anehus, R., and Fredholm, D. 1999. The optimal acetate buffered acetic acid technique for extracting phosphatic fossils. *Journal of Paleontology* 73: 964–972.

Kaźmierczak, J.O. 1967. Morphology and palaeoecology of the productid *Horridonia horrida* (Sowerby) from Zechstein of Poland. *Acta Palaeontologica Polonica* 12: 239–264.

King, W. 1850. The Permian fossils of England. *Monograph of the Palaeontographical Society of London* 37: 1–253.

Koot, M.B. 2013. *Effects of the Late Permian Mass Extinction on Chondrichthyan Palaeobiodiversity and Distribution Patterns*. 859 pp. Ph.D. dissertation, University of Plymouth, Plymouth.

Koot, M.B., Gilles, C., Orchard, M.J., Richoz, S., Hart, M.B., and Twitchett, R.J. 2015. New hybodontiform and neoselachian sharks from the Lower Triassic of Oman. *Journal of Systematic Palaeontology* 13: 891–917.

Landon, E.N., Duffin, C.J., Hildebrandt, C., Davies, T.G., Simms, M.J., and Benton, M.J. 2017. The first discovery of crinoids and cephalopod hooklets in the British Triassic. *Proceedings of the Geologists' Association* 128: 360–373.

Liszkowski, J. and Racki, G. 1992. Ichthyoliths and deepening events in the Devonian carbonate platform of the Holy Cross Mountains. *Acta Palaeontologica Polonica* 37: 407–426.

Manzanares, E., Plá, C., Martínez-Pérez, C., Rasskin, D., and Botella, H. 2014. The enameloid microstructure of euselachian (Chondrichthyes) scales. *Paleontological Journal* 48: 1060–1066.

Menning, M. 1995. A numerical time scale for the Permian and Triassic Periods. *In*: P.A. Scholle, T. Peryt, D.S. Ulmer-Scholle (eds.), *The Permian of Northern Pangea. Vol. 1: Paleogeography, Paleoclimates, Stratigraphy*, 77–97. Springer, Heidelberg.

Near, T.J., Eytan, R.I., Dornburg, A., Kuhn, K.L., Moore, J.A., Davis, M.P., Wainwright, P.C., Friedman, M., and Smith, W.L. 2012. Resolution of ray-finned fish phylogeny and timing of diversification. *Proceedings of the National Academy of Sciences* 109: 13698–13703.

Nielsen, E. 1952. On new or little known Edestidae from the Permian and Triassic of East Greenland. *Palaeozoologica Groenlandica* 6: 5–55.

Nurgaliev, D.K., Silantiev, V.V., and Nikolaeva, S.V. (eds.) 2015. *Type and Reference Sections of the Middle and Upper Permian of the Volga and Kama River Regions. A Field Guidebook of XVIII International Congress on Carboniferous and Permian.* 208 pp. Kazan University Press, Kazan.

Owen, R. 1846. *Lectures on comparative anatomy and Physiology of Vertebrate Animals. Part 1. Fishes*. 51 pp. Royal College of Physicians of London, London.

Patterson, C. 1966. British Wealden sharks. *Bulletin of the British Museum (Natural History)* 11: 283–350.

Peryt, T.M. 1978. Sedimentology and paleoecology of the Zechstein Limestone (upper Permian) in the Fore-Sudetic area (western Poland). *Sedimentary Geology* 20: 217–243.

Pindakiewicz, M., Tałanda, M., Sulej, T., Niedźwiedzki, G., Sennikov, A.G., Bakaev, A S., Bulanov, V.V., Golubev, V.K., and Minikh, A. 2020. Feeding convergence among ray-finned fishes: teeth of the herbivorous actinopterygians from the latest Permian of East European Platform, Russia. *Acta Palaeontologica Polonica* 65: 71–79.

Poszytek, A. and Suchan, J. 2016. A tight-gas reservoir in the basinal facies of the upper Permian Ca1 in the southwestern Zechstein Basin, Poland. *Facies* 62: 1–13.

Purnell, M.A. and Darras, L.P. 2015. 3D tooth microwear texture analysis in fishes as a test of dietary hypotheses of durophagy. *Surface Topography: Metrology and Properties* 4: 014006.

Raczyński, P. 1997. Depositional conditions and paleoenvironments of the Zechstein deposits in the North Sudetic Basin, SW Poland. *Przegląd Geologiczny* 45: 693–699.

Ramsay, W. 1878. A synopsis of the genus *Pomatorhinus*. *Ibis* 20: 129–145.
Reif, W.E. 1978. Types of morphogenesis of the dermal skeleton in fossil sharks. *Paläontologische Zeitschrift* 52: 110–128.
Romano, C., Koot, M. B., Kogan, I., Brayard, A., Minikh, A.V., Brinkmann, W., Bucher, H., and Kriwet, J. 2016. Permian–Triassic Osteichthyes (bony fishes): diversity dynamics and body size evolution. *Biological Reviews* 9: 106–147.
Scupin, H. 1933. Der Buntsandstein der Nordsudeten. *Zeitschrift der Deutschen Geologischen Gesellschaft* 85: 161–189.
Sinitshenkova, N.D. 2003. Main ecological events in aquatic insects history. *Acta Zoologica Cracoviensia* 46: 381–392.
Suveizdis, P.I. 1975. *Permskaâ sistema Pribaltiki (fauna i stratigrafiâ)*. 305 pp. Mintis, Vilnius.
Szaniawski, H. 1968. Three new polychaete jaw apparatuses from the upper Permian of Poland. *Acta Palaeontologica Polonica* 13: 252–281.
Tverdokhlebov, V.P., Tverdokhlebova, G.I., Minikh, A.V., Surkov, M.V., and Benton, M.J. 2005. Upper Permian vertebrates and their sedimentological context in the South Urals, Russia. *Earth-Science Reviews* 69: 27–77.
Wang, N.Z., Zhang, X., Zhu, M., and Zhao, W.J. 2009. A new articulated hybodontoid from late Permian of northwestern China. *Acta Zoologica* 90: 159–170.
Yamagishi, H. and Fujimoto, T. 2011. Chondrichthyan remains from the Akasaka Limestone Formation (Middle Permian) of Gifu Prefecture, Central Japan. *Bulletin of the Kanagawa Prefectural Museum of Natural Science* 40: 1–6.

First aphidiine wasp from the Sakhalinian amber

ELENA M. DAVIDIAN, MARYNA O. KALIUZHNA, and EVGENY E. PERKOVSKY

Davidian E.M., Kaliuzhna M.O., and Perkovsky E.E. 2021. First aphidiine wasp from the Sakhalinian amber. *Acta Palaeontologica Polonica* 66 (Supplement to 3): S59–S65.

The first ichneumonoid aphidiine wasp species from Sakhalinian amber (middle Eocene) is described. *Ephedrus rasnitsyni* Davidian and Kaliuzhna sp. nov. is the oldest named aphidiine female, the first fossil aphidiine from Asia, and the oldest named species of the *Ephedrus*. *Ephedrus rasnitsyni* Davidian and Kaliuzhna sp. nov. and the two fossil species of *Ephedrus*, i.e., *Ephedrus primordialis* from Baltic amber (late Eocene) and *Ephedrus mirabilis* from Camoins-les-Bains (early Oligocene), presumably belong to the *Ephedrus plagiator* species group of the subgenus *Ephedrus* sensu stricto, and new species differs from them in having a longer petiole and a rather long 3M vein that does not reach the forewing margin. It additionally differs from *E. primordialis* by having longer ovipositor sheaths. The new species is most similar to the extant *Ephedrus validus* and *Ephedrus carinatus,* from which it differs by the less elongated F1, absence of notauli, and by ovipositor sheaths that are 3.0 times as long as wide.

Key words: Hymenoptera, Ichneumonoidea, Braconidae, Aphidiinae, Eocene, Oligocene, Baltic amber, Sakhalinian amber.

Elena M. Davidian [GDavidian@yandex.ru; ORCID: https://orcid.org/0000-0003-3804-4618], All-Russian Institute of Plant Protection (FSBSI VIZR), Podbelskogo, 3, St. Petersburg – Pushkin, 196608 Russian Federation.
Maryna O. Kaliuzhna [kaliuzhna.maryna@gmail.com; ORCID: https://orcid.org/0000-0002-9265-0195], I.I. Schmalhausen Institute of Zoology of NAS of Ukraine, B. Khmelnytskogo Str. 15, 01030 Kyiv, Ukraine.
Evgeny E. Perkovsky [perkovsk@gmail.com; ORCID: https://orcid.org/0000-0002-7959-4379], I.I. Schmalhausen Institute of Zoology of NAS of Ukraine, B. Khmelnytskogo Str. 15, 01030 Kyiv, Ukraine; A.A. Borissiak Paleontological Institute of the Russian Academy of Sciences, Profsoyuznaya Str. 123, 117997 Moscow, Russian Federation.

Received 15 October 2020, accepted 8 January 2021, available online 11 June 2021.

Introduction

Middle Eocene Sakhalinian amber (43–47 Ma) is the typical rumanite from the Dolinsk District (south of Sakhalin Island). It is much older than European succinites (Kodrul 1999; Perkovsky et al. 2007; Baranov et al. 2015), and its biota is poorly studied (Simutnik 2014, 2015, 2020; Fedotova and Perkovsky 2016; Radchenko and Perkovsky 2016; Marusik et al. 2018; Dietrich and Perkovsky 2019; Azar and Maksoud 2020; Batelka et al. 2020; Perkovsky et al. 2021; Tykhonenko et al. 2021). Aphids are extremely abundant in Sakhalinian amber. Only Late Cretaceous *Baeomorpha* Realm faunas display similar abundance of aphids (Gumovsky et al. 2018). Sakhalinian amber fauna is unique for Cenozoic amber in the rarity of ants (Kazantsev and Perkovsky 2019, and references therein), with only a single species of cantharine beetles as an aphid predator (Kazantsev and Perkovsky 2019). Thus, there is a high abundance of aphid parasitoids in Sakhalinian amber, unknown from any other amber fauna (Rasnitsyn 1980).

Aphidiinae is a small, globally distributed subfamily of specialized aphid parasitoids belonging to Braconidae, Hymenoptera (Yu et al. 2016; Chen and van Achterberg 2019), but it was once considered a separate family within Ichneumonoidea (Starý 1970; Tobias and Chiriac 1986; Davidian 2007, 2018, 2019). According to different estimates, there are 505 (Žikić et al. 2017) to 619 (Yu et al. 2016) extant species of aphidiines recognized worldwide, and the process of generic revision and new species description continues (Rakhshani et al. 2017; Čkrkić et al. 2019; Kocić et al. 2019, 2020; Tomanović et al. 2020). More than half of all species are known from the Palaearctic Region (Yu et al. 2016). Aphidiines are an essential part of the aphidophagous guild, and due to their practical importance, this group is well studied (Žikić et al. 2017; Chen and van Achterberg 2019); however, questions remain regarding the evolution and phylogeny of the group (Belshaw and Quicke 1997; Belshaw et al. 2000; Sanchis et al. 2000; Ortega-Blanco et al. 2009; Chen and van Achterberg 2019) and genera therein (Gärdenfors 1986; Kocić et al. 2019, 2020; Čkrkić et al. 2020). The study of fossil material may contribute to resolving these problems.

The fossil fauna of Aphidiinae includes 14 genera and 26 species (Ortega-Blanco et al. 2009). The oldest fossil genus and species, *Archephedrus stolamissus* Ortega-Blanco, Bennett, Delclòs, and Engel, 2009, was described from a single male specimen from the late Albian (Early Cretaceous) Álava amber of Spain (Ortega-Blanco et al. 2009), and this species was assigned to Ephedrini (Yu et al. 2016). The majority of fossil aphidiines have been described from the early Rupelian (Oligocene) Anna pit in the Alsace potash field (Quilis 1940; Starý 1973; Berger et al. 2005; Ortega-Blanco et al. 2009). Aphidiinae are also found in the late Eocene Baltic (Brues 1933; Starý 1970, 1973) and Rovno ambers (MOK and EEP unpublished data). Aphidiines are prevalent in middle Eocene Sakhalinian amber (Rasnitsyn 1980); however, detailed study is in its infancy, with short reports on *Ephedrus* Haliday, 1833, specimens (Kaliuzhna et al. 2019) and the differentiation of possible new species (Kaliuzhna et al. 2020).

Ephedrus contains about 50 living and extinct species altogether, most of which are known from the Palaearctic Region (Yu et al. 2016; Kocić et al. 2019; Tomanović et al. 2020). Among Ephedrini, the *Ephedrus* is the only genus with rich extant fauna and includes two fossil species described from Europe (Oligocene of France and Baltic amber; Yu et al. 2016). Diagnostic morphological characters of the genus are 11-segmented antennae in both sexes (an exception is *E. antennalis* Tomanović, 2020, described from a single female with 12-segmented antennae), complete venation of the forewing, with present 2RS and r-m veins, and also seven complete cells (marginal, 1st and 2nd submarginal, 1st discal, basal, subbasal, and 1st subdiscal). The ovipositor sheaths are more or less elongate, straight or slightly curved upward, usually with sparse setae.

According to the review by Kocić et al. (2019), the extant fauna of the *Ephedrus* is represented by three subgenera: *Ephedrus* sensu stricto, *Breviephedrus* Gärdenfors, 1986, and *Fovephedrus* Chen, 1986. The monotypic subgenus *Lysephedrus* Starý, 1958, is assigned by the same authors as a junior synonym of *Ephedrus* sensu stricto, according to the results of molecular analysis (Kocić et al. 2019). The fossil species *Ephedrus primordialis* Brues, 1933, from Baltic amber and *E. mirabilis* Timon-David, 1944, from early Oligocene Camoins-les-Bains Marls near Marseille presumably belong to the subgenus *Ephedrus* sensu stricto as far as we can conclude from the original descriptions (Brues 1933; Timon-David 1944).

Institutional abbreviations.—FSBSI VIZR, All-Russian Institute of Plant Protection, St. Petersburg-Pushkin, Russian Federation; PIN, A.A. Borissiak Paleontological Institute of the Russian Academy of Sciences, Moscow, Russian Federation; SIZK, I.I. Schmalhausen Institute of Zoology of NAS of Ukraine, Kyiv, Ukraine.

Other abbreviations.—F1–F9, antennal flagellomeres; Pt, pterostigma; r, cross vein connecting pterostigma and radial sector; RS, radial sector; 3RSa, the first section of 3rd abscissa of radial sector; 3M, 3rd abscissa of media; 2RS, 2nd abscissa of radial sector; r-m, cross vein connecting radius and media.

Nomenclatural acts.—This published work and the nomenclatural act it contains, have been registered in ZooBank: urn:lsid:zoobank.org:pub:CBF2F8F0-B33C-4A4E-A6CA-0FAA15FD3084.

Material and methods

Amber insects were collected in the southern part of Sakhalin Island, Russian Far East, by an expedition of the Paleontological Institute of Academy of Science of USSR in 1972 (Dietrich and Perkovsky 2019, and references therein).

In total, 36 amber specimens were studied under Axio Imager M1 Carl Zeiss microscope in FSBSI VIZR and under Leica Z16 APO microscope equipped with a Leica DFC 450 camera and LAS V3.8 software in SIZK. Photos were made using Axio Imager M1 Carl Zeiss microscope in FSBSI VIZR. The examined material housed in PIN.

Classification of aphids is given after Heie and Węgierek (2009). The morphological terminology used in this paper follows Sharkey and Wharton (1997) and Hymenoptera Anatomy Ontology Project, the latter is an illustrated glossary of morphological terms (Hymenoptera Anatomy Consortium available online at http://glossary.hymao.org).

Systematic palaeontology

Order Hymenoptera Linnaeus, 1758

Superfamily Ichneumonoidea Latreille, 1802

Family Braconidae Nees, 1811

Subfamily Aphidiinae Haliday, 1833

Genus *Ephedrus* Haliday, 1833

Type species: *Bracon plagiator* Nees, 1811; Sickershausen, Germany (destroyed); Hermanovce, Preśovské hory, Slovakia (neotype), extant.

Ephedrus rasnitsyni Davidian and Kaliuzhna sp. nov.

Figs. 1, 2.

2008 Aphidiinae (Braconidae); Zherikhin et al. 2008: 197, text-fig. 76.

Zoobank LSID: urn:lsid:zoobank.org:act:7C703563-7681-41BC-AA73-824655228560

Etymology: The species named after famous paleoentomologist Alexandr Pavlovich Rasnitsyn.

Holotype: PIN 3387/79, single female imago.

Type locality: Starodubskoye, Dolinsk District, Sakhalin Province, Sakhalin Island, Russian Federation.

Type horizon: Middle Eocene.

Diagnosis.—The complete pubescence of the elongate ovipositor sheaths (Fig. 1A$_4$) distinguishes the new species

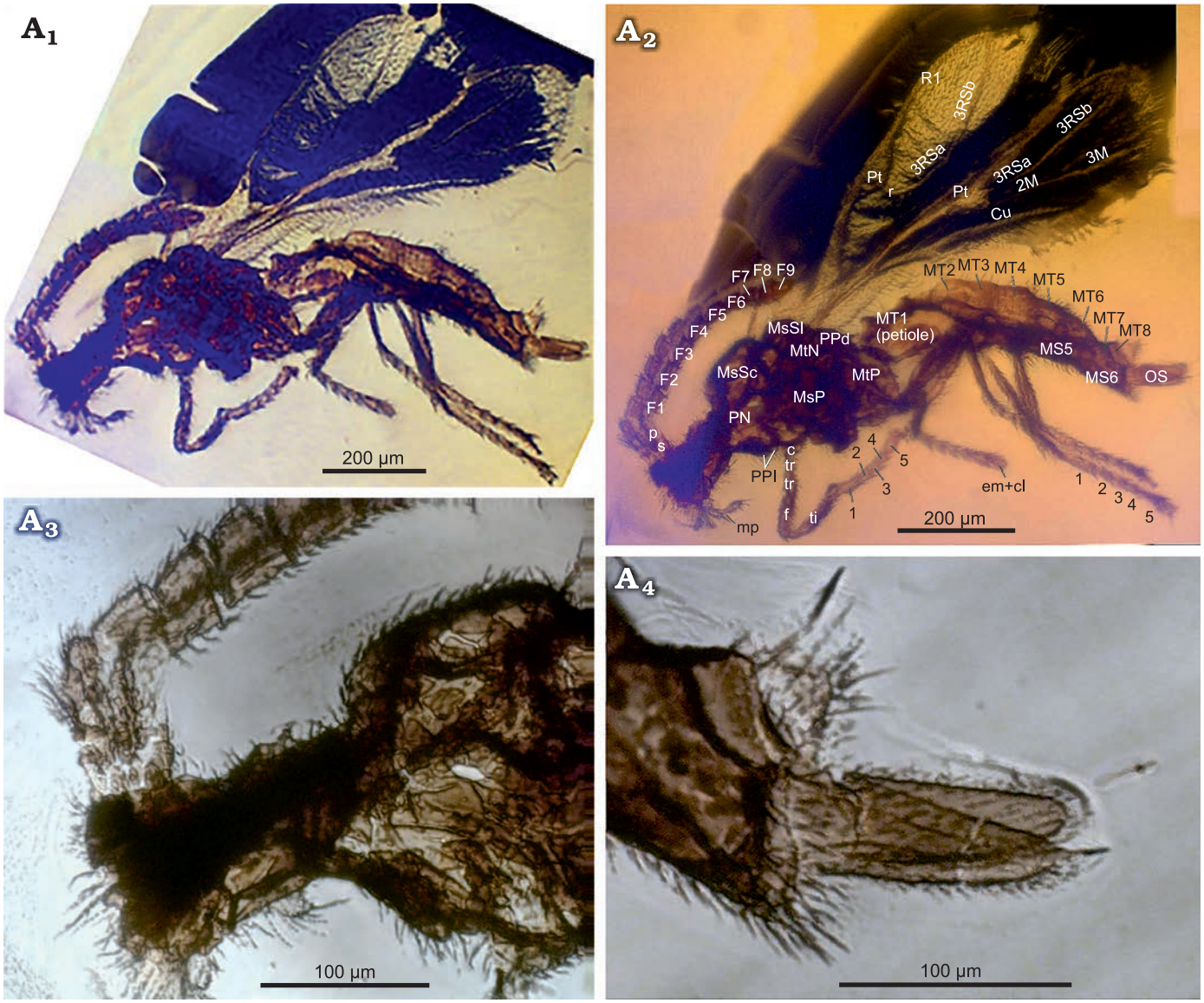

Fig. 1. Aphidiine wasp *Ephedrus rasnitsyni* Davidian and Kaliuzhna sp. nov., holotype PIN 3387/79, Starodubskoye, Sakhalinian amber (Russia), middle Eocene. Specimen in lateral view (A_1), explanatory morphology (A_2), anterolateral part of the specimen (A_3), ovipositor sheaths inlateral view (A_4). Abbreviations: body: c, coxa; em+cl, empodium and claws; f, femur; F1–F9, flagellomeres 1–9; mp, maxillary palp; MS5-6, metasomal sternites 5 and 6; MsP, mesopleuron; MsSc, mesoscutum; MsSl, mesoscutellum; MT1 (petiole), first metasomal tergite, petiole; MT2–MT8, metasomal tergites 2–8; MtN, metanotum; MtP, metapleuron; OS, ovipositor sheaths; p, pedicellus; PN, pronotum; PPd, propodeum; PPl, propleuron; s, scape; ti, tibia; tr, trochanter; 1–5, tarsomeres; venation: Pt, pterostigma; R1, metacarp, anterior branch of radius; r, cross vein connecting pterostigma and radial sector; Pt, pterostigma; RS, radial sector; 3RSa, 3RSb, a and b sections of 3rd abscissa of radial sector; 2M, 3M, 2nd, and 3rd abscissae of media; Cu, cubitus.

from all other species of the *Ephedrus* and places it closer to the extant *E. validus* (Haliday, 1833) and *E. carinatus* Tomanović, 2020. From these two species *E. rasnitsyni* Davidian and Kaliuzhna sp. nov. differs in following characters: first flagellomere (F1) less elongate, 2.5 times as long as wide (Fig. $1A_3$), notauli absent, ovipositor sheaths 3.0 times as long as wide (Fig. $1A_4$) and overall smaller body size. *Ephedrus rasnitsyni* Davidian and Kaliuzhna sp. nov. differs from known fossil species *E. mirabilis* and *E. primordialis* by a longer petiole, and rather long 3M vein that, however, does not reach the forewing margin (Figs. $1A_1$, A_2, 2). The new species additionally differs from the *E. primordialis* by more elongate ovipositor sheaths.

Description.—Description is based on a single female, male forms are unknown.

Head (Fig. $1A_1$–A_3) distinctly densely pubescent. Maxillary palp with three visible palpomeres; labial palp with two palpomeres. Maxillary palpomere oval; two times as long as wide, completely pubescent, covered with short setae and with two–three long setae apically. Antenna with 11 antennomeres, short, barely reaching the apex of thorax, covered with dense setae that are slightly shorter than the width of F1; each flagellomere also with two semi-erected longer setae apically. F1–F3 parallel-sided (Fig. $1A_3$); other flagellomeres beginning with F4 are strongly widened towards apex, possibly flattened in amber. The apical flagellomeres

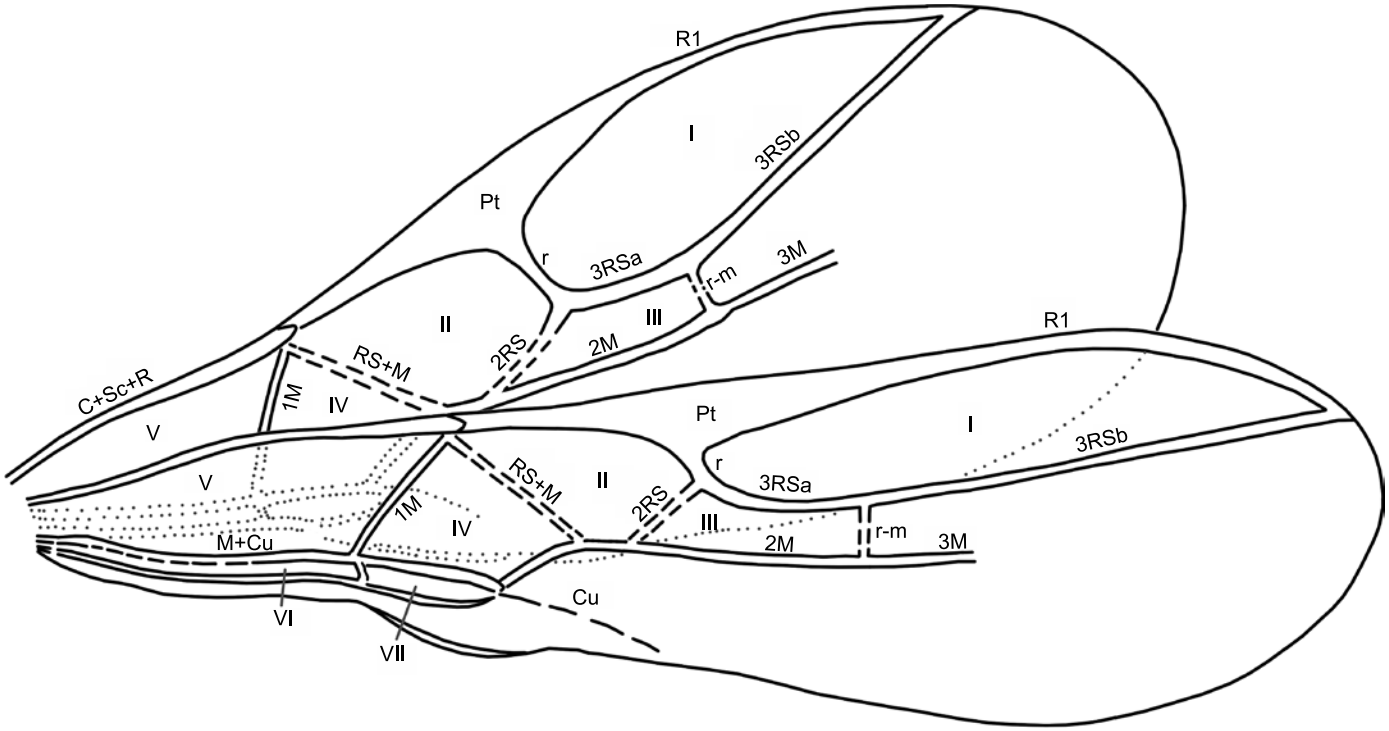

Fig. 2. Schema of forewing venation of aphidiine wasp *Ephedrus rasnitsyni* Davidian and Kaliuzhna sp. nov., holotype PIN 3387/79, Starodubskoye, Sakhalinian amber (Russia), middle Eocene. Abbreviations: Veins: C+Sc+R, costa+subcosta+radius; Pt, pterostigma; R1, metacarp, anterior branch of radius; r, cross vein connecting pterostigma and radial sector; Pt, pterostigma; RS, radial sector; 3RSa, 3RSb, a and b sections of 3rd abscissa of radial sector; 1M, 2M, 3M, 1st, 2nd and 3rd abscissae of media; RS+M, radial sector+media; 2RS, 2nd abscissa of radial sector; r-m, cross vein connecting radius and media; M+Cu, media+cubitus; Cu, cubitus. Cells: I, marginal; II, 1st submarginal; III, 2nd submarginal; IV, 1st discal; V, basal; VI, subbasal; VII, subdiscal.

tightly jointed to each other, forming a club. F1 is broken in basal third, approximately equal in length to F2, 2.5 times as long as wide in the middle; F3 and F4 2.0 times as long as wide, F5 and F6 1.5 times as long as wide; F7 and F8 almost square, i.e., the same length and width; F9 1.3 times as long as wide at base (Fig. $1A_1$, A_2). F1 and F2 with one longitudinal placode; other flagellomeres with two placodes each.

Mesosoma densely pubescent (Fig. $1A_1$–A_3). Propodeum with central areola.

The venation (Figs. $1A_1$, A_2, 2) of the forewing complete, including 2RS and r-m veins and seven closed cells, however, only marginal, 1st and 2nd submarginal and basal cells are clearly visible. Pterostigma approximately two times as long as wide. 3RSa slightly longer than 2RS; 3M not reaching wing margin. Hind wing with complete basal cell. The surface of both wings densely covered with long setae. The setae along the wing edge are longer than on the wing surface.

Legs densely pubescent. First fore tarsomere 2.0 times as long as second tarsomere, first hind tarsomere 2.7 times as long as second tarsomere.

Metasoma (Fig. $1A_1$, A_2, A_4) elongate, lanceolate, densely pubescent. Petiole inverted and its shape is difficult to observe; approximately two times as long as wide at the level of the spiracular tubercles. Eight metasomal tergites clearly visible. Hypopygium and elongate ovipositor sheaths completely covered with short dense setae. Ovipositor sheaths elongate, 3.0 times as long as wide in the middle; dorsal margin of ovipositor sheaths straight, apex rounded, ventral margin slightly curved upwards. Left ovipositor sheath broken at midlength (Fig. $1A_4$).

Coloration of the body is brown, antennae and legs are slightly lighter; palpi are light yellow.

Body length 1.2 mm, the length of antennae 0.5 mm.

Remarks.—Left side of the specimen is convex towards observer. The head is strongly deformed, it is not possible to observe the eyes and clypeus. The specimen has clearly visible mesosoma, legs, metasomal tergites, ovipositor sheaths; the wings and petiole are partly visible.

Ephedrus rasnitsyni Davidian and Kaliuzhna sp. nov. is the first Aphidiinae species described from Sakhalinian amber, and the oldest named female of subfamily.

Ephedrus rasnitsyni sp. nov. presumably belongs to *E. plagiator* species group of the subgenus *Ephedrus* sensu stricto (Gärdenfors 1986; Kocić et al. 2019) on the basis of following characters: 11-segmented antennae, complete venation of the forewing, with 3RSa slightly longer than 2RS, and rather long petiole (Figs. $1A_1$, A_2, 2).

Ephedrus rasnitsyni sp. nov., as well as other studied Sakhalinian Aphidiinae, are much shorter than extant species of the *E. plagiator* group. This group includes 12 extant species, with only some specimens of two species, i.e., *E. laevicollis* (Thomson, 1895) (1.3–1.9 mm) and *Ephedrus koponeni* Halme, 1992 (1.4–1.9 mm), smaller than 1.5 mm, while all known specimens of six species are longer than 1.7 mm, with the largest being *Ephedrus prociphili* Starý,

1982 (2.5–3.5 mm; Gärdenfors 1986; Tomanović et al. 2020). Compared to fossil species, *Ephedrus rasnitsyni* Davidian and Kaliuzhna sp. nov. is larger than *E. primordialis* (0.6–0.7 mm) and smaller than *E. mirabilis* (1.56 mm).

Stratigraphical and geographic range.—Middle Eocene, Starodubskoye, Dolinsk District, Sakhalin Province, Sakhalin Island, Russian Federation.

Concluding remarks

Among studied aphidiine specimens from Sakhalinian amber, the most abundant species are from the genus *Ephedrus*, tribe Ephedrini Haliday, 1833 (29 out of 36 specimens).

Ephedrus rasnitsyni Davidian and Kaliuzhna sp. nov. clearly belongs to the *Ephedrus*. We compared this specimen with all known genera of Ephedrini according to the electronic catalog Taxapad (Yu et al. 2016): *Ephedrus* Haliday, 1833, *Parephedrus* Starý and Carver, 1971, *Toxares* Haliday, 1840, *Diospilites* Brues, 1933, *Indoephedrus* Samanta, Pramanik, and Raychaudhuri, 1983, and *Archephedrus* Ortega-Blanco, Bennet, Delclòs, and Engel, 2009.

Among these genera, *Diospilites* and *Indoephedrus* have been erroneously assigned to Aphidiinae in Taxapad (Yu et al. 2016). We agree with Tobias (1987), who redescribed the fossil *Diospilites brevicornis* Brues, 1933, from Baltic amber and erected for him the monotypic subfamily Diospilitinae. The *Indoephedrus* was erected for two parasitoids of Greenideidae from Meghalaya (northeast India): *I. reticulata* Samanta, Pramanik, and Raychaudhuri, 1983, and *I. neoficicola* Samanta, Pramanik, and Raychaudhuri, 1983. According to the description by Samanta et al. (1983), the structure of the head (oval head shape, long temples, narrow face with sparse setae, reticular region between the antennal fossae and simple eyes), venation of the forewings, long antennae (25-segmented in *I. neoficicola* and 33- in *I. reticulata*) as well as the structure of the long narrow ovipositor sheaths completely covered with setae, are similar to those of some genera of the subfamily Braconinae Nees, 1811 (Sergey A. Belokobylskij, personal communication 2020) and does not belong to Aphidiinae. This opinion is also shared by other aphidiine specialists (Ehsan Rakhshani, personal communication 2020), and the genus was not included to the list of world aphidiine parasitoids of greenideids (Starý et al. 2010).

The fossil *Archephedrus stolamissus* Ortega-Blanco, Bennet, Delclòs, and Engel, 2009, was described based on a single male from Early Cretaceous (late Albian) Álava amber (Peñacerrada I) from Spain. It differs from the new species by having 16-segmented antennae that clearly narrow towards the apex and by the 5-segmented maxillary palps.

The *Parephedrus* and *Toxares* are represented exclusively by extant species. The Australian *Parephedrus*, despite the absence of notauli, is characterized by sparse pubescence of the ovipositor sheaths, as well as having two thickened setae at the apex of the sheath, similar to species of the *Praon* Haliday, 1833. The *Toxares* occupies an isolated position in the group because it has 16–23-segmented antennae and a plow-shaped ovipositor sheath that is curved downward and widens towards the apex.

Ephedrus rasnitsyni Davidian and Kaliuzhna sp. nov. has all of the plesiomorphic features of the *Ephedrus*: 11-segmented antennae, complete wing venation, propodeum with central areola, hind wings with a complete basal cell, a straight, triangular ovipositor sheath. The absence of notauli is characteristic to both previously described fossil *Ephedrus* species and modern *Parephedrus* (Starý 1973; Gärdenfors 1986). Apomorphic features of Ephedrini include posterior position of propodeal spiracles, an elongated petiole, free cuspises of male genitalia, and black colored aphid host mummies (Gärdenfors 1986). The only clearly visible apomorphy of the new species is an elongated petiole; other characters are hardly visible or not present in the available specimen.

The fossil species *E. mirabilis* and *E. primordialis* can be easily distinguished from the new species. The former has a short petiole and a very short 3M that is approximately equal to r (Timon-David 1944; Starý 1973). *E. primordialis* has a short, wide, and almost square petiole and a long 3M vein that reaches the apical margin of the wing, and rather short, narrow, triangular ovipositor sheaths (the character of pubescence is absent in the description) (Brues 1933; Starý 1973). The new species has a longer petiole, a long 3M vein that does not reach the forewing margin, and more elongated ovipositor sheaths that are completely covered with setae.

Ephedrus rasnitsyni Davidian and Kaliuzhna sp. nov. is most similar to the extant *E. validus* and *E. carinatus* in the pubescence of the ovipositor sheaths but differs from these species in the following characters: the F1 is shorter, 2.5 times as long as wide; notauli are absent; and the ovipositor sheaths are 3.0 times as long as wide. In the related extant species, the F1 is much longer (in *E. validus*, it is 4.2–4.7 times as long as wide, and in *E. carinatus*, 5.8 times as long as wide); the notauli are well developed; and the ovipositor sheaths are about two times as long as wide (Starý 1958; Tomanović et al. 2020). Interestingly, *E. validus* was at one time included in the monotypic subgenus *Lysephedrus* established based on morphological and ecological data (Starý 1958). The main diagnostic characters that differentiate *Lysephedrus* from the rest of the subgenera are the reticulated sculpture of the propodeum and petiole and the continuous pubescence of the ovipositor sheath. *Lysephedrus* was also considered a subgenus in the *Ephedrus* monograph by Gärdenfors (1986). In several other studies, *Lysephedrus* was considered as a genus (Mackauer 1968; Starý 2006; Davidian 2018, 2019). On the other hand, *Ephedrus carinatus* (*Ephedrus* sensu stricto) from Austria was described from a single female already in the nominative subgenus (Tomanović et al. 2020). This species, like *E. validus*, is characterized by pubescent ovipositor sheaths. This morphological character could be an adaptation to the

parasitization of root aphids (e.g., subfamily Eriosomatinae), such as in *E. validus* (Starý and Schlinger 1967; Tobias and Chiriac 1986; Davidian 2007; Yu et al. 2016) and a similar host was assumed by Tomanović et al. (2020) for *E. carinatus*. Eriosomatidae are known from Sakhalinian amber as well (Piotr Węgierek, personal communication 2020), and because *E. rasnitsyni* Davidian and Kaliuzhna sp. nov. has the same character, it could also be a parasite of root aphids.

Sakhalinian amber is potentially the best source to reveal the crucial information in understanding the early stages of aphid-aphidiine coevolution. The Sakhalinian amber biota existed after the rise of ants and after the establishment of close ant-aphid relationships (Perkovsky and Węgierek 2018, and references therein), but ants are rare in this amber—four times less abundant than in Baltic and Rovno ambers (Perkovsky et al. 2007; Radchenko and Perkovsky 2016, and references therein).

Acknowledgements

The authors are grateful to Alexandr P. Rasnitsyn and Irina D. Sukatsheva (both PIN), who provided the amber material; to Andranik R. Manukian (Senior Researcher of the Kaliningrad Regional Amber Museum, Kaliningrad, Russian Federation) who kindly helped in separating inclusions and polishing amber; to Ehsan Rakhshani (University of Zabol, Zābol, Iran), Dmitri V. Logunov (Curator of Arthropods at the Manchester Museum, the University of Manchester, UK), and Hirotsugu Ono (National Museum of Nature and Science, Tokyo, Japan), who provided a copy of the *Indoephedrus* description. Piotr Węgierek (Silesian University, Katowice, Poland) is thanked for discussion and Sarah C. Crews (California Academy of Sciences, San Francisco, USA) for editing of the English text. Authors are grateful to reviewers of this article Sergey A. Belokobylskij (Zoological Institute of Russian Academy of Sciences, St. Petersburg, Russian Federation) and Michael Sharkey (University of Kentucky, Lexington, USA) for useful recommendations and corrections.

References

Azar, D. and Maksoud, S. 2020. New psychodid flies from the Upper Cretaceous Yantardakh amber and Eocene Sakhalin amber (Diptera: Psychodidae: Psychodinae). *Palaeoentomology* 3: 500–512.

Baranov, V., Andersen, T., and Perkovsky, E.E. 2015. Orthoclads from Eocene amber from Sakhalin (Diptera: Chironomidae, Orthocladiinae). *Insect Systematics & Evolution* 46: 359–378.

Batelka, J., Perkovsky, E.E., and Prokop, J. 2020. Diversity of Eocene Ripiphoridae with descriptions of the first species of Pelecotominae and larva of Ripidiinae (Coleoptera). *Zoological Journal of the Linnean Society* 188: 412–433.

Belshaw, R. and Quicke, D.L.J. 1997. A molecular phylogeny of the Aphidiinae (Hymenoptera: Braconidae). *Molecular Phylogenetics and Evolution* 7: 281–293.

Belshaw, R., Dowton, M., Quicke, D.L.J., and Austin, A.D. 2000. Estimating ancestral geographical distributions: a Gondwanan origin for aphid parasitoids? *Proceedings of the Royal Society of London, Series B, Biological Sciences* 267: 491–496.

Berger, J.P., Reichenbacher, B., Becker, D., Grimm, M., Grimm, K., Picot, L., Storni, A., Pirkenseer, C., and Schaefer, A. 2005. Eocene–Pliocene time scale and stratigraphy of the Upper Rhine Graben (URG) and the Swiss Molasse Basin (SMB). *International Journal of Earth Sciences* (*Geologische Rundschau*) 94: 711–731.

Brues, C.T. 1933. The parasitic Hymenoptera of the Baltic amber: Part I. *In*: K. Andrée (ed.), *Bernstein-Forschungen* (*Amber Studies*) *3*, 4–178. Walter de Gruyter & Co., Berlin.

Chen, X. and van Achterberg, C. 2019. Systematics, phylogeny, and evolution of braconid wasps: 30 years of progress. *Annual Review of Entomology* 64: 335–358.

Čkrkić, J., Petrović, A., Kocić, K., Mitrović, M., Kavallieratos, N.G., van Achterberg, C., Hebert, P.D.N., and Tomanović, Ž. 2020. Phylogeny of the subtribe Monoctonina (Hymenoptera, Braconidae, Aphidiinae). *Insects* 11 (3): 160 [published online, https://doi.org/10.3390/insects11030160]

Davidian, E.M. [David'ân, E.M.] 2007. Family Aphidiidae [in Russian]. *In*: A.S. Leley (ed.), *Opredelitel' nasekomyh Dal'nego Vostoka Rossii*, 192–254. Dal'nauka, Vladivostok.

Davidian, E.M. 2018. Check-list of the aphidiid-wasp subfamily Ephedrinae (Hymenoptera, Aphidiidae) from Russia and adjacent countries. *Entomological Review* 98: 1091–1104.

Davidian, E.M. [David'ân, E.M.] 2019. Family Aphidiidae [in Russian]. *In*: S.A. Belokobyl'skij, K.G. Samartsev, and A.S. Il'inskaya (eds.), Annotated Catalogue of the Hymenoptera of Russia. Volume II. Apocrita: Parasitica. *Trudy Zoologičeskogo instituta Rossijskoj akademii nauk* (Supplement 8): 329–340.

Dietrich, C.H. and Perkovsky, E.E. 2019. First record of Cicadellidae (Insecta, Hemiptera, Auchenorrhyncha) from Eocene Sakhalinian amber. *ZooKeys* 886: 127–134.

Fedotova, Z.A. and Perkovsky, E.E. 2016. A new genus and species of gall midges of the supertribe Heteropezidi (Diptera, Cecidomyiidae) found in Eocene amber from Sakhalin. *Paleontological Journal* 50: 1033–1037.

Gärdenfors, U. 1986.Taxonomic and biological revision of Palearctic *Ephedrus* Hal. (Hymenoptera, Braconidae, Aphidiinae). *Entomologica Scandinavica*, Supplement 27: 1–95.

Gumovsky, A., Perkovsky, E., and Rasnitsyn, A. 2018. Laurasian ancestors and "Gondwanan" descendants of Rotoitidae (Hymenoptera: Chalcidoidea): what a review of Late Cretaceous *Baeomorpha* revealed. *Cretaceous Research* 84: 286–322.

Heie, O.E. and Węgierek, P. 2009. A classification of the Aphidomorpha (Hemiptera: Sternorrhyncha) under consideration of the fossil taxa. *Redia* 92: 69–77.

Kaliuzhna, M.O., Davidian, E.M., and Perkovsky, E.E.2019. Fossil aphidiine wasps (Hymenoptera: Braconidae, Aphidiinae): an overview of the known records and new ones from Sakhalinian amber. *In*: M.Yu. Proshchalykin (executive editor), A.S. Lelej, V.M. Loktionov, A.G. Radchenko, S.V. Triapitsyn, and A.V. Fateryga (eds.), *IV Euroasian Symposium on Hymenoptera. Book of Abstracts*, 13–14. FSC Biodiversity FEB RAS, Vladivostok.

Kaliuzhna, M.O., Davidian, E.M., and Perkovsky, E.E. 2020. Fossil *Ephedrus* species (Hymenoptera, Braconidae, Aphidiinae): from Sakhalinian amber. *In*: *2nd Palaeontological Virtual Congress. Book of Abstracts. Palaeontology in the Virtual Era*, 36. Published by Evangelos Vlachos, Esther Manzanares, Vicente D. Crespo, Carlos Martínez-Pérez, Humberto G. Ferrón, José Luis Herráiz, Arturo Gamonal, Fernando Antonio M. Arnal, Francesc Gascó, and Paolo Citton.

Kazantsev, S.V. and Perkovsky, E.E. 2019. A new genus of soldier beetles (Insecta: Coleoptera: Cantharidae: Cantharinae) from Sakhalinian amber. *Paleontological Journal* 53: 300–304.

Kocić, K., Petrović, A., Čkrkić, J., Kavallieratos, N.G., Rakhshani, E., Arnó, J., Aparicio, Y., Hebert, P.D.N., and Tomanović, Ž. 2020. Resolving the taxonomic status of potential biocontrol agents belonging to the neglected genus *Lipolexis* Förster (Hymenoptera, Braconidae, Aphidiinae) with descriptions of six new species. *Insects* 11 (10): 667.

Kocić, K., Petrović, A., Čkrkić, J., Mitrović, M., and Tomanović, Ž. 2019. Phylogenetic relationships and subgeneric classification of European *Ephedrus* species (Hymenoptera, Braconidae, Aphidiinae). *ZooKeys* 878: 1–22.

Kodrul, T.M. 1999. Paleogene phytostratigraphy of the South Sakhalin [in

Russian]. *Trudy Geologičeskogo Instituta Rossijskoj Akademii Nauk* 519: 1–150.

Mackauer, M. 1968. Aphidiidae. *In*: C. Ferrière and J. van der Vecht (eds.), *Hymenopterorum Catalogus 3*, 1–103. Dr. W. Junk N.V., The Hague.

Marusik, Y.M., Perkovsky, E.E., and Eskov, K.Y. 2018. First records of spiders (Arachnida: Aranei) from Sakhalinian amber with description of a new species of the genus *Orchestina* Simon, 1890. *Far Eastern Entomologist* 367: 1–9.

Ortega-Blanco, J., Bennett, D.J., Delclòs, X., and Engel, M.S. 2009. Primitive aphidiine wasp in Albian amber from Spain and a Northern Hemisphere origin for the subfamily (Hymenoptera: Braconidae: Aphidiinae). *Journal of the Kansas Entomological Society* 82: 273–282.

Perkovsky, E.E. and Węgierek, P. 2018. Aphid-*Buchnera*-ant symbiosis, or why are aphids rare in the tropics and very rare further south? *Earth and Environmental Science Transactions of the Royal Society of Edinburgh* 107: 297–310.

Perkovsky, E.E., Háva, J., and Zaitsev, A.A. 2021. The first finding of a skin beetle (Coleoptera, Dermestidae) from Sakhalinian amber. *Paleontological Journal* 55: 184–192.

Perkovsky, E.E., Rasnitsyn, A.P., Vlaskin, A.P., and Taraschuk, M.V. 2007. A comparative analysis of the Baltic and Rovno amber arthropod faunas: representative samples. *African Invertebrates* 48: 229–245.

Quilis, P.M. 1940. Los Aphidiidae fósiles de Wittenheim (Haut-Rhin, Francia) (Hym. Brac.). *Eos*, *Revista Española de Entomología* 14: 23–61.

Radchenko, A.G. and Perkovsky, E.E. 2016. The ant *Aphaenogaster dlusskyana* sp. nov. (Hymenoptera, Formicidae) from the Sakhalin amber—the earliest described species of an extant genus of Myrmicinae. *Paleontological Journal* 50: 936–946.

Rakhshani, E., Pons, X., Lumbierres, B., Havelka, J., Pérez Hidalgo, N., Tomanović, Ž., and Starý, P. 2017. A new parasitoid (Hymenoptera: Braconidae: Aphidiinae) of the invasive bamboo aphids *Takecallis* spp. (Hemiptera: Aphididae) from Western Europe. *Journal of Natural History* 51: 1237–1248.

Rasnitsyn, A.P. [Rasnicyn, A.P.] 1980. Origin and evolution of Hymenoptera [in Russian]. *Trudy Paleontologičeskogo instituta Akademii Nauk SSSR* 174: 1–191.

Samanta, A.K., Pramanik, D.R., and Raychaudhuri, D. 1983. Some new aphid parasitoids (Hymenoptera: Aphidiidae) from Meghalaya, North East India. *Akitu* 54: 1–8.

Sanchis, A., Amparo, L., González-Candelas, F., and Michelena, J.M. 2000. An 18S rDNA-based molecular phylogeny of Aphidiinae (Hymenoptera: Braconidae). *Molecular Phylogenetics and Evolution* 14: 180–194.

Sharkey, M.J. and Wharton, R.A. 1997. Morphology and terminology. *In*: R.A. Wharton, P.M. Marsh, and M.J. Sharkey (eds.), *International Society of Hymenopterists Special Publication I, Manual of the New World Genera of the Family Braconidae*, 19–37. The International Society of Hymenopterists, Washington.

Simutnik, S.A. 2014. First record of Encyrtidae (Hymenoptera, Chalcidoidea) from the Sakhalin amber. *Paleontological Journal* 48: 621–623.

Simutnik, S.A. 2015. Description of two new monotypic genera of encyrtid wasps (Hymenoptera, Chalcidoidea: Encyrtidae), based on males from the middle Eocene Sakhalin amber. *Entomological Review* 95: 937–940.

Simutnik, S.A. 2020. The earliest Encyrtidae (Hymenoptera, Chalcidoidea). *Historical Biology* [published online, https://doi.org/10.1080/08912963.2020.1835887].

Starý, P. 1958. A taxonomic revision of some aphidiine genera with remarks on the subfamily Aphidiinae (Hymenoptera, Braconidae). *Acta Faunistica Entomologica Musei Nationalis Pragae* 3: 53–96.

Starý, P. 1970. *Biology of Aphid Parasites (Hymenoptera: Aphidiidae) With Respect to Integrated Control. Series Entomologica 6*. 643 pp. Dr. W. Junk B.V., Hague.

Starý, P. 1973. A revision of the fossil Aphidiidae (Hymenoptera). *Annotationes Zoologicae et Botanicae* 87: 1–22.

Starý, P. and Schlinger, E.I. 1967. *A revision of the Far East Asian Aphidiidae* (*Hymenoptera*). *Series Entomologica* 3: 1–204. Dr. W. Junk Publisher, The Hague.

Starý, P. 2006. *Aphid Parasitoids of the Czech Republic (Hymenoptera: Braconidae, Aphidiinae)*. 430 pp. Academia, Praha.

Starý, P., Rakhshani, E., Havelka, J., Tomanović, Ž., Kavallieratos N.G., and Sharkey, M. 2010. Review and key to the world parasitoids (Hymenoptera: Braconidae: Aphidiinae) of Greenideinae aphids (Hemiptera: Aphididae), including notes on invasive pest species. *Annals of the Entomological Society of America* 103: 307–321.

Timon-David, J. 1944. Insectes fossiles de l'Oligocène inférieur des Camoins (Bassin de Marseille). II. Hyménoptères. *Bulletin de la Société Entomologique de France* 49: 40–45.

Tobias, V.I. 1987. New taxa of Braconidae from Baltic amber (Hymenoptera) [in Russian]. *Entomologičeskoe obozrenie* 66 (4): 845–859.

Tobias, V.I. and Chiriac, I.G. [Kiriâk I.G.] 1986. Family Aphidiidae [in Russian]. *In*: G.S. Medvedev (ed.), *Opredelitel'nasekomyh evropejskoj časti SSSR 3 (5)*, 232–308. Nauka, Lenindrad.

Tomanović, Ž., Petrović, A., Kocić, K., Čkrkić, J., and Žikić, V. 2020. Two new morphologically interesting species of the genus *Ephedrus* Haliday (Hymenoptera, Braconidae, Aphidiinae). *Journal of Hymenoptera Research* 77: 167–174.

Tykhonenko, Y.Y., Hayova, V.P., Sukhomlyn, M.M., Ignatov, M.S., Vasilenko, D.V., and Perkovsky, E.E. 2021. The first record of the rust fungus spores (Pucciniales) from middle Eocene Sakhalinian amber. *Paleontological Journal* 55: 105–110.

Yu, D.S., van Achterberg, C., and Horstmann, K. 2016. *World Ichneumonoidea 2015: Taxonomy, Biology, Morphology and Distribution*. CD/DVD. Taxapad, Vancouver.

Zherikhin, V.V. [Žerihin V.V.], Ponomarenko, A.G. [Ponomarenko, A.G.], and Rasnitsyn, A.P. [Rasnicyn, A.P.] 2008. *Vvedenie v paleoèntomologiû*. 371 pp. KMK, Moskva.

Žikić, V., Lazarević, M., and Milosević, D. 2017. Host range patterning of parasitoid wasps Aphidiinae (Hymenoptera: Braconidae). *Zoologischer Anzeiger* 268: 75–83.

Hippopotamid dispersal across the Mediterranean in the latest Miocene: a re-evaluation of the Gravitelli record from Sicily, Italy

ROBERTA MARTINO, JOHANNES PIGNATTI, LORENZO ROOK, and LUCA PANDOLFI

Martino, R., Pignatti, J., Rook, L., and Pandolfi, L. 2021. Hippopotamid dispersal across the Mediterranean in the latest Miocene: a re-evaluation of the Gravitelli record from Sicily, Italy. *Acta Palaeontologica Polonica* 66 (Supplement to 3): S67–S78.

The first dispersal of Hippopotamidae out of Africa is recorded around 6 Ma, but this event is documented only in a few European localities. Among them, the uppermost Miocene deposits of Gravitelli in Sicily yielded particularly abundant hippopotamid remains. These specimens, published at the beginning of the 20th century, went lost during the 1908 earthquake that destroyed the city of Messina. The specimens from Gravitelli were ascribed to a new species, *Hippopotamus siculus*; their generic attribution was not questioned during the first half of the past century and they have not been revised in recent decades. The remains of the Gravitelli hippopotamid were mainly represented by isolated teeth and a few postcranial remains. Morphological and dimensional characters of the specimens, such as long lower premolars, low-crowned molars, a lower canine with longitudinal ridges and a groove on the lateral surface and the overall dimensions suggest that the Sicilian hippopotamid was characterized by plesiomorphic features. The morphology of the specimens collected from Gravitelli is similar to that of *Hexaprotodon*? *crusafonti*, *Archaeopotamus harvardi*, *Hexaprotodon sivalensis* and *Hexaprotodon garyam*. *Hexaprotodon*? *siculus* is also morphometrically similar to *Hexaprotodon sivalensis*, but the lower premolars in the former are longer and wider than in the latter. Accordingly, we provisionally refer the Gravitelli hippopotamid to the genus *Hexaprotodon*. *Hexaprotodon*? *siculus* is dimensionally different from the Spanish latest Miocene hippopotamid, herein referred to as *Archaeopotamus crusafonti*, and the two species are considered as valid taxa. The paleobiogeography of the latest Miocene hippopotamids from the Mediterranean Basin is discussed.

Key words: Mammalia, Hippopotamidae, dental morphology, Miocene, Gravitelli, Italy.

Roberta Martino [roberta.aska@gmail.com], via Ninfa, 9, Latina, Italy.
Johannes Pignatti [johannes.pignatti@uniroma1.it], Dipartimento di Scienze della Terra, "Sapienza" Università di Roma, Piazzale Aldo Moro 5, 00185 Rome, Italy.
Lorenzo Rook [lorenzo.rook@unifi.it] and Luca Pandolfi [luca.pandolfi@unifi.it], Dipartimento di Scienze della Terra, Università degli Studi di Firenze, Viale Giorgio La Pira 4, 50121 Florence, Italy.

Received 14 October 2020, accepted 26 March 2021, available online 10 August 2021.

Introduction

The first dispersal of Hippopotamidae out of Africa took place around 6 Ma (Boisserie 2007). In Europe, hippopotamid remains occur in the uppermost Miocene deposits of Spain and Italy and they were ascribed to different species. In Spain, the scanty hippopotamid remains were referred to *Hexaprotodon*? *crusafonti* (Aguirre, 1963) (Fig. 1), whilst in Italy two different species were recorded: *Hexaprotodon*? *pantanellii* (Joleaud, 1920) from the Casino Basin, Tuscany (Pantanelli 1879; Boisserie 2005) and *Hexaprotodon*? *siculus* (Hooijer, 1946) from Gravitelli, Sicily (Seguenza 1902, 1907; Hooijer 1946; Boisserie 2005; Fig. 1). In contrast to the other circum-Mediterranean records, the hippopotamid material collected at the beginning of 19th century from Gravitelli was particularly abundant. Seguenza (1902, 1907) described and figured part of the collected remains and ascribed them to *Hippopotamus sivalensis* Falconer and Cautley, 1836. The faunal list of Gravitelli, now attributed to the Mammal Neogene Zone 13 (MN 13), includes several mammal taxa such as *Mesopithecus* sp. (aff. ?*Mesopithecus monspessulanus*), *Metailurus parvulus*, Viverridae indet., *Thalassictis hyaenoides*, *Zygolophodon borsoni* (recte *Mammut borsoni*), *Zygolophodon turicensis*, *Diceros* cf. *D. pachygnathus* (recte *Ceratotherium* sp.), Reduncini indet., ?*Gazella deperdita*, ?*Parabos* sp., and *Microstonyx major erymanthius* (recte *Propotamochoerus* sp.) (Rook 1992; Kotsakis et al. 1997; Rook 1999; Van der Made 1999; Gallai

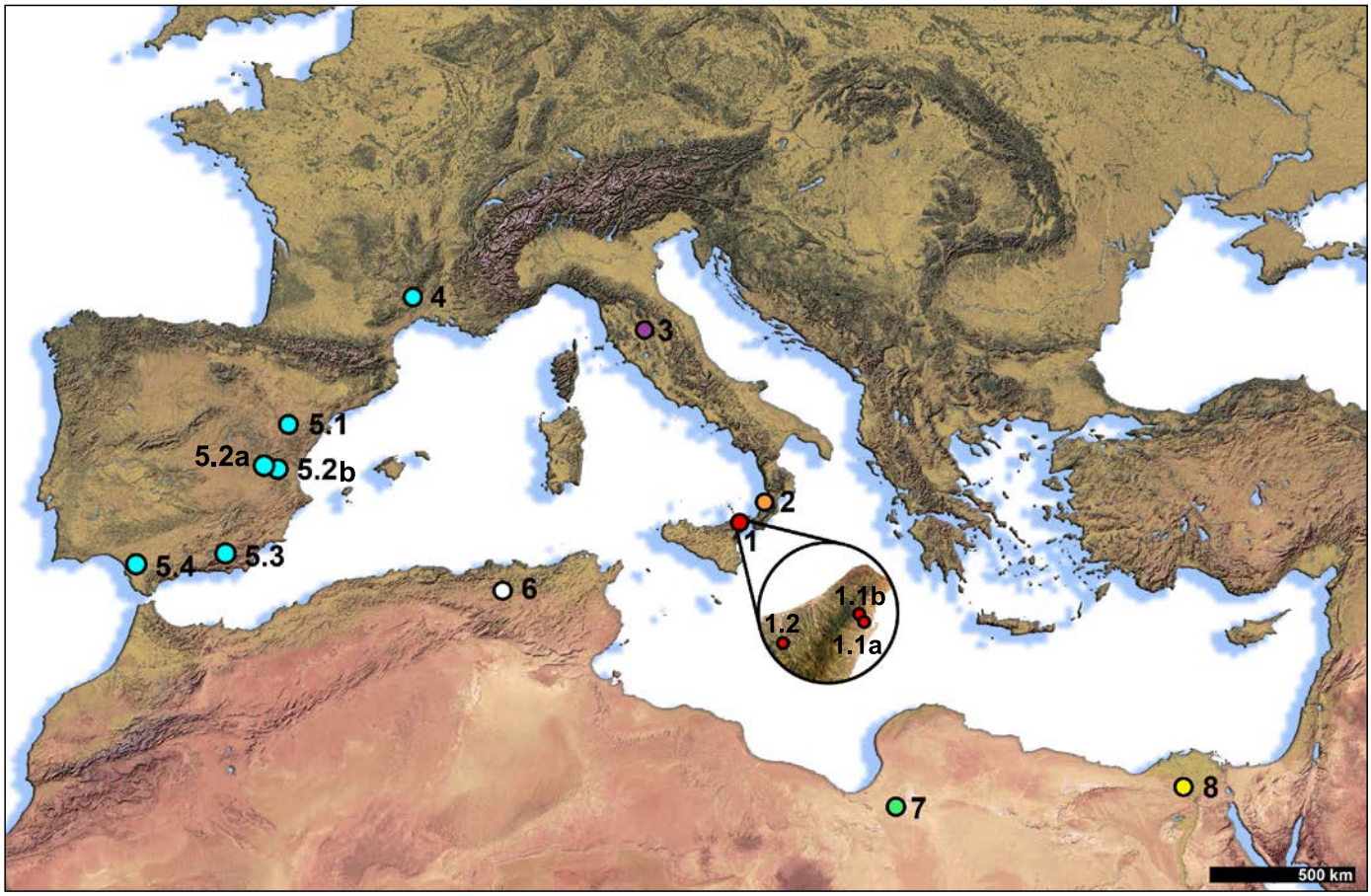

Fig. 1. Selected records of circum-Mediterranean hippopotamids during the latest Miocene–earliest Pliocene. 1, *Hexaprotodon*? *siculus* (Hooijer, 1946) (1.1a, Gravitelli and 1.1b Scirpi; San Pier Niceto) Messina, Sicily, late Miocene; 2, ?Hippopotamidae indet., Cessaniti, Calabria, late Miocene; 3, *Hexaprotodon*? *pantanellii* (Joleaud, 1920), Casino Basin, Tuscany, late Miocene; 4, *Archaeopotamus crusafonti* (Aguirre, 1963), La Mosson (Montpellier), France, early Pliocene; 5, *Archaeopotamus crusafonti* (Aguirre, 1963) (5.1, Las Casiones, Teruel; 5.2a, Venta del Moro and 5.2b, La Portera, Valencia; 5.3, Arenas del Rey, Granada; 5.4, El Arquillo, Siviglia), Spain, late Miocene; 6, *Hexaprotodon*? *hipponensis* (Gaudry, 1876), Pont-de-Duvivier, Algeria, early Pliocene; 7, *Hexaprotodon*? *sahabiensis* (Gaziry, 1987), As Sahabi, Libya, late Miocene; 8, *Hexaprotodon protamphibius andrewsi* (Arambourg, 1947), Egypt, early Pliocene.

and Rook 2006; Rook et al. 2006; Pandolfi and Rook 2017; Pandolfi et al. 2021). The faunal assemblage of Gravitelli is considered close to that from Cessaniti (Calabria) and As Sahabi (Libya) and has been used for paleobiogeographic considerations on dispersal events of latest Miocene mammals from Africa to Europe (Bernor and Rook 2008; Marra et al. 2017). Unfortunately, all the specimens described by Seguenza (1902, 1907) went lost during the 1908 earthquake that destroyed the city of Messina, and all subsequent considerations on the mammal remains from Gravitelli are based only on the published figures. Hooijer (1946) revised the works by Seguenza (1902, 1907) and, based on morphological traits, erected the new hippopotamid species *Hippopotamus siculus*, which was later provisionally assigned to *Hexaprotodon* (Boisserie 2005). Nevertheless, the hippopotamid from Gravitelli has not been revised in the last decades.

The hippopotamid remains published by Seguenza (1902, 1907) are here revised in order to clarify and update their systematic position and their paleobiogeographic implications.

Institutional abbreviations.—MSNAF, Museo di Storia Naturale dell'Accademia dei Fisiocritici, Siena, Italy; RMCA, Royal Museum of Central Africa, Tervuren, Belgium.

Other abbreviations.—C/c, canine; DP/dp, deciduous upper/lower premolar; MN, Mammal Neogene Zone; M/m, upper/lower molar; P/p, upper/lower premolar.

Material and methods

The morphological terminology for the teeth follows Thenius (1989) and Boisserie et al. (2010) (Fig. 2). The morphological terminology for the postcranial remains follows Mazza (1995). The material collected from Gravitelli was published by Seguenza (1902, 1907). Descriptions and figures reported by Seguenza (1902, 1907) are scarce and most of the remains are represented only in part (Figs. 3, 4). The revised remains are morphologically and morphometrically compared with late Miocene and early Pliocene hippopotamids: *Hexaprotodon garyam* Boisserie, Likius, Vignaud,

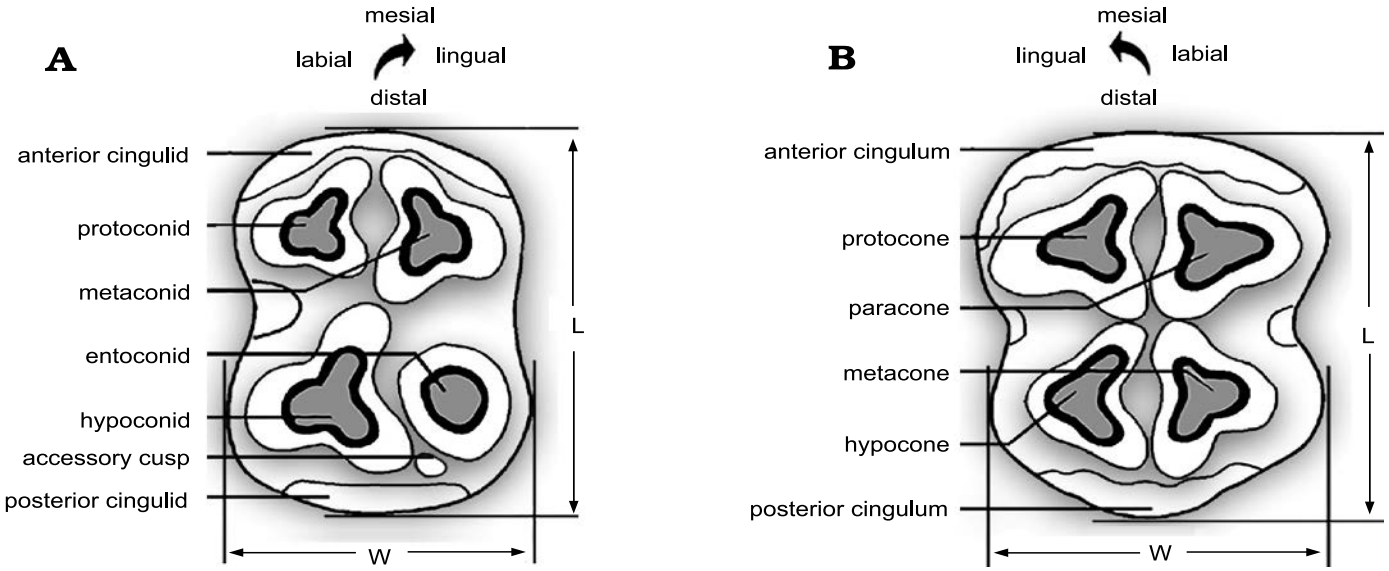

Fig. 2. Hippopotamid cheek teeth nomenclature based on the left m2 and M2 in occlusal view. Accessory cusps may be present or absent on upper and lower teeth. The m3 is characterized by a fifth distal cusp called hypocolunid. Modified from Htike (2012).

and Brunet, 2005, *Hexaprotodon sivalensis* (Falconer and Cautley, 1836), *Saotherium mingoz* Boisserie, 2005, *Archaeopotamus harvardi* (Coryndon, 1977), *A. lothagamensis* (Weston, 2000), *A. qeshta* Boisserie in Boisserie et al., 2017, *Hexaprotodon*? *crusafonti* (Aguirre, 1963), *Hexaprotodon*? *sahabiensis* (Gaziry, 1987), *Hexaprotodon*? *hipponensis* (Gaudry, 1876), *Hexaprotodon protamphibius* (Arambourg, 1944), and *Hexaprotodon protamphibius andrewsi* (Arambourg, 1947). *Hexaprotodon*? *siculus* remains are also compared with the living species *Hippopotamus amphibius* Linnaeus, 1758; and *Choeropsis liberiensis* (Morton, 1844). The measurements of *Hexaprotodon*? *siculus* were published by Seguenza (1902, 1907).

Systematic palaeontology

Cetartiodactyla Montgelard, Catzeflis, and Douzery, 1997

Cetancodonta Arnason, Gulerg, Solweig, Ursing, and Janke, 2000

Hippopotamoidea Gray, 1821 (sensu Gentry and Hooker 1988)

Hippopotamidae Gray, 1821

Hippopotaminae Gray, 1821

Genus *Hexaprotodon* Falconer and Cautley, 1836

Type species: *Hexaprotodon sivalensis* Falconer and Cautley, 1836, from Mio-Pliocene strata of the Siwalik Hills, India/Pakistan.

Hexaprotodon? *siculus* (Hooijer, 1946)

Figs. 3–5, $6B_1$, B_2.

1902 *Hippopotamus* (*Hexaprotodon*) *sivalensis* Falconer and Cautley, 1836; Seguenza 1902: 115–175, pl. 7: 1–14, 20, 22, 23.

1907 *Hippopotamus* (*Hexaprotodon*) *sivalensis* Falconer and Cautley, 1836; Seguenza 1907: 89–122, pl. 6: 1–22, pl. 7: 1–16.

1946 *Hippopotamus siculus* sp. nov.; Hooijer 1946: 301–319.

2005 *Hexaprotodon*? *siculus* (Hooijer, 1946); Boisserie 2005: 143.

Material.—Material from the late Miocene of Sicily, listed in Seguenza (1902: pl. 7; here Fig. 3): a maxillary fragment with DP3, DP4, M1 (pl. 7: 1–3) and a fragment of a DP? (pl. 7: 20) from San Pier Niceto; left astragalus (pl. 7: 4–7, 8, 9) from Scirpi or Gravitelli; a partial M (pl. 7: 10, 11), an C (pl. 7: 13, 14), and an unciform (pl. 7: 22, 23) from Gravitelli. Material from late Miocene of Sicily (Gravitelli site), listed in Seguenza (1907: pls. 6 and 7; here Figs. 4 and 5 respectively): mandible fragment with a m1 (pl. 6: 1–3), a cervical vertebra (pl. 6: 4–6), a M3 (pl. 6: 7, 8), a M1 or M2 (pl. 6: 9, 10), a C fragment (pl. 6: 11), two dp3 (pl. 6: 14–16), a P2 (pl. 6: 17, 18), a dp (pl. 6: 19, 20), m2–m3 (pl. 7: 1, 2), a m1 (pl. 7: 3, 4), a p2 (pl. 7: 5, 6), a p3 (pl. 7: 7, 8), a p4 (pl. 7: 9, 10), a c (pl. 7: 11, 12), and some incisor fragments (pl. 7: 13–16), a fragment of a radius (pl. 5: 49, 50).

Seguenza (1907) attributed to *Hippopotamus* a portion of a distal radius (pl. 5: 49, 50) a proximal part of a radius (pl. 5: 51, 52), a scapula fragment (pl. 6: 12, 13), and a distal part of a metacarpal (pl. 6: 21, 22) from late Miocene of Sicily (Gravitelli site). Hooijer (1946) attributed the distal part and the proximal part of the radius to *Parabos*? and the scapula fragment together with the distal part of a metacarpal to a rhinoceros. We do not agree with the attribution of the radius to a bovid, due to both morphological and morphometric traits of the figured bone, and we include it within the Hippopotamidae material.

Description.—Dental characters cannot be easily recognized due to the impossibility to observe the original specimens lost in 1908. Photos and descriptions in Seguenza (1902, 1907) are therefore the only documentation of the presence of a hippopotamid in Sicily during the late Miocene

(Figs. 3, 4, 5). Deciduous premolars do not display useful diagnostic features. Four fragmentary incisors were figured by Seguenza (1907; Fig. 5). According to the available text and figures, two grooves, one on each side, are present on the lower incisors. Seguenza (1907: 116–117) reported the presence of six different partial incisors that were all collected from a single mandible, completely destroyed during the excavation. This statement, anyway, testifies to the hexaprotodonty (presence of six incisors, while the extant *Hippopotamus amphibius* is characterized by four incisors, the tetraprotodont condition) of the Sicilian species. The upper canines are characterized by a deep posterior groove and by two less defined lateral grooves, one on the medial side and one on the lateral side (Fig. 3). A lower canine fragment described by Seguenza (1907) displays a rough enamel, longitudinal striae and transversal growth striae (Fig. 4). The lower canine has longitudinal ridges and a groove on the lateral surface (Fig. 5). The P2 is mostly triangular and simply built (Fig. 4). The lower premolars (p2 and p3) are mainly triangular and partially incomplete (Fig. 5). The p2 has a distolingual cusp. The p3 is characterized by a distolingual cusp surrounded by a crenulated cingulid and more developed than one of the p2. The p4 of the Sicilian species is broken and worn. A single cusp is visible, but a second lower and less developed cusp was probably present distally. In lateral view the cingulid is strongly elevated whilst, in occlusal view, some well-developed cristae are visible in the distal part of the tooth. All molars from Gravitelli are low crowned. The M1 in the maxillary fragment displays a thick crenulated cingulum and a finely striated enamel (Fig. 3). M1–M2 (Fig. 4) is characterized by a trefoil wear pattern not completely developed. The enamel is relatively thick on the protocone and the cingulum is crenulated on the lingual side. An upper molar, referred to M2 by Hooijer (1946), is partially broken, and only the metacone and paracone are present (Fig. 3). The cingulum is crenulated on these cusps and the enamel is finely striated. The posterior cusps of M3 (Fig. 4) are narrower than the anterior cups (Hooijer 1946). This tooth is unworn and the crown is not particularly high; the cusps are simple with not particularly well-developed

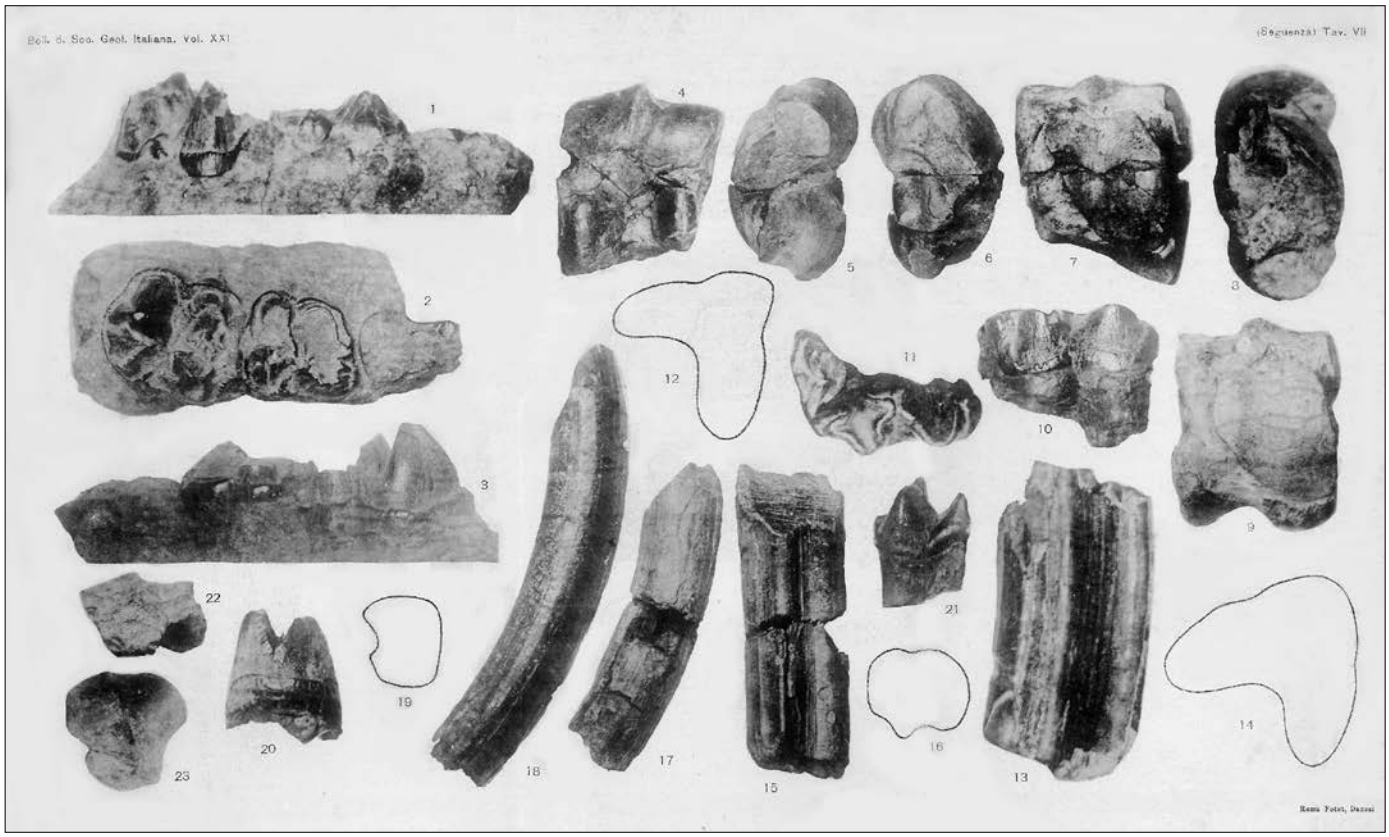

Fig. 3. Late Miocene hippopotamid *Hexaprotodon*? *siculus* (Hooijer, 1946) from Sicily, Italy; original plate from Seguenza (1902: pl. 7). Maxillary fragment with DP3, DP4, and M1 from San Pier Niceto, in lingual (1), occlusal (2), and labial (3) views. Fragment of a upper deciduous? tooth from San Pier Niceto (20), two left astragali one from Gravitelli and one from Scirpi (4, anterior view; 5 and 8, medial view; 6, lateral view; 7 and 9, posterior view), partial left M from Gravitelli (10, labial view; 11, occlusal view), C section from Gravitelli (12, view of the transverse section), C and its section from Gravitelli (13, labial view; 14, view of the transverse section), unciform from Gravitelli (22, lateral? view; 23, anterior view).

Fig. 4. Late Miocene hippopotamid *Hexaprotodon*? *siculus* (Hooijer, 1946) from Gravitelli, Sicily, Italy; original plate from Seguenza (1907: pl. 6). → Mandible fragment with M1, in labial (1), occlusal (2), and lingual (3) views, cervical vertebra in ventral (4), caudal (5), and cranial (6) views, left M3 (7, labial view; 8, occlusal view), right M1–M2 (9, labial view; 10, occlusal view), C fragment (11, labial? view), right dp3 (14, labial view; 15, occlusal view), left dp3 (16, lingual view), P2 (17, lingual view; 18, occlusal view), dp (19, lingual view; 20, occlusal view).

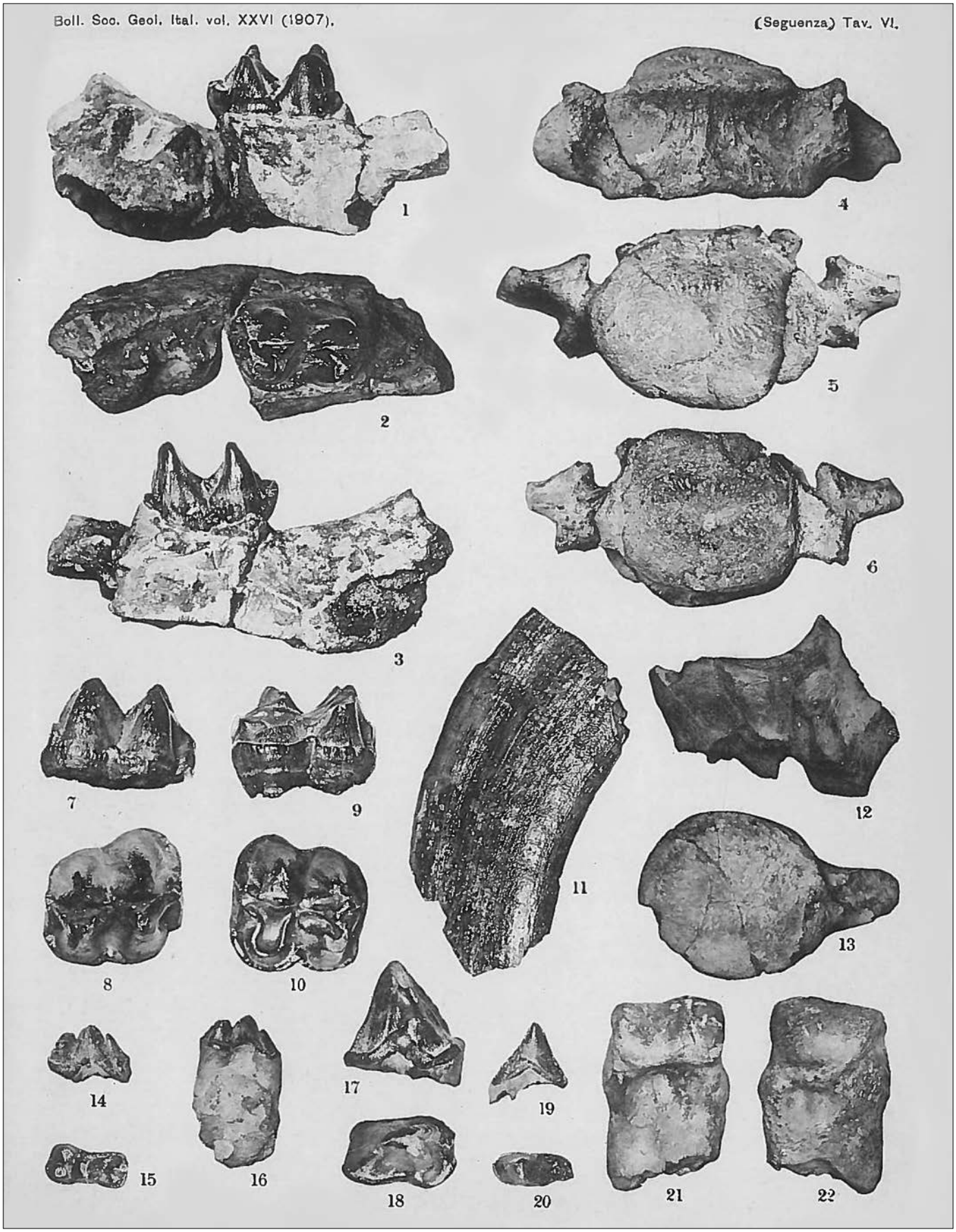
Boll. Soc. Geol. Ital. vol. XXVI (1907).
(Seguenza) Tav. VI.
1
2
3
4
5
6
7
8
9
10
11
12
13
14
15
16
17
18
19
20
21
22

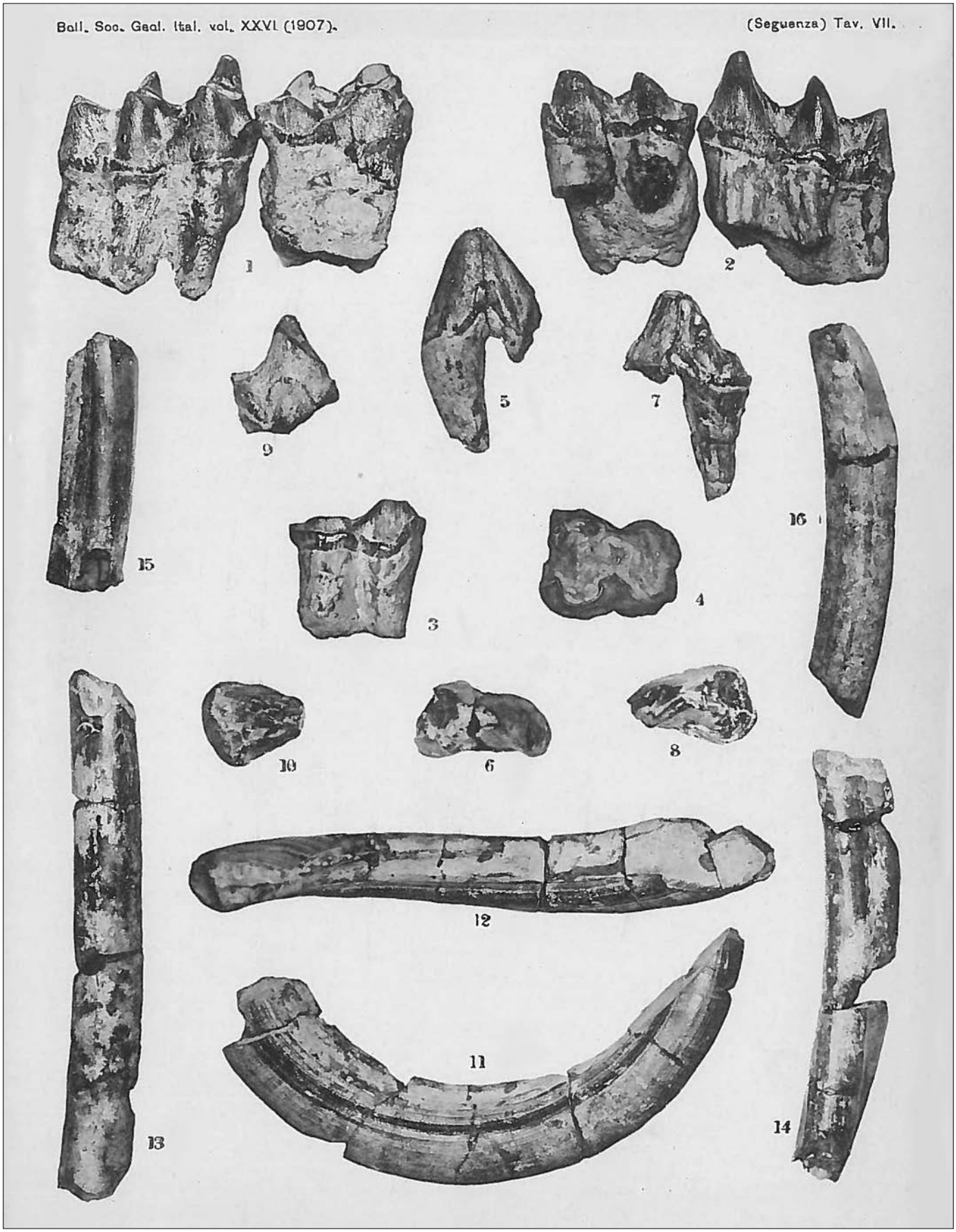
Boll. Soc. Geol. Ital. vol. XXVI (1907).
(Seguenza) Tav. VII.
1
2
5
7
9
15
16
3
4
10
6
8
12
11
13
14

grooves. The cingulum is crenulated, and it is higher and more complex on the posterior cusps compared to the anterior cups.

The lower molars from Gravitelli are low-crowned. The m1 displays a longitudinal valley between metaconid and protoconid, located labial to the valley between entoconid and hypoconid (Hooijer 1946; Fig. 4). The unworn cusps are particularly slender, the cingulid is crenulated and only visible on the posterior cusps. The m3 and m2 were partially figured by Seguenza (1907), who did not provide their occlusal view (Fig. 5). The m2 does not display a posterior lobe on the entoconid. The m3 is characterized by slender cusps and a large hypoconulid. The cingulid on this tooth is crenulated and higher on the labial side of the hypoconulid. The cusps are almost unworn, and the enamel is finely striated.

The vertebra cervicalis is severely damaged (Fig. 4). It displays a ventral spine that is not particularly prominent. The posterior face of the vertebra is larger than the anterior. The radius is broken and displays on the distal epiphysis an antero-posteriorly oriented crest between the articular surfaces for the scaphoid and with the lunar (Seguenza 1907: pl. 5: 49, 50). The unciform displays a concave articulation with the cuneiform and a narrow articulation with the lunar. Two astragali were figured by Seguenza (1902), one collected from Gravitelli and the other one from Scirpi (Fig. 3). Unfortunately, one astragalus lacks a part of the proximal throclea and the other astragalus was only figured in plantar view by Seguenza (1902). These bones display a comparable size of the oblique articular surface for the cuboid and of the articular surface for the navicular. The complete astragalus is rather subquadrangular in plantar view; on this specimen it is also possible to observe a stop facet that could limit the degree of flexion of the tarsus.

Stratigraphic and geographic range.—Upper Miocene of Gravitelli, San Pier Niceto, and Scirpi (Messina, Sicily, South Italy), European Mammal Neogene Zone 13.

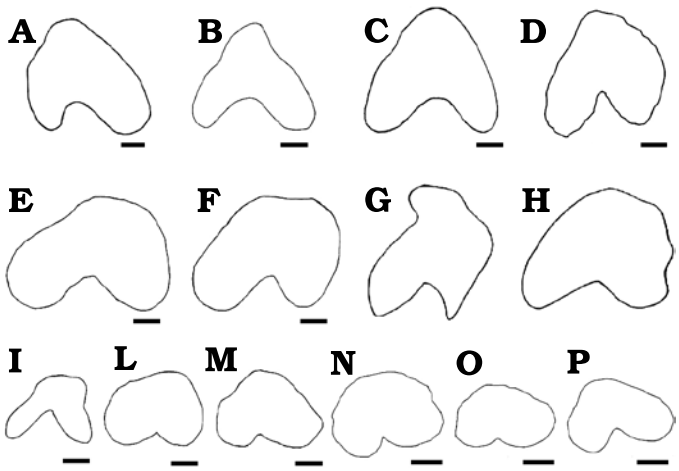

Fig. 6. Upper canine of various hippopotamids in cross section. **A**. *Archaeopotamus crusafonti* (Aguirre, 1963), Arenas del Rey (Spain), late Miocene (Aguirre 1963). **B**. *Hexaprotodon*? *siculus* (Hooijer, 1946), Gravitelli (Sicily, Italy), late Miocene (Seguenza 1902; Hooijer 1946). **C**. *Hexaprotodon*? *siculus* (Hooijer, 1946), Gravitelli (Sicily, Italy), late Miocene (Seguenza 1902; Hooijer 1946). **D**. *Hexaprotodon garyam* Boisserie, Likius, Vignaud, and Brunet, 2005, Toros-Menalla (Chad), late Miocene (Boisserie et al. 2005). **E**. *Hexaprotodon sivalensis* (Falconer and Cautley, 1836), Siwalik Hills (India/Pakistan), late Miocene–early Pliocene (Hooijer 1946). **F**. *Hexaprotodon sivalensis* (Falconer and Cautley, 1836), Siwalik Hills (India/Pakistan), late Miocene–early Pliocene (Hooijer 1946). **G**. Subadult *Archaeopotamus harvardi* (Coryndon, 1977), Lothagam (Kenya), late Miocene (Weston 2003). **H**. Adult *Archaeopotamus harvardi* (Coryndon, 1977), Lothagam (Kenya), late Miocene (Weston 2003). **I**. *Choeropsis liberiensis* (Morton, 1844), Leiden Museum collection (Hooijer 1946). **L**. *Hexaprotodon*? *protamphibius andrewsi* (Arambourg, 1947), Wadi-Natrum (Egypt), early Pliocene (Stromer 1914). **M**. *Hippopotamus amphibius* Linnaeus, 1758, Leiden Museum collection (after Hooijer 1946). **N**–**P**. Subadult *Hexaprotodon amphibius* Linnaeus, 1758, Zaire, Holocene; original data sampled by LP at the Royal Museum of Central Africa, Tervuren, Belgium. RMCA n. A6035M127 (**N**), RMCA n. A6035M194 (**O**), RMCA n. A6035M190 (**P**). Scale bars 10 mm. A, scale redrawn form Aguirre (1963); B,C, E, F, I, L, M, scales redrawn from Hooijer (1946); D, scale redrawn from Boisserie et al. (2005); G, H, scale not provided in Weston (2003).

Discussion

Comparison with late Miocene–early Pliocene peri-Mediterranean hippopotamids.—The morphological comparison highlights an affinity of the Sicilian hippopotamus with *Hexaprotodon*? *crusafonti*. The upper canine section typical of the Gravitelli *Hexaprotodon*? *siculus* specimens is also shared by *He.*? *crusafonti* (Aguirre 1963; Fig. 6). Nevertheless, a deep posterior groove is also displayed in species confidently attributed to the *Hexaprotodon* (Boisserie 2005), and in the *Saotherium* (Boisserie et al. 2003) and *Archaeopotamus* (Weston 2000, 2003). This character can therefore be considered as a plesiomorphic feature within the Hippopotamidae and is thus not diagnostic at the genus level. The lower canine from Gravitelli displays longitudinal ridges and a groove on the lateral surface as in *Archaeopotamus harvardi* (see Weston 2003). In *Hexaprotodon sivalensis* several specimens do not display the groove on the lateral side, but this character is variable, being documented in some fossil remains (De Visser 2008). However, a shallow groove on the lateral side of the lower canine is more or less developed in several hippopotamid species and usually well-expressed in later ontogenetic stages (Boisserie 2005). The enamel of *Saotherium mingoz* is slightly ridged or smooth and without a well-defined groove (Boisserie et al. 2003). P2 from Gravitelli is wide, mostly triangular in shape, with a main singular cusp as

← Fig. 5. Late Miocene hippopotamid *Hexaprotodon*? *siculus* (Hooijer, 1946) remains from Gravitelli, Sicily, Italy; original plate from Seguenza (1907: pl. 7). Left m2 and m3 in labial (1) and lingual (2) views, right m1 (3, labial view; 4, occlusal view); left p2r (r, refuse) (5, labial view; 6, occlusal view), right p3 (7, lingual view; 8, occlusal view), right p4 (9, labial view; 10, occlusal view), lower canine (11, lingual view; 12, dorsal view), and some incisor fragments (13–16, lateral view).

Table 1. Comparative dimensions of upper and lower teeth of Miocene hippopotamids (minimum–maximum dimension in mm; mean; number of specimens). Data for *Hexaprotodon*? *siculus* from Seguenza (1902, 1907), Hooijer (1946, 1950); *Archaeopotamus crusafonti* from Aguirre (1963); *Archaeopotamus crusafonti* from Alcalá et al. (1986); *Hexaprotodon*? *sahabiensis* from Gaziry (1987), Pavlakis (2008); *Archaeopotamus harvardi* from Coryndon (1977), *Archaeopotamus lothagamensis* from Weston (2000, 2003); *Hexaprotodon garyam* from Boisserie et al. (2005); *Hexaprotodon sivalensis* from De Visser (2008); *Archaeopotamus qeshta* from Boisserie et al. (2017). Values of *Hexaprotodon*? *pantanelli* were measured at MSNAF (n.2828). The second lower premolar reported of *Hexaprotodon*? *pantanellii* is partially broken and it was reported in Pantanelli (1879) as 32 mm but the specimen measured at MSNAF is 29.56 mm; this tooth was probably broken after Pantanelli (1879). Abbreviations: L, length, W, width.

Species/ tooth		*He.*? *siculus*	*He.*? *pantanellii*	*A. crusafonti*	*He.*? *sahabiensis*	*He.*? *hipponensis*	*A. harvardi*	*A. lothagamensis*	*A. qeshta*	*He. garyam*	*He. sivalensis*
p2	L	>41.7	>29.56–32(?)	41			31.3–41; 36.27; 6		29.2–40.2; 34.7; 2	29.8–47.1; 36; 17	31–34; 32.5; 2
	W	27	19.69	?			21.4–24.7; 22.85; 5		18.2–19.7; 18.95; 2	19–27.6; 22.12; 17	19.5; 19.5; 2
p3	L	>40.6		37.5		35	36.5–45.1; 40.04; 6		35.7–39.1; 37.4; 2	31.7–48; 39.42; 20	31.3–39; 35.15; 2
	W	26		21			22.5–26.6; 24.62; 6		19.6–23.1; 21.35; 2	18–32.9; 24.17; 19	19.2
p4	L	36		30–37; 33.5; 2	36		36.4–41.6; 38.66; 8	30.7–33.6; 32.15; 2	33.9–34.5; 34.2;2	33.4– 43.1; 39.1; 19	29.3–35.9; 32.25; 8
	W	29		24–25.6; 24.8;2	25		24.9–30.6; 27.41; 8	20.5–23.8; 22.15; 2	22.4–23.8; 23.1; 2	21.7– 32.5; 27.81; 18	20.6–22.4; 22.33; 7
m1	L	40.5–41; 40.75; 2		36–40.5; 38.25; 2	36–36.42; 36.21; 2		35.5–41; 38.25; 8	36.5–40; 38.25; 2		23–28; 25.5; 20	31–41; 36.67; 3
	W	28–32; 30; 2		25–26.5; 25.75; 2	25.78–30; 27.89; 2		26.1–35; 31.34; 9	24–30; 28; 2	25.2–25.7; 25.45; 2	19–23; 21; 20	24–33; 29; 4
m2	L	46–50; 48; 2	44.6	37–40.4; 37.43; 3	39		41.2–51.3; 47.44; 11	41.1–42.7; 41.90; 2	41.5–44.8; 43.15; 2	41.6–54; 49.28; 31	43–52; 48.17; 9
	W	35–39; 37; 2	33	28–29; 28.5; 2	34		33–38.4; 36.16; 10	27.8–34.0; 30.90; 2	31.8–33.7; 32.75; 2	30.8–45.2; 37.53; 26	31–40; 36.5; 10
m3	L	63		>53–55; 54; 3	59		58.3–68; 63.1; 16	49.8–51.1; 50.45; 2	54.9–62.9; 58.9; 2	59.1–70.7; 63.26; 31	56–72; 65.55; 12
	W	35		28.2–>36.1; 29.1; 3	33		32–40.2; 35.9; 15	28.3–29.2; 28.75; 2	31.5	31.9–45.2; 38.12; 31	33–42; 38.55 ;12
M1	L	40			34		35–46; 40.5; 11			36–49; 42.5; 21	31–46; 41.86; 10
	W	37			33		38–46; 42; 11			31–43; 37; 21	36–41; 38.5; 10
M3	L	44			39		44.0–51.7; 47.17; 13			37.8–57.4; 47.74; 49	36.8–51; 47; 10
	W	44			42		41.4–56.2; 46.48; 13			40.8–52.2; 46.54; 48	35.15–52; 48.4; 10

in *Hexaprotodon sivalensis*, *Archaeopotamus harvardi*, *Hexaprotodon garyam*, and *Saotherium mingoz* (Hooijer 1950; Boisserie et al. 2003, 2005; Weston 2003). The p2 from Gravitelli is wider and longer than in *He. sivalensis* (Table 1). The distolingual cusp displayed by the studied p3 also characterizes *He. sivalensis*, *S. mingoz*, *A. harvardi*, *He.*? *crusafonti*, and *He. garyam* (Hooijer 1950; Lacomba et al. 1986; Boisserie et al. 2003, 2005; Weston 2003); this tooth is distally wide as in *A. harvardi* and *He.*? *crusafonti* (Aguirre 1963; Lacomba et al. 1986; Weston 2000, 2003). The p3 in *Hexaprotodon*? *hipponensis* shows more tubercles and a lingual cusp more developed than in *He.*? *siculus* (Gaudry 1876). The length of p3 from Gravitelli is similar to that of *A. harvardi*, whereas it is smaller in *He. sivalensis* (Table 1). The fourth lower premolar in *He.*? *siculus* is distinctly wider in its distal part; this character is also shared by *He.*? *crusafonti*, *He. garyam*, and occasionally, *A. harvardi* (Lacomba et al. 1986; Weston 2003; Boisserie et al. 2005). Dimensionally, the p4 from Gravitelli is closer to *A. harvardi* and *He. garyam*, whereas the dimensions of *He. sivalensis* are considerably smaller (Table 1, Fig. 7). The lower premolars of *He.*? *siculus* are morphometrically closer to *A. harvardi* and *He. garyam*, whereas the dimensions of *He. sivalensis* are always smaller than in the Sicilian specimens. The grooves on M3 from Gravitelli are less developed than in *He. sivalensis* and *He.*? *hipponensis* (Hooijer 1946). The crown on M3 from Gravitelli is more brachyodont than in *He. sivalensis*. Low-crowned

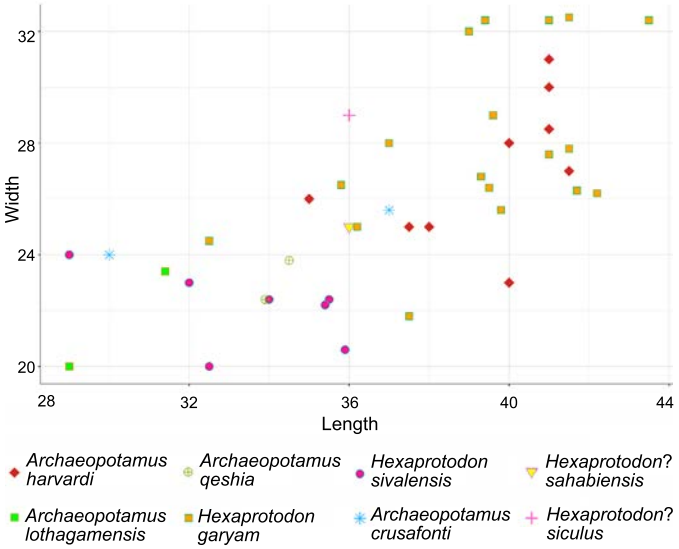

Fig. 7. Length-width diagram (in mm) of p4 in different hippopotamid species. Measurements from the literature (see Table 1).

teeth are typical of African species such as *A. harvardi* and *He. garyam*, whereas Asian hippos display higher crowned teeth (Boisserie 2005). Low-crowned teeth are also typical of the late Miocene species *He.*? *crusafonti* (Aguirre 1963; Lacomba et al. 1986). In general, the observed trend in the Hippopotamidae is towards higher crowned molars (Boisserie 2005). In the third lower molar of *A. harvardi* the cingulid is not continuous and may be separated from the mesial and distal cusps by a ridge (Weston 2003), as in the Sicilian species. In the Gravitelli hippopotamid, the cusps on the m3 are more slender and the hypoconulid is more developed than in *He. sivalensis*. The morphology of the third lower molar resembles that of *He.*? *crusafonti* in lingual and labial views. Dimensionally, the m3 from Gravitelli is close to *A. harvardi*, *He. sivalensis*, *He.*? *sahabiensis*, and *He. garyam* (Hooijer 1950; Gaziry 1987; Weston 2003; Boisserie et al. 2005; Table 1). The stop facet observed on the astragalus of the Sicilian species is also documented on some specimens from Lothagam, attributed to *A. harvardi* (Weston 2003). The height difference between the articular surface for the cuboid and the articular surface for the navicular in *A. harvardi* is similar to that displayed by the Sicilian specimens, whereas in *He. sivalensis* the height difference is greater. A single astragalus attributed to *Hexaprotodon*? *crusafonti* was described by Alcalá (1994) from Las Casiones (Spain). Similarly, to the specimens from Sicily, the height between the articulations of the navicular and cuboid is comparable. A single *He. protamphibius andrewsi* astragalus is figured by Stromer (1914). This bone is less quadrangular, smaller and more slender than in the Sicilian specimens and it possibly lacks the stop facet. In addition, the astragalus of *He. protamphibius andrewsi* displays a well-developed tuberosity below the medial ridge, similarly to *He. sivalensis*. The astragalus of the Sicilian species is morphologically more similar to that of *Hippopotamus amphibius* than to *Choeropsis liberiensis* (Fig. 8). Some studies highlight that astragalus morphology in bovids is a useful tool for paleohabitat reconstructions (DeGusta and Vrba 2003 and references therein). A study based on hippopotamuses' astragali has not yet been performed, but it could probably test terrestrial versus aquatic adaptations in the different fossil hippopotamid species. The astragalus index ([max. width = 84 mm/max. length = 109 mm] × 100 = 77; measured by Seguenza 1902) in the Gravitelli hippopotamid is close to the values of *He. protamphibius andrewsi*, *A. harvardi*, *He. sivalensis*, and *He. protamphibius* (Stromer 1914; Hooijer 1946; Harrison 1997). The radius of *He. sivalensis* displays a distal crest less directed antero-posteriorly than in the material from Gravitelli (Hooijer 1946). In addition, the articulation between cuneiform and unciform is less concave and the articulation between unciform and lunar is narrower in *He. sivalensis* than in the Sicilian specimens (Hooijer 1946).

An overview of late Miocene–early Pliocene hippopotamids from the circum-Mediterranean area.—The morphology of the specimens collected from Gravitelli and assigned as *Hexaprotodon*? *siculus* is similar to that of *He.*? *crusafonti*, *Archaeopotamus harvardi*, *He. sivalensis*, and *He. garyam*. The dimensions of the cranial remains from Gravitelli fall within the variability of *A. harvardi* and *He. garyam*. *Hexaprotodon*? *siculus* is also morphometrically similar to *He. sivalensis* but the lower premolars in the former are always longer and larger than in the latter. Accordingly, and considering its hexaprotodont condition, we tentatively refer the Gravitelli hippopotamid to the genus *Hexaprotodon* in agreement with Boisserie (2005).

Due to the tetraprotodont condition and the clear morphometrical differences with *Hexaprotodon*? *siculus*, the Spanish Miocene hippopotamid *He.*? *crusafonti* is considered as a valid species. *Hexaprotodon*? *crusafonti* was firstly described from the upper Miocene deposit of Arenas del Rey by Aguirre (1963). This Spanish species was later identified at Venta del Moro (Aguirre et al. 1973, Morales 1984), El Arquillo (Crusafont et al. 1964; Alcalá and Montoya 1998), Las Casiones (Alcalá 1994) and La Portera (Lacomba et al.

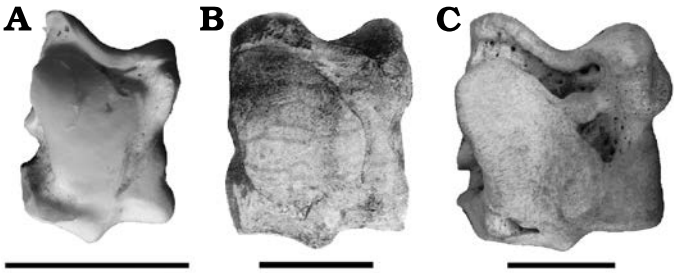

Fig. 8. Astragali of hippopotamids in plantar view. **A**. *Choeropsis liberiensis* (Morton, 1844) (RMCA n. RG35716), Holocene, specimen from zoo, Recent. **B**. *Hexaprotodon*? *siculus* (Hooijer, 1946) (Seguenza 1902: pl. 7: 9), late Miocene, Gravitelli or Scirpi, Sicily, Italy. **C**. *Hippopotamus amphibius* Linnaeus, 1758 (RMCA n. RG508), Holocene, Zaire. Scale bar in B estimated according to the maximum height of the astragalus (97 mm) indicated by Seguenza (1902). Scale bars 50 mm.

1986). *Hexaprotodon*? *crusafonti* was also collected from the lower Pliocene deposit of La Mosson, France (Faure and Méon 1984). The material from La Portera (Lacomba et al. 1986) includes a left semi-complete hemimandible with the mandibular symphysis, two broken first incisors and two second incisor alveoli, suggesting the tetraprotodont condition of this species. Two important features characterize this taxon: a premolar row longer than the molar row and a mandibular symphysis that is long and narrow. These characters are both diagnostic of the *Archaeopotamus* (Boisserie 2005). The tetraprotodont condition displayed by the Spanish species could suggest an evolutionary stage more advanced than the African coeval forms, such has *A. harvardi*, *A. lothagamensis*, and *He. garyam*. *Hexaprotodon protamphibius* collected from different geological sequences from Shungura (Ethiopia) testifies to a well-defined evolutionary trend in hippopotamids: from an archaic hexaprotodont condition towards a more advanced tetraprotodont condition (Coryndon 1978). *Hexaprotodon*? *crusafonti* is therefore closer to *Archaeopotamus* than to species confidently attributed to *Hexaprotodon* (as previously suggested by Weston 2000, 2003), and it could thus be more properly referred to as *Archaeopotamus crusafonti*. The re-attribution of these specimens to *Archaeopotamus* suggests that this genus originally recorded in Africa (Kenya and possibly Tanzania) and Arabia (Abu Dhabi) was also present in Southern Europe (Harrison 1997; Weston 2003; Boisserie 2005; Boisserie et al. 2017). The peri-Mediterranean area was intensively colonized by hippopotamids during the latest Miocene. In addition to the Italian species (*He.*? *siculus* and *He.*? *pantanellii*) and the Spanish species (*A. crusafonti*), some other forms were collected from Libya (*He.*? *sahabiensis*, Gaziry 1987), Algeria (*He.*? *hipponensis*, Gaudry 1876) and Egypt (*He. protamphibius andrewsi*; Andrews 1902; Stromer 1914; Arambourg 1947) (Fig. 1). Since these remains are scarce and mainly fragmentary, a proper and exhaustive study is problematic. Remains attributed to *He.*? *pantanellii* and ascribed to the late Miocene (late MN13) were collected during the 19th century from the Casino Basin, Siena, Italy (Pantanelli 1879; Joleaud 1920; Boisserie 2005; Gallai 2005). These remains include a mandibular symphysis fragment with four broken incisors, some isolated incisors, a broken second lower premolar, a second lower molar and a fragment of a lower canine. Unfortunately, the original second lower molar described and figured by Pantanelli (1879) was lost. The scarce and fragmentary record from Casino does not support the validity of *He.*? *pantanellii* as a separate species, and these specimens should be, more cautiously, assigned to Hippopotamidae indet. This taxon probably arrived through the Iberian Peninsula and colonized Tuscany during the Messinian (Martino et al. 2020). The remains from Gravitelli, along with some fragmentary elements from the Casino Basin in Tuscany (Martino et al. 2020), are the only evidence of the presence of hippopotamids in Italy during the late Miocene. Hippopotamid remains were also doubtfully reported from Cessaniti, Calabria (Ferretti et al. 2003; Marra et al. 2011, 2017), and attributed to a time span between 8.1 and 7.2 Ma (Marra et al. 2017; Fig. 1). Recently, this scarce material, an incisor and a femur previously assigned to a hexaprotodontid hippopotamid, has been attributed to an anthracotheriid (Marra 2019). Pending further evidence, the remains from Gravitelli indicate that around 6 Ma African hippopotamids dispersed in Southern Europe. *Hexaprotodon*? *sahabiensis* was collected from As Sahabi, Libya, a site dated around 6.5 Ma (Bernor and Rook 2008). The teeth described by Gaziry (1987) show several archaic features, such as the sub-selenodont or selenodont aspect of the molar cusps. Weston (2003) noticed that some features displayed by *He.*? *sahabiensis*, such as the premolar row as long as the molar row, upper incisors with a mesial-lingual groove and molars dimensions, are similar to those of *Archaeopotamus*. A mandibular portion from Sahabi was later described by Pavlakis (2008). This fragment confirmed the hexaprotodont condition of the Sahabi species. The sagittal cross section of the mandible of *He.*? *sahabiensis* is peculiar among the Hippopotamidae (Boisserie 2005; Pavlakis 2008) but the mandibular portion was probably deformed by taphonomic processes that affected the mandibular symphysis. Pavlakis (2008) highlighted a strong morphologic and morphometric affinity between *He.*? *sahabiensis* and *A. lothagamensis*. Following Pavlakis (2008), the relationship between these two species should be reinvestigated. *Hexaprotodon*? *hipponensis* was collected from the lower Pliocene of Pont-de-Duvivier, Algeria (Gaudry 1876), and is represented by very scarce remains: four semi-complete incisors, two broken incisors, two lower premolars, a broken molar and two canine fragments. The third premolar is characterized by an additional cusp and by tubercles that originated from the cingulid, which is highly crenulated. The incisors are long and straight. The wear surface is delimitated by a tracked margin, a characteristic that is typical of this species. Some other remains were later collected from Wadi Natrum, Egypt, and initially attributed to *He.*? *hipponensis* by Andrews (1902) and Stromer (1914). Arambourg (1947), in contrast with previous authors, noticed a closer affinity with *He. protamphibius* (Arambourg 1944) and attributed the lower Pliocene material from Egypt to the subspecies *He. protamphibius andrewsi*. Two upper molars were illustrated by Andrews (1902), in particular an unworn M3 and a M2 with a weak wear on the lingual cusps. These molars are both quadrangular with a crenulated high cingulum and striated enamel. In the transverse valleys of the M3 there are also several tubercles probably originating from the cingulum (Andrews 1902). The remains from Egypt, subsequently partially described and figured by Stromer (1914), are quite abundant but they have not been revised recently and their location is unclear, preventing any useful considerations on these specimens.

To sum up, during the latest Miocene–early Pliocene, the circum-Mediterranean area was characterized by the presence of at least five different hippopotamid taxa: *He.*? *siculus* in Sicily (late Miocene), *A. crusafonti* in Spain (late Miocene) and in France (early Pliocene), *He.*? *hipponensis* in Algeria (early Pliocene), *He.*? *sahabiensis* in Libya

(late Miocene), and *He. protamphibius andrewsi* in Egypt (early Pliocene). The last three taxa need to be revised in detail, being based on fragmentary and poorly preserved remains. Furthermore, *He.*? *pantanellii* cannot be considered as a valid species because the material collected from the Casino Basin is too scarce and fragmentary for a generic and specific determination and it should be assigned as Hippopotamidae indet.

Conclusions

The morphological and morphometric characters of the hippopotamid remains from the uppermost Miocene deposits of Gravitelli are difficult to assess because all the original material was lost in 1908 due to the catastrophic earthquake that destroyed the city of Messina. The specimens were described and partially figured by Seguenza (1902, 1907). Seguenza (1902) also reported that some material (a maxillary fragment, a partial premolar, and a astragalus) were collected from San Pier Niceto and Scirpi. This information indicates that during the late Miocene at least three different Sicilian localities were inhabited by hippopotamids. The hippopotamid specimens from Gravitelli are mainly represented by teeth and a few poorly preserved postcranial remains. Some characters of the teeth, such as the length of the lower premolars, the low-crowned molars with crenulated cingulids, the weak trefoil wear pattern and hexaprotodonty suggest that *He.*? *siculus* displays archaic features. The characters displayed by the Sicilian hippopotamid differ from those of other species collected from the peri-Mediterranean area. In particular, *A. crusafonti* is morphometrically smaller than *He.*? *siculus* and is characterised by a tetraprotodont condition. *Hexaprotodon*? *hipponensis* has incisors characterised by a tracked margin and lower premolars with a well-developed additional cusp, whilst *He.*? *sahabiensis* has sub-selenodont or selenodont molar cusps. *Hexaprotodon*? *siculus* is morphologically closer to *Archaeopotamus harvardi*, *Hexaprotodont sivalensis* and *He. garyam*, and it is morphometrically similar to *He. sivalensis*. Accordingly, we provisionally refer the Gravitelli hippopotamid to the genus *Hexaprotodon*. *Hexaprotodon*? *siculus* arrived in Sicily during the Messinian, probably from the North African coast, but its ancestor is still unknown. The hippopotamids that colonized the Mediterranean area around the Mio-Pliocene transition were probably closely related, but the scant collected material, which is generally poorly figured and described, does not permit a detailed study. Our analysis of the published figures and descriptions reveals that some of them are probably related to *Archaeopotamus*, thus suggesting a dispersal of this genus from East Africa to North Africa, and later to Southern Europe. A re-analysis of all the late Miocene hippopotamid remains from the circum-Mediterranean area is necessary to shed light on the evolutionary history of these species as well as to resolve their phylogenetic relationships.

Acknowledgements

Thanks to the reviewers: Athanassios Athanassiou (Ministry of Culture, Ephorate of Palaeoanthropology and Speleology, Athens, Greece) and an anonymous reviewer, the editor Olivier Lambert (Terre et Histoire de la Vie, Institut Royal des Sciences Naturelles de Belgique, Brussels, Belgium) for their constructive and useful advices. This work originates within a project on late Neogene vertebrate evolution developed at the University of Florence (coordinator LR). LP prepared this paper within the research project "Ecomorphology of fossil and extant Hippopotamids and Rhinocerotids" of the University of Florence ("Progetto Giovani Ricercatori Protagonisti" initiative). LP thanks the European Commission's Research Infrastructure Action, EU-SYNTHESYS+ project BE-TAF-1367; part of this research received support from the SYNTHESYS+ Project http://www.synthesys.info/. This work is part of the "Augusto Azzaroli (1921–2015) centennial papers" by the Vertebrate Paleontology Group at the Earth Sciences Department, University of Florence.

References

Aguirre, E.D. 1963. *Hippopotamus crusafonti* n. sp. del Plioceno inferior de Arenas del Rey (Granada). *Notas y comunicaciones del Instituto Geológico y Minero de España* 69: 215–230.

Aguirre, E.D., Robles, F., Thaler, L., López Martínez, N., Alberdi, M.T., and Fuentes, C. 1973. Venta del Moro, nueva fauna finimiocena de Moluscos y Vertebrados. *Estudios geológicos* 29: 569–578.

Alcalá, L. 1994. *Macromamíferos neógenos de la fosa de Alfambra-Teruel*. 554 pp. Instituto de Estudios Turolenses-Museo Nacional de Ciencias Naturales-CSIC, Teruel.

Alcalá, L. and Montoya, P. 1998. *Hexaprotodon crusafonti* (Hippopotamidae, Mammalia) del Mioceno superior de El Arquillo (Fosa de Teruel). *Boletín de la Real Sociedad Española de Historia Natural (Sección Geológica)* 94: 93–100.

Andrews, C.W. 1902. Note on a Pliocene vertebrate fauna from the Wadi-Natrun, Egypt. *Geological Magazine* 9: 433–439.

Arambourg, C. 1944. Au sujet de l'*Hippopotamus hipponensis* Gaudry, 1876. *Bulletin de la Société géologique de France (Série 5)* 14: 147–152.

Arambourg, C. 1947. Contribution a l'étude géologique et paléontologique du bassin du lac Rudolphe et de la basse vallée de l'Omo. Mission scientifique de l'Omo 1932–1933. *Géologie-Anthropologie* 1: 232–562.

Arnason, U., Gulerg, A., Solweig, G., Ursing, B., and Janke, A. 2000. The mitochondrial genome of the sperm whale and a new molecular reference for estimating eutherian divergence rate. *Journal of Molecular Evolution* 50: 569–578.

Bernor, R.L. and Rook, L. 2008. A current view of As Sahabi large mammal biogeographic relationships. *Garyounis Scientific Bulletin Special Issue* 5: 283–290.

Boisserie, J.-R. 2005. The phylogeny and taxonomy of Hippopotamidae (Mammalia: Artiodactyla): a review based on morphology and cladistic analysis. *Zoological Journal of the Linnean Society*, 143: 1–26.

Boisserie, J.-R. 2007. Family Hippopotamidae. *In*: D.R. Prothero and S.E. Foss (eds.), *The Evolution of Artiodactyls*, 106–119. Johns Hopkins University Press, Baltimore.

Boisserie, J.-R., Brunet, M., Andossa, L., and Vignaud P. 2003. Hippopotamids from the Djurab Pliocene faunas, Chad, Central Africa. *Journal of African Earth Sciences* 36: 15–27.

Boisserie, J.-R., Lihoreau, F., Orliac, M., Fisher, R.E., Weston, E.M., and Ducrocq, S. 2010. Morphology and phylogenetic relationships of the earliest known hippopotamids (Cetartiodactyla, Hippopotamidae, Kenyapotaminae). *Zoological Journal of the Linnean Society* 158: 325–366.

Boisserie, J.-R., Likius, A., Vignaud, P., and Brunet, M. 2005. A new late Miocene hippopotamid from Toros-Ménalla, Chad. *Journal of Vertebrate Paleontology* 25: 665–673.

Boisserie, J.-R., Schuster, M., Beech, M.J., Hill, A., and Bibi, F. 2017. A new species of hippopotamine (Cetartiodactyla, Hippopotamidae)

from the late Miocene Baynunah Formation, Abu Dhabi, United Arab Emirates. *Palaeovertebrata* 41: e2.

Coryndon, S.C. 1977. The taxonomy and nomenclature of the Hippopotamidae (Mammalia, Artiodactyla) and a description of two new fossil species. *Proceedings of the Koninklijke Nederlandse Akademie van Wetenschappen* 80: 61–88.

Coryndon, S.C. 1978. Hippopotamidae. *In*: V.J. Maglio and H.B.S. Cooke (eds.), *Evolution of African Mammals*, 483–495. Harvard University Press, Cambridge.

Crusafont, M., Adrover, R., and Golpe, J.M. 1964. Découverte dans le Pikermien d'Espagne du plus primitif des hippopotames: *Hippopotamus (Hexaprotodon) primaevus* n. sp. *Comptes rendus hebdomadaires des séances de l'Académie des sciences* 258: 1572–1575.

De Visser, J.A. 2008. *The Extinct Genus* Hexaprotodon *Falconer & Cautley, 1836 (Mammalia, Artiodactyla, Hippopotamidae) in Asia: Paleoecology and Taxonomy.* 390 pp. Ph.D. Thesis, Universiteit Utrecht, Utrecht.

DeGusta, D. and Vrba, E. 2003. A method for inferring paleohabitats from the functional morphology of bovid astragali. *Journal of Archaeological Science* 30: 1009–1022.

Falconer, H. and Cautley, P.T. 1836. Note on the fossil *Hippopotamus* of the Siwalik hills. *Asiatic Researches* 19: 39–53.

Faure, M. and Méon, H. 1984. L'*Hippopotamus crusafonti* de La Mosson (près Montpellier). Première reconnaissance d'un Hippopotame néogène en France. *Comptes-rendus des séances de l'Académie des sciences. Série 2, Mécanique-physique, chimie, sciences de l'univers, sciences de la Terre* 298 (3): 93–98.

Ferretti, M., Rook, L., and Torre, D. 2003. *Stegotetrabelodon* (Proboscidea, Elephantidae) from the late Miocene of Southern Italy. *Journal of Vertebrate Paleontology* 23: 659–666.

Gallai, G. 2005. Tafonomia e paleobiologia della fauna mammaliana turoliana (Miocene superiore) del bacino del Casino (Siena): risultati preliminari. *Rendiconti Società Paleontologica Italiana* 2: 119–125.

Gallai, G. and Rook, L. 2006. *Propotamochoerus* sp (Suidae, Mammalia) from the late Miocene of Gravitelli, (Messina, Sicily, Italy) rediscovered. *Rivista Italiana di Paleontologia e Stratigrafia* 112: 317–321.

Gaudry, A. 1876. Sur un Hippopotame fossile découvert à Bone (Algérie). *Bulletin de la Société géologique de France (Série* 3) 4: 502–504.

Gaziry, A.W. 1987. *Hexaprotodon sahabiensis* (Artiodactyla, Mammalia): a new hippopotamus from Libya. *In*: N.T. Boaz, A. El-Arnauti, A.W. Gaziry, J. de Heinzelin, and D. Boaz (eds.), *Neogene Paleontology and Geology of Sahabi*, 303–315. Alan R. Liss, New York.

Gentry, A. and Hooker, J. 1988. The phylogeny of the Artiodactyla. *In*: M. Benton (ed.), *The Phylogeny and Classification of the Tetrapods, Vol. 2*, 235–272. Clarendon Press, Oxford.

Gray, J.E. 1821. On the natural arrangement of vertebrate animals. *London Medical Repository* 15: 296–310.

Harrison, T. 1997. The anatomy, paleobiology, and phylogenetic relationships of the Hippopotamidae (Mammalia, Artiodactyla) from the Manonga Valley, Tanzania. *In*: T. Harrison (ed.). *Neogene Paleontology of the Manonga Valley, Tanzania*, 137–190. Plenum Press, New York.

Hooijer, D.A. 1946. Notes on some Pontian mammals from Sicily figured by Seguenza. *Archives néerlandaises de Zoologie* 7: 301–333.

Hooijer, D.A. 1950. The fossil Hippopotamidae of Asia, with notes on the Recent species*. Zoologische Verhandelingen* 8: 1–124.

Htike, T. 2012. Review on the taxonomic status of *Hexaprotodon iravaticus* (Mammalia, Artiodactyla, Hippopotamidae) from the Neogene of Myanmar*. Shwebo University Research Journal* 3: 94–110.

Joleaud, L. 1920. Contribution à l'étude des hippopotames fossiles. *Bulletin de la Société géologique de France (Série 4)* 20: 13–26.

Kotsakis, T., Barisone, G., and Rook, L. 1997. Mammalian biochronology in an insular domain: the Italian Tertiary faunas. *Mémoires et travaux de l'Institut de Montpellier* 21: 431–441.

Lacomba, J.I., Morales, J., Robles, F., Santisteban, C., and Alberdi, M.T. 1986. Sedimentologia y paleontologia del yacimiento finimioceno de La Portera (Valencia*). Estudios geologicos Instituto de Investigaciones deológicas Lucas Mallada* 42: 167–180.

Linnaeus, C. 1758. *Systema naturae per regna tria naturae, secundum classes, ordines, genera, species, cum characteribus, differentiis, synonymis, locis. Editio decima, reformata*. 824 pp. Laurentii Salvii, Stockholm.

Marra, A.C. 2019. Contribution of the late Miocene mammals from Calabria and Sicily to the palaeogeography of the central Mediterranean. *Atti della Accademia Peloritana dei Pericolanti-Classe di Scienze Fisiche, Matematiche e Naturali* 97 (S2): A29-1–12.

Marra, A.C., Carone, G., Agnini, C., Ghinassi, M., Oms, O., and Rook, L. 2017. Stratigraphic and chronologic framework of the upper Miocene Cessaniti succession (Vibo Valentia, Calabria, Italy). *Rivista Italiana di Paleontologia e Stratigrafia (Research In Paleontology and Stratigraphy)* 123: 379–393.

Marra, A.C., Solounias, N., Carone, G., and Rook, L. 2011. Palaeogeographic significance of the giraffid remains (Mammalia, Arctiodactyla) from Cessaniti (Late Miocene, Southern Italy). *Geobios* 44: 189–197.

Martino, R., Pignatti, J., Rook, L., and Pandolfi, L. 2020. Systematic revision of hippopotamid remains from the Casino Basin, Tuscany, Italy. *Fossilia* 2020: 29–31.

Mazza, P. 1995. New evidence on the Pleistocene hippopotamuses of Western Europe. *Geologica Romana* 31: 61–241.

Montgelard, C., Catzeflis, F. M., and Douzery, E. 1997. Phylogenetic relationships of artiodactyls and cetaceans as deduced from the comparison of cytochrome b and 12S rRNA mitochondrial sequences. *Molecular Biology and Evolution* 14 (5): 550–559.

Morales, J. 1984. *Venta del Moro: su Macrofauna de mamíferos y biostratigrafía continental del Mioceno terminal mediterráneo*. 340 pp. Ph.D. Thesis, Universidad Complutense de Madrid, Madrid.

Morton, S.G. 1844. On a supposed new species of *Hippopotamus*. *Proceedings of the National Academy of Sciences, Philadelphia* 2: 4–27.

Pandolfi, L. and Rook, L. 2017. Rhinocerotidae (Mammalia, Perissodactyla) from the latest Turolian localities (MN 13; late Miocene) of central and northern Italy. *Bollettino della Società Paleontologica Italiana* 56: 45–56.

Pandolfi, L., Marra, A.C., Carone, G., Maiorino, L., and Rook, L. 2021. A new rhinocerotid (Mammalia, Rhinocerotidae) from the latest Miocene of Southern Italy. *Historical Biology* 33: 194–208.

Pantanelli, D. 1879. Sugli strati miocenici del Casino (Siena) e considerazioni sul Miocene superiore. *Atti della Reale Accademia dei Lincei, Memorie della classe di scienze fisiche, matematiche e naturali (Ser. 3)* 3: 309–327.

Pavlakis, P. 2008. Rediscovered hippopotamid remains from As Sahabi. Circum-Mediterranean geology and biotic evolution during the Neogene period: The perspective from Libya. *Garyounis Scientific Bulletin,* Special Issue 5: 179–187.

Rook, L. 1992. Italian Messinian localities with vertebrate faunas. *Paleontologia y Evolució* 24–25: 141–147.

Rook, L. 1999. Late Turolian *Mesopithecus* (Mammalia, Primates, Colobinae) from Italy. *Journal of Human Evolution* 36: 535–547.

Rook, L., Gallai, G., and Torre, D. 2006. Lands and endemic mammals in the late Miocene of Italy: constrains for paleogeographic outlines of Tyrrhenian area. *Palaeogeography, Palaeoclimatology, Palaeoecology* 238: 263–269.

Seguenza, G. 1902. I vertebrati fossili della Provincia di Messina. Parte seconda. Mammiferi e geologia del Piano Pontico. *Bollettino della Società Geologica Italiana* 21: 115–175.

Seguenza, G. 1907. Nuovi resti di mammiferi pontici di Gravitelli presso Messina. *Bollettino della Società Geologica Italiana* 26: 89–122.

Stromer, E. 1914. Mitteilungen über Wirbeltierreste aus dem Mittelpliocän des Natrontales (Ägypten), 3. Artiodactyla: A. Bunodontia: Flußpferd. *Zeitschrift der Deutschen Geologischen Gesellschaft* 66: 1–33.

Thenius, E. 1989. *Zähne und Gebiß der Säugetiere. Handbuch der Zoologie VIII (56)*. 513 pp. De Gruyter, Berlin.

Van der Made, J. 1999. Biogeography and stratigraphy of the Mio-Pleistocene mammals of Sardinia and the description of some fossils. *Deinsea* 7 (1): 337–360.

Weston, E.M. 2000. A new species of hippopotamus *Hexaprotodon lothagamensis* (Mammalia: Hippopotamidae) from the late Miocene of Kenya. *Journal of Vertebrate Paleontology* 20: 177–185.

Weston, E.M. 2003. Fossil Hippopotamidae from Lothagam. *In*: M.G. Leakey and J.M. Harris (eds.), *Lothagam. The Dawn of Humanity in Eastern Africa*. 441–483. Columbia University Press, New York.

The glyptodont *Eleutherocercus solidus* from the late Neogene of north-western Argentina: Morphology, chronology, and phylogeny

ALIZIA NÚÑEZ-BLASCO, ALFREDO E. ZURITA, ÁNGEL R. MIÑO-BOILINI, RICARDO A. BONINI, and FRANCISCO CUADRELLI

Núñez-Blasco, A., Zurita, A.E., Miño-Boilini, A.R., Bonini, R.A., and Cuadrelli, F. 2021. The glyptodont *Eleutherocercus solidus* from the late Neogene of North-Western Argentina: Morphology, chronology, and phylogeny. *Acta Palaeontologica Polonica* XX (Supplement to 3): S79–S99.

Glyptodonts (Mammalia, Xenarthra, Glyptodontidae) represent a diversified radiation of large armored herbivores, mainly related to open biomes in South America, with an extensive fossil history since the late Eocene (ca. 33 Ma) until their extinction in the latest Pleistocene–earliest Holocene. During the Pliocene and Pleistocene, glyptodonts arrived in Central and North America as part of the Great American Biotic Interchange. Within glyptodont diversity, one of the most enigmatic groups (and also one of the least known) are the Doedicurinae, mainly recognized by the enormous Pleistocene *Doedicurus*, with some specimens reaching ca. two tons. Almost nothing is known about the Neogene evolutionary history of this lineage. Some very complete specimens of the previously scarcely known *Eleutherocercus solidus*, which in turn becomes the most complete Neogene Doedicurinae, are here described in detail and compared to related taxa. The materials come from the Andalhuala and Corral Quemado formations (north-western Argentina), specifically from stratigraphic levels correlated to the Messinian–Piacenzian interval (latest Miocene–Pliocene). The comparative study and the cladistic analysis support the hypothesis that Doedicurinae forms a well supported monophyletic group, located within a large and diversified clade mostly restricted to southern South America. Within Doedicurinae, the genus *Eleutherocercus* (*E. antiquus* + *E. solidus*) is the sister group of the Pleistocene *Doedicurus*. Unlike most of the late Neogene and Pleistocene lineages of glyptodonts, doedicurins show along its evolutionary history a latitudinal retraction since the Pleistocene, ending with the giant *Doedicurus* restricted to the Pampean region of Argentina, southernmost Brazil, and southern Uruguay. This hypothetic relationship between body mass and latitudinal distribution suggests that climate could have played an active role in the evolution of the subfamily.

Key words: Mammalia, Xenarthra, Doedicurinae, anatomy, taxonomy, phylogeny, Pliocene, South America.

Alizia Núñez-Blasco [alizia_zgz12@hotmail.com], Alfredo E. Zurita [aezurita74@yahoo.com.ar], Ángel R. Miño-Boilini [angelmioboilini@yahoo.com.ar], and Francisco Cuadrelli [f.cuadrelli@gmail.com], Laboratorio de Evolución de Vertebrados y Ambientes Cenozoicos; Centro de Ecología Aplicada del Litoral (CECOAL-CONICET) Ruta 5, Km 2,5 cc 128 (3400) y Universidad Nacional del Nordeste (UNNE), Corrientes Capital, Argentina.
Ricardo A. Bonini [rbonini@fcnym.unlp.edu.ar], Instituto de investigaciones Arqueológicas y paleontológicas del Cuaternario Pampeano (INCUAPA-CONICET), Facultad de Ciencias Sociales, Universidad Nacional del Centro de la Provincia de Buenos Aires, Olavarría, Argentina. Av. Del Valle 5737, 7400, Olavarría, Buenos Aires, Argentina.

Received 24 September 2020, accepted 15 December 2020, available online 23 August 2021.

Introduction

Xenarthra is a peculiar clade of placental mammals characteristic for the Neotropical region (Gaudin and Croft 2015; Gibb et al. 2015; Delsuc et al. 2016), with a long fossil history since the early Eocene (Bergqvist et al. 2004; Lindsey et al. 2020). Their records are remarkably abundant in various Cenozoic sites mainly in South America (particularly in Argentina, see Scillato-Yané 1986), but also in Central America and North America (McDonald 2005; Brandoni et al. 2016; Gillette et al. 2016). Within Xenarthra, two large clades can be recognized, Cingulata and Pilosa, the latter containing the anteaters Vermilingua and the sloths Folivora (or Tardigrada or Phyllophaga, see Delsuc et al. 2001; Lindsey et al. 2020).

Historically, Pilosa (especially Folivora) is much better known from several viewpoints, including ecology (e.g., Bargo et al. 2006), evolutionary history (Gaudin 2004), diet (Hofreiter et al. 2000), and habitat (Bargo et al. 2006) compared to the other large clade, Cingulata (except for the "armadillos" Dasypodidae) (Gaudin and Lyon 2017),

although Cingulata represents the most diversified clade among Xenarthra (Abba et al. 2012).

Cingulata (early Eocene–Recent) is morphologically characterized mainly by the presence of a cephalic shield, dorsal carapace, and caudal armor formed by hundreds of osteoderms that cover and protect the body (Gilette and Ray 1981; Gaudin and Wible 2006; Soibelzon et al. 2010). Six families are included in Cingulata: Chlamyphoridae, Dasypodidae, Pampatheriidae, Pachyarmatheriidae, Peltephilidae, and Glyptodontidae (Delsuc et al. 2016; Mitchell et al. 2016; Fernicola et al. 2018).

Within this diversity, glyptodonts (late Eocene–latest Pleistocene/earliest Holocene) are a clade composed of large to very large grazing armored herbivores, with body masses ranging between 100 kg to ca. 2000 kg (Vizcaíno et al. 2011; Soibelzon et al. 2012; Quiñones et al. 2020). In a phylogenetic framewok, there is consensus that pampatheres (Pampatheriidae) is the sister group of glyptodonts (Gaudin and Wible 2006; Gaudin and Lyon 2017; Fernicola et al. 2018; but see Delsuc et al. 2016; Mitchell et al. 2016 for an alternative view).

The early evolutionary history of glyptodonts, during the Paleogene, is poorly known, but the records increase markedly during the Neogene and Pleistocene (Gaudin and Croft 2015; Zurita et al. 2016), especially in southern South America (Zurita et al. 2016; Toriño and Perea 2018).

Though the diversity and phylogenetic relationships of glyptodonts are under study with promising results (see, among others, Fernicola 2008; Fernicola and Porpino 2012; Zurita et al. 2013; Gillette et al. 2016; Cuadrelli et al. 2019, 2020), the subfamily Doedicurinae (late Neogene–late Pleistocene) remains one of the most enigmatic groups. It is mostly known by the Pleistocene species *Doedicurus clavicaudatus* (Owen, 1847), one of the largest and most bizarre Quaternary forms, with some specimens having body masses of ca. 2000 kg (see Soibelzon et al. 2012). The most conspicuous characters of this clade include a caudal tube in which the distal part is dorso-ventrally compressed and laterally expanded, with terminal rugose concave areas, probably for the insertion of corneous "spines" (see Lydekker 1895: pl. 27). The fossil record (e.g., MLP 16-25) and recent biomechanical analyses show that this caudal tube would make a formidable weapon against predators or to be used in intraspecific combats (see Alexander et al. 1999; Blanco et al. 2009). Another intriguing character of Doedicurinae is the exposed surface of the osteoderms of the dorsal carapace, where large foramina cross the entire thickness of the osteoderms, a unique feature among glyptodonts, and even among Cingulates (see Zurita et al. 2014, 2016), the most remarkable example being the late Pleistocene terminal species *D. clavicaudatus*. Finally, the geographic distribution along doedicurine evolutionary history is also peculiar, since a latitudinal retraction is especially evident in the Pleistocene genus *Doedicurus* Burmeister, 1874, with most records being restricted to southern South America (i.e., Argentina, Uruguay, and southernmost Brazil; Zurita et al. 2009, 2014; Varela et al. 2018).

Although the anatomy of *Doedicurus* is relatively well known, almost nothing is known about the Neogene diversity achieved by the Doedicurinae in southern South America, with a fossil record mostly limited to one dorsal carapace, several fragments of associated osteoderms, and some caudal tubes (see Ameghino 1887, 1889, 1920; Moreno 1888; Lydekker, 1895; Rovereto 1914; Castellanos 1927, 1940; Cabrera 1944). In a historical framework, and despite a large number of very poorly characterized species, only the species currently named *Eleutherocercus antiquus* (Ameghino, 1887) is known by a relatively complete dorsal carapace associated with a caudal tube (MLP 16-25, holotype of *E. copei* (Moreno, 1888) (see Ameghino 1887, 1889, 1920; Moreno 1888; Lydekker 1895) originating from the early Pliocene of the Atlantic coast of Argentina (sensu Tomassini et al. 2013). In this context, Zurita et al. (2014) first described and included in a phylogenetic framework the two only known late Neogene Doedicurinae skulls associated with some osteoderms of the dorsal carapace coming from the late Neogene–earliest Pleistocene of the Pampean region of Argentina (ca. 4.5–2.8 Ma). The results indicate that the group including the genera *Doedicurus* and *Eleutherocercus* Koken, 1888 (Doedicurinae) is monophyletic, supported mainly by cranial and dorsal carapace synapomorphies (Zurita et al. 2014).

However, and despite the advance in the knowledge of these late Neogene Doedicurinae of the Pampean region of Argentina, other records of the subfamily from Northwestern Argentina, where one of the most complete late Neogene continental sequences is exposed, are very scarce (see Quiñones et al. 2019). In fact, the last revision of glyptodonts from this area was carried out by Cabrera (1944), and Doedicurinae were among the least addressed. According to this revision, only one species of Doedicurinae was recognized in the Neogene sequences, *Eleutherocercus solidus* (Rovereto, 1914), the type material (MACN 8335) being represented by osteoderms of the dorsal carapace, and coming from Santa María Valley (SMV).

During many years, the Santa María Valley was a valuable source of palaeontological data, and palaeontologists studied the abundant fossil remains discovered there (e.g., Moreno and Mercerat 1891; Ameghino 1891; Lydekker 1895; Rovereto 1914, among others). On the other hand, the nearby outcrops of the Villavil–Quillay Basin (VQB; Catamarca Province, North-western Argentina; see Fig. 1A) have not been prospected until 1926, during the expedition led by Elmer S. Riggs of the Field Museum of Natural History, Chicago, and immediately followed by Ángel Cabrera and collaborators of the Museo de La Plata in 1927, 1929, and 1930 (see Bonini 2014). During Riggs' field expedition, several remains of mammals including the most complete specimens of Glyptodontidae were obtained in the VQB, with precise data for their stratigraphic provenance.

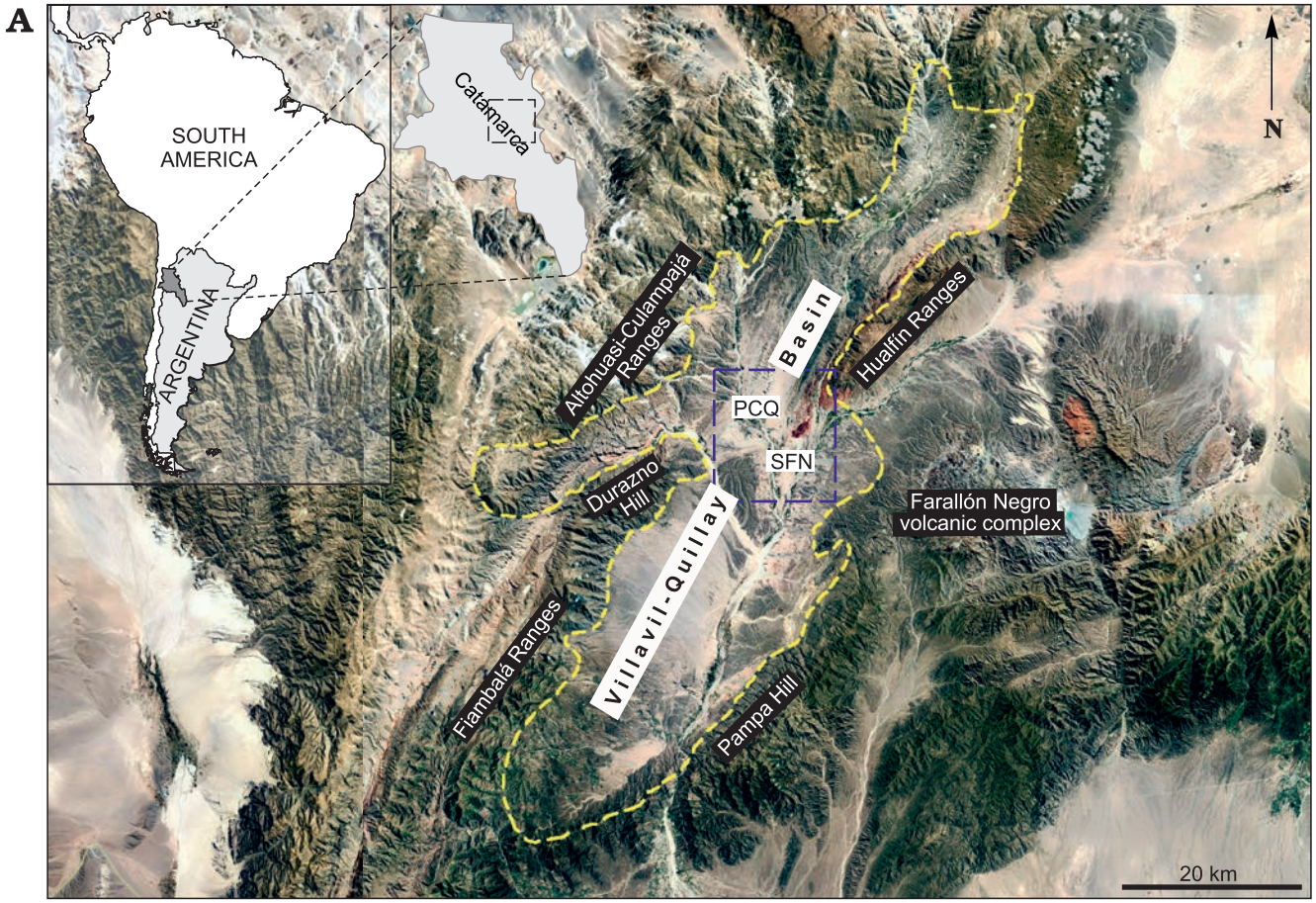

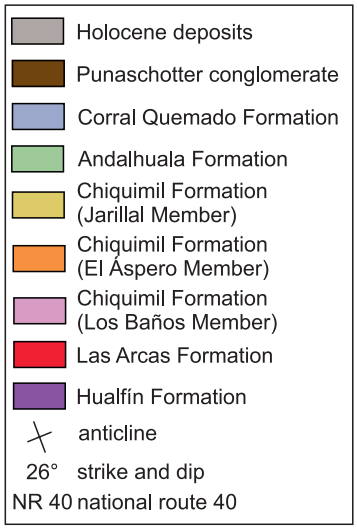

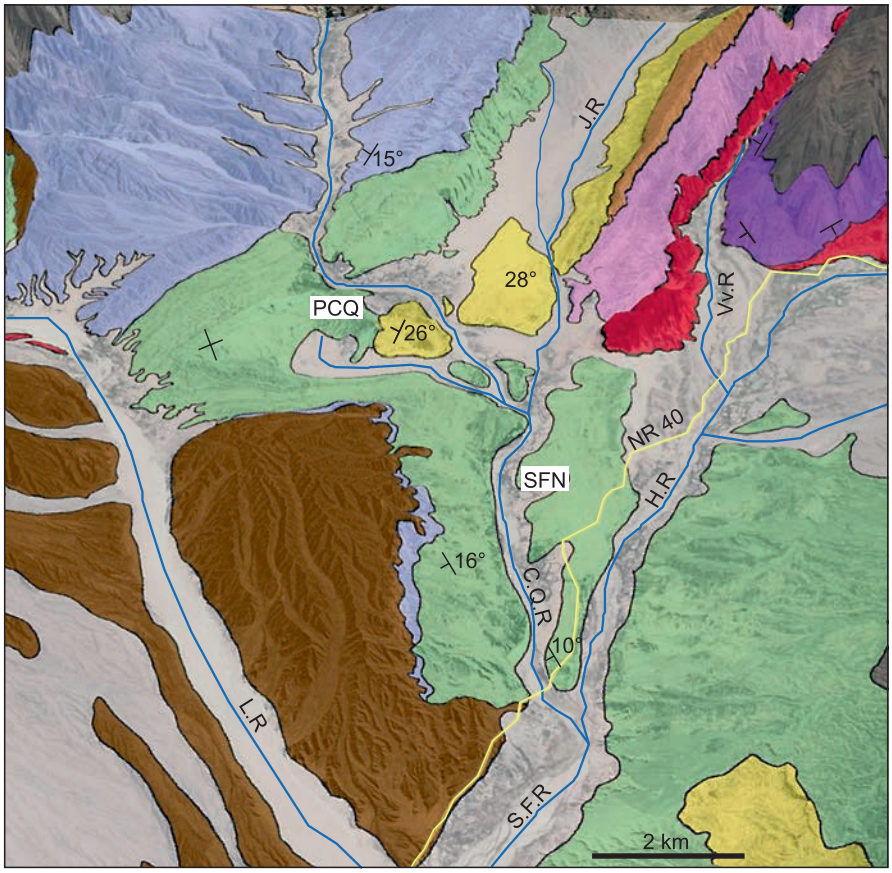

Fig. 1. Geographic and geological maps of the Villavil–Quillay Basin, North-western Argentina showing location of studied localities in Catamarca Province (**A**) and exposed lithostratigraphic units in the Villavil–Quillay Basin (**B**). Abbreviations: CQR, Corral Quemado River; HR, Hualfín River; JR, Jarillal River; LR, Loconte River; PCQ, Puerta de Corral Quemado; SFN, San Fernando Norte; VvR, Villavil River.

In this context, and as a result of fieldwork carried out in the upper Neogene from the Villavil–Quillay Basin, in addition to a careful revision of paleontological collections from the USA and Argentina, new and more complete specimens of Doedicurinae are described here, representing the most complete late Neogene glyptodonts ever known. This sample offers the opportunity to carry out a detailed morphological and phylogenetic study of these enigmatic cingulates, as well as to perform a comparative analysis with the relatively well known Doedicurinae from the Pampean region of Argentina, and to test their biostratigraphic importance.

The aims of this paper are: (i) to carry out a detailed description and comparison of new and more complete materials referred to *E. solidus*; (ii) to provide a taxonomic revision of this species and assess its biostratigraphic value; (iii) to test its relationships within Doedicurinae in a cladistic framework; and (iv) to discuss some aspects concerning the evolutionary history of Doedicurinae in high and middle latitudes of South America.

Institutional abbreviations.—FMNH-P, Paleontological collection, Field Museum of Natural History, Chicago, USA; MACN, Sección Paleontología Vertebrados, Museo Argentino de Ciencias Naturales "Bernardino Rivadavia", Buenos Aires, Argentina; MCH P, Sección Paleontología, Museo Arqueológico Condor Huasi, Belén, Catamarca, Argentina; MLP, División Paleontología Vertebrados, Facultad de Ciencias Naturales y Museo, Universidad Nacional de La Plata, Buenos Aires, Argentina; MMP, Museo Municipal de Ciencias Naturales "Lorenzo Scaglia", Mar del Plata, Buenos Aires, Argentina; Xen, Collection "Cementos Avellaneda", Olavarría, Buenos Aires, Argentina.

Other abbreviations.—FAD, First Appearance Datum; Mf/mf, upper/lower molariforms; PCQ, Puerta de Corral Quemado; SFN, San Fernando Norte; VQB, Villavil–Quillay Basin.

Material and methods

The analysis is mainly based on specimens FMNH-P 14437 and FMNH-P 14446, housed in the Paleontological collection of the Field Museum of Natural History, and MLP 29-X-10-29, housed in the Vertebrate Paleontological collection of Museo de La Plata.

Systematics partially follow Hoffstetter (1958), Paula-Couto (1979), McKenna and Bell (1997), and Fernicola (2008). All the values included in tables are expressed in millimeters, with an error range of 0.5 mm. The description and terminology for osteoderms and molariforms follow Zurita (2007), Krmpotic et al. (2009), and González-Ruiz et al. (2015).

The description of the units of the Santa María Group exposed in the Villavil–Quillay Basin (VQB; i.e., Puerta de Corral Quemado and San Fernando Norte localities) was based on different stratigraphical and geochronological proposals (Fig. 1B). Therefore, we perform here a theoretical model using this information, including stratigraphic, geochronological, and biostratigraphic data of the specimens of Doedicurinae found in VQB, in order to provide the chronological context of the fossils studied here. The provenance of the fossils collected by the expedition of Riggs in 1926 is provided in Marshall and Patterson (1981: appendix 5), while the correlation of the volcanic tuffaceous levels was made from the contributions of Latorre et al. (1997) and Bonini et al. (2017) (see Fig. 2).

In order to test the relationships of *Eleutherocercus solidus* within Doedicurinae, as well as the monophyly of Doedicurinae, we performed a cladistic analysis. The matrix includes 23 taxa and 57 morphological characters (see SOM, Supplementary Online Material available at http://app.pan.pl/SOM/app66-Nunez_etal_SOM.pdf). Most characters are based on previous analyses (Fernicola 2008; Porpino et al. 2010; Zamorano and Brandoni 2013; Zurita et al. 2013, 2014, 2017; Cuadrelli et al. 2020), with the addition of six new characters. The characters include five characters from teeth, thirteen from the skull, two from the mandible, three from the appendicular skeleton, two from the cephalic shield, twenty one from the dorsal carapace, and eleven from the caudal armor. The new characters are: angle between naso-frontal and parietal regions located at orbital notch level (in lateral view) (char. 5); angle between posterior margin of the orbital notch and the plane of the palate, near 90° (char. 7); small foramina with nearly homogenous distribution along the exposed surface of the osteoderms without ornamentation pattern (char. 34); posterior region of the dorsal carapace with a hypertrophied dome-shaped glandular structure (char. 38); transverse contour of the distal third of the caudal tube (char. 49); and ornamentation pattern of the dorsal osteoderms of the caudal tube (char. 51). There are 43 binary characters and 14 non-binary. All the characters considered in this study were scored via direct observation of the specimens and from photographs taken by the authors, and they were treated with the same weight (1.0). Character states that were not preserved were coded as "?". The matrix was obtained with Mesquite 3.04 (Maddison and Maddison 2018). The character-taxon matrix was analyzed via "Implicit enumeration" using TNT (Goloboff et al. 2008), under the criterion of maximum parsimony. Clade support was assessed via Relative and Absolute Bremer support (retained trees suboptimal by 4 steps; see Bremer 1994; Goloboff and Farris 2001); in addition to the Jackknife analysis, we used the option "Implicit enumeration" with 100 replicates.

In the phylogenetic analysis the in-group includes the following taxa: *Eleutherocercus solidus*, *E. antiquus*, and *Doedicurus clavicaudatus*. The remaining genera of Doedicurinae (*Castellanosia* Kraglievich, 1932, *Comaphorus* Ameghino, 1886, *Daedicuroides* Castellanos, 1941, *Prodaedicurus* Castellanos, 1927, *Xiphuroides* Castellanos, 1927, and *Plaxhaplous* Ameghino, 1884) were excluded from this analysis due to the scarcity of characters present

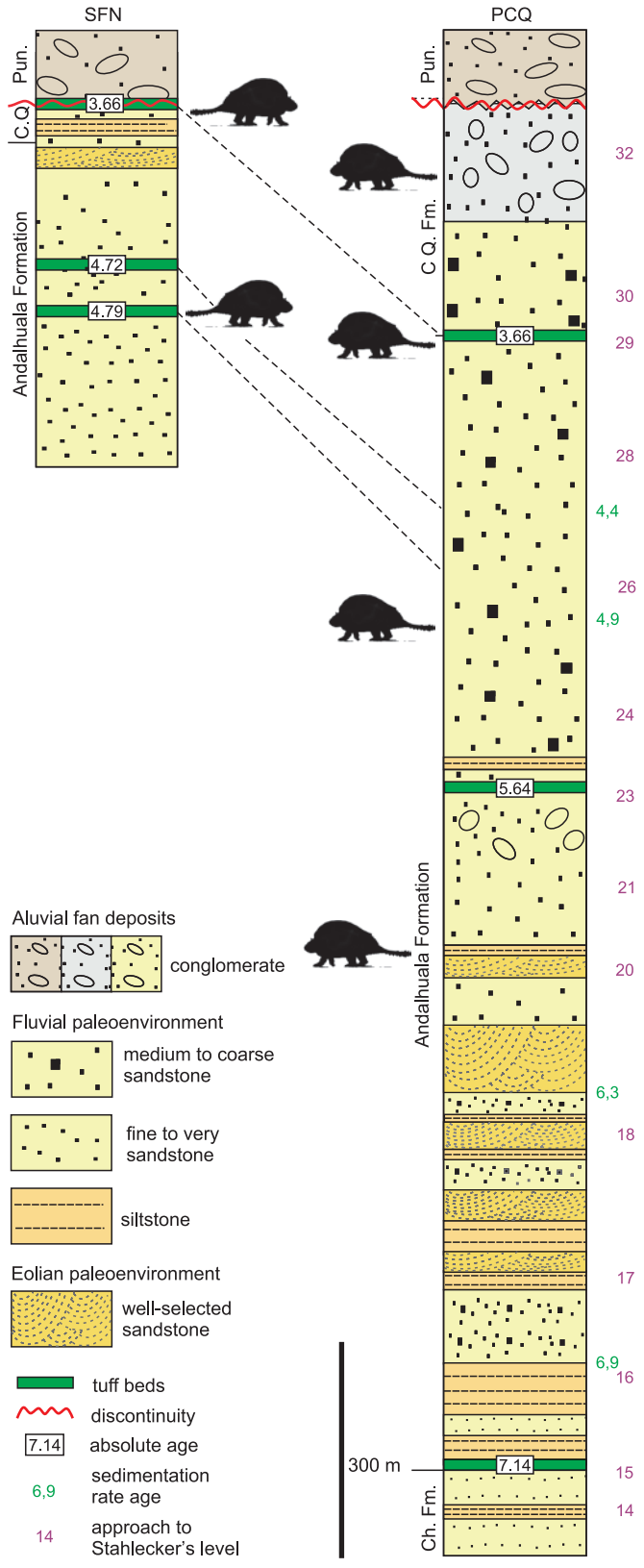

Fig. 2. Lithostratigraphic, chronological, and paleoenvironmental synthesis of San Fernando Norte and Puerta de Corral Quemado sections showing the stratigraphical and chronological distribution of *Eleutherocercus solidus* Rovereto, 1914 (modified from Georgieff et al. 2017; Bonini et al. 2020). Abbreviations: Ch. Fm., Chiquimil Formation; CQ. Fm., Corral Quemado Formation; Pun., Punaschotter.

in the type materials (mostly limited to very fragmentary osteoderms of the dorsal carapace and caudal tube) and their dubious specific validity. More specifically, a detailed taxonomic revision of these genera is needed before including them in a phylogenetic analysis. The extant dasypodid *Euphractus sexcintus* Linnaeus, 1758, and the pampathere *Pampatherium humboldtii* (Lund, 1839) were used to root the tree. In addition, the out-group is composed of *Boreostemma venezolensis* Simpson, 1947 (*Boreostema acostae* (Villarroel, 1983), *Glyptodon jatunkhirkhi* Cuadrelli, Zurita, Toriño, Miño-Boilini, Perea, Luna, Gillette, and Medina, 2020, *Glyptodon munizi* Ameghino, 1881, *Glyptodon reticulatus* Owen, 1845, *Glyptotherium texanum* Osborn, 1903, *Glyptotherium cylindricum* (Brown, 1912) (Glyptodontinae), *Propalaehoplophorus australis* Ameghino, 1887, *Eucinepeltus petestatus* Ameghino, 1891, *Cochlops muricatus* Ameghino, 1889 ("Propalaehoplophorinae"), *Plohophorus figuratus* Ameghino, 1887, *Pseudoplohophorus absolutus* Perea, 2005 ("Plohophorini"), *Neosclerocalyptus ornatus* (Owen, 1845), *Glyptotherium paskoensis* (Zurita, 2002) (Neosclerocalyptini), *Hoplophorus euphractus* Lund, 1839, *Propanochthus bullifer* (Burmeister, 1874), *Panochthus intermedius* Lydekker, 1895, and *P. tuberculatus* (Owen, 1845) (Hoplophorini, Hoplophorinae).

Geological setting

The specimens described here come from late Neogene sediments cropping out in Puerta de Corral Quemado (PCQ) (27°13'S/66°55' W) and San Fernando Norte (SFN) (27°16' S/66°54' W) in the Villavil–Quillay Basin (VQB), Belén Department, Catamarca Province, north-western Argentina. These localities are included in the geological province known as north-western Pampean Ranges, and they are bounded to the NW by Sierra de Altohuasi and Culampajá, to the W by Cerro Durazno, to the SW by Sierra de Fiambalá, to the NE by Sierra de Hualfín, to the E by the Farallón Negro volcanic complex, and to the SE by the Cerro Pampa and Sierra de Belén (Fig. 1).

The glyptodonts studied here come from levels of the "Araucanense" and Corral Quemado horizons (sensu Riggs and Patterson 1939), cropping out in PCQ, which, with some differences at the boundary of units, were correlated with the Andalhuala and Corral Quemado formations, respectively (for more details about the correlations see Bossi et al. 1987; Bossi and Muruaga 2009; Bonini 2014; Esteban et al. 2014; Georgieff et al. 2017). Several authors reported radiometric datings obtained from the tuff levels interbedded in the Andalhuala Formation exposed in both localities (Marshall et al. 1979; Butler et al. 1984; Latorre et al. 1997; Sasso 1997; Bonini et al. 2017). These absolute ages enabled the correlation of both localities and constrained chronologically the fossiliferous levels, which highlighted their biostratigraphic value, as was indicated by Nuñez-Blasco et al. (2020). The specimens studied here and collected in SFN were exhumed

from levels of the Andalhuala and Corral Quemado formations that span from ca. 4.8 to 3.6 Ma in this locality, according to the absolute ages proposed by Bonini et al. (2017). On the other hand, those coming from PCQ were found in levels ranging from ca. 5.64 to 3.66 Ma, following the absolute ages proposed by Latorre et al. 1997 (Fig. 2).

Historical background

The species currently known as *Eleutherocercus solidus* was first recognized and described by Rovereto (1914) as *Neuryurus solidus*. The holotype (MACN 8335) consists of a small fragment of dorsal carapace**,** exhumed from the Andalhuala locality, Catamarca Province. Some years later, Castellanos (1927) included the species in the genus *Eleutherocercus* Koken 1888, proposing a new combination, *Eleutherocercus solidus* (Rovereto, 1914). In the same contribution, Castellanos (1927) included another species in *Eleutherocercus*, namely *E. tucumanus*, originally *Plaxhaplus tucumanus* Castellanos, 1927, and designated as holotype the specimen MACN 2893, which consists of the distal part of a caudal tube, discovered in the vicinity of Tiopunco, Tucumán Province. Finally, Cabrera (1944) established *Eleutherocercus tucumanus* (Castellanos, 1927) as a junior synonym of *Eleutherocercus solidus*. Our observations are in agreement with the synonymy proposed by Cabrera (1944) since no significant differences are seen when comparing the caudal tubes of both species (see description and comparisons).

Systematic palaeontology

Xenarthra Cope, 1889

Cingulata Illiger, 1811

Glyptodontia Ameghino, 1889

Glyptodontoidea Gray 1869

Glyptodontidae Gray, 1869

Doedicurinae Trouessart, 1897

Genus *Eleutherocercus* Koken, 1888

Type species: *Eleutherocercus setifer* Koken, 1888; Messinian–Zanclean of Uruguay.

Emended diagnosis.—Medium sized glyptodont, and smaller compared to the giant *Doedicurus clavicaudatus*. Skull with the naso-frontal area ventrally inclined with respect to the parieto-occipital region, forming an angle of ca. 140° and showing some similitude with the genus *Panochthus* Burmeister, 1866. Orbital notch with vertical posterior margin, delimiting an angle with respect to the palatal plane of ca. 90°. Palate transversally expanded at the level of Mf1, but not as evident as in *Doedicurus.* Mf1 and mf1 simple and subcircular in outline, somewhat similar to those of *Doedicurus*; the remaining upper molariforms almost identical to *Doedicurus*. Dorsal carapace with the posterior region forming a "dome", perhaps of glandular origin. Exposed surface of the osteoderms of the dorsal carapace rugose and uniformly perforated by numerous and small foramina, a few of them crossing the entire thickness of the osteoderms; in *Doedicurus* instead, the foramina are larger and mainly concentrated in the central area of the osteoderms, with most of them crossing the entire thickness. Caudal tube similar to *Doedicurus*, but with its distal part not as laterally expanded; dorsal area of the caudal tube with numerous small foramina (as in the dorsal carapace), but preserving in some restricted areas a "rosette" ornamentation pattern (i.e., a central figure surrounded by several small figures).

Eleutherocercus solidus (Rovereto, 1914)

1927 *Eleutherocercus tucumanus*; Castellanos 1927: 282.

Holotype: MACN 8335, fragment of carapace composed of three anatomically connected osteoderms, and one isolated osteoderm.

Type locality: Andalhuala, Santa María Department, Catamarca Province, Argentina.

Type horizon: "Araucanian", late Neogene.

Material.—FMNH-P 14437, almost complete skull, mandible, carapace fragment (postero-dorsal region), complete caudal tube, left and right femora, left and right tibio-fibula, from Puerta de Corral Quemado, Belén Department, Catamarca Province, Argentina, levels 23–28 (sensu Marshall and Patterson 1981: appendix 5), Andalhuala Formation (sensu Bossi et al. 1987), ~5.64 Ma, Zanclean, early Pliocene; FMNH-P 14446, highly deformed dorsoventral skull, carapace fragment (middle or cephalic region), left hemimandible, incomplete caudal tube, vertebra, foot bones, and scapula, from Puerta de Corral Quemado, Belén Department, Catamarca Province, Argentina, level 32 (sensu Marshall and Patterson 1981: appendix 5), Corral Quemado Formation (sensu Bossi et al. 1987), above ca. 3.66 Ma, latest Zanclean–Piacenzian, Pliocene; FMNH-P 14475, complete skull without molariforms, rib, fragment of humerus, vertebrae, and foot bones, from Puerta de Corral Quemado, Belén Department, Catamarca Province, Argentina, level 20 (sensu Marshall and Patterson 1981: appendix 5), Andalhuala Formation (sensu Esteban et al. 2014), Messinian, late Miocene; MLP 29-X-10-9, highly deformed skull, from Puerta de Corral Quemado, Belén Department, Catamarca Province, Argentina, unknown stratigraphic level, probably upper levels of Andalhuala Formation or lower levels of Corral Quemado Formation, Zanclean–Piacenzian, Pliocene; MCH-P 188, small fragment of carapace, San Fernando Norte, Belén Department, Catamarca Province, Argentina, located between tuffs dated at ca. 4.78–4.72 Ma, Andalhuala Formation, Zanclean, Pliocene; MCH-P 253, isolated osteoderm from San Fernando Norte, Belén Department, Catamarca Province, Argentina, 5 m below the tuff dated at 3.66 Ma, Corral Quemado Formation, Zanclean, early Pliocene; MCH-P 325, small fragment of carapace, from San Fernando Norte (SE), Belén Department,

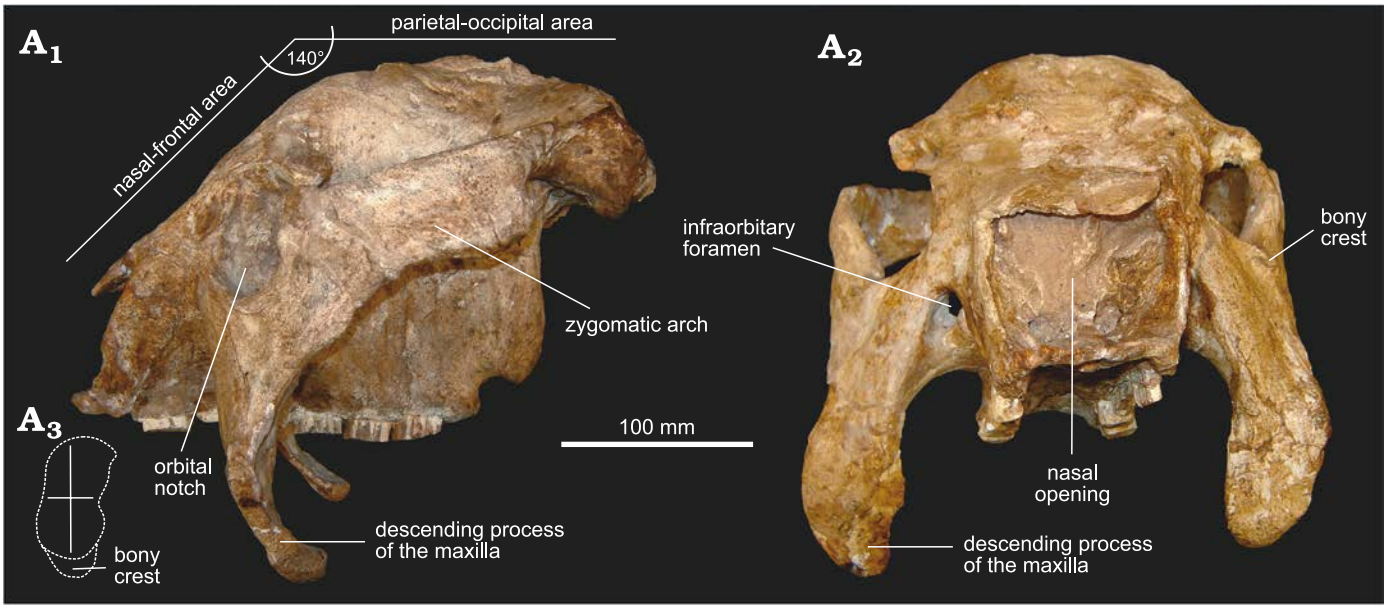

Fig. 3. Skull of doedicurine glyptodont *Eleutherocercus solidus* (Rovereto, 1914), FMNH-P 14437, from upper Miocene–Pliocene, Puerta de Corral Quemado, Andalhuala Formation, levels 23–28, Argentina; in left lateral (A_1) and frontal (A_2) views; drawing of detail of orbit notch (A_3).

Catamarca Province, Argentina, found between tuffs dated at ca. 3.6 and ca. 4.72 Ma, Zanclean, early Pliocene; MLP 29-X-10-21, caudal tube from Puerta de Corral Quemado (near the road to Loconte), Department of Belén, Catamarca Province, Argentina, unknown stratigraphic level, near the limit between Andalhuala and Corral Quemado formations, Pliocene; MACN 2893, medial-distal portion of caudal tube, holotype of *Eleutherocercus tucumanus* (Castellanos, 1927), from Tiopunco, Deparment of Tafi del Valle, Tucumán Province, Argentina, unknown stratigraphic level.

Emended diagnosis.—Glyptodont similar in size to *E. antiquus* (Table 1). Skull with an evident convex surface delimiting the rostral and parieto-occipital areas, more developed than in *E. antiquus.* Nasal openings sub-rectangular in contour, and somewhat different from the more curved lateral margins of *E. antiquus* and *Doedicurus*. In dorsal view, rostral area more elongated and subrectangular, different from the more subtriangular rostral area observed in *E. antiquus* and *Doedicurus*. Zygomatic arches with a great antero-posterior diameter. In lateral view, posterior margin of the orbital notch with an angle of ca. 90° to the palatal plane. In occlusal view, widening of the palate at the level of the Mf1 less developed compared to *E. antiquus* and *Doedicurus.* Very high horizontal ramus, almost identical to that of *Doedicurus*. Exposed surface of the osteoderms of the dorsal carapace very similar to *E. antiquus* and very different from *Doedicurus*. Caudal tube similar to *E. antiquus* in general morphology and preserving in some restricted areas a "rosette" ornamentation pattern, different from the completely perforated surface observed in *Doedicurus.*

Description.—*Skull and dentition*: The skull FMNH-P 14437 is almost complete and is the best preserved skull of Neogene doedicurine, since the two other coming from the upper Neogene of the Atlantic coast in the Pampean region do not preserve most of the parieto-occipital region (see Zurita et al. 2014) and since no cranial remains belonging to Doedicurinae are known outside Argentina.

In lateral view (Fig. $3A_1$), it can be observed that the dorsal profile of the skull resembles mainly that of cf. *Eleutherocercus antiquus* (MMP 4860) and, to a lesser extent, that of *Doedicurus* (MACN 2762, MMP 4251, MLP 16-24) (Zurita et al. 2014). The naso-frontal area is ventrally inclined to the parieto-occipital region, forming an angle of ca. 140°. This particular morphology is similar to that of the *Panochthus*, but in *E. solidus* this character appears behind the orbital notch, while in *Panochthus* it is just at the level

Table 1. Skull linear measurements (in mm) of *Eleutherocercus solidus* (FMNH-P 14437) and cf. *Eleutherocercus antiquus* (MMP 4860).

	FMNH-P 14437	MMP 4860
Total length	285	230.74
Maximum transverse diameter between zygomatic arches	218	235.18
Height of narial aperture	55.27	71.70
Transverse diameter of narial aperture	71.46	98.82
Transverse diameter of post-orbital region	115.49	108.14
Length of the tooth series	182	144.44 (M1–M6)
Length of the palate	221	157.28
Transverse diameter of the palate at the level of Mf1	47	115.20

of the orbital notch. As in cf. *E. antiquus*, a conspicuous convex surface separates both regions of the skull, a potential synapomorphy for the genus. In turn, the orbital notch is slightly sub-elliptical, with the main axis dorso-ventrally oriented, but less developed compared to cf. *E. antiquus* and some specimens of *Doedicurus* (MMP 4251). In fact, the morphology of the orbital notch seems to be more similar between cf. *E. antiquus* and *Doedicurus*, compared to *E. solidus*. However, this morphology is different from that of *Glyptodon* and *Glyptotherium*, in which the orbital notch is more circular in outline. The ventral margin of the orbital notch shows a bony crest, very similar to that in cf. *E. antiquus* and *Doedicurus* but less developed than in *E. solidus*. In turn, the posterior margin of the orbital notch is remarkably vertical, drawing an angle with respect to the palatal plane of ca. 90°, as in cf. *E. antiquus* and *Doedicurus*. The descending process of the maxillae is more dorso-ventrally elongated than in cf. *E. antiquus* and much more elongated compared to *Doedicurus*, curving towards the posterior region of the skull, which is especially evident in the ventral third of this process. The transverse diameter of the zygomatic arch is constant from the region behind the orbital notch to the contact with the temporal bone, but the curved end is less developed than in *Doedicurus*. The zygomatic arch, remarkably antero-posteriorly developed, is very different from that of cf. *E. antiquus* and *Doedicurus*, in which it is clearly less antero-posteriorly developed but dorso-ventrally higher. The dorsal margin is straight and ventrally inclined towards the orbital notch, unlike cf. *E. antiquus* in which this dorsal margin delimits a more concave surface. In general, this results in a very different morphology for both species (i.e., *E. solidus* and *E. antiquus*).

In frontal view (Fig. $3A_2$), the nasal openings are sub-rectangular, as in *D. clavicaudatus* (MLP 16-24), but different from cf. *E. antiquus* and *Doedicurus* sp. (MACN 2762), in which the lateral margins are somewhat convex, as in *Plohophorus figuratus* and *Eosclerocalyptus tapinocephalus* (Cabrera, 1939). In general morphology, the outline of the nasal openings is very different from *Glyptodon* (*G. reticulatus* and *G. munizi*), which shows a clear and inverted subtriangular outline (see Cuadrelli et al. 2019). In turn, the frontal bone shows a great vertical development, similar to cf. *E. antiquus*, and very different from *D. clavicaudatus*, *Plohophorus figuratus*, and *G. munizi*, in which it is clearly less developed. As observed in lateral view, the ventral margin of the orbital notch has a bony crest, similar in morphology to that of *Doedicurus* and much less developed compared to cf. *E. antiquus*. The infraorbitary foramina are sub-circular, and in the same relative position as in cf. *E. antiquus* and *Doedicurus.* In *G. munizi and G. reticulatus*, these foramina are circular, and developing a ventral channel (see Zurita et al. 2013; Cuadrelli et al. 2019) not present in Doedicurinae. The descending processes of the maxillae are in this frontal view very particular and different from those of cf. *E. antiquus* and *Doedicurus.* In *E. solidus*, this structure is much more massive, with a great transverse diameter (especially in its ventral half), also resembling *D. clavicaudatus*. In *Glyptodon*, these processes have a similar transverse diameter, but in their ventral-most part, they become clearly pointed (see Cuadrelli et al. 2019, 2020).

In dorsal view (Fig. $4A_1$), the general morphology of the skull is similar to that of cf. *E. antiquus*. It is also somewhat similar to *D. clavicaudatus*. but some differences can be noted. In *E. solidus*, the rostral area ahead of the orbital notches is more antero-posteriorly elongated than in cf. *E. antiquus* and *Doedicurus*, delimiting a sub-rectangular contour. On the contrary, in *D. clavicaudatus* and *Doedicurus* sp., the rostral area is more sub-triangular, as in *Panochthus tuberculatus* and *Plohophorus figuratus*. As in cf. *E. antiquus* and *Doedicurus*, the orbital notches are posteriorly closed by a well-developed post-orbital bar. In *E. solidus*, this post-orbital bar draws an angle of ca. 90° with the sagittal plane of the skull, while in the species of *Doedicurus* this angle ranges between 40–50°. The zygomatic arches of *E. solidus* are straight in their antero-posterior length, while in *Doedicurus* they are more laterally expanded, making a semicircle. The parietal and frontal bones are remarkably wide, especially between the orbital notches and the posterior-most region of the zygomatic arches. The maximum diameter of the fronto-parietal region coincides with the post-orbital bar. In cf. *E. antiquus* this morphology is similar, although this lateral expansion is not so evident compared to *E. solidus*. On the contrary, in other taxa such us *D. clavicaudatus*, *Doedicurus* sp., *G. munizi*, *Panochthus tuberculatus*, and *Plohophorus figuratus,* there is a well-developed post-orbital narrowing, weekly developed in *E. solidus*.

In occlusal view (Fig. $4A_3$, A_4), some of the most remarkable characters for *E. solidus* involve the morphology of the molariforms, the difference in size and shape between the Mf1 and the rest of the tooth series, together with the expansion of the palate at the level of Mf1. This set of characters is also seen in cf. *E. antiquus*, *D. clavicaudatus*, and *Doedicurus* sp., constituting potential synapomorphies for Doedicurinae (see Zurita et al. 2014). Mf1 are not lobed, as in *Doedicurus* and cf. *E. antiquus*. However, in *E. solidus* and *Doedicurus* it has a circular or sub-circular cross section, unlike cf. *E. antiquus*, in which Mf1 is more elliptical. Although there is a clear widening of the palate at the level of Mf1, this seems to be less obvious than in cf. *E. antiquus* and species of *Doedicurus*. The pattern of Mf2 tends to trilobation, while Mf3 is clearly trilobated. This feature is close to the morphology seen in *Doedicurus*, in which Mf2 already shows a high degree of lobulation, unlike in cf. *E. antiquus* where Mf2 is bilobated. The Mf3 of cf. *E. antiquus* and species of *Doedicurus* are similar, but in *E. solidus* and cf. *E. antiquus* the anterior margin of the first lobe is more rounded. In *E. solidus*, from Mf4 onwards, the trilobation is very marked and there are no significant differences between the other molariforms in the series, except that the anterior margin of the first lobe tends to be convex in Mf3–Mf4, flat in Mf5, and concave in the last three molariforms (Mf6–Mf8). In comparative terms, the Mf4–Mf6

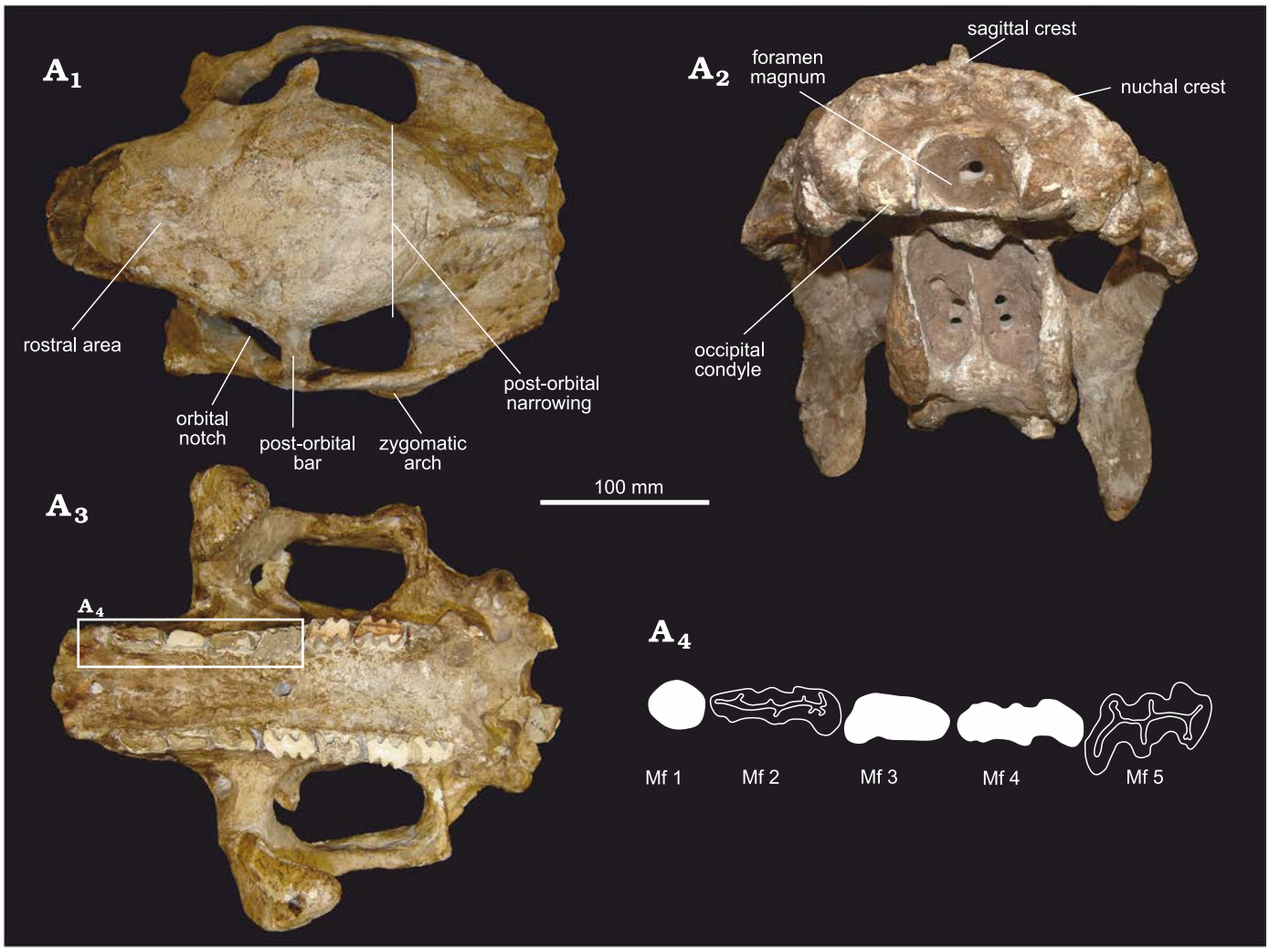

Fig. 4. Skull of doedicurine glyptodont *Eleutherocercus solidus* (Rovereto, 1914), FMNH-P 14437, from the late Miocene–early Pliocene of Argentina, Puerta de Corral Quemado, Andalhuala Formation, levels 23–28, Argentina; in dorsal (A_1) and occipital (A_2), and (A_3) occlusal views; drawing of detail of the first five molariforms (A_4). In white teeth the occlusal surface is covered by sediment.

of cf. *E. antiquus*, *D. clavicaudatus,* and *Doedicurus* sp. are very similar to each other, showing a concavity in the labial half of the posterior margin of the third lobe, a small detail also seen in other species of more distantly related genera, such as *Plohophorus* and *Glyptodon*. This character is also present in *E. solidus*, but beginning at the level of Mf5 instead of Mf4. In *E. solidus*, the minimum width of the palate is observed at the Mf3 and Mf4 level, while this narrowing is observed at the Mf4 and Mf5 level in cf. *E. antiquus*, and at the Mf4 level in *Doedicurus*. In cf. *E. antiquus* and *Doedicurus*, two large foramina with an anterior canal are present on the palate at the Mf3–Mf4 border, unlike in *E. solidus* in which those could not be detected. Likewise, in *E. solidus* the main axis of Mf1–Mf4 is parallel to the longitudinal axis of the tooth series, whereas in cf. *E. antiquus* only the main axis of Mf2 is parallel to the longitudinal axis, and in *Doedicurus* sp. only in the last molariforms of the series (Mf6–Mf8) are parallel. In other groups, such as *Plohophorus* and *Glyptodon*, this character is observed from Mf4–Mf8. It is worth noting that the skull MLP 29-X-10-9 presents supernumerary teeth, thus having a total of nine molariforms due to the duplication of Mf8. This feature was already described on this specimen by Cabrera (1944), making the first record of hyperdontia in *Eleutherocercus* and the second record for Glyptodontidae (see González-Ruiz et al. 2015).

In occipital view (Fig. $4A_2$), the specimen FMNH-P 14437 is slightly deformed due to compaction, mainly affecting the maxillary bone. The dorsal outline of the supraoccipital is rounded and convex, similar to cf. *E. antiquus*, and a marked sagittal crest extends to the nuchal crest. In *D. clavicaudatus* and *Doedicurus* sp. the dorsal profile of the supraoccipital is slightly quadrangular and concave, and the sagittal crest cannot be seen in this view. In *G. reticulatus* the dorsal profile of the supraoccipital is convex and continues laterally with the nuchal crest. In *E. solidus*, the foramen magnum is sub-elliptical, with its main axis transversally oriented. In *D. clavicaudatus* and *Doedicurus* sp. it is circular, while in *G. reticulatus* it is distinctly rhomboidal.

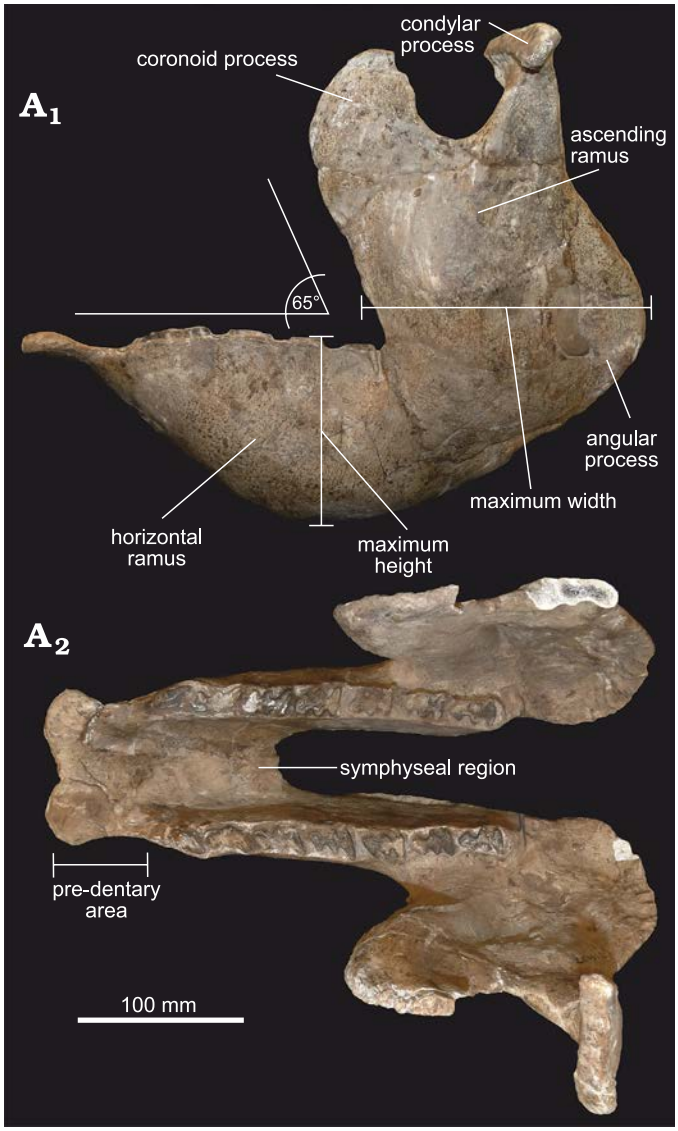

Fig. 5. Mandible of doedicurine glyptodont *Eleutherocercus solidus* (Rovereto, 1914), FMNH-P 14437, from, upper Miocene–Pliocene, Puerta de Corral Quemado, Andalhuala Formation, levels 23–28, Argentina; in left lateral external (A_1), and occlusal (A_2) views.

Mandible: The material includes FMNH-P 14437 (Fig. 5), represented by a complete and very well-preserved mandible, in addition to another hemi-mandible (FMNH-P 14446). The general morphology is almost identical to that of *Doedicurus*, although both taxa are temporally separated by more than 4 My. This highlights the conservative dentary morphology observed in this lineage, coinciding with the observations carried out in other glyptodont clades, such as the Neosclerocalyptini *Neosclerocalyptus* (see Quiñones et al. 2020).

In lateral view (Fig. $5A_1$), the mandible is very robust, at the level of both the ascending and horizontal rami, as in *Doedicurus*. The ventral margin of the horizontal ramus is notably concave, much more than that of *Glyptodon*, *Panochthus*, and *Neosclerocalyptus*, reaching its maximum height at the level of the mf4 and mf5. The angle between the symphysial region and the middle and posterior border of the mandibular body is ca. 140°, as in *Doedicurus*, somewhat different from *Glyptodon*, in which this angle reaches 150°. Like the mandibular body, the ascending ramus is very robust, with a great antero-posterior diameter, which represents the total length of the tooth series from mf1 to mf6, as in *Doedicurus*. As in *Doedicurus*, *Neosclerocalyptus*, and *Glyptodon*, the ascending ramus is inclined forwards, drawing an angle of 65° between its anterior margin and the alveolar margin; this anterior margin is at the level of mf5, as in the genera *Doedicurus* and *Glyptodon,* and different from *Neosclerocalyptus*, in which it is located at the level of mf6. The sigmoid notch is very developed and similar to the notch in *Doedicurus*, while the posteroventral margin of the ascending ramus shows a very conspicuous angular process at the level of the posterior margin of the third lobe of mf8. In turn, the posterior margin of the ascending ramus is concave, especially in its dorsal-most third, as in *Doedicurus*, but different from *Neosclerocalyptus*, *Panochthus*, and *Glyptodon*, which show a straighter edge.

In occlusal view (Fig. $5A_2$), the pre-dental region of the symphysis is 76 mm long proximo-distally, widening in the most distal portion, where two large mental foramina are seen on the ventral side. The mandibular symphysis ends at the level of the second lobe of mf4, as in *Neosclerocalyptus*, *Glyptodon*, and *Panochthus.*

Molariforms: (Fig. $5A_2$). The mf1 is sub-circular in section, and the smallest compared to the rest of the molariforms (mf2–mf8). In *Doedicurus* sp. and cf. *E. antiquus* this molariform is subcircular to subtriangular and similarly smaller than other molariforms. The mf2 of *E. solidus* is elliptical in outline, with irregular edges, lacking a defined pattern, so that no clear tendency towards bilobulation or trilobulation is observed. On the contrary, in *Doedicurus* sp., mf2 is completely trilobulated. This particular morphology observed in the mf1, mf2 of Doedicurinae markedly contrasts with that of *Glyptodon*, in which a very conspicuous trilobulation is seen from the mf1 (this character being a synapomorphy of the genus; see Zurita et al. 2013; Cuadrelli et al. 2020), together with a limited variation of size along the molariform series. The mf3 shows some tendency towards trilobulation, but not as marked as in the rest of the posterior molariforms. The mf4–mf8 are completely trilobulated, as in cf. *E. antiquus*; in addition, the general morphology of the last molariforms of *E. antiquus* and *E. solidus* is very similar to those of *D. clavicaudatus* and *Doedicurus* sp.

Osteoderms: Associated with the material described above, some fragments of dorsal carapace were found. This allows for careful comparisons with the holotype of *E. solidus* (MACN 8335; see Fig. 6A) and, consequently, to refer the specimens here analyzed to this species, greatly improving its morphological characterization. Other remains were found in nearby localities, but mostly corresponding to isolated osteoderms and small fragments of carapace (MCH-P 188, 253, and 325; Fig. 6D).

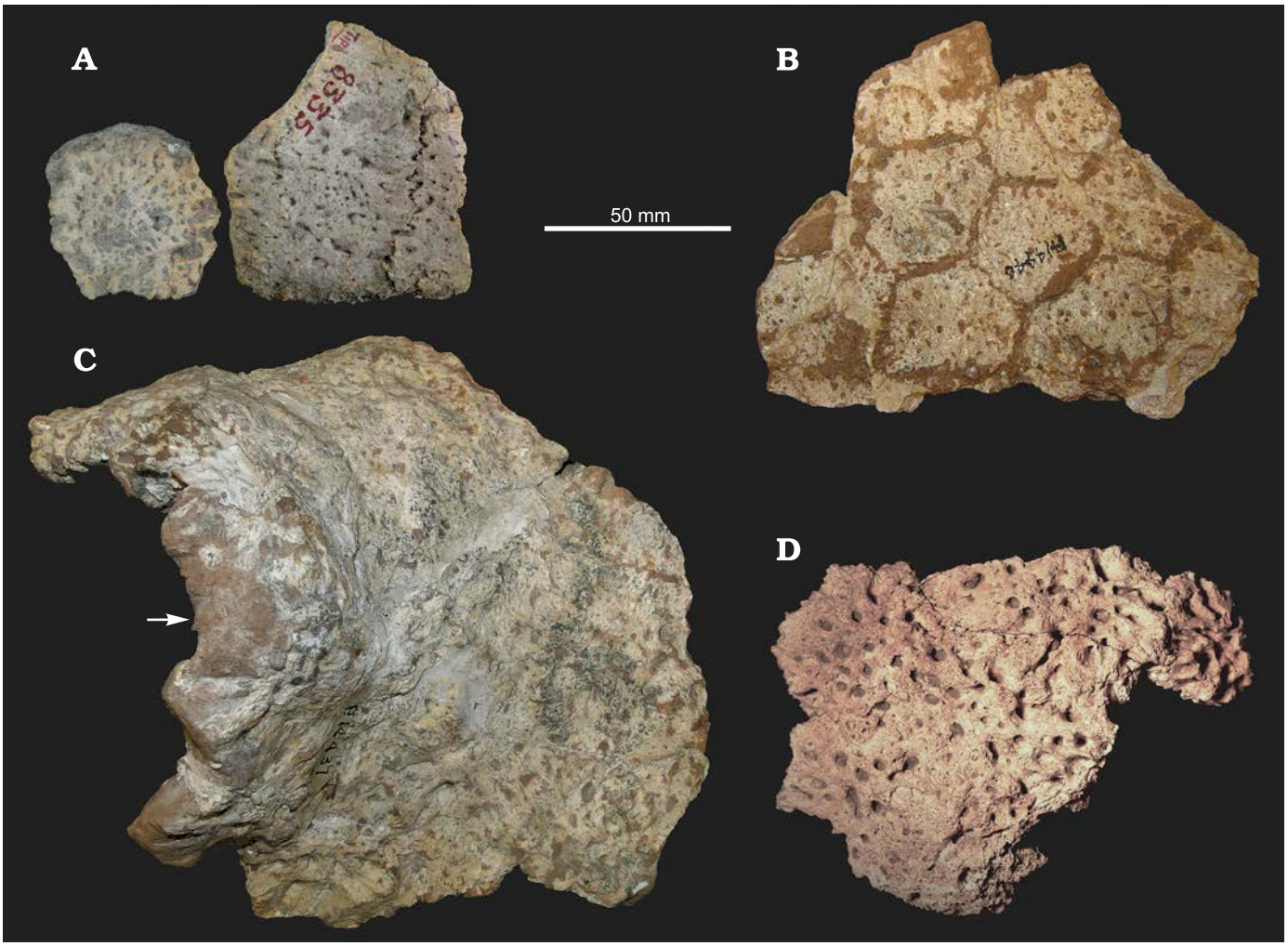

Fig. 6. Osteoderms of doedicurine glyptodont *Eleutherocercus solidus* (Rovereto, 1914) from Pliocene of Argentina. **A**. MACN 8335 (holotype), small carapace fragment, from Andalhuala, "Araucanian" (late Neogene). **B**. FMNH-P 14446, carapace fragment (middle or cephalic region), from Puerta de Corral Quemado, Corral Quemado Formation, level 32. **C**. FMNH-P 14437, carapace fragment (the arrow is pointing the postero-dorsal region showing the modified osteoderms that constitute the "dome" structure), from Puerta de Corral Quemado, Andalhuala Formation, levels 23–28. **D**. MCH-P 188, small fragment of carapace, from San Fernando Norte, Andalhuala Formation.

The fragment of dorsal carapace of FMNH-P 14446 (Fig. 6B) is composed of 11 associated osteoderms, of which six are complete. The osteoderms are hexagonal and probably correspond to the middle or cephalic part of the carapace, as observed in other glyptodonts. The exposed surface is rugose and has several small foramina irregularly distributed. Most of these foramina do not penetrate the entire thickness of the osteoderms, as in cf. *E. antiquus* (see Zurita et al. 2014) and the type material of *E. solidus*. This clearly differs from the morphology observed in *Doedicurus*, in which the osteoderms are much thicker, and the foramina tend to be, in small number, located in the middle region of the osteoderm, piercing its entire thickness. The other fragment (FMNH-P 14437; see Fig. 6C) belongs to the postero-dorsal region. The high degree of fusion between osteoderms prevents from inferring their exact number in this fragment. As in FMNH-P 14446 and the holotype of *E. solidus*, the exposed surface shows several small foramina irregularly distributed (see Rovereto 1914). The most marginal osteoderms are extremely irregular in shape and have an anomalous fibrous texture. On the left lateral half of this fragment, part of an irregular dome-like structure can be seen. The high degree of fusion indicates that this is the anterior region of the "dome". This particular structure (of glandular origin?) has been reported by other authors as characterizing the genus *Eleutherocercus* (see Moreno 1888; Lydekker 1895; Ameghino 1920; Chimento et al. 2010). We therefore suggest, agreeing with the proposal of Chimento et al. (2010), that it could represent part of a glandular system located at the level of the posterior part of the pelvic girdle. Supporting this hypothesis, several specimens of the Glyptodontinae *Glyptodon* show very large foramina at the intersection between the annular and radial sulci, in the same region of the dorsal carapace (see Zurita et al. 2016; Cuadrelli et al. 2019).

Caudal tube: FMNH-P 14437 includes an almost complete caudal tube, but its exposed surface is not well preserved, precluding the observation of the ornamentation

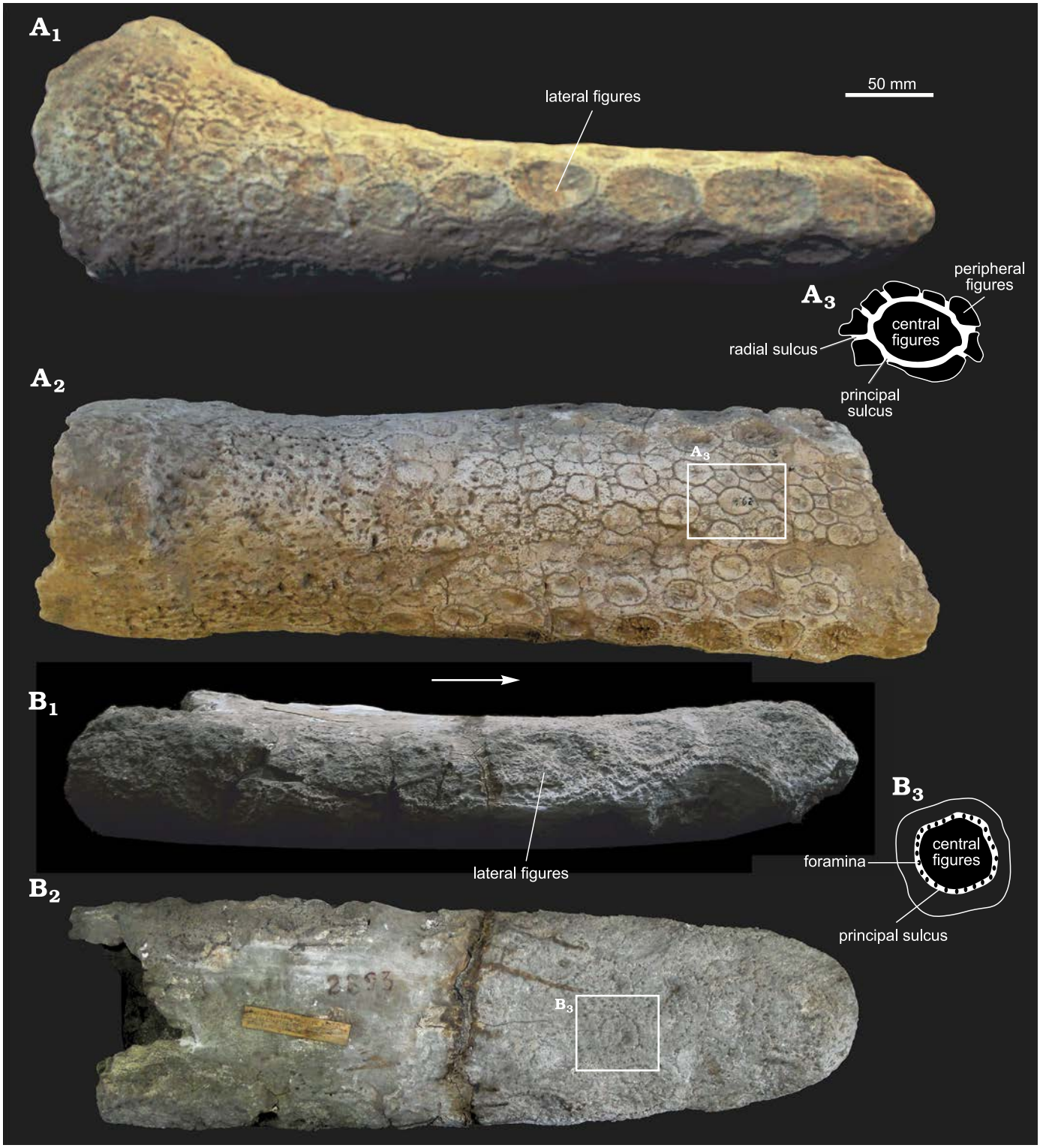

Fig. 7. Caudal tubes of doedicurine glyptodont *Eleutherocercus solidus* (Rovereto, 1914), from upper Miocene–Pliocene of Argentina. **A**. MLP 29-X-10-21, from Puerta de Corral Quemado (near the road to Loconte), unknown stratigraphic level; in lateral (A_1) and dorsal (A_2) views; drawing of detail of dorsal osteoderm (A_3). **B**. MACN 2893 (holotype of *E. tucumanus* Castellanos) from Tiopunco, unknown stratigraphic level; in lateral (B_1) and dorsal (B_2) views; drawing of detail of dorsal osteoderm (B_3).

pattern. However, its general morphology can be inferred. Although its transverse diameter is quite similar along its antero-posterior length, the caudal tube is slightly more laterally expanded at the proximal end, whereas the distal-most part is clearly rounded and blunt. In lateral view, the caudal tube shows a greater dorso-ventral diameter (ca. 30%) in its proximal part, being more flattened towards the distal end. MLP 29-X-10-21 (Fig. 7A) and MACN 2893 (holotype of

E. tucumanus, Fig. 7B) preserve the exposed surface, with a clear ornamentation pattern. In dorsal view, the ornamentation displays a "rosette" pattern. In each osteoderm the central figure is slightly concave, surrounded by 7–8 smaller and angular peripheral figures. The principal sulcus surrounding the central figure bears several small foramina. In some specimens (e.g., MLP 29-X-10-21) the foramina are more developed in the proximal half of the caudal tube, while in others (e.g., MACN 2893) they are present along the antero-posterior diameter, but this could be probably due to taphonomic factors. On the lateral sides, near both margins, there is a row of large figures with a very rugose surface, which become more numerous towards the distal end of the tube. In lateral view, six or seven lateral figures are present, increasing in size towards the distal end, as in *Panochthus* and *Doedicurus*. Unlike in *Panochthus*, in *Eleutherocercus* (as well as in *Doedicurus*) the surface of these figures is concave, very rugose and striated. Instead, in *Panochthus* and *Hoplophorus* these figures display a "spine-like" morphology. In *E. solidus*, lateral figures are separated from each other by a single row of foramina, but the proximal ones also show some peripheral figures. On the distal end of MACN 2893, there are two large figures on each margin, one being more dorsal and the other being more ventral and somewhat larger. The contact area between both figures (dorsal and ventral) coincides with the midline of the lateral sides of the tube. Despite some similarities with *Doedicurus*, the morphology of the caudal tube of *Eleutherocercus* shows some differences. In *Doedicurus*, the distal end of the caudal tube is very laterally expanded, similar to a club. The rosette ornamentation pattern of *Eleutherocercus* is not observed in *Doedicurus*; in the latter, the surface is smooth with numerous foramina similar in morphology to those of the dorsal carapace.

However, the most evident differences between the genera *Doedicurus* and *Eleutherocercus* are observed at the distal end of the caudal tube, specifically in the location and number of the large rugose figures. In *Eleutherocercus* these figures are numerous, ranging 10–14 depending on the specimen. From the most distal end of the tube to a proximal position they are located as follows: four at the most distal end, grouped into two pairs, one pair placed in the dorsal surface, and the other two in the ventral surface, the latter being a larger pair; in the dorsal area of the distal end there is a total of up to five figures, grouped into a distal row of three and another more proximal composed of two figures. In turn, the ventral area shows the same ornamentation pattern to that observed in the dorsal surface. On the other hand, in *Doedicururs* these figures are reduced in number to only 8. From the most distal end of the tube to a proximal position they are located as follows: a pair of symmetrical figures at the most distal end of the caudal tube; four immediately behind, in a more proximal position and grouped in two pairs, one pair in a dorsal position and the other in a ventral position; and finally two more symmetrical figures in a mid-lateral position, the latter being the largest.

Phylogenetic affinities of *Eleutherocercus solidus*

The cladistic analysis resulted in one most parsimonious tree (MPT) (RI = 0.91 and CI = 0.79; length = 97 steps), see Fig. 8.

Two major radiations are observed in the topology. In the first one, supported by synapomorphies 20:0 and 40:0, *Propalaehoplophorus australis* is the most basal taxon. However, "Propalaehoplophorinae" is not a monophyletic group, since the three species generally placed in that group (*P. australis*, *Eucinepeltus petestatus*, and *Cochlops muricatus*) branch sequentially, with *Cochlops muricatus* being recovered as the sister group of the remaining diversity, recognized as valid in this analysis (Plohophorini, Neosclerocalyptini + Hoplophorini [Hoplophorinae] and Doedicurinae sensu Zurita et al. 2014; synapomorphy 48:2 and the ambiguous synapomorphies 24:1; 42:0; 52:1). This is in agreement with the topologies reported by Zurita et al. (2013, 2014), Quiñones et al. (2020), and Cuadrelli et al. (2020).

The clade formed by *Pseudoplohophorus absolutus* and *Plohophorus figuratus* (ambiguous synapomorphy 29:1) is recovered as the sister group of the remaining members of this radiation (Doedicurinae and Hoplophorinae [Hoplophorini + Neosclerocalyptini] sensu Zurita et al. 2014; synapomorphy 17:2). In turn, the subfamily Doedicurinae appears as a well supported clade, condition based on several cranial and postcranial characters (synapomorphies 7:1; 12:1; 16:1; 26:0; 27:2; 30:2; 35:3; 50:2; 54:1 and ambiguous synapomorphies 11:1; 42:3; 49:1). It includes the genera *Doedicurus* and *Eleutherocercus*, and shows a similar topology to that obtained by Zurita et al. (2014). Within Doedicurinae, the genus *Eleutherocercus* includes the two species (*E. antiquus* + *E. solidus*) and several cranial and postcranial characters support its condition of natural group (synapomorphies 34:1; 38:1; 56:1 and ambiguous synapomorphies 4:0; 45:0). On the other hand, within Hoplophorinae sensu Zurita et al. 2014 (synapomorphies 2;1 14:1; 21:1) a sister group relationship between the tribes Neosclerocalyptini (*N. ornatus* + *N. paskoensis*; synapomorphies 3:1; 9:3; 37:0) and Hoplophorini (synapomorphies 8:1; 41:1; 53:1 and ambiguous synapomorphy 49:1) is recovered, with the genus *Hoplophorus* as sister taxon of *Propanochthus* + *Panochthus* (26:3; 33:1; 51:2 and ambiguous synapomorphy 29:1). The position of *Propanochthus bullifer* as sister group of *Panochthus* spp. suggests that the former may be interpreted as belonging to the latter genus.

The second radiation of Glyptodontidae is that of Glyptodontinae (synapomorphies 17:3; 22:0; 40:1 and ambiguous synapomorphy 15:0). This subfamily includes the tribes Boreostemmini (sensu Cuadrelli 2020), represented by *Boreostemma* (synapomorphies 43:1 and the ambiguous synapomorphy 31:1) and Glyptodontini (sensu Cuadrelli 2020; synapomorphies 0:1; 6:1; 9:1; 23:0; 26:1; 28:1; 42:2 and the ambiguous synapomorphy 24:1). In turn, Glyptodontini

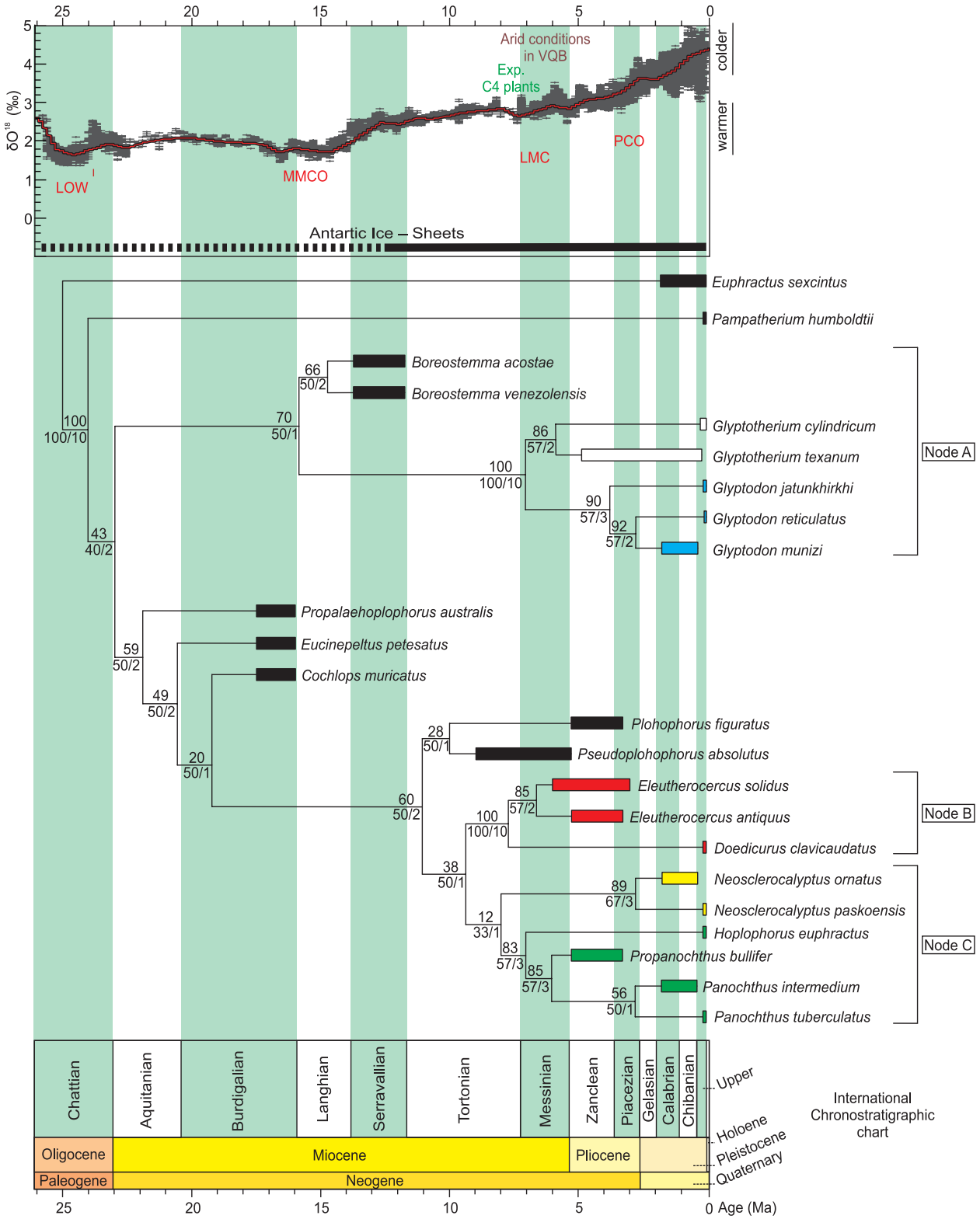

Fig. 8. Phylogeny of Glyptodontidae based on TNT parsimony analysis of 57 osteological characters from 23 taxa (tree length 97 steps; Consistency Index 0.79; Retention Index 0.91). The numbers above each node represent Jackknife values; numbers under each node show relative Bremer support (right) and absolute Bremer support (left). Node A: Glyptodontinae (taxa in white correspond to Glyptotheriini; taxa in blue correspond to Glyptodontini); Node B: Doedicurinae (taxa in red); Node C: Hoplophorinae (taxa in yellow correspond to Neosclerocalyptini; taxa in green correspond to Hoplophorini). Chronostratigraphic calibration of the phylogenetic relationships of Neogene Glyptodontidae is compared to benthic foraminifera $\delta^{18}O$ values from Zachos et al. (2001) to visualize the evolution of the Doedicurinae clade in the context of paleoenvironment and climate changes throughout the Neogene in north-western Argentina. Abbreviations: LOW, Late Oligocene Warming; MMCO, Middle Miocene Climatic Optimun; LMC, Late Miocene Cooling; PCO, Pliocene Climatic Optimun; Exp. C4 plants, expansion of C4 plants; VQB, Villavil-Quillay Basin.

is divided into two subtribes, Glyptodontina (synapomorphies 1:1; 10:1; 14:0; 32:1; 55:0) that gathers species of the *Glyptodon*, and Glyptotheriina (synapomorphies 35:1; 36:1; 55:1) including species of the *Glyptotherium*.

Discussion

Glyptodonts constitute one of the most spectacular cingulate radiations in America (Zurita et al. 2016), and their evolutionary history appears to be mostly related to the appearance and development of open biomes since the late Eocene–Oligocene (Carlini et al. 2010; Mitchell et al. 2016; Zachos et al. 2001, 2008; Fig. 8). The biomechanical evidence interpreted glyptodonts as grazers, although some kind of niche partitioning was suggested by some authors (Vizcaíno et al. 2012).

Although the Paleogene evidence is still very scarce and mostly limited to osteoderms of the dorsal carapace, an interesting diversification is observed, represented by two morphotypes, one included in the subfamily "Propalaehoplophorinae" and the other in the poorly known "Glyptatelinae". This early diversification could be related to the progressive aridization and development of open areas since the latest Eocene–early Oligocene, and is mostly restricted to the Patagonian region of South America (Cuadrelli et al. 2020).

Since the early–middle Miocene (ca. 19–17 Ma) a marked increase in the records of glyptodonts is observed, with the first well-documented Neogene radiation represented by the "Propalaeoplophorinae" and the enigmatic *Parapropalaehoplohorus septentrionalis* in southern South America (Croft et al. 2007; Vizcaíno et al. 2010; González Ruiz et al. 2020). This evolutionary process may have coincided, at least in part, with the Middle Miocene Climatic Optimum (MMCO) (Zachos et al. 2001; Croft et al. 2016).

From an evolutionary standpoint, the "Propalaehoplophorinae" (i.e., *Propalaehoplophorus*, *Eucinepeltus*, and *Cochlops*) are the most basal taxa of a large southern South American radiation that includes most of the known diversity of glyptodonts, the other large radiation being represented by the Glyptodontinae (Carlini et al. 2008; Zurita et al. 2013; Cuadrelli et al. 2020). In this framework, this first large southern lineage that begins with *Propalaehoplophorus australis*, underwent, according to the fossil record, a diversification process since the late Miocene–earliest Pliocene, with the first record of several lineages, some of them with long biochrons that reached the latest Pleistocene (Zurita et al. 2016). Interestingly, this major diversification seems to have mainly occurred in high latitudes instead of tropical and intertropical regions of South America, where the diversification was mostly limited to the subfamily Glyptodontinae during the Miocene and Pliocene (Zurita et al. 2013; Cuadrelli et al. 2020).

In this context, in our phylogenetic analysis, Doedicurinae appears as a well supported clade, including until now the genera *Eleutherocercus* and *Doedicurus* as sister groups. In turn, Doedicurinae is included in a large southern South American clade, which is in agreement with several previous analyses (see Zurita et al. 2013; Cuadrelli et al. 2020; but see Fernicola 2008; Fernicola and Porpino 2012 for another interpretation). As occurs with most of the taxa composing this large clade, the evolutionary history of Doedicurinae was restricted to high and middle latitudes.

From a chronostratigraphic view point, the records of *E. solidus* come from the Corral Quemado and Andalhuala formations, specifically, the stratigraphic levels chronologically located in a latest Messinian to Piacenzian interval (ca. 6–3 Ma, latest Miocene–Pliocene). FMNH-P 14475 is considered here as the First Appearance Datum (FAD) of *Eleutherocercus solidus* in VQB, recorded in level 20 (sensu Stahlecker in Marshall and Patterson 1981: appendix 5), which is located in the stratigraphic section 1100–1200 m at ca. 6 Ma (see Fig. 2). This inferred interval is similar to the one postulated for the geological units in the Pampean region of Argentina where remains of *E. antiquus* (Monte Hermoso Formation) and cf. *E. antiquus* (Chapadmalal and El Polvorin formations) are recorded, which span ca. 5.2–2.8 Ma (Zanclean to Piacenzian) (Zárate et al. 2007; Beilinson et al. 2017; Quiñones et al. 2020). This implies that both species of the genus partially overlap in time (Pliocene), but in different regions of southern South America (Zurita 2007; Cione et al. 2000).

During the late Miocene–early Pliocene, a series of paleoenvironmental changes have been documented in the fossiliferous sediments of northwestern Argentina. These changes have been related to floristic (i.e., C3/C4 ratio), tectonic (i.e., rising of mountain ranges), and climatic events (i.e., generalized aridification, seasonality) (Hynek et al. 2012; Georgieff et al. 2017; Armella and Bonini 2020), which probably affected the development and evolution of herbivorous faunas (Cerling et al. 1998; MacFadden et al. 1999; MacFadden 2005). The FAD of *E. solidus* in VQB is synchronous to large eolian deposits representing arid conditions, which are identified in different locations along the basin (see Muruaga 2001; Hynek et al. 2012; Esteban et al. 2014; Georgieff et al. 2017). Likewise, these deposits coincide with the period in which C4 becomes an important component in the diet of large herbivores (Hynek 2011), before becoming dominant after 4 Ma (Latorre et al. 1997). As stated above, the general morphology of the mandible and teeth of *E. solidus* is almost identical to that of *Doedicurus*, which has the highest hypsodonty index among glyptodonts (Vizcaíno et al. 2011). These anatomical features can be interpreted as a way of increasing the mechanical capacity in relation to accidental consumption of abrasive particles (i.e., sand, dust, volcanic glass) adhering to the surface of plants (Janis 1988; Candela and Bonini 2017) or the ingestion of large amounts of food with low nutritive value (Vizcaíno et al. 2011; see Fig. 9).

The high frequency of records suggests that Doedicurinae were dominant elements in the late Neogene palaeofauna in both the Pampean and northwestern regions. However, preliminary studies of the El Polvorín Formation

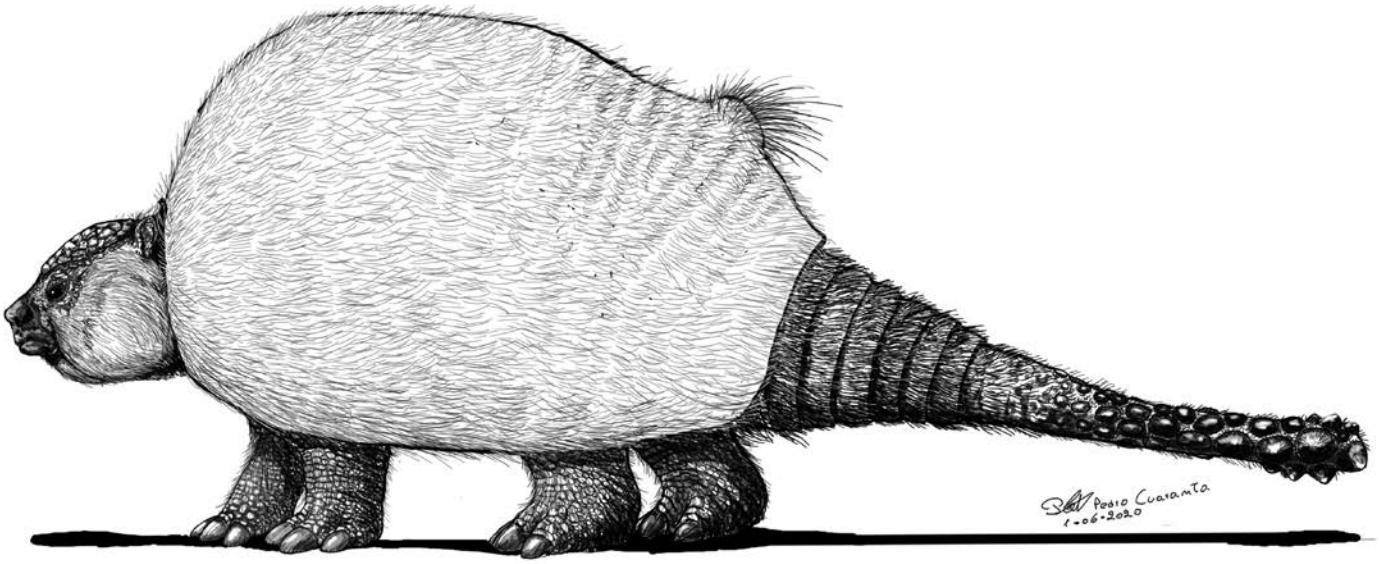

Fig. 9. Hypothetical life reconstruction of the extinct *Eleutherocercus solidus* (Rovereto, 1914), based on the new specimens described here. Credit: Pedro Cuaranta.

(Pliocene–earliest Pleistocene) reveal a decrease in the frequency of records of Doedicurinae towards the Pleistocene (Quiñones et al. 2020). In this framework, and taking into account that most of the glyptodonts present a rich fossil record in South America (see Zurita et al. 2009), we suggest that this very low frequency of records of Pleistocene Doedicurinae in most of South America (perhaps except for some areas of Uruguay) is reflecting a genuine process in which Pleistocene Doedicurinae were very reduced in the number of specimens compared to the other genera (ie., *Glyptodon*, *Panochthus*, and *Neosclerocalyptus*). It is interesting to note that it is quite common to find some associated specimens of Pleistocene glyptodonts in southern South America, suggesting some kind of gregarious habit. However, this was not reported for *Doedicurus* since all the records correspond to single specimens. Although more evidence is necessary, this could suggest that *Doedicurus* developed solitary habits.

Outside Argentina, Neogene Doedicurinae is also recorded in the Pliocene of Inchasi, Bolivia (ca. 3.3–4 Ma; see MacFadden et al. 1993; Cione and Tonni 1996), and Uruguay (Koken 1888; Toriño and Perea 2008), at high and middle latitudes. Doedicurinae (together with Glyptodontinae) were some of the most frequently recorded glyptodonts in the Pliocene sequences of Inchasi, Bolivia (AEZ, personal observations). The northernmost record of a Doedicurinae comes from the Pliocene of Ayo Ayo, near La Paz (Bolivia), at a latitude of ca. 16°30′. Based on the high frequency of Neogene records of Doedicurinae in Uruguay, some authors recognized several endemic taxa, among them *Prodaedicurus* and *Castellanosia* (Toriño and Perea 2008). However, it cannot be ruled out that some (if not all) could belong to the same taxon. More complete remains are needed to test this taxonomic hypothesis. Indeed, unlike north-western and Pampean regions of Argentina, where Doedicurinae is represented by several relatively complete specimens, the remains from Bolivia and Uruguay are mostly represented by osteoderms of the dorsal carapace and some caudal tubes, a situation that hinders their taxonomic identification. No remains of Doedicurinae are known from the Pleistocene of Bolivia and Peru. However, it seems that during the late Neogene (latest Miocene–Pliocene) Doedicurinae reached a wide latitudinal distribution from ca. 16°30′ (La Paz, Bolivia) to ca. 38°58′ (Monte Hermoso, Argentina), being a frequent component within glyptodont assemblages.

During the Pleistocene (ca. 2.6–0.011 Ma), Doedicurinae underwent a marked latitudinal retraction as the *Doedicurus* is geographically restricted to the Pampean region of Argentina (Ameghino 1889; Carlini and Scillato-Yané 1999), Uruguay (Ubilla et al. 2004; Zurita et al. 2009) and southernmost Brazil (Oliveira 1992; Pereira et al. 2012). In this scenario, the paleontological evidence agrees with the geographic distribution predicted by Varela et al. (2018; species distribution models).

It is worth noting that the largest (*Doedicurus*) and the smallest (*Neosclerocalyptus*) glyptodonts were the most latitudinally restricted during the Pleistocene, with *Doedicurus* being the most geographically constrained (Zurita et al. 2009; Quiñones et al. 2020). This progressive latitudinal retraction of Doedicurinae since the Pleistocene is quite intriguing because it is exactly opposite to that of the other Pleistocene lineages (e.g., *Glyptodon* and *Panochthus*) of South American glyptodonts. In the latter, an increase in body mass is related to an increase in the latitudinal distribution (see Cuarelli et al. 2020), as is currently observed in some African megamammals (i.e., *Hippopotamus amphibius*) that have a body mass similar to that inferred for *Doedicurus* (ca. two tons; Soibelzon et al. 2012; Vizcaíno et al. 2011). The co-ocurrence of *Doedicurus* and at least three other genera of glyptodonts (i.e., *Neosclerocalyptus*,

Panochthus, and *Glyptodon*) in the Pampean region of Argentina, Uruguay, and southern Brazil, suggests niche partitioning, in agreement with evidence from stable isotope analyses (see Domingo et al. 2012; Melo-Franca et al. 2015) and biomechanical studies (see Vizcaíno et al. 2011; Pomi 2008). According to Cione et al. (2015), the hypothetically low primary productivity of these glacial ecosystems could have led to a lower number of individuals for each species, also stimulating a partition of resources as a key strategy to survive in these areas, especially during glacial stages (see Domingo et al. 2020).

Accordingly, our observations reveal that the frequency of records of *Doedicurus* is one of the lowest within Pleistocene glyptodont diversity in southern South America. Therefore, it is possible that the number of individuals of *Doedicurus* living in the same area at the same time was low, as suggested by the fossil record.

This geographic retraction, which probably started in the latest Neogene or early Pleistocene, could be related to the progressive cooling and aridization observed since the Pliocene, which intensified during the Pleistocene in southern South America. Despite this phenomenon, *Doedicurus* is one of the last survivors of the South American Pleistocene megafauna, as it is recorded until the latest Pleistocene in the Pampean region, a pattern that suggests that this area acted as a refuge for the last member of the megafauna before its extinction (see Politis et al. 2019).

Conclusions

(i) *Eleutherocercus solidus* is the only well characterized Doedicurinae in North-western Argentina, with a biochron that spans from the latest Miocene to Pliocene; (ii) the mandibular and dental morphology of *E. solidus* (almost identical to *Doedicurus*, the most hypsodont glyptodont ever known) reveals that the temporal distribution of this species coincides with a spread of C4 plants in northwestern of Argentina; (iii) the other species of the genus, *E. antiquus*, shows a similar temporal distribution (Pliocene), but living in a different biogeographical area (i.e., the Pampean region of Argentina); (iv) the *Eleutherocercus* is a well supported clade, sister group of the giant late Pleistocene *Doedicurus clavicaudatus*; (v) *Eleutherocercus* spp. + *Doedicurus* constitutes the subfamily Doedicurinae, which in turn forms part of a large southern South American glyptodont radiation starting, at least, in the early Miocene, in the Patagonian region of Argentina; (vi) contrary to what was observed for the diversity of the other Pleistocene glyptodonts (i.e., *Neosclerocalyptus*, *Panochthus*, and *Glyptodon*), Doedicurinae underwent a latitudinal retraction ending with the giant *Doedicurus* being limited to the Pampean region of Argentina, Uruguay, and southernmost Brazil during the late Pleistocene; (vii) the hypothetic relationship between body mass (with some specimens of *Doedicurus* achieving ca. two tons) and latitudinal retraction suggests that the cyclic climate changes during the Pleistocene could have played an active role in the final steps of the evolutionary history of glyptodonts in South America.

Acknowledgements

We thank Marcelo Reguero (MLP), Laura Cruz (MACN), William Simpson and Keneth Angielczyk (both FMNH), and the Museo "Condor Huasi" Belén for granting us access to their collections, and Dirección de Antropología de Catamarca for giving us the permission to work in Catamarca Province. We also thank Pedro Cuaranta (Universidad Nacional del Nordeste, Corrientes, Argentina) for drawing the reconstruction of *Eleutherocercus solidus* and Sergio Miguel Georgieff (Universidad Nacional de Tucumán, Tucumán, Argentina) who helped in the field trip and provided comments on the stratigraphic context, and we thank Emilia Sferco and Federico Degrange (both CICTERRA-CONICET-UNC, Córdoba, Argentina), Eugenia García (Dirección Provincial de Antropología de Catamarca, San Fernando del Valle de Catamarca, Argentina), Agustín Scanferla (CONICET-Instituto de Bio y Geociencias del NOA (IBIGEO), Salta, Argentina), Javier Ochoa (Museo Arqueológico e Histórico Regional "Florentino Ameghino", Int De Buono y San Pedro, Río Tercero, Córdoba, Argentina), Damián Voglino (Museo de Ciencias Naturales "Rvdo. P. Antonio Scasso", San Nicolás de los Arroyos, Argentina), Miguel Lugo (Museo de historia Hércules Rabagliati, Ramallo, Argentina), and Matias A. Armella (Universidad Nacional de Tucumán y Museo Miguel Lillo, Tucumán, Argentina) for the help during fieldwork. Finally, special thanks are due to the reviewers David Gillette (Institut royal des Sciences naturelles de Belgique, Brussels, Belgium) and Daniel Perea (Universidad de La República, Montevideo, Uruguay) and the editor Olivier Lambert (Institut royal des Sciences naturelles de Belgique, Brussels, Belgium) for their critical reading of the manuscript and their suggestions wich helped to improve the manuscript. This contribution was partially supported by grants PI Q002/17, PICT 2017-0765, and PICT 2015-0724.

References

Abba, A.M., Tognelli, M.F. Seitz, V.P., Bender, J. B., and Vizcaíno, S.F. 2012. Distribution of extant xenarthrans (Mammalia: Xenarthra) in Argentina using species distribution models. *Mammalia* 76: 123–136.

Alexander, R.M. Fariña, R., and Vizcaíno, S.F. 1999. Tail blow energy and carapace fractures in a large glyptodont (Mammalia, Xenarthra). *Zoological Journal of the Linnean Society* 126: 41–49.

Ameghino, F. 1881. *La antigüedad del hombre en el Plata. Vol. 2*. 557 pp. Masson-Igon Hermanos, París.

Ameghino, F. 1884. Excursiones geológicas y paleontológicas en la provincia de Buenos Aires. *Boletín de la Academia Nacional de Ciencias en Córdoba* 6: 1–257.

Ameghino, F. 1886. Contribuciones al conocimiento de los mamíferos fósiles de los terrenos terciarios antiguos del Paraná. *Boletín de la Academia Nacional de Ciencias en Córdoba* 9: 5–228.

Ameghino, F. 1887. Apuntes preliminares sobre algunos mamíferos extinguidos del yacimiento de "Monte Hermoso" existentes en el "Museo La Plata". *Boletín del Museo de La Plata* 1: 1–18.

Ameghino, F. 1889. Contribuciones al conocimiento de los mamíferos fósiles de la República Argentina. *Actas de la Academia Nacional de Ciencias de Córdoba* 6: 1–1027.

Ameghino, F. 1891. Sobre algunos restos de mamíferos fósiles, recogidos por el Señor Manuel B. Zavaleta en la formación miocena de Tucumán y Catamarca. *Revista Argentina de Historia Natural* 1: 88–101.

Ameghino, F. 1920. Sur les Edentés fossiles de l'Argentine; Examen cri-

tique, revisión et correction de l'ouvrage de M.R. Lydekker. *Obras Completas y Correspondencia Científica* 11: 448–907.

Armella, M.A. and Bonini, R.A. 2020. Biostratigraphic significance of the presence of *Protypotherium* cf. *P. antiquum* Ameghino 1885 (Interatheriidae, Notoungulata) in the late Miocene of Northwestern Argentina. *Journal of South American Earth Sciences* 102: 102676.

Bargo, M.S., De Iuliis, G., and Vizcaíno, S.F. 2006. Hypsodonty in Pleistocene ground sloths. *Acta Palaeontologica Polonica* 51: 53–61.

Beilinson, E., Gasparini, G.M., Tomassini, R.L., Zárate, M.A., Deschamps, C.M., Barendregt, R.W., and Rabassa, J. 2017. The Quequén Salado River Basin: geology and biochronostratigraphy of the Mio-Pliocene boundary in the southern Pampean plain, Argentina. *Journal of South American Earth Sciences* 76: 362–374.

Bergqvist, L.P., Abrantes, E.A.L., and Avilla, L. dos S. 2004. The Xenarthra (Mammalia) of São José de Itabora Basin (upper Paleocene, Itaboraian), Rio de Janeiro, Brazil. *Geodiversitas* 26: 323–337.

Blanco, R.E., Jones, W.W., and Rinderknecht, A. 2009. The sweet spot of a biological hammer: the centre of percussion of glyptodont (Mammalia: Xenarthra) tail clubs. *Proceedings of the Royal Society B: Biological Sciences* 276 (1675): 3971–3978.

Bonini, R.A. 2014. *Bioestratigrafía y Diversidad de los Mamíferos del Neógeno de San Fernando y Puerta de Corral Quemado, Catamarca, Argentina*. 337 pp. Ph.D. Thesis, Universidad Nacional de La Plata, La Plata.

Bonini, R.A., Candela, A.M., Georgieff, S.M., and Reguero, M.A. 2016. Bioestratigrafía, geocronología y diversidad de los mamíferos del Neógeno de San Fernando, Departamento Belén, Catamarca. *Ameghiniana* 53 (3 Supplement): R5–R6.

Bonini, R.A., Georgieff, S.M., and Candela, A.M. 2017. Stratigraphy, geochronology, and paleoenvironments of Miocene–Pliocene boundary of San Fernando, Belén (Catamarca, northwest of Argentina). *Journal of South American Earth Sciences* 79: 459–471.

Bonini, R.A., Miño-Boilini, A.R., Brandoni, D., and Georgieff, S.M. 2020. New data on the diversity and chronology of late Neogene sloths (Xenarthra, Folivora) from the Villavil–Quillay Basin, Catamarca, Argentina. *Historical Biology* [published online, https://doi.org/10.1080/08912963.2020.1826470].

Bossi, G.E. and Muruaga, C. 2009. Estratigrafía e inversión tectónica del rift neógeno en el Campo del Arenal, Catamarca, NO Argentina. *Andean Geology* 36: 311–340.

Bossi, G.E., Ovejero, R., and Strecker, M. 1987. Correlación entre los perfiles del Terciario superior en la Puerta de Corral Quemado-Hualfín y Entre Ríos (Chiquimil). Provincia de Catamarca, Argentina. *En Actas del X Congreso Geológico Argentino* 2: 117–120.

Brandoni, D., Sclillato-Yané, G.J., Miño-Boilini, A.R., and E. Favotti. 2016. Los Tardigrada (Mammalia, Xenarthra) de Argentina: diversidad, evolución y biogeografía. *Contribuciones del MACN* 6: 261–272.

Bremer, K. 1994. Branch support and tree stability. *Cladistics* 10: 295–304.

Brown, B. 1912. *Brachyostracon*, a new genus of glyptodonts from México. *American Museum of Natural History Bulletin* 31: 167–177.

Burmeister, G. 1866. Lista de los mamíferos fósiles del terreno diluviano. *Anales del Museo Público de Buenos Aires* 1: 121–232.

Burmeister, G. 1870–1874. Monografía de los Glyptodontes en el Museo Público de Buenos Aires. *Anales del Museo Publico de Buenos Aires* 2: 1–412.

Butler, R.F., Marshall, L. G., Drake, R.E., and Curtis, G.H. 1984. Magnetic polarity stratigraphy and 40K-40Ar dating of late Miocene and early Pliocene continental deposits, Catamarca province, NW Argentina. *Journal of Geology* 92: 623–636.

Cabrera A. 1939. Sobre vertebrados fósiles del Plioceno de Adolfo Alsina. *Revista del Museo de La Plata* 2 (6): 3–35.

Cabrera, A. 1944. Los Gliptodontoideos del Araucaniano de Catamarca. *Revista del museo de La Plata (Nueva Serie)* 3: 5–76.

Candela, A.M. and Bonini, R.A. 2017. A new guinea pig (Rodentia, Caviomorpha) from northwestern Argentina: implications for the origin of the genus *Cavia*. *Journal of Vertebrate Paleontology* 37 (4): e1352591.

Carlini, A.A. and Scillato-Yané, G.J. 1999. Evolution of quaternary xenarthrans (Mammalia) of Argentina. *Quaternary of South America and Antarctic Peninsula* 12: 149–175.

Carlini, A.A., Ciancio, M.R., and Scillato-Yané, G.J. 2010. Middle Eocene–early Miocene Dasypodidae (Xenarthra) of southern South America, successive faunas in Gran Barranca; biostratigraphy and palaeoecology. *In*: R.H. Madden, A.A. Carlini, M.G. Vucetich, and R.F. Kay (eds.), *The Paleontology of Gran Barranca: Evolution and Environmental Change through the Middle Cenozoic of Patagonia*, 106–129. Cambridge University Press, Cambridge.

Carlini, A.A., Zurita, A.E., and Scillato-Yane, G.J. 2008. A new glyptodont species from Codore Formation (Pliocene), Estado Falcón (Venezuela), and the *Asterostemma* problem. *Paläontologische Zeitschritt* 82: 125–138.

Castellanos, A. 1927. Descripción de un fragmento de tubo caudal de un nuevo Doedicurino en relación con sus géneros afines. *Anales del Museo de Historia Natural de Montevideo* 2: 265–300.

Castellanos, A. 1940. A propósito de los géneros *Plohophorus*, *Nopachthus* y *Panochthus* (2º parte). *Publicaciones del Instituto de Fisiografía y Geología*. *Facultad de Ciencias Matemáticas, Fisico-Químicas y Naturales aplicadas a la Industria de la Universidad Nacional del Litoral* 1 (6): 1–418.

Castellanos, A. 1941. A propósito de los géneros *Plohophorus*, *Nopachthus* y *Panochthus*. *Publicaciones del Instituto de Fisiografía y Geología*. *Facultad de Ciencias Matemáticas, Fisico-Químicas y Naturales aplicadas a la Industria de la Universidad Nacional del Litoral* 2 (8): 279–418.

Cerling, T.E., Ehleringer, J.R., and Harris, J.M. 1998. Carbon dioxide starvation, the development of C4 ecosystems, and mammalian evolution. *Philosophical Transactions of the Royal Society of London. Series B: Biological Sciences* 353: 159–171.

Chimento, N.R., Ciancio, M.R., Cornero, S., and Carlini, A.A., 2010. La coraza de *Eleutherocercus* (Xenarthra, Glyptodontidae): presencia de una estructura posiblemente vinculada a una gran masa glandular. *In*: E.B. Casanave (ed.), *Libro de Actas de XXIII Jornadas argentinas de Mastozoologia Resúmenes* 15. Bahía Blanca.

Cione, A.L. and Tonni, E.P. 1996. Reassesment of the Pliocene–Pleistocene continental time scale of South America. Correlation of the type Chapadmalalan with Bolivian sections. *Journal of South American Earth Sciences* 9: 221–236.

Cione, A.L., Azpelicueta, M.D.L.M, Bond, M., Carlini, A.A., Casciotta, J.R., Cozzuol, M.A., De La Fuente, M., Gasparini, Z., Goin, F.L., Noriega, J.I., Scillato-Yané, G.J., Soibelzon, L.H., Tonni, E.P., Verzi, D., and Vucetich, M.G. 2000. Miocene vertebrates from Entre Ríos province, Eastern Argentina. El Neógeno de Argentina. *Serie Correlación Geológica* 14: 191–237.

Cione, A.L., Gasparini, G.M., Soibelzon, E., Soibelzon, L.H., and Tonni, E.P. 2015. *The Great American Biotic Interchange: A South American Perspective*. 97 pp. Springer Briefs in Earth System Sciences, Springer, Dordrecht.

Cope, E.D. 1889. The edentate of North America. *American Naturalist* 23: 657–664.

Croft, D.A., Carlini, A.A., Ciancio, M.R., Brandoni, D., Drew, N.E., Engelman, R.K., and Anaya, F. 2016. New mammal faunal data from Cerdas, Bolivia, a middle-latitude Neotropical site that chronicles the end of the Middle Miocene Climatic Optimum in South America. *Journal of Vertebrate Paleontology* 36 (5): e1163574.

Croft, D.A., Flynn, J.J., and Wyss, A.R. 2007. A new basal glyptodontoid and other Xenarthra of the early Miocene Chucal fauna, northern Chile. *Journal of Vertebrate Paleontology* 27: 781–797.

Cuadrelli, F. 2020. *Los Glyptodontidae Glyptodontinae (Mammalia, Xenarthra): morfología, sistemática y filogenia de los taxones de la radiación austral*. 254 pp. Ph.D. Thesis, Facultad de Ciencias Exactas, Físicas y Naturales, Universidad Nacional de Córdoba, Córdoba.

Cuadrelli, F., Zurita, A.E. Toriño. P. Miño-Boilini, A.R., Perea, D., Luna, C.A., Gillette. D.D., and Medina, O. 2020. A new species of glyptodontine (Mammalia, Xenarthra, Glyptodontidae) from the Quaternary of the Eastern Cordillera, Bolivia: phylogeny and palaeobiogeogra-

phy, *Journal of Systematic Palaeontology* [published online, https://doi.org/10.1080/14772019.2020.1784300].

Cuadrelli, F., Zurita, A.E., Toriño, P., Miño-Boilini, A.R., Rodríguez-Bualó, S., Perea, D., and Acuña Suárez, G.E. 2019. Late Pleistocene Glyptodontinae (Mammalia, Xenarthra, Glyptodontidae) from southern South America: a comprehensive review. *Journal of Vertebrate Paleontology* 38 (5): e1525390.

Delsuc, F., Catzeflis, F.M., Stanhope, M.J. and Douzery, E.J. P. 2001. The evolution of armadillos, anteaters and sloths depicted by nuclear and mitocondrial phylogenies: implications for the status of the enigmatic fossil *Eurotamandua. Proceedings of the Royal Society of London series B* 268: 1605–1615.

Delsuc, F., Gibb, G.C., Kuch, M., Billet, G., Hautier, L., Southon, J., Rouillard, J.M., Fernicola, J.C., Vizcaíno, S. F., MacPhee, R. D., and Poinar, H.N. 2016. The phylogenetic affinities of the extinct glyptodonts. *Current Biology* 26: 155–156.

Domingo, L., Prado, J.L., and Alberdi, M.T. 2012. The effect of paleoecology and paleobiogeography on stable isotopes of Quaternary mammals from South America. *Quaternary Science Review* 55: 102–112.

Domingo, L., Tomassini, R.L, Montalvo, C.I., Sanz-Pérez, D., and Alberdi, M.T. 2020. The Great American Biotic Interchange revisited: a new perspective from the stable isotope record of Argentine Pampas fossil mammals. *Scientific Reports* 10 (1): 1–10.

Esteban, G., Nasif, N., and Georgieff, S. M. 2014. Cronobioestratigrafía del Mioceno tardío-Plioceno temprano, Puerta de Corral Quemado y Villavil, provincia de Catamarca, Argentina. *Acta geológica lilloana* 26: 165–192

Fernicola, J.C. 2008. Nuevos aportes para la sistemática de los Glyptodontia Ameghino, 1889 (Mammalia, Xenarthra, Cingulata). *Ameghiniana* 45: 553–574.

Fernicola, J.C. and Porpino, K.O. 2012. Exoskeleton and Systematics: A Historical Problem in the Classification of Glyptodonts. *Journal of Mammal Evolution* 19 (3): 171–183.

Fernicola, J.C., Rinderknecht, A., Washington, J., Vizcaíno, S.F., and Porpino, K.O. 2018. A new species of *Neoglyptatelus* (Mammalia, Xenarthra, Cingulata) from the late Miocene of Uruguay provides new insights on the evolution of the dorsal armor in cingulates. *Ameghiniana* 55: 233–252.

Gaudin, T.J. 2004. Phylogenetic relationship among sloths (Mammalia, Xenarthra, Tardigrada): the craniodental evidence. *Zoological Journal of the Society* 140: 255–305.

Gaudin, T.J. and Croft, D.A. 2015. Paleogene Xenarthra and the evolution of South American mammals. *Journal of Mammalogy* 96: 622–634.

Gaudin, T.J. and Lyon, L.M. 2017. Cranial osteology of the pampathere *Holmesina floridanus* (Xenarthra: Cingulata; Blancan NALMA), including a description of an isolated petrosal bone. *PeerJ* 5: e4022.

Gaudin, T.J. and Wible, J.R. 2006. The phylogeny of living and extinct armadillos (Mammalia, Xenarthra, Cingulata): a craniodental analysis. *In*: M.T. Carrano, T.J. Gaudin, R.W. Blob, and J.R. Wible (eds.), *Amniote Paleobiology: Perspectives on the Evolution of Mammals, Birds and Reptiles*, 153–198. University of Chicago Press, Chicago.

Georgieff, S.M., Muruaga, C., Ibañez, L.M., Spagnuolo, M.C., Bonini, R.A., Esteban, G., Nasif, N.L., and Del Pero, M. 2017. Estilos de deformación, cronoestratigrafía y evolución paleoambiental de las unidades neógenas de las Sierras Pampeanas Noroccidentales de Catamarca y Tucumán, Argentina. *In*: C. Muruaga and P. Grosse (eds.), *Relatorio XX Congreso Geológico Argentino*. 34 pp. Universidad Nacional de Tucumán, San Miguel de Tucumán.

Gibb, G.C., Condamine, F.L., Kuch, M., Enk, J., Moraes-Barros, N., Superina, M., Poinar, H.N., and Delsuc, F. 2015. Shotgun mitogenomics provides a reference phylogenetic framework and timescale for living xenarthrans. *Molecular Biology and Evolution* 33: 621–642.

Gillette, D.D. and Ray, C.E. 1981. Glyptodonts of North America. *Smithsonian Contributions to Paleobiology* 40:1–251.

Gillette, D.D., Carraza-Castañeda, O., White, R.S., Morgan, G.S., Thrasher, L.C., McCord, R., and McCullough, G. 2016. Ontogeny and sexual dimorphism of *Glyptotherium texanum* (Xenarthra, Cingulata) from the Pliocene and Pleistocene (Blancan and Irvingtonian NALMA) of Arizona, New Mexico, and Mexico. *Journal of Mammalian Evolution* 23: 133–154.

Goloboff, P.A. and Farris, J.S. 2001. Methods for quick consensus estimation. *Cladistics* 17: 26–34.

Goloboff, P., Farris, J., and Nixon, K. 2008. TNT, a free program for phylogeny analysis. *Cladistics* 24: 774–786.

González-Ruiz, L.R., Brandoni, D., Zurita, A.E., Green, J.L., Novo, N.M., Tauber, A.A., and Tejedor, M.F. 2020. Juvenile glyptodont (Mammalia, Cingulata) from the Miocene of Patagonia, Argentina: Insights into mandibular and dental characters. *Journal of Vertebrate Paleontology* 40 (1): e1768398.

González-Ruiz, L.R., Ciancio, M.R. Martin, G.M., and Zurita, A.E. 2015. First record of supernumerary teeth in Glyptodontidae (Mammalia, Xenarthra, Cingulata). *Journal of Vertebrate Paleontology* 35: e885033.

Gray, J.E. 1869. *Catalogue of Carnivorous, Pachydermatous and Edentate Mammalia in the British Museum*. 398 pp. British Museum (Natural History), London.

Hoffstetter, R. 1958. Xenarthra. *In*: J. Piveteau (ed.), *Traité de paléontologie. Vol. 6*, 535–636. Masson & Co, Paris.

Hofreiter, M., Poinar, H.N., Spaulding, W.G., Bauer, K., Martin, P.S., Possnert, G., and Paabo, S. 2000. A molecular analysis of ground sloth diet through the last glaciation. *Molecular Ecology* 9: 1975–1984.

Hynek, S.A. 2011. *Mio-Pliocene Geology of the Southem Puna Plateau Margin, Argentina*. 329 pp. Ph.D. Thesis. University of Utah, Salt Lake City.

Hynek, S.A., Passey, B.H., Prado, J.L., Brown, F.H., Cerling, T.E., and Quade, J. 2012. Small mammal carbon isotope ecology across the Miocene–Pliocene boundary, northwestern Argentina. *Earth and Planetary Science Letters* 321: 177–188.

Illiger, C. 1811. *Prodromus systematis mammalium et avium; additis terminis zoographicis utriusque classis, eurumque versione germanica.* 301 pp. C. Safeld, Berlin.

Janis, C.M. 1988. Estimation of tooth volume and hypsodonty indices in ungulate mammals, and the correlation of these factors with dictary preference. *Mémoires du Muséum National d'Histoire Naturelle, série C* 53: 367–387.

Koken E. 1888. *Eleutherocercus*, ein neuer Glyptodont aus Uruguay. *Anhang zu den Abhandlungen Königlichen Akademie der Wissenschaften zu Berlin* 1888: 1–28.

Kraglievich, L. 1932. Nuevos apuntes para la geología y paleontología uruguayas. *Anales del Museo de Historia Natural de Montevideo* 3: 257–320.

Krmpotic, C.M., Ciancio, M.R., Barbeito, C., Mario, R.C. and Carlini, A.A. 2009. Osteoderm morphology in recent and fossil euphractine xenarthrans. *Acta Zoologica* 90: 339–351.

Latorre, C., Quade, J., and Mclntosh, W.C. 1997. The expansion of C_4 grasses and global change in the table Miocene: stable isotope evidence from the Americas. *Earth and Planetary Science Letters* 146: 83–96.

Lindsey, E.L., López Reyes, E.X., Matzke, G.E., Rice, K.A., and McDonald, G.H. 2020. A monodominant late-Pleistocene megafauna locality from Santa Elena, Ecuador: Insight on the biology and behavior of gigant ground sloths. *Palaeogeography, Palaeoclimatology, Palaeoecology* 544: 109599.

Linnaeus, C. 1758. *Systema naturae per regna tria naturae, secundum classes, ordines, genera, species, cum characteribus, differentiis, synonymis, locis*. 824 pp. Laurentii Salvii, Holmiae.

Lydekker, R. 1895. Contributions to a knowledge of the fossil vertebrates of Argentina. The extinct edentates of Argentina. *Anales del Museo de La Plata*, *Paleontología Argentina* 3: 1–118.

Lund, P.W. 1839. Blik paa Brasiliens dyreverden för sidste jordomvaeltning. Anden afhandling: Pattedyrene (Lagoa Santa d. 16de novbr. 1837). *Det kongelige Danske Videnskabernes Selskabs naturvidenskabelige og mathematiske Afhandlinger* 8: 61–144.

MacFadden, B.J. 2005. Diet and habitat of toxodont megaherbivores

(Mammalia, Notoungulata) from the late Quaternary of South and Central America. *Quaternary Research* 64: 113–124.

MacFadden, B.J., Anaya, F., and Argollo, J. 1993. Magnetic stratigraphy of Inchasi: a Pliocene mammal-bearing locality from the Bolivian Andes deposited just before the Great American Interchange. *Earth and Planetary Science Letters* 114: 229–241.

MacFadden, B.J., Cerling, T.E., Harris, J.M., and Prado, J. 1999. Ancient latitudinal gradients of C3/C4 grasses interpreted from stable isotopes of New Word Pleistocene horse (Equus) teeth. *Global Ecology and Biogeography* 8: 137–149.

Maddison, W.P. and Maddison, D.R. 2018. *Mesquite: a Modular System for Evolutionary Analysis.* Version 3.04. Available at http://mesquiteproject.org

Marshall, L.G. and Patterson, B. 1981. Geology and geochronology of the mammal-bearing Tertiary of the Valle de Santa María and Río Corral Quemado, Catamarca Province, Argentina. *Fieldiana Geology* 9: 1–80.

Marshall, L.G., Butler, R.F., Drake, R.E., Curtis, G.H., and Tedford, R.H. 1979. Calibration of the Great American Interchange. *Science* 204: 272–279.

McDonald, G.H. 2005. Paleoecology of extinct Xenarthrans and the Great American Biotic Interchange. *Bulletin of the Florida Museum of Natural History* 45: 319–340.

McKenna, M.C. and Bell, S.K. 1997. *Classification of Mammals Above the Species Level*. 631 pp. Columbia University Press, New York.

Melo-Franca, L., Asevedo, L., Dantas, M.A.T., Bocchiglieri, A., Dos Santos Avilla, L., Lopes, R.P., and Da Silva, J.L.L. 2015. Review of feeding ecology data of late Pleistocene mammalian herbivores from South America and discussion on niche differentiation. *Earth-Science Reviews* 140: 158–165.

Mitchell, K. J., Scanferla, A., Soibelzon, E., Bonini, R., Ochoa, J., and Cooper, A. 2016. Ancient DNA from the extinct South America giant glyptodont *Doedicurus* sp. (Xenarthra: Glyptodontiae) reveals that glyptodonts evolved from Eocene armadillos. *Molecular Ecology* 25: 3499–3508.

Moreno, F.P. 1888. Informe preliminar de los progresos del Museo La Plata, durante el primer semestre de 1888. *Boletín del Museo de La Plata* 2: 1–35.

Moreno, F.P. and Mercerat, A. 1891. Exploración arqueológica de la Provincia de Catamarca: Paleontología. *Revista del Museo de La Plata* 1: 1–71.

Muruaga, C.M., 2001. Estratigrafía y desarrollo tectosedimentario de los sedimentos terciarios en los alrededores de la Sierra de Hualfín, borde suroriental de la Puna, Catamarca, Argentina. *Latin American Journal of Sedimentology and Basin Analysis* 8: 27–50.

Nuñez-Blasco, A., Zurita, A.E., Miño-Boilini, A.R., and Bonini, R.A. 2020. Chronologic distribution of the Glyptodontidae (Mammalia, Cingulata) recorded in the Villavil–Quillay Basin, Catamarca, Argentina. *In*: V. Crespo and P. Citton (eds.), *2nd Palaeontological Virtual Congress*, 187. Valencia.

Oliveira, E.V. 1992. *Mamíferos fósseis do Quaterário do Estado do Rio Grande do Sul, Brasil*. 118 pp. M.Sc. Thesis, Programa de Pós-Graduação em Geociências, Universidade Federal do Rio Grande do Sul, Porto Alegre.

Osborn, H.F., 1903. *Glyptotherium texanum*, a new glyptodont, from the lower Pleistocene of Texas. *Bulletin of the American Museum of Natural History* 19: 491–494.

Owen, R. 1845. *Descriptive and illustrated catalogue of the fossil organic remains of Mammalia and Aves contained in the Museum of the Royal College of Surgeons of London, England*. 391 pp. Richard and John E. Taylor, London.

Paula-Couto, C. 1979. *Tratado de paleomastozoologia*. 590 pp. Academia Brasileira de Ciências. Rio de Janeiro.

Perea, D. 2005. *Pseudoplohophorus absolutus* n. sp. (Xenarthra, Glyptodontidae), variabilidad en Sclerocalyptinae y redefinición de una biozona del Mioceno Superior de Uruguay. *Ameghiniana* 42: 175–190.

Pereira, J.C., Lopes, R.P., and Kerber, L. 2012. New remains of late Pleistocene mammals from the Chuí Creek, Southern Brazil. *Revista Brasileira de Paleontologia* 15: 228–239.

Politis, G.G., Messineo, P.G., Stafford, T.W., and Lindsey, E.L. 2019. Campo Laborde: a late Pleistocene gigant ground sloth kill and butchering site in the Pampas. *Science Advances* 5 (3): 2–10.

Pomi, L.H. 2008. Tafonomía y paleoecología de los Glyptodontidae (Mammalia) pleistocénicos de la provincia de Buenos Aires, Argentina. *In*: *Congreso Latinoamericano de Paleontología de Vertebrados 3, 2008. Resumenes*, 200. Neuquén,

Porpino, K.O., Fernicola, J.C., and Bergqvist, L.P. 2010. Revisiting the intertropical Brazilian species *Hoplophorus euphractus* (Cingulata, Glyptodontoidea) and the phylogenetic affinities of *Hoplophorus*. *Journal of Vertebrate Paleontology* 30: 911–927.

Quiñones, S.I., de Los Reyes, M., Zurita, A.E., Cuadrelli, F., Miño-Boilini, A.R., and Poiré, D. 2020. *Neosclerocalyptus* Paula Couto (Xenarthra, Glyptodontidae) in the late Pliocene–earliest Pleistocene of the Pampean region (Argentina): its contribution to the understanding of evolutionary history of Pleistocene glyptodonts. *Journal of South American Earth Sciences* 103: 102701.

Quiñones, S.I., Miño-Boilini, A.R. Zurita, A.E. Contreras, S., Luna, C.A. Candela, A.M. Camacho, M., Ercoli, M.D., Solís, N., and Brandoni, D. 2019. New records of Neogene Xenarthra (Mammalia) from eastern Puna (Argentina): diversity and biochronology. *Journal of Paleontology* 93: 1258–1275.

Riggs, E.S. and Patterson, B. 1939. Stratigraphy of Late Miocene and Pliocene deposits of the Province of Catamarca (Argentina) with notes on the faunae. *Physis* 14: 143–162.

Rovereto, C. 1914. Los estratos araucanianos y sus fósiles. *Anales del Museo Nacional de Historia Natural de Buenos Aires* 25: 1–247.

Sasso, A.M. 1997. *Geological Evolution and Metallogenic Relationships of the Farallón Negro Volcanic Complex, NW Argentina*. 268 pp. Ph.D. Thesis, Queens University, Kingston.

Scillato-Yané, G.J. 1986. Los Xenarthra fósiles de Argentina (Mammalia, Edentata). *Actas del IV Congreso Argentino de Paleontología y Bioestratigrafía* 2: 151–155.

Simpson, G.G. 1947 A Miocene glyptodont from Venezuela. *American Museum Novitates* 1368: 1–10

Soibelzon, E., Miño-Boilini, A.R., Zurita, A.E., and Krmpotic, C.M. 2010. Los Xenarthra (Mammalia) del Ensenadense (Pleistoceno inferior a medio) de la Región Pampeana (Argentina). *Revista Mexicana de Ciencias Geológicas* 27: 449–469.

Soibelzon, L.H., Zamorano, M., Scillato-Yané, G. J., Piazza, D., Rodríguez, S., Soibelzon, E., and Tonni, E.P. 2012. Un Glyptodontidae de gran tamaño en el Holoceno temprano de la región Pampeana, Argentina. *Revista Brasileira de Paleontología* 15: 105–112.

Tomassini, R.L., Montalvo, C.I., Deschamps, C.M., and Manera, T. 2013. Biostratigraphy and biochronology of the Monte Hermoso Formation (early Pliocene) at its type locality, Buenos Aires Province, Argentina. *Journal of South American Earth Sciences* 48: 31–42.

Toriño, P. and Perea, D. 2008. Tertiary Glyptodontids from Uruguay. I: Glyptatelinae, Doedicurinae and Glyptodontinae. *In*: *III Congreso Latinoamericano de Paleontología de Vertebrados. Libro de resúmenes* 250: 22–25. Neuquén.

Toriño, P. and Perea, D. 2018. New contributions to the systematic of the "Plohophorini" (Mammalia, Cingulata, Glyptodontidae) from Uruguay. *Journal of South American Earth Sciences* 86:410–430.

Ubilla, M., Perea, D., Aguilar, C.G., and Lorenzo, N. 2004. Late Pleistocene vertebrate from northern Uruguay: tools for biostratigraphic, climatic and environmental reconstruction. *Quaternary International* 114: 129–142.

Varela, L., Tambusso, P.S., Patiño, S.J., Di Giacomo, M., and Fariñaa, R.A. 2018. Potential distribution of fossil xenarthrans in South America during the late Pleistocene: co-occurrence and provincialism. *Journal of Mammalian Evolution* 25: 539–550.

Villarroel, C. 1983. Descripción de *Asterostemma*? *acostae*, nueva especie de propalaehoplophorino (Glyptodontidae, Mammalia) del Mioceno de La Venta, Colombia. *Geologia Norandina* 7: 29–34.

Vizcaíno, S.F., Bargo, M.S., Kay, R.F., Fariña, R.A., Di Giacomo, M., Perry, J.M., Precosti, F.J., Toledo, N., Cassini, G.H., and Fernicola, J.C.

2010. A baseline paleoecological study for the Santa Cruz Formation (late–early Miocene) at the Atlantic coast of Patagonia, Argentina. *Palaeogeography, Palaeoclimatology, Palaeoecology* 292: 507–519.

Vizcaíno, S.F., Cassini, G.H., Fernicola, J.C., and Bargo, M.S. 2011. Evaluating hábitats and feeding habits through ecomorphological features in glyptodonts (Mammalia, Xenarthra). *Ameghiniana* 48: 305–319.

Vizcaíno, S.F., Cassini, G.H., Toledo, N., and Bargo, M.S. 2012. On the evolution of large size in mammalian herbivores of Cenozoic. *In*: D. Bruce, B.D. Patterson, and L.P. Costa (eds.), *Bones, Clones, and Biomes: the History and Geography of Recent Neotropical Mammals*. 432 pp. The University of Chicago Press, Chicago.

Zachos, J.C., Shackleton, N.J., Revenaugh, J.S., Pälike, H., and Flower, B.P. 2001. Climate response to orbital forcing across the Oligocene–Miocene boundary. *Science* 292: 274–278.

Zachos, J.C., Dickens, G.R., and Zeebe, R.E. 2008. An early Cenozoic perspective on greenhouse warming and carbon-cycle dynamics. *Nature* 451: 279–283.

Zamorano, M. and Brandoni, D. 2013. Phylogenetic analysis of the Panochthini (Xenarthra, Glyptodontidae), with remarks on their temporal distribution. *Alcheringa* 37: 442–45.

Zárate, M.A., Schultz, P.H., Blasi, A., Heil, C., King, J., and Hames, W. 2007. Geology and geochronology of type Chasicoan (late Miocene) mammal-bearing deposits of Buenos Aires (Argentina). *Journal of South American Earth Sciences* 23: 81–90.

Zurita, A.E. 2002. Nuevo gliptodonte (Mammalia, Glyptodontoidea) del Cuaternario de la provincia de Chaco, Argentina. *Ameghiniana* 39: 175–182.

Zurita, A.E. 2007. *Sistemática y evolución de los Hoplophorini (Xenarthra, Glyptodontidae, Hoplophorinae. Mioceno tardío-Holoceno temprano). Importancia bioestratigráfica, paleobiogeográfica y paleoambiental*. 376 pp. Ph.D. Thesis, Facultad de Ciencias Naturales y Museo, Universidad Nacional de La Plata, La Plata.

Zurita, A.E., González-Ruiz, L.R., Gómez-Cruz, A.J., and Arenas-Mosquera, J.E. 2013. The most complete known Neogene Glyptodontidae (Mammalia, Xenarthra, Cingulata) from northern South America: taxonomic, paleobiogeographic, and phylogenetic implications. *Journal of Vertebrate Paleontology* 33: 696–708.

Zurita, A.E, Miño-Boilini A.R., Soibelzon, E., Carlini, A.A., and Paredes Ríos, F. 2009. The diversity of Glyptodontidae (Xenarthra, Cingulata) in the Tarija Valley (Bolivia): systematic, biostratigraphic and paleobiogeographic aspects of a particular assemblage. *Neues Jahrbuch fur Geologie und Paläontologie Abhandlungen* 251: 225–237.

Zurita, A.E., Tagliorettí, M., De los Reyes, M., Cuadrelli, F., and Poire, D. 2016. Regarding the real diversity of Glyptodontidae (Mammalia, Xenarthra) in the late Pliocene (Chapadmalalan age/stage) of Argentina. *Anais da Academia Brasileira de Ciências* 88: 809–827.

Zurita, A.E., Tagliorettí, M., De los Reyes, M., Oliva, C., and Scaglia, F. 2014. First Neogene skull of Doedicurinae (Xenarthra, Glyptodontidae): morphology and phylogenetic implications. *Historical Biology* 28: 423–432.

Zurita, A.E., Zamorano, M., Scillato-Yané, G.J., Iriondo, S.F.M, and Gillette, D.D. 2017. A new species of *Panochthus* Burmeister (Xenarthra, Cingulata, Glyptodontidae) from the Pleistocene of the Eastern Cordillera, Bolivia. *Historical Biology* 29: 1076–1088.

A large hadrosaurid dinosaur from Presa San Antonio, Cerro del Pueblo Formation, Coahuila, Mexico

ROGELIO ANTONIO REYNA-HERNÁNDEZ, HÉCTOR E. RIVERA-SYLVA, LUIS E. SILVA-MARTÍNEZ, and JOSÉ RUBÉN GUZMAN-GUTIÉRREZ

Reyna-Hernández, R.A., Rivera-Sylva, H.E., Silva-Martínez, L.E., and Guzman-Gutiérrez, J.R. 2021. A large hadrosaurid dinosaur from Presa San Antonio, Cerro del Pueblo Formation, Coahuila, Mexico. *Acta Palaeontologica Polonica* 66 (Supplement to 3): S101–S110.

New hadrosaurid postcranial material is reported, collected near Presa San Antonio, Parras de la Fuente municipality, Coahuila, Mexico, in a sedimentary sequence belonging to the upper Campanian of the Cerro del Pueblo Formation, in the Parras Basin. The skeletal remains include partial elements from the pelvic girdle (left ilium, right pubis, ischium, and incomplete sacrum), a distal end of a left femur, almost complete right and left tibiae, right metatarsals II and IV, cervical and caudal vertebrae. Also, partially complete forelimb elements are present, which are still under preparation. The pubis shows characters of the Lambeosaurinae morphotypes, but the lack of cranial elements does not allow us to directly differentiate this specimen from the already described hadrosaurid taxa from the studied area, such as *Velafrons coahuilensis*, *Latirhinus uitstlani*, and *Kritosaurus navajovius*. This specimen, referred as Lambeosaurinae indet., adds to the fossil record of the hadrosaurids in southern Laramidia during the Campanian.

Key words: Dinosauria, Hadrosauridae, Lambeosaurinae, Cretaceous, Campanian, Mexico.

Rogelio Antonio Reyna-Hernández [rogelio.reynahr@gmail.com], Luis E. Silva-Martínez [luis.silva.paleo@gmail.com], Laboratorio de Paleobiología, Facultad de Ciencias Biológicas, Universidad Autónoma de Nuevo León, Av. Pedro de Alba y Manuel L. Barragán s/n, Ciudad Universitaria, San Nicolás de los Garza, Nuevo León, México. C.P. 66455.
Héctor E. Rivera-Sylva [hrivera@museodeldesierto.org] (corresponding author), José Rubén Guzman-Gutiérrez [paleovert@yahoo.com.mx], Departamento de Paleontología, Museo del Desierto, Carlos Abedrop Dávila 3745, Saltillo, Coahuila, México. C.P. 25022.

Received 1 October 2020, accepted 15 January 2021, available online 14 June 2021.

Introduction

Hadrosaurids are a very distinctive and common group of ornithopod dinosaurs in Late Cretaceous ecosystems. Their stratigraphic range begins in the late Santonian and ends together with the other non-avian dinosaurs at the K/Pg extinction event at the end of the Maastrichtian. They also have a wide geographical distribution, as specimens of this clade have been found on all continents except Oceania (Horner et al. 2004; Lund and Gates 2006; Prieto-Márquez 2010a; Longrich et al. 2021). These ornithopods differ from the other groups of dinosaurs due to the adaptations of the nasal region, where the bones have been modified in specialized structures such as cranial crests (e.g., Lull and Wright 1942; Ostrom 1961b). Furthermore, they present a complex dental arrangement made up of different series of rows of teeth and keratinous bills that allowed them a more efficient herbivorous diet (Morris 1970; Nabavizadeh 2014; Nabavizadeh and Weishampel 2016). Most of the diagnostic elements for this family are found in the cranial region (Prieto-Márquez 2010b), from which large number of species has been differentiated. However, the pectoral and pelvic girdles also provide a wide range of taxonomic information that does not always receives the proper importance (Brett-Surman 1989; Campione 2014).

In Mexico, the Hadrosauridae presents the widest record of any group of dinosaurs, with most of the reports coming from the northern region (Ramírez-Velasco et al. 2014; Rivera-Sylva and Carpenter 2014; Ramírez-Velasco and Hernández-Rivera 2015). Despite this, the study of Mexican specimens has been relatively scarce due to the fragmentary condition of most of the specimens, although the number of hadrosaurid studies in Mexico has recently increased (Kirkland et al. 2006; Serrano-Brañas et al. 2006; Ramírez-Velasco et al. 2014; Serrano-Brañas

and Espinosa-Chávez 2017; Rivera-Sylva et al. 2019a; Rybakiewicz et al. 2019).

The Cerro del Pueblo Formation is one of the most studied geological formations in Mexico with a very diverse faunal record, composed mainly of dinosaurs and other reptiles (Wolleben 1977; Rodriguez-de la Rosa and Cevallos-Ferriz 1998; Kirkland et al. 2000; Cifuentes-Ruiz et al. 2006; Rivera-Sylva and Espinosa-Chávez 2006; Loewen et al. 2010; Brinkman 2014; Rivera-Sylva et al. 2018, 2019b; Serrano-Brañas et al. 2020), flora (Rodriguez-de la Rosa and Cevallos-Ferriz 1994; Estrada-Ruiz and Cevallos-Ferriz 2007; Estrada-Ruiz et al. 2009; Cevallos-Ferriz and Vázquez-Rueda 2016), and trace fossils (Rodriguez-de la Rosa and Cevallos-Ferriz 1998; Rodríguez-de la Rosa 2007; Rivera-Sylva et al. 2017; Serrano-Brañas et al. 2018a, b, 2019). Three hadrosaurid taxa are known so far from this formation: *Kritosaurus navajovius* Brown, 1910 (Kirkland et al. 2006; Prieto-Márquez 2014b), *Latirhinus uitstlani* Prieto-Márquez and Serrano Brañas, 2012 (Prieto-Márquez and Serrano Brañas 2012) and *Velafrons coahuilensis* Gates, Sampson, Delgado de Jesús, Zanno, Eberth, Hernandez-Rivera, Aguillón-Martínez, and Kirkland, 2007 (Gates et al. 2007). The latter species was described based on cranial elements only, despite the fact that there are a number of preserved postcranial elements.

We describe a new hadrosaurid specimen consisting only of postcranial material from the Cerro del Pueblo Formation collected in Parras de la Fuente municipality, Coahuila, Mexico. The study of these materials would allow for better overview of the faunal diversity within the fossil ecosystems of the Upper Cretaceous in Mexico and provide a more robust anatomical knowledge of the species of the region.

Institutional abbreviations.—AEHM, Amur Natural History Museum of the Far Eastern Institute of Mineral Resources, FEB RAS, Blagoveshchensk, Russia; CPC, Colección Paleobiológica de Coahuila, Museo del Desierto, Saltillo, Mexico; FCBUANL, Colección Paleobiológica, Facultad de Ciencias Biológicas, Universidad Autónoma de Nuevo León, San Nicolás de los Garza, Mexico; GMH, Geological Museum of Heilongjiang, Harbin, China; IGM, Museo de Paleontología, Instituto de Geología, Universidad Nacional Autónoma de México, Mexico City, Mexico; LACM, Natural History Museum of Los Angeles County, Los Angeles, USA.

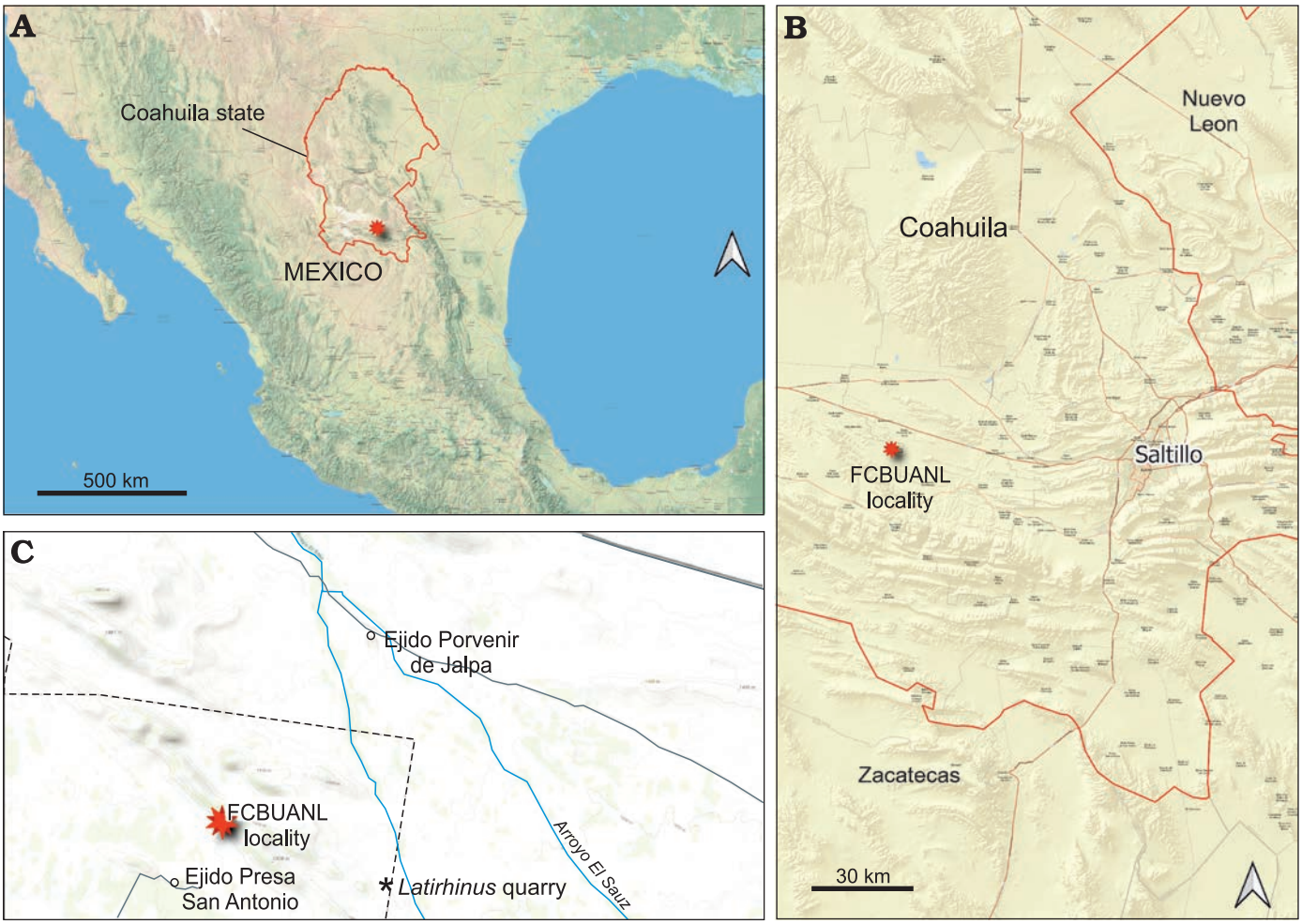

Fig. 1. Map showing location of the Coahuila state (**A**) and FCBUANL locality (**B**) where studied fossils were found. Detailed map indicating the principal localities of Cerro del Pueblo Formation (**C**), FCBUANL_2711 locality represented by red star.

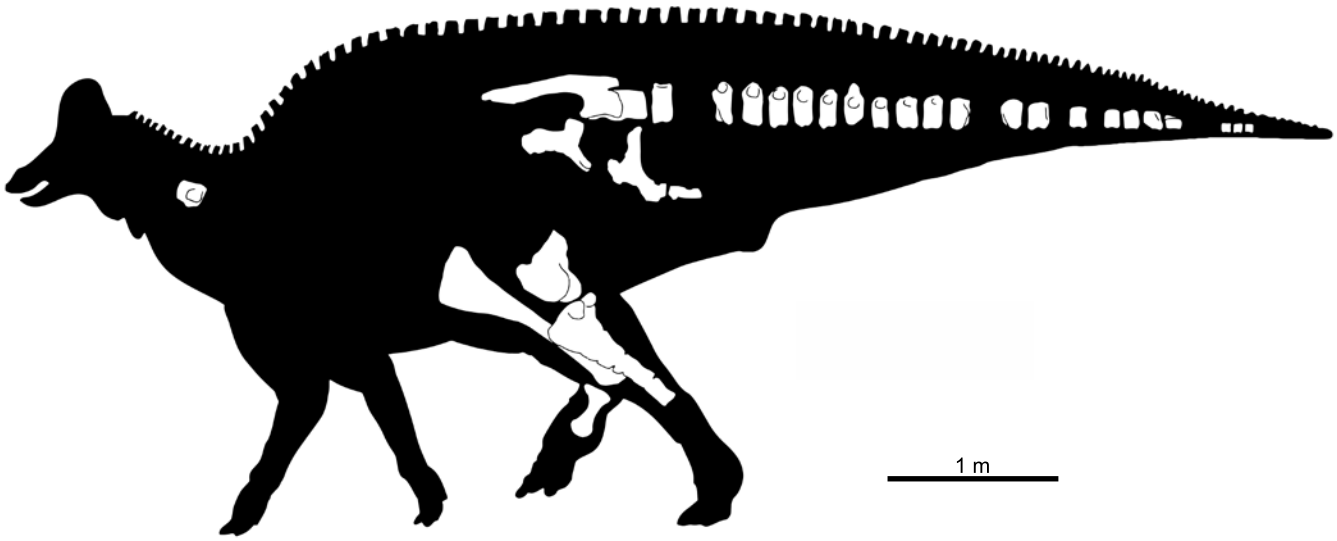

Fig. 2. Skeletal composition of the FCBUANL_2711. The silhouette was obtained from phylopic.org vectorized by T. Michael Keesey from the work of Dmitry Bogdanov.

Material and methods

The specimen FCBUANL_2711 was collected by a team of the Laboratorio de Paleobiología, FCB UANL, during 1992 near the Ejido Presa San Antonio, located in the Parras de la Fuente municipality, Coahuila state, northeastern Mexico (Fig. 1). The specimen was deposited in the Colección Paleobiológica of the UANL Facultad de Ciencias Biológicas. The preparation process has been slow due to space restrictions. Mechanical techniques have been used for this purpose with tools as electric engravers and brushes. The present material was photographed with a Canon EOS Rebels XT camera and Canon 28 mm lens and Canon PowerShot SX280 HS.

Systematic palaeontology

Dinosauria Owen, 1842
Ornithischia Seeley, 1887
Ornithopoda Marsh, 1881
Hadrosauridae Cope, 1870
Lambeosaurinae Parks, 1923
Lambeosaurinae indet.

Material.—FCBUANL_2711, left ilium, right pubis, right ischium, partial sacrum, distal end of left femur, right and left tibiae, II and IV right metatarsals, one cervical and 21 caudal vertebrae (Fig. 2); from Near Ejido Presa San Antonio, Parras de la Fuente municipality, Coahuila, Mexico. The material was recovered from a thick lodolite layer dominated by the gastropod *Tympanotonus nodosa* with thin sandstone intercalations, at Cerro del Pueblo Formation, upper Campanian.

Description.—*Ilium*: Only the left ilium is preserved, missing the posterior region, including the supracetabular crest. The length of the preserved portion is 780 mm (Fig. $3A_1$). The preacetabular process is thick and shows a deep projection close to the anterior end, extruding posteriorly in the direction of the tip. The lateral surface is flattened and in dorsal view it shows a slight concavity with respect to the lateral plane (Fig. $3A_2$). This process is 597 mm in length and shows a minimal degree of ventral deflection

Table 1. Measurements (in mm) of the caudal vertebrae centra of Lambeosaurinae indet. FCBUANL_2711. Element numbers are tentative and do not consider the missing vertebrae.

Element	Height	Width	Length
1	172	194	83
2	182	179	98
3	187	166	91
4	177	176	93
5	178	157	91
6	174	142	85
7	165	152	82
8	155	144	95
9	152	120	98
10	141	135	92
11	147	120	92
12	123	129	96
13	119	114	101
14	113	84	79
15	91	83	84
16	81	85	88
17	96	90	88
18	?	80	91
19	51	63	55
20	54	66	52
21	47	50	58

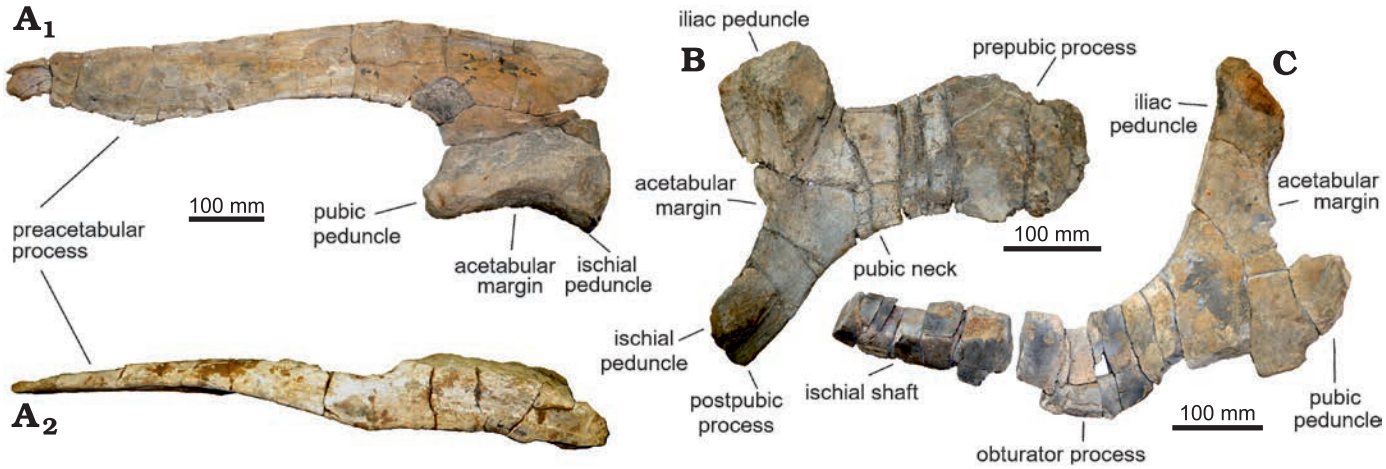

Fig. 3. Lambeosaurinae indet., pelvic gridle elements of FCBUANL_2711, from Ejido Presa San Antonio, Coahuila, Mexico, upper Campanian. **A**. Left ilium in lateral (A_1) and dorsal (A_2) views. **B**. Right pubis in lateral view. **C**. Right ischium in lateral view.

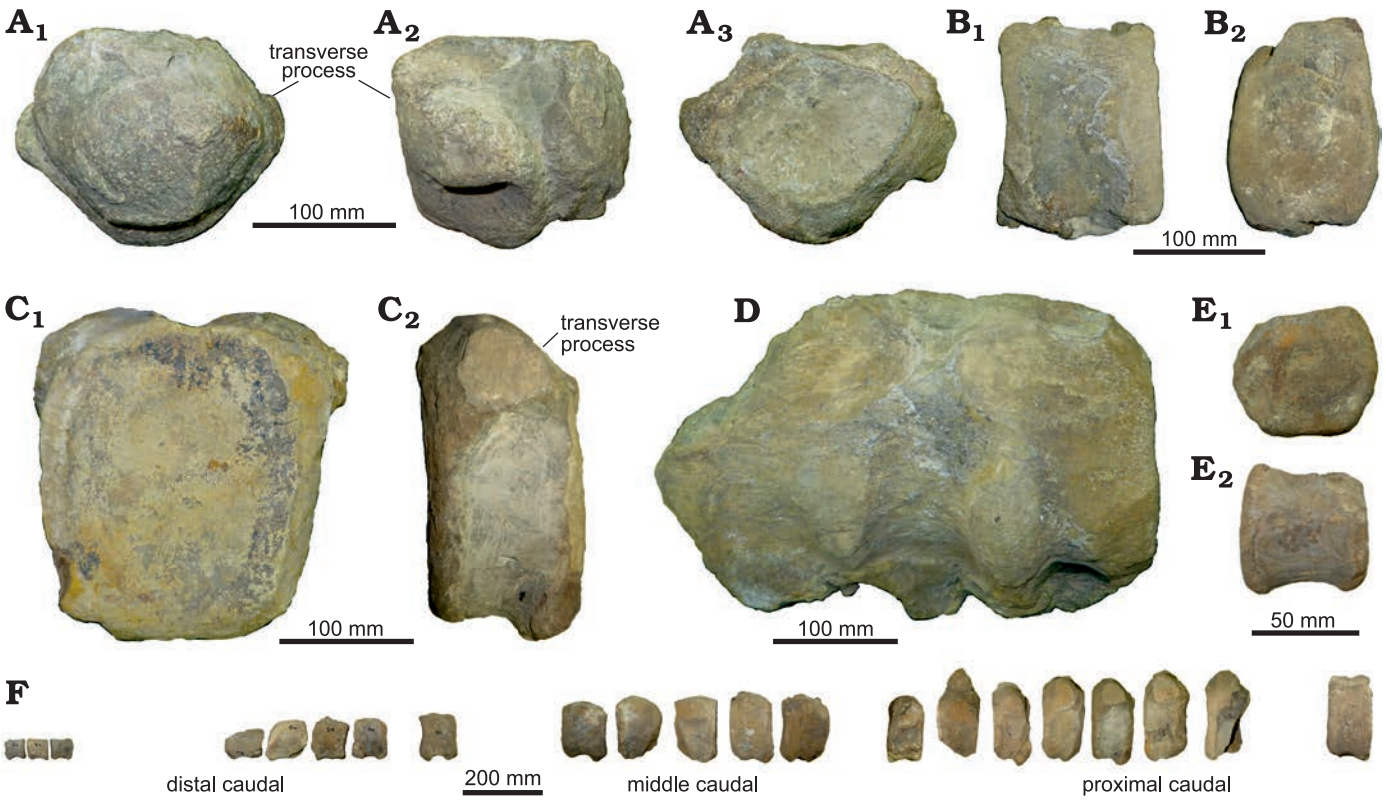

Fig. 4. Vertebrae of Lambeosaurinae indet.(FCBUANL_2711) from Ejido Presa San Antonio, Coahuila, Mexico, upper Campanian. **A**. Cervical vertebrae, in cranial (A_1), lateral (A_2), and caudal (A_3) views. **B**. Middle caudal vertebra, in lateral (B_1) and cranial (B_2) views. **C**. Proximal caudal vertebra, in cranial (C_1) and lateral (C_2) views. **D**. Sacrum in ventral view. **E**. Distal caudal vertebra in cranial (E_2) and lateral (E_2) views. **F**. Caudal vertebrae in lateral view.

(164°). The ratio between the length of the preacetabular process and the length of the acetabulum is 3.14. Although the length measurements seem to indicate that this process has a considerable elongation compared to the ilium, it is not possible to confirm this assumption this without knowing the proportions of the postacetabular process.

Pubis: The pubis (Fig. 3B) has a wide and short pubic blade. The dorsal margin starts to project notably dorsally at the beginning of the prepubic process, while the ventral margin does the same in the ventral direction. Due to the absence of the dorsal and ventral margins of the distal portion of the prepubic process, the shape of this region cannot be determined. However, this process is hypothesized to be short, based on its distal margin. The iliac peduncle is massive and wide, with a triangular section and mediodorsally expanded in the distal region. The distal end of the ischiadic peduncle is absent, and the proximal region shows a protuberance at the base. The distal region of the postpubic process is not preserved and the base is slightly ventrally projected. The acetabular margin is concave and an angle

of 134° is observed between the portion of the margin that corresponds to the iliac peduncle and the margin of the ischial peduncle, giving the appearance of an abrupt change of direction in the margin.

Ischium: Only the proximal region of the right ischium is present, and it is poorly preserved (Fig. 3C). The iliac peduncle is strongly dorsally projected, giving a longer appearance in comparison with the pubic peduncle, which is eroded. The dorsal and ventral margins of the iliac peduncle are convergent. The dorsal one is nearly straight from the base to the tip of the iliac peduncle, and the vertex between dorsal and articular margin is slightly dorsally projected. Only the base of the obturator process is preserved, and it is strongly eroded. The ischiadic shaft shows a clockwise torsional deformation at the base.

Cervical vertebra: Only one cervical vertebra was collected (Fig. 4A). It presents a markedly opisthocoelus condition with a length close to 110 mm. The centrum is wider than high, and the neural canal is wide. There is no neural arch associated with this vertebra and both transverse processes are short and centrally located.

Sacrum: The sacrum (Fig. 4D) is preserved as a single fragmented block composed of 3 sacral vertebrae. It has an approximate length of 350 mm. The last centrum is as tall as wide. Dorsally, it has a neural arch and associated spines. The ventral side is heavily eroded.

Caudal vertebrae: 21 elements are preserved, eight proximal, five middle and eight distal caudal vertebrae (Fig. 4B, C, E, F). Table 1 lists the measurements of the caudal vertebrae. The proximal caudal vertebrae (Fig. 4C) have amphicoelus centra, rectangular to pentagonal in anterior view, being taller than wide and compressed craniocaudally. The neural canal is relatively narrow. Vascular foramina are present in the lateral sides of the centra. In the first vertebra the transverse processes on the centrum are eroded and missing, whereas the following vertebrae present them on the upper lateral part. Also, the articular surfaces of the chevrons are absent on the first vertebra, but they are present on the following elements. The neural arches and spines are present however they are still under preparation. The middle caudal vertebrae (Fig. 4B) are smaller than the proximal caudal vertebrae and hexagonal in anterior view. The articular surfaces of the chevrons are slightly projected

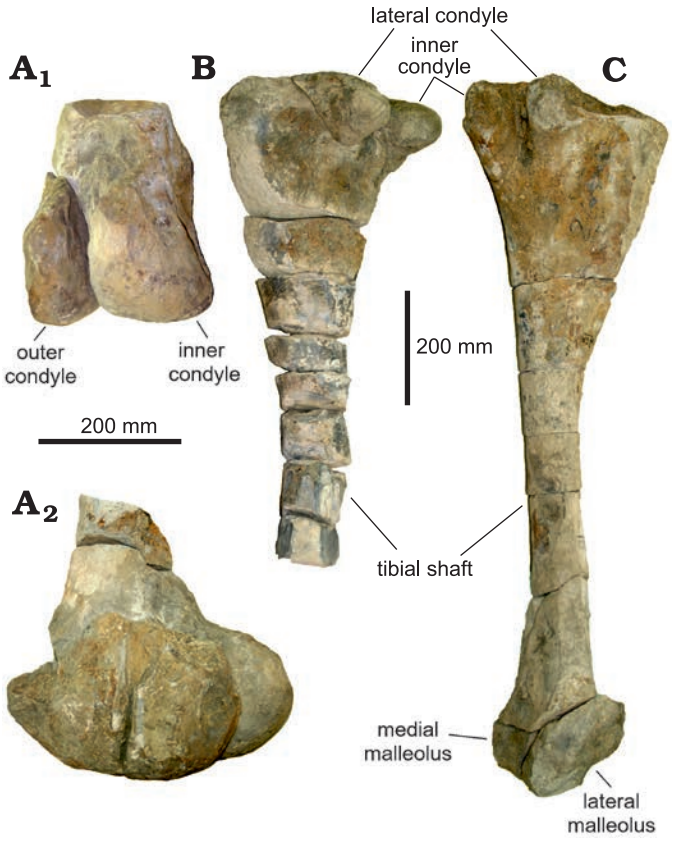

Fig. 5. Hindlimb elements of Lambeosaurinae indet. (FCBUANL_2711) from Ejido Presa San Antonio, Coahuila, Mexico, upper Campanian. **A**. Distal end of the left femur, in caudal (A_1) and lateral (A_2) views. **B**. Left tibia in lateral view. **C**. Right tibia in lateral view.

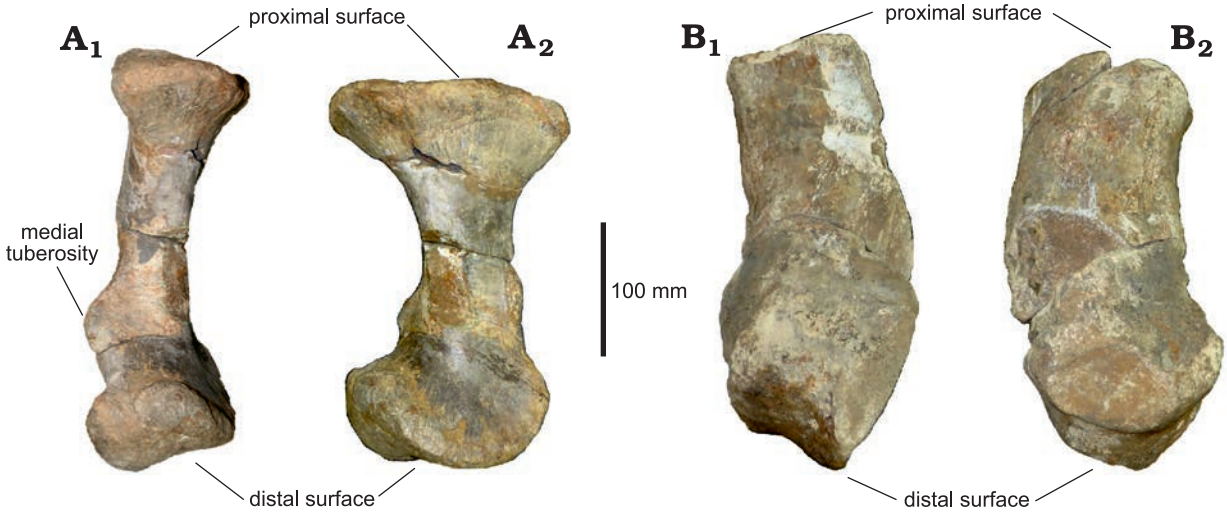

Fig. 6. Metatarsals of Lambeosaurinae indet. (FCBUANL_2711) from Ejido Presa San Antonio, Coahuila, Mexico, upper Campanian. **A**. Metatarsus II, in dorsal (A_1) and lateral (A_2) views. **B**. Metatarsus IV, in dorsal (B_1) and lateral (B_2) views.

ventrally. The centra are less compressed than the proximal vertebrae, maintaining the amphicoelus centra and the narrow neural canal. The distal caudal vertebrae (Fig. 4E) have the smallest centra with cubic proportions. They lack the transverse processes, and the articular surfaces of the chevrons are completely reduced.

Femur: Only the distal end of the left femur is preserved (Fig. $5A_2$). The cranial portion is absent, the outer condyle is smaller and more lateromedially compressed than the inner condyle. The latter is more caudally projected, the intercondylar groove is narrow distally, widening proximally (Fig. $5A_1$).

Tibiae: Both tibiae are present (Fig. 5B, C). However, the left one is missing the distal end and the shaft is transversely fragmented multiple times (Fig. 5B). The right tibia is complete (Fig. 5C), with minor eroded areas and a total length of about 1300 mm. Both tibiae have a wide craniocaudal expansion at their proximal ends and the inner condyle is larger than the lateral condyle, forming a well-defined intercondylar groove. The cnemial crests are eroded on both tibiae. The central shaft of the tibia is sub-cylindrical and very thin compared to the width of the proximal end. In the right tibia the lateral malleolus is smaller than the medial malleolus.

Metatarsals: The right metatarsal IV (Fig. 6B) measures about 330 mm in length. Near mid-length, the bone is strongly deflected laterally. The proximal surface is markedly concave. The distal surface is heavily eroded on the sides. The right metatarsal II (Fig. 6A) is much better preserved than the previous one, with a length of approximately 340 mm. The proximal surface is flat, unlike metatarsal IV, and expanded dorsoplantarly. A medial tuberosity is located above the distal end of metatarsal II, where the bone curves medially.

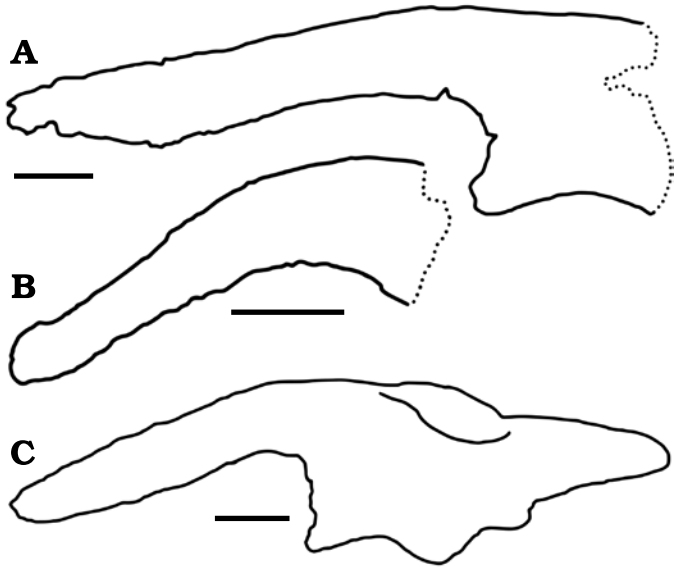

Fig. 7. Comparision of ilia of hadrosaurids from Cerro del Pueblo Formation. **A**. Lambeosaurinae indet., FCBUANL_2711. **B**. *Latirhinus uitstlani* (Prieto-Márquez and Serrano Brañas 2012). **C**. *Velafrons coahuilensis*, CPC 59 (Gates et al. 2007). Scale bars 100 mm.

Discussion

Comparisons with *Latirhinus* and *Velafrons*.—*Latirhinus uitstlani* Prieto-Márquez and Serrano Brañas, 2012 is the only species described so far with postcranial material from the Cerro del Pueblo Formation (Prieto-Márquez and Serrano Brañas 2012). The ilium of FCBUANL_2711 (Fig. 7A) differs markedly from *L. uitstlani* IGM 6583 (Fig. 7B) by presenting a sigmoidal curvature in the ventral margin of the preacetabular process, which narrows anteriorly. The distal

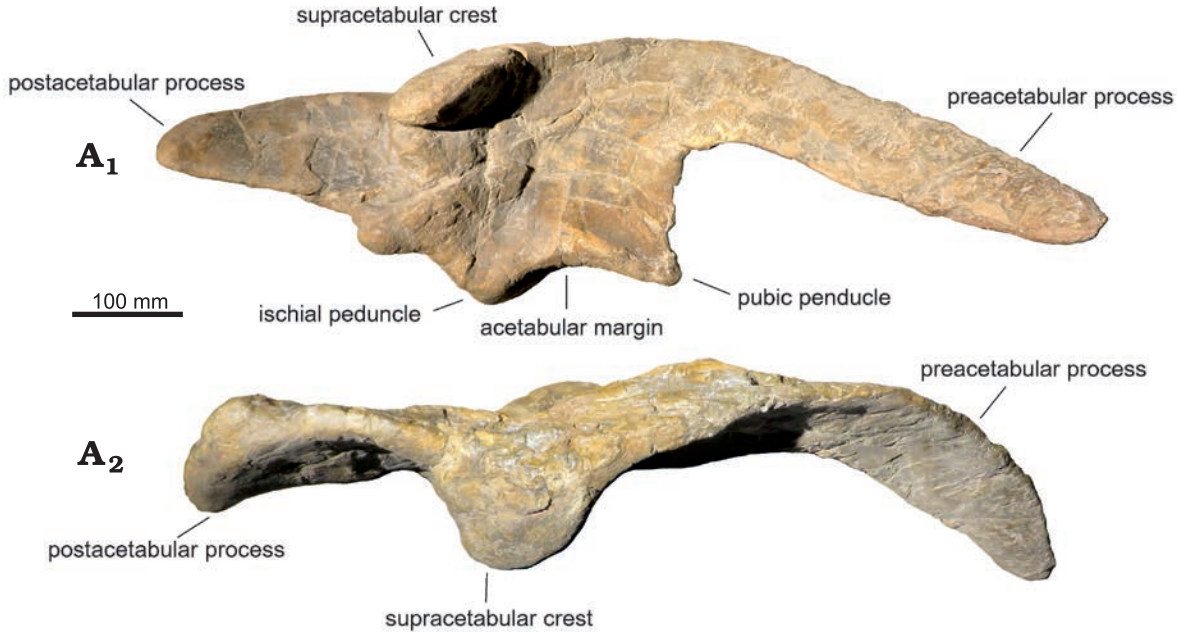

Fig. 8. Ilium of hadrosaurid dinosaur *Velafrons coahuilensis* Gates, Sampson, Delgado de Jesús, Zanno, Eberth, Hernandez-Rivera, Aguillón-Martínez, and Kirkland, 2007 (CPC 59) from Rincón Colorado, Coahuila, Mexico, upper Campanian; in lateral (A_1) and dorsal (A_2) views.

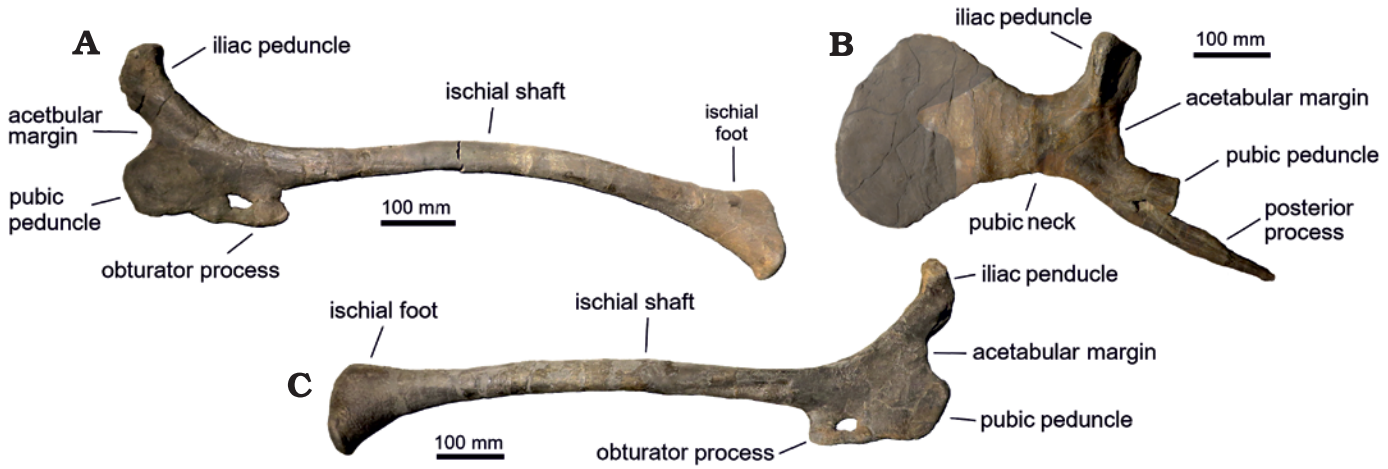

Fig. 9. Pelvic gridle elements of hadrosaurid dinosaur *Velafrons coahuilensis* Gates, Sampson, Delgado de Jesús, Zanno, Eberth, Hernandez-Rivera, Aguillón-Martínez, and Kirkland, 2007 (CPC 59) from Rincón Colorado, Coahuila, Mexico, upper Campanian. **A**. Left ischium in lateral view. **B**. Left pubis in lateral view, shading indicates the reconstructed area. **C**. Right ischium in lateral view.

end of the iliac peduncle of one of the ischias is also assigned to IGM 6583, but due to its fragmentary condition, a direct comparison is not possible.

The holotype of the hadrosaurid *Velafrons coahuilensis* (CPC 59) includes the right ilium, left pubis and both ischia, but these elements were never described. The ilium of CPC 59 (Fig. 7C) has a total length of 690 mm and shows a wide and straight preacetabular process in lateral view (Fig. $8A_1$), whereas in dorsal view this process is strongly craniolaterally curved (Fig. $8A_2$). The preacetabular notch is wide and the ischiadic peduncle is not strongly projected cranially. In contrast, the preacetabular process of FCBUANL_2711 is concave in dorsal view with respect to the lateral axis but it does not present a deformation as marked as in CPC 59. Furthermore, the preacetabular notch is narrower, highlighting the cranial projection of the pubic peduncle, which is more robust than in CPC 59. The ilium of FCBUANL_2711, despite being incomplete, is longer than the ilium of CPC 59, which has been previously regarded as a juvenile specimen (Gates et al. 2007). Both specimens show a ventral deflection of the preacetabular process greater than 150°, 153° in CPC 59 and 164° in FCBUANL_2711. According to Brett-Surman and Wagner (2007), this character is highly variable, even between the two ilia of the same individual, therefore a difference of 10° of ventral deflection is not sufficient for the differentiation of FCBUANL_2711 from *V. coahuilensis*. The designation of FCBUANL_2711 as an adult specimen of *V. coahuilensis* is possible, however Prieto-Márquez (2014a) indicates that in *Edmontosaurus annectens* Marsh, 1892, there is an ontogenetic change in the ventral deflection of the preacetabular process of the ilium. In juveniles it is slightly deflected (157° to 165°) whereas adults shows a more pronounced deflection (138° to 147°) (Prieto-Marquez 2014a). A more detailed study of this character in other species is necessary to determine whether ontogenetic variation of the deflection of this process is generalized among hadrosaurids, or if it is only present in *E. annectens*.

The left pubis of CPC 59 (Fig. 9B) shows the common morphology of lamebosaurines, presenting a high iliac peduncle with triangular cross-section and a short prepubic constriction. The prepubic process is incompletely preserved. The margins of the prepubic constriction are divergent, and the dorsal margin arises dorsally without reaching the level of the proximal end of the iliac peduncle. The pubis of FCBUANL_2711 and that of CPC 59 are similar, differing in the more robust iliac peduncle in the former and the slightly narrower prepubic constriction in CPC 59.

CPC 59 preserves both complete ischia (Fig. 9A, C), characterized by the "thumb-like" shape of the dorsal and articular margin of the iliac peduncle. The distal end of the ischiadic shaft ends in the typical lambeosaurine "foot" shape, but it lacks the "heel", a feature also absent in species of *Corythosaurus* and *Lambeosaurus* (Brett-Surmann 1989). The ischium is the least well preserved element of the three pelvic bones of FCBUANL_2711, showing the "thumb like" iliac peduncle as well, although erosion reduces the visibility of this character. Both the pubic peduncle, the obturator process, and the notch are not well preserved, preventing a more extensive comparison with the material assigned to *Velafrons*. The absence of the distal end of the ischial shaft precludes a more accurate assignment of this material to Lambeosaurinae, as well as its differentiation from *V. coahuilensis*.

Comparisons with other hadrosaurids.—The angle of ventral deflection of the ilium greater than 150°, present in FCBUANL_2711 and *Velafrons coahuilensis*, is also present in the material tentatively referred to the Asian hadrosaurine *Kundurosaurus nagornyi* Godefroit, Bolotsky, and Lauters, 2012b, AENM 2/922-7L (Godefroit et al. 2012b), relegated as a junior synonym of *Kerberosaurus manakini* Bolotsky and Godefroit, 2004, by Xing et al. (2014), in the south American hadrosaurine *Bonapartesaurus rionegrensis* Cruzado-Caballero and Powell, 2017 (Cruzado-Caballero and Powell 2017), and the Asian lambeosaurine *Sahaliyania elunchunorum* Godefroit, Shulin, Tingxiang, and Lauters,

2008 (Godefroit et al. 2008). The ilium of FCBUANL_2711 differs from *K. manakini* by having a wide preacetabular process, a notable characteristic in lambeosaurines (Brett-Surman 1989). The preacetabular process of the ilium also shows a ventral projection close to the cranial end where it narrows distally, as in other lambeosaurine specimens like FMNH P27393 *Parasaurolophus cyrtocristatus* Ostrom, 1961a (Ostrom 1961a), LACM 20874 *Magnapaulia laticaudus* Morris, 1981 (Prieto-Márquez et al. 2012) and AEHM 2/846 *Olorotitan arharensis* Godefroit, Bolotsky, and Alifanov, 2003 (Godefroit et al. 2012a). The ilium shows a similar morphology to the GMH W103 an ilium referred to *S. elunchunorum* (Godefroit et al. 2008), but the preacetabular notch of FCBUANL_2711 is narrower than in GMH W103. The absence of the supracetabular crest and postacetabular process prevents a more extensive comparison, since in these regions possess important diagnostic characters for the clade (Prieto-Márquez 2010b).

The pubis of FCBUANL_2711 resembles the V morphotype proposed by Brett-Surmann (1989) which corresponds to the Parasaurolophini clade, while differs from the morphotypes of the Hadrosaurinae by having a short and wide prepubic constriction. Despite the incomplete condition, the prepubic process is similar to the morphology of the *Hypacrosaurus stebingeri* Horner and Currie, 1994, pubis (see Guenther 2009: fig. 10c). The material referred to *S. elunchunorum* includes a left pubis (GMH W179) that differs from FCBUANL_2711 in having an almost straight ventral margin of the prepubic process, resulting in a more elongated appearance of the bone, similar to the V morphotype of Brett-Surmann (1989). The pubis of GMH W179 bears a robust iliac peduncle, although to a lesser extent than in FCBUANL_2711. The incomplete condition of the prepubic process complicates a better systematic resolution, but the recognized features suggest lambeosaurine affinities.

Conclusions

The hadrosaurid specimen described in this paper shows lambeosaurine affinities, therefore distinct from *Kritosaurus navajovius* and *Latirhinus uitstlani*, both present in the Cerro del Pueblo Formation. The differentiation from to *Velafrons coahuilensis* is not clear; because FCBUANL_2711 is a large individual, it is possible that it is a fully developed adult individual of this species, but an osteohistological analysis would be necessary to confirm this. The lack of cranial elements in FCBUANL_2711 prevents the assignment of the specimen to *V. coahuilensis* or to a different species. Therefore, this specimen is referred only as Lambeosaurinae indet. Paleontological studies of this clade, along with other groups of dinosaurs, have increased in recent years in Mexico, but several other materials need to be studied from other geological formations of Campanian–Maastrichtian Mexico. This will allow a better understanding of the terrestrial environments during these ages in southern Laramidia.

Acknowledgements

We thank Claudia Hernández Pérez, Rogelio Reyna de Labra, and José Martínez (Monterrey, Mexico) for their collaboration and help with the photographs and assistance in the preparation of the figures. Thanks to the reviewer Filippo Bertozzo (Queen's University Belfast, UK) and the anonymous reviewer for their detailed and helpful comments on the manuscript. We would like to thank Erick C. Oñate-González and Hidalgo Rodríguez-Vela (both Universidad Autónoma De Nuevo León, Mexico) for their reviews and the helpful comments. Financial support for the field work was provided by Programa de Apoyo a la Investigación Científica y Tecnológica (PAICYT) Proyecto N° CN1181-11 and Facultad de Ciencias Biológicas, Universidad Autónoma de Nuevo León.

References

Bolotsky, Y.L. and Godefroit, P. 2004. A new hadrosaurine dinosaur from the Late Cretaceous of Far Eastern Russia. *Journal of Vertebrate Paleontology* 24: 351–365.

Brett-Surman, M.K. 1989. *A Revision of the Hadrosauridae (Reptilia: Ornithischia) and Their Evolution During the Campanian and Maastrichtian*. 272 pp. Unpublished Ph.D. Thesis, George Washington University, Washington D.C.

Brett-Surman, M.K. and Wagner, J.R. 2007. Discussion of character analysis of the appendicular anatomy in Campanian and Maastrichtian North American hadrosaurids—variation and ontogeny. *In*: K. Carpenter (ed.), *Horns and Beaks*, 135–170. Indiana University Press, Bloomington.

Brinkman, D.B. 2014. Turtles of the Mesozoic of Mexico. *In*: H.E. Rivera-Sylva, K. Carpenter, and E. Frey (eds.), *Dinosaurs and Other Reptiles from the Mesozoic of Mexico*, 30–43. Indiana University Press, Bloomington.

Brown, B. 1910. The Cretaceous Ojo Alamo beds of New Mexico with description of the new dinosaur genus *Kritosaurus*. *Bulletin of the American Museum of Natural History* 28: 267–274.

Campione, N.E. 2014. Postcranial anatomy of *Edmontosaurus regalis* (Hadrosauridae) from the Horseshoe Canyon Formation, Alberta, Canada. *In*: D.A. Eberth, D.C. Evans, and P.E. Ralrick (eds.), *Hadrosaurs*, 208–244. Indiana University Press, Bloomington.

Cevallos-Ferriz, S.R.S. and Vázquez-Rueda, M.A. 2016. Permineralized infructescence from the Cerro del Pueblo Formation, Upper Cretaceous, Coahuila, Mexico. *Botany* 94: 773–785.

Cifuentes-Ruiz, P., Vršanský, P., Vega, F.J., Cevallos-Ferriz, S.R.S., González-Soriano, E., and Delgado de Jesús, C.R. 2006. Campanian terrestrial arthropods from the Cerro del Pueblo Formation, Difunta Group in northeastern Mexico. *Geologica Carpathica* 57: 347–354.

Cope, E.D. 1870. Synopsis of the extinct Batrachia and Reptilia of North America. *Transactions of the American Philosophical Society* 14: 1–252.

Cruzado-Caballero, P. and Powell, J. 2017. *Bonapartesaurus rionegrensis*, a new hadrosaurine dinosaur from South America: implications for phylogenetic and biogeographic relations with North America. *Journal of Vertebrate Paleontology* 37: e1289381.

Estrada-Ruiz, E. and Cevallos-Ferriz, S.R.S. 2007. Infructescences from the Cerro del Pueblo Formation (Late Campanian), Coahuila, and El Cien Formation (Oligocene–Miocene), Baja California Sur, Mexico. *International Journal of Plant Sciences* 168: 507–519.

Estrada-Ruiz, E., Calvillo-Canadell, L., and Cevallos-Ferriz, S.R.S. 2009. Upper Cretaceous aquatic plants from Northern Mexico. *Aquatic Botany* 90: 282–288.

Gates, T.A., Sampson, S.D., Delgado de Jesús, C.R., Zanno, L.E., Eberth, D., Hernandez-Rivera, R., Aguillón-Martínez, M.C., and Kirkland, J.I. 2007. *Velafrons coahuilensis*, a new lambeosaurine hadrosaurid (Di-

nosauria: Ornithopoda) from the Late Campanian Cerro del Pueblo Formation, Coahuila, Mexico. *Journal of Vertebrate Paleontology* 27: 917–930.

Godefroit, P., Bolotsky, Y.. and Alifanov, V. 2003. A remarkable hollow-crested hadrosaur from Russia: An Asian origin for lambeosaurines. *Comptes Rendus Palevol* 2: 143–151.

Godefroit, P., Bolotsky, Y.L., and Bolotsky, I.Y. 2012a. Osteology and relationships of *Olorotitan arharensis*, a hollow-crested hadrosaurid dinosaur from the latest Cretaceous of far eastern Russia. *Acta Palaeontologica Polonica* 57: 527–560.

Godefroit, P., Bolotsky, Y.L., and Lauters, P. 2012b. A new saurolophine dinosaur from the Latest Cretaceous of far eastern Russia. *PLoS ONE* 7 (5): e36849.

Godefroit, P., Shulin, H., Tingxiang, Y., and Lauters, P. 2008. New hadrosaurid dinosaurs from the uppermost Cretaceous of northeastern China. *Acta Palaeontologica Polonica* 53: 47–74.

Guenther, M.F. 2009. Influence of sequence heterochrony on hadrosaurid dinosaur postcranial development. *Anatomical Record* 292: 1427–1441.

Horner, J.R., Weishampel, D.B., and Foster, C.A. 2004. Hadrosauridae. *In*: D.B. Weishampel, P. Dodson, and H. Osmólska (eds.), *The Dinosauria*, 438–463. University of California Press, Berkeley.

Kirkland, J.I., Hernández Rivera, R., Aguillón Martínez, M.C., Delgado de Jesús, C.R., Gómez Nuñez, R., and Vallejo, I. 2000. The Late Cretaceous Difunta Group of the Parras Basin, Coahuila, Mexico, and its vertebrate fauna. *In*: *Society of Vertebrate Paleontology Annual Meeting 2000 Field Trip Book*, 133–172. UNAM, Mexico City.

Kirkland, J.I., Hernández-Rivera, R., Gates, T., Paul, G.S., Nesbitt, S., Serrano-Brañas, C.I., and Garcia-de la Garza, J.P. 2006. Large hadrosaurine dinosaurs from the Latest Campanian of Coahuila, Mexico. *New Mexico Museum of Natural History and Science Bulletin* 35: 299–315.

Loewen, M.A., Sampson, S.D., Lund, E.K., Farke, A.A., Aguillón-Martínez, M.C., de León, C.A., Rodríguez-de la Rosa, R.A., Getty, M.A., and Eberth, D.A. 2010. Horned dinosaurs (Ornithischia: Ceratopsidae) from the Upper Cretaceous (Campanian) Cerro del Pueblo Formation, Coahuila, Mexico. *In*: M.J. Ryan, B.J. Chinnery-Allgeier, D.A. Eberth, and P.E. Ralrick (eds.), *New Perspectives on Horned Dinosaurs*, 99–116. Indiana University Press, Bloomington.

Longrich, N.R., Suberbiola, X.P., Pyron, R.A. and Jalil, N.-E. 2021. The first duckbill dinosaur (Hadrosauridae: Lambeosaurinae) from Africa and the role of oceanic dispersal in dinosaur biogeography. *Cretaceous Research* 120: 104678.

Lull, R.S. and Wright, N.E. 1942. Hadrosaurian dinosaurs of North America. *Geological Society of America Special Papers* 40: 1–272.

Lund, E.K. and Gates, T.A. 2006. A historical and biogeographical examination of hadrosaurian dinosaurs. *New Mexico Museum of Natural History and Science Bulletin* 35: 263–276.

Marsh, O.C. 1881. Principal characters of American Jurassic dinosaurs. Part IV. *American Journal of Science* 21: 167–170.

Marsh, O.C. 1892. Notice of new reptiles from the Laramie Formation. *American Journal of Science* 43: 449–453.

Morris, W.J. 1970. Hadrosaurian dinosaur bills-morphology and function. *Contributions in Science* 193: 1–14.

Morris, W.J. 1981. A new species of hadrosaurian dinosaur from the Upper Cretaceous of Baja California—?*Lambeosaurus laticaudus*. *Journal of Paleontology* 55: 453–462.

Nabavizadeh, A. 2014. Hadrosauroid jaw mechanics and the functional significance of the predentary bone. *In*: D.A. Eberth, D.C. Evans, and P.E. Ralrick (eds.), *Hadrosaurs*, 467–483. Indiana University Press, Bloomington.

Nabavizadeh, A. and Weishampel, D.B. 2016. The predentary bone and its significance in the evolution of feeding mechanisms in ornithischian dinosaurs. *The Anatomical Record* 299: 1358–1388.

Ostrom, J.H. 1961a. A new species of hadrosaurian dinosaur from the Cretaceous of New Mexico. *Journal of Paleontology* 35: 575–577.

Ostrom, J.H. 1961b. Cranial morphology of the hadrosaurian dinosaurs of North America. *Bulletin of the American Museum of Natural History* 122: 33–186.

Owen, R. 1842. Report on British fossil reptiles. Part II. *Reports of the British Association for the Advancement of Science* 11: 60–204.

Parks, W.A. 1923. Corythosaurus intermedius, a new species of trachodont dinosaur. *University of Toronto Studies, Geological Series* 15: 5–57.

Prieto-Márquez, A. 2010a. Global historical biogeography of hadrosaurid dinosaurs. *Zoological Journal of the Linnean Society* 159: 503–525.

Prieto-Márquez, A. 2010b. Global phylogeny of hadrosauridae (Dinosauria: Ornithopoda) using parsimony and bayesian methods. *Zoological Journal of the Linnean Society* 159: 435–502.

Prieto-Márquez, A. 2014a. A juvenile *Edmontosaurus* from the late Maastrichtian (Cretaceous) of North America: Implications for ontogeny and phylogenetic inference in saurolophine dinosaurs. *Cretaceous Research* 50: 282–303.

Prieto-Márquez, A. 2014b. Skeletal morphology of *Kritosaurus navajovius* (Dinosauria: Hadrosauridae) from the Late Cretaceous of the North American south-west, with an evaluation of the phylogenetic systematics and biogeography of Kritosaurini. *Journal of Systematic Palaeontology* 12: 133–175.

Prieto-Márquez, A. and Serrano Brañas, C.I. 2012. *Latirhinus uitstlani*, a "broad-nosed" saurolophine hadrosaurid (Dinosauria, Ornithopoda) from the late Campanian (Cretaceous) of northern Mexico. *Historical Biology* 24: 607–619.

Prieto-Márquez, A., Chiappe, L.M., and Joshi, S.H. 2012. The lambeosaurine dinosaur *Magnapaulia laticaudus* from the Late Cretaceous of Baja California, northwestern Mexico. *PLoS ONE* 7 (6): e38207.

Ramírez-Velasco, A.A. and Hernández-Rivera, R. 2015. Diversity of Late Cretaceous dinosaurs from Mexico. *Boletín Geológico y Minero* 126: 63–108.

Ramírez-Velasco, A.A., Hernández-Rivera, R., and Servin-Pichardo, R. 2014. The hadrosaurian record from Mexico. *In*: D.A. Eberth, D.C. Evans, and P.E. Ralrick (eds.), *Hadrosaurs*, 340–360. Indiana University Press, Bloomington.

Rivera-Sylva, H.E. and Carpenter, K. 2014. The ornithischian dinosaurs of Mexico. *In*: H.E. Rivera-Sylva, K. Carpenter, and E. Frey (eds.), *Dinosaurs and Other Reptiles from the Mesozoic of Mexico*, 156–180. Indiana University Press, Bloomington.

Rivera-Sylva, H.E. and Espinosa-Chávez, B. 2006. Ankylosaurid (Dinosauria: Thyreophora) osteoderms from the Upper Cretaceous Cerro del Pueblo Formation of Coahuila, Mexico. *Carnets de Géologie (Notebooks on Geology)* 2006: CG2006_L02.

Rivera-Sylva, H.E., Barrón-Ortíz, C.I., Vivas González, R., Nava Rodríguez, R.L., Guzmán-Gutiérrez, J.R., Cabral Valdez, F., and de León Dávila, C. 2019a. Preliminary assessment of hadrosaur dental microwear from the Cerro del Pueblo Formation (Upper Cretaceous: Campanian) of Coahuila, northeastern Mexico. *Paleontología Mexicana* 8 (1): 17–28.

Rivera-Sylva, H.E., Frey, E., Schulp, A.S., Meyer, C., Thüring, B., Stinnesbeck, W., and Vanhecke, V. 2017. Late Campanian theropod trackways from Porvenir de Jalpa, Coahuila, Mexico. *Palaeovertebrata* 41 (2): e1.

Rivera-Sylva, H.E., Frey, E., Stinnesbeck, W., Amezcua, N., and Flores Huerta, D. 2018. First occurrence of Parksosauridae in Mexico, from the Cerro del Pueblo Formation (Late Cretaceous; late Campanian) at Las águilas, Coahuila. *Boletín de la Sociedad Geológica Mexicana* 70: 779–784.

Rivera-Sylva, H.E., Frey, E., Stinnesbeck, W., Amezcua Torres, N., and Flores Huerta, D. 2019b. Terrestrial vertebrate paleocommunities from the Cerro del Pueblo Formation (Late Cretaceous; late Campanian) at Las Aguilas, Coahuila, Mexico. *Palaeovertebrata* 42 (2): e1.

Rodríguez de la Rosa, R.A. 2007. Hadrosaurian footprints from the Late Cretaceous Cerro del Pueblo Formation of Coahuila, Mexico. *In*: E. Díaz-Martínez and I. Rábano (eds.), *4th European Meeting on the Palaeontology and Stratigraphy of Latin America. Cuadernos Del Museo Geominero No. 8*, 339–343. Instituto Geológico y Minero de España, Madrid.

Rodriguez-de la Rosa, R.A. and Cevallos-Ferriz, S.R.S. 1994. Upper Creta-

ceous zingiberalean fruits with in situ seeds from southeastern Coahuila, Mexico. *International Journal of Plant Sciences* 55: 786–805.

Rodriguez-de la Rosa, R.A. and Cevallos-Ferriz, S.R.S. 1998. Vertebrates of the El Pelillal locality (Campanian, Cerro Del Pueblo Formation), southeastern Coahuila, Mexico. *Journal of Vertebrate Paleontology* 18: 751–764.

Rybakiewicz, S., Rivera-Sylva, H.E., Stinnesbeck, W., Frey, E., Guzmán-Gutiérrez, J.R., Vivas González, R., Nava Rodríguez, R.L., and Padilla-Gutiérrez, J.M. 2019. Hadrosaurs from Cañada Ancha (Cerro del Pueblo Formation; upper Campanian–?lower Maastrichtian), Coahuila, northeastern Mexico. *Cretaceous Research* 104: 104199.

Seeley, H.G. 1887. Researches on the structure, organization, and classification of the fossil reptilia. I. On *Protorosaurus speneri* (von Meyer). *Philosophical Transactions of the Royal Society of London B* 178: 187–213.

Serrano-Brañas, C.I. and Espinosa-Chávez, B. 2017. Taphonomic history of a "duck-bill" dinosaur (Dinosauria: Ornithopoda) from the Cerro del Pueblo Formation (Upper Cretaceous, Campanian) Coahuila, Mexico: Preservational and paleoecological implications. *Cretaceous Research* 74: 165–174.

Serrano-Brañas, C.I., Espinosa-Chávez, B., and Maccracken, S.A. 2018a. *Gastrochaenolites* Leymerie in dinosaur bones from the Upper Cretaceous of Coahuila, north-central Mexico: Taphonomic implications for isolated bone fragments. *Cretaceous Research* 92: 18–25.

Serrano-Brañas, C.I., Espinosa-Chávez, B., and Maccracken, S.A. 2018b. Insect damage in dinosaur bones from the Cerro del Pueblo Formation (Late Cretaceous, Campanian) Coahuila, Mexico. *Journal of South American Earth Sciences* 86: 353–365.

Serrano-Brañas, C.I., Espinosa-Chávez, B., and Maccracken, S.A. 2019. *Teredolites* trace fossils in log-grounds from the Cerro del Pueblo Formation (Upper Cretaceous) of the state of Coahuila, Mexico. *Journal of South American Earth Sciences* 95: 102316.

Serrano-Brañas, C.I., Espinosa-Chávez, B., Maccracken, S.A., Gutiérrez-Blando, C., de León-Dávila, C., and Flores Ventura, J. 2020. *Paraxenisaurus normalensis*, a large deinocheirid ornithomimosaur from the Cerro del Pueblo Formation (Upper Cretaceous), Coahuila, Mexico. *Journal of South American Earth Sciences* 101: 102610.

Serrano-Brañas, C.I., Hernández-Rivera, R., Torres-Rodríguez, E., and Espinosa Chávez, B. 2006. A natural hadrosaurid endocast from the Cerro del Pueblo Formation (Upper Cretaceous) of Coahuila, Mexico. *New Mexico Museum of Natural History and Science Bulletin* 35: 317–322.

Wolleben, J.A. 1977. Paleontology of the Difunta Group (Upper Cretaceous–Tertiary) in Northern Mexico. *Journal of Paleontology* 51: 373–398.

Xing, H., Zhao, X., Wang, K., Li, D., Chen, S., Mallon, J.C., Zhang, Y., and Xu, X. 2014. Comparative osteology and phylogenetic relationship of *Edmontosaurus* and *Shantungosaurus* (Dinosauria: Hadrosauridae) from the Upper Cretaceous of North America and East Asia. *Acta Geologica Sinica (English Edition)* 88: 1623–1652.

First Miocene megafossil of arrowhead, alismataceous plant *Sagittaria*, from South America

JUAN M. ROBLEDO, SILVINA A. CONTRERAS, JOHANNA S. BAEZ, and CLAUDIA I. GALLI

Robledo, J.M., Contreras, S.A., Baez, J.S., and Galli, C.I. 2021. First Miocene megafossil of arrowhead, alismataceous plant *Sagittaria*, from South America. *Acta Palaeontologica Polonica* 66 (Supplement to 3): S111–S122.

The first pre-Quaternary representative of Alismataceae from South America is reported based on achenes of *Sagittaria montevidensis* from the Palo Pintado Formation (upper Miocene) in the south of Salta Province, Argentina. Achenes are laterally compressed, have a lateral beak and a single recurved seed inside them. The fruits were found both in the base (10 Ma) and the top of the formation (~5 Ma), suggesting similar environmental conditions during this time period. A cursory review of the Alismataceae family in the fossil record, with a special interest in those South American reports is given. During the Oligocene–Miocene *Sagittaria* may have arrived from tropical Africa to South America and thence to North America.

Key words: Alismataceae, *Sagittaria*, achene, aquatic plants, fossil fruits, Neogene, Argentina.

Juan M. Robledo [robledomanuel182@gmail.com] and Silvina A. Contreras [sailcontreras11@gmail.com], Laboratorio de Paleobotánica y Palinología desde el Neógeno hasta la Actualidad en el Norte de Argentina, Centro de Ecología Aplicada del Litoral (CONICET-UNNE), Ruta 5, km 2.5. W3400, Corrientes, Argentina and Facultad de Ciencias Exactas, Naturales y Agrimensura-Universidad Nacional del Nordeste. Av. Libertad 5450, W3400. Corrientes, Argentina.
Johanna S. Baez [johannasbaez@gmail.com], Laboratorio de Xilotafofloras del Neopaleozoico y Triásico de Sudamérica y Neógeno del Noroeste Argentino, Centro de Ecología Aplicada del Litoral (CONICET-UNNE), Ruta 5, km 2.5. W3400. Corrientes, Argentina.
Claudia I. Galli [cgalli@unsa.edu.ar], Instituto de Ecorregiones Andinas (INECOA-UNJu), Av. Bolivia 1661, S.S. de Jujuy, Universidad Nacional de Salta, Facultad de Ciencias Naturales. Av Bolivia 5150, Salta, Argentina.

Received 12 October 2020, accepted 2 February 2021, available online 6 August 2021.

Introduction

The monocot family Alismataceae sensu lato (including Limnocharitaceae Takhtajan ex Cronquist, 1981) contains about 12 genera and approximately 100 species (Dahlgren 1980; APG III 2009; Chen et al. 2012). The family has a cosmopolitan distribution (Haynes and Holm-Nielsen 1994; Costa and Forni-Martins 2003; Soltis et al. 2005; Lehtonen 2009) and includes aquatic or semi-aquatic herbs with erect or floating leaves (Haynes and Holm-Nielsen 1994). Fossils of this family have been reported from the Lower and Upper Cretaceous and the Paleocene in North America, Europe, Siberia, and Africa (Berry 1925; Brown 1962; Golovneva 1997; Riley and Stockey 2004; Coiffard and Mohr 2018), but researchers disagree about whether all these fossil reports actually represent Alismataceae (Chandler 1963; Haggard and Tiffney 1997; Haynes and Les 2004; Chen et al. 2012).

The alismataceous genus *Sagittaria* has been considered to include up to 139 named species, but only about 20 of them are currently considered as legitimate (www.tropicos.org; Zepeda and Lot 2005). Species of *Sagittaria*, commonly named arrowheads, are mostly distributed in America, from Canada to Argentina and Chile, although four species are reported in Europe, Asia, and Oceania (Haynes and Holm-Nielsen 1994; Adair et al. 2012). Three species of *Sagittaria* are recorded from Argentina (Rataj 1970, 1972; Matias and Irgang 2006). The fruits of *Sagittaria* consist of aggregates of achenes. These achenes are laterally compressed (flattened) and have different shapes, from sub-circular to lanceolate and oblanceolate. Among the most striking morphological characters, a lateral beak (persistent style) stands out, which has different degrees of development, and a strongly recurved seed. Chen (1989) suggested that *Sagittaria* originated in tropical wetlands and lake areas of Africa, during the Late Cretaceous. Then, it might have dispersed to South America and subsequently to North America (Chen et al. 2012). Data concerning the biogeographic history of Alismataceae family in South America are still scarce.

Recently, Neogene impressions of *Sagittaria* fruits

(described in this paper) were found in the Palo Pintado Formation from northwestern Argentina. This formation has been studied since the 1980-ies and nowadays discoveries still occur. Deposits of the Palo Pintado Formation indicate water bodies of low energy, as a wandering fluvial system that in rainfall periods overflowed from the channel, generating lagoons and swamps during late Miocene to Pliocene (Herbst et al. 1987; Galli et al. 2011).

In order to contribute to the history of the Alismataceae in Argentina and South America, in this paper the following objectives are proposed: (i) to describe the first record of *Sagittaria* from the Palo Pintado Formation; (ii) to perform a review of the Alismataceae in South America; (iii) and associate these data with stratigraphic, sedimentological and paleontological features.

Institutional abbreviations.—CTES-PB, Colección Paleontológica de la UNNE Dr. Rafael Herbst, Paleontological Collection of the Universidad Nacional del Nordeste, Corrientes, Argentina.

Geological setting

The study area is located in the Eastern Cordillera, from 25°30’ S to 66°15’ W and 25°45’ S to 66°00’ W, approximately 200 km south of the city of Salta in northwestern Argentina (Fig. 1). Cenozoic sedimentary strata crop out in the Calchaquí Valleys as part of the regional Andean foreland basin that extended into the Eastern Cordillera.

The Payogastilla Group (Díaz and Malizzia 1983) in the Calchaquí Valleys is composed of continental deposits, including in ascending order formations Los Colorados (middle Eocene to Oligocene), Angastaco (middle to upper Miocene), Palo Pintado (upper Miocene) and San Felipe (Pliocene to lower Pleistocene). The Palo Pintado Formation is ~800 m thick and contains a tuff that has been dated at 10.29 ± 0.11 Ma (K/Ar) by Galli et al. (2008). Near the top is another pyroclastic unit that was dated at 5.27 ± 0.28 Ma ($^{206}Pb/^{238}U$) by Coutand et al. (2006) and at 5.98 ± 0.32 Ma by Bywater-Reyes et al. (2010). The unit com-

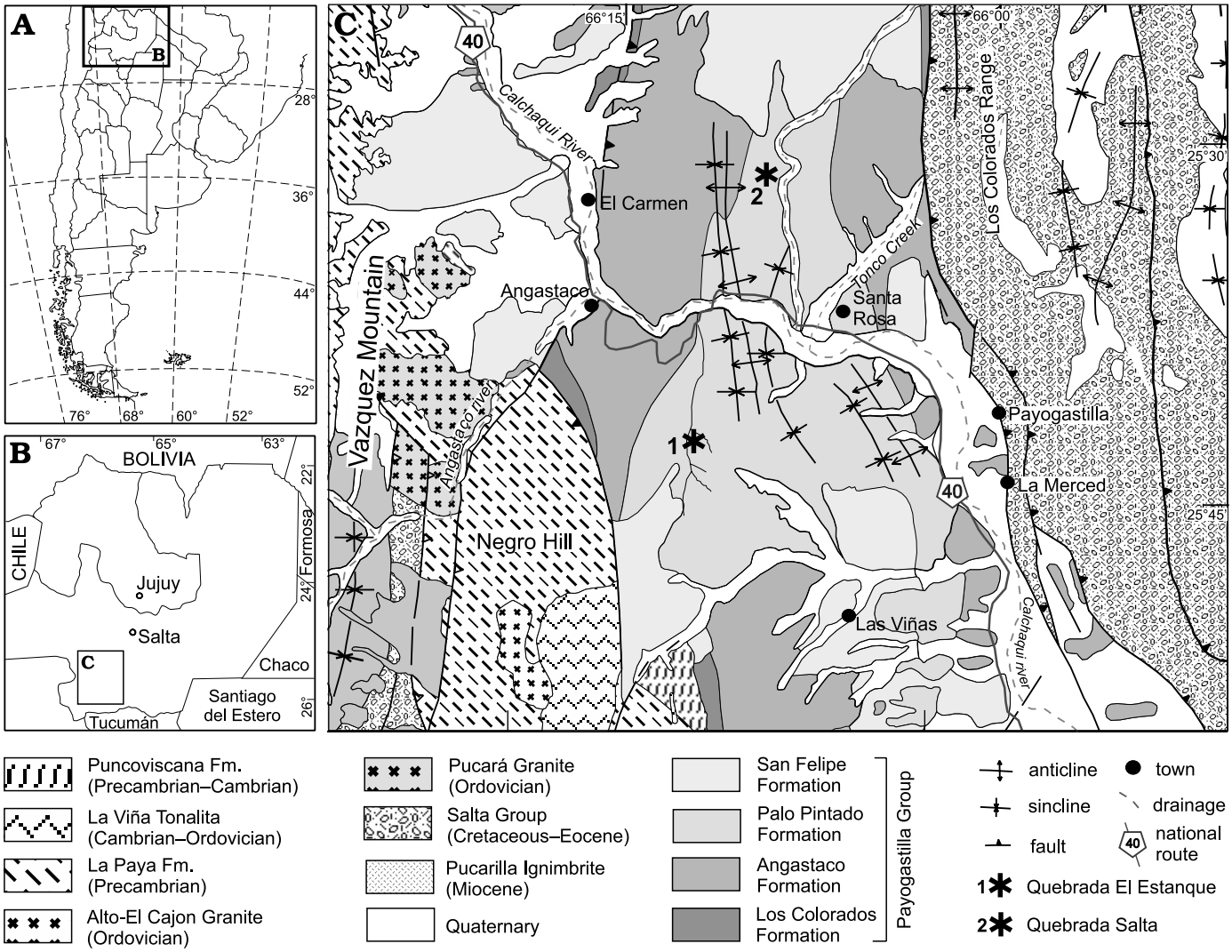

Fig. 1. **A**, **B**. Map showing location of the study area within Argentina. **C**. Geological map with indicated fossil localities of Quebrada El Estanque and Quebrada Salta.

prises thickening and coarsening-upward cycles, including matrix-supported conglomerate, fine to medium sandstone, and fine-grained sublithic sandstone that end in levels of green, brown and gray siltstone. These deposits consist of a transitional style between low- and high-sinuosity rivers that form wandering sand-gravel fluvial systems with small lakes. The geometry and the fluvial architectural characteristics are a direct consequence of allogenic controls, such as tectonic activity, under constant climatic conditions (Galli et al. 2011; Galli and Reynolds 2012). The sedimentological and paleontological evidence indicates that the sediments were deposited while the region was suffering changes regarding the hydric regimen, from a wet phase (late Miocene) to a drier one (Pliocene), due mainly to the formation of an intermountain basin (Angastaco Basin) that was bordered to the west by the Sierra de Quilmes and to the east by the uprising of the Sierras Los Colorados and León Muerto (Starck and Anzótegui 2001; Bywater-Reyes et al. 2010; Rohrmann et al. 2016; Robledo et al. 2020b).

During the late Miocene, the uplift of the basin caused an increase in the sedimentary accommodation/deposition (A/D) rate and was also associated with a change in the petrologic composition of the deposits (Galli et al. 2011, 2017). The resulting orographic barriers produced a warmer and wetter climate (Starck and Anzótegui 2001). The deposits of the San Felipe Formation at the top of the Payogastilla Group are more than 600 m thick in the southeastern Calchaquí Valley and are affected by numerous faults and folds. The transition between the Palo Pintado Formation and the San Felipe Formation is sharp and unconformable; it contains considerable clast-supported conglomerate with overlapping clasts and a lower proportion of sandstone and siltstone, which are interpreted as a gravel-braided fluvial system (Galli and Reynolds 2012). Different analyses of deposits of Palo Pintado Formation, like the presence of clay minerals in the floodplain sub-environment, or the presence of illite, smectite and kaolinite indicate generation by hydrolysis in a temperate-humid climate (Galli et al. 2011); stable isotope data from pedogenic carbonates demonstrated relatively more humid conditions between 10 to 6 Ma (Bywater-Reyes et al. 2010). Paleomagnetism studies in Palo Pintado Formation deposits indicate that at approximately 6.6 Ma there is an increase in the rate of sedimentation of 0.11–0.66 mm/y which is associated with a higher percentage of Salta Group clasts. Paleocurrents from the south to the southeast indicate the tectonic reactivation of the deposition area from the Sierra León Muerto and its continuation to the north as the Sierra Los Colorados (Galli et al. 2014). Isotope analysis of δDg recorded in volcanic glass reveal that between -6.5 to 5.3 Ma, values from the Angastaco Basin decrease by -23 ± 6‰ (absolute δDg = -95‰), which is interpreted to be the result of surface uplift in this area, with altitude and aridization in a paleoenvironment like the present-day (Pingel et al. 2016).

In the global context, the ancestor assemblage floras of the current communities already were established and diversifying during the Miocene (Bell et al. 2010). This event

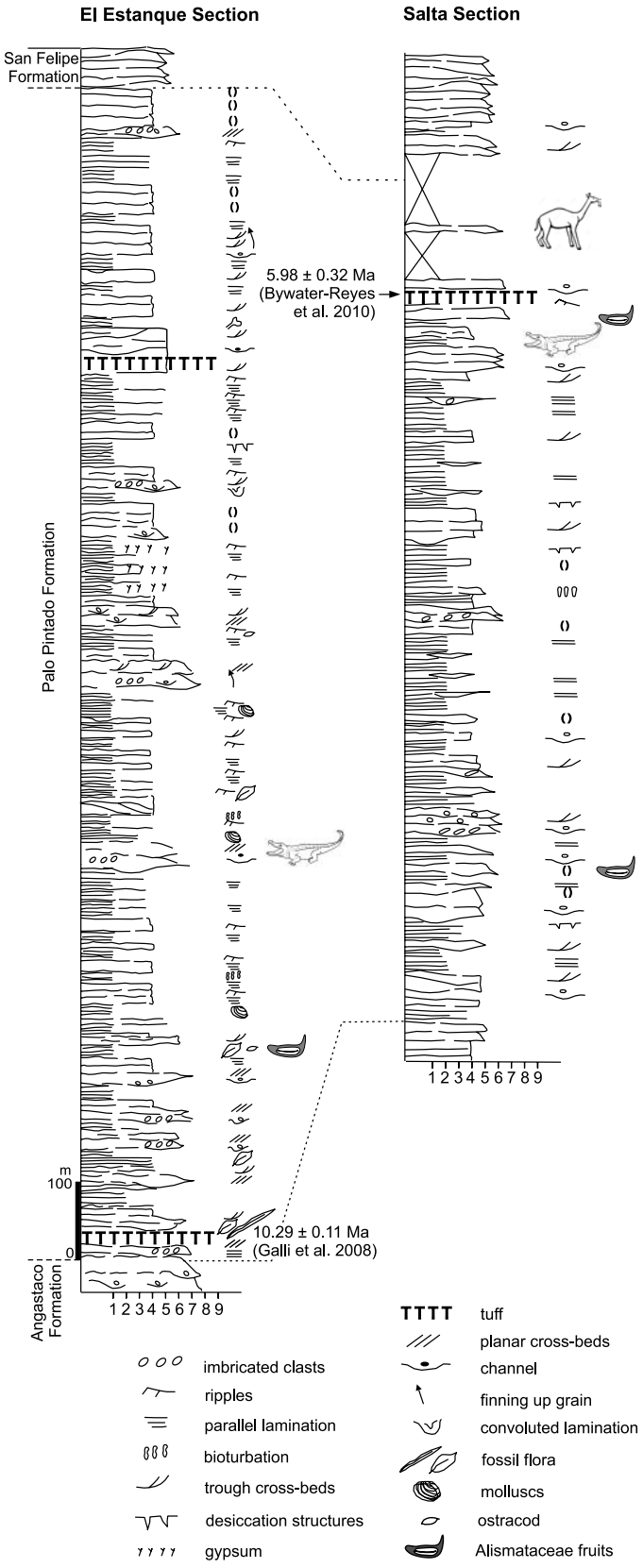

Fig. 2. Stratigraphic correlation of the Quebrada Salta and Quebrada El Estanque localities (Palo Pintado Formation, upper Miocene). 1, clay; 2, limolite; 3, fine sandstone; 4, middle sandstone; 5, coarse sandstone; 6, fine conglomerate; 7, middle conglomerate; 8, coarse conglomerate; 9, ash.

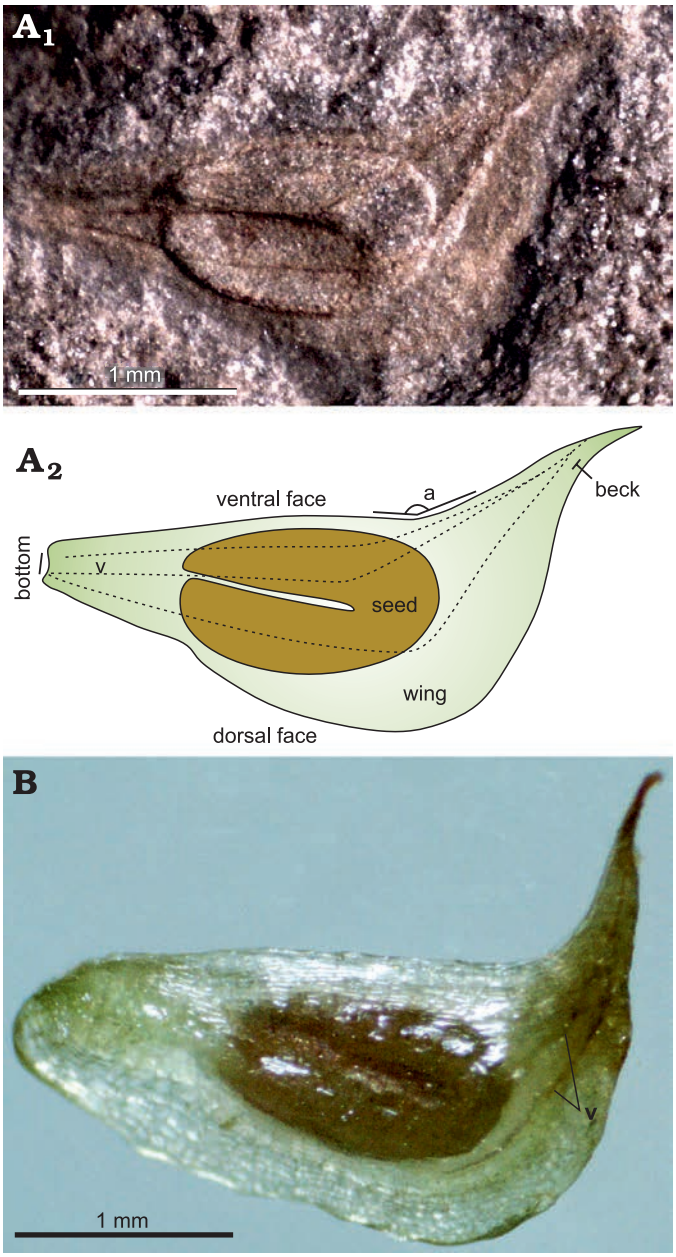

Fig. 3. Fossil and extant fruits of alismataceous plant *Sagittaria montevidensis* Chamisso and Schlectendal, 1827. **A**. CTES-PB 12911, Quebrada El Estanque (Palo Pintado Formation), upper Miocene, fossil fruit (A_1), explanatory drawing (A_2), dotted lines (v) represent veins present in the fossil fruit (a, angle formed by the beak and the ventral face); **B**. Recent fruit where the veins (v) are present, but with a slight development. The Recent material is deposited in the CTES herbarium (Corrientes City), as *Sagittaria montevidensis* Chamisso and Schlectendal, 1827 subsp. *montevidensis*.

is also observed in South American paleofloras (Barreda et al. 2007). In turn, the Miocene is a critical moment during which the great spread of the savannas took place (Quade et al. 1989; Cerling et al. 1997; Osborne 2008).

In addition to the *Sagittaria* fossils described below, various other vegetal remains were found at the Quebrada Salta and Quebrada El Estanque localities, which developed in an environment with fresh or brackish permanent water. These fossils include algae, ferns, monocots, and dicots (Herbst et al. 1987; Anzótegui and Horn 2011; Horn et al. 2011; Anzótegui et al. 2015). The taxa identified reflect that at least four paleoenvironments have been developed in these localities: aquatic, marsh, riparian and open terrestrial. The fossil fauna recorded here, at the moment corresponds to fragments of a turtle shell, a mandible of *Caiman latirostris* Daudin, 1802 (Bona et al. 2014; Bona and Barrios 2015), a tail tube and osteoderms of two glyptodons, Pampatheriidae osteoderms, fish scales, molluscs (Herbst et al. 2000), and insect wings.

Material and methods

Two sedimentological profiles from the north and south locations of the Palo Pintado Formation in the study area were analyzed at a scale of 1: 500 (i) Quebrada El Estanque and (ii) Quebrada Salta (Figs. 1, 2), from Salta Province, Argentina. The samples described here were collected from these outcrops of the Palo Pintado Formation. The fossils are deposited at the Colecciones Paleontológicas "Dr. Rafael Herbst", of the Universidad Nacional del Nordeste, Corrientes Province, Argentina (CTES-PB 12911–12917). The fruits analyzed here are formally considered as achenes, because those are dry fruits with a single seed inside, which does not adhere to the pericarp (Fig. 3). The specimens are well preserved, some samples containing organic remains, although others are incomplete, lacking the bases or the beaks. The fossil fruits were compared with herbarium (CTES-IBONE), field samples, and literature. The fossils were examined with a Nikon binocular stereomicroscope, model SMZ-445, and photographed with a Nikon mounted camera (model 590U). All measurements were digitally performed with the software Micrometrics. Photographs were processed with the software Corel Draw. The systematics in paper are according to APG IV 2016 (Byng et al. 2016).

Systematic paleobotany

Division: Angiospermae Linnaeus, 1753

Class: Monocotyledoneae De Candolle, 1817

Order Alismatales Brown ex von Berchtold and Presl, 1820

Family Alismataceae Ventenat, 1799

Genus *Sagittaria* Linnaeus, 1753

Type species: *Sagittaria sagittifolia* Linnaeus, 1753; Recent, Eurasia.

Sagittaria montevidensis Chamisso and Schlectendal, 1827

Fig. 4A–G.

Material.—CTES-PB 12911–12917 (Fig. 4A–C, E–G) from Miocene of Quebrada Salta and Quebrada El Estanque outcrops, Palo Pintado Formation, Salta Province, Argentina. All specimens correspond to achenes.

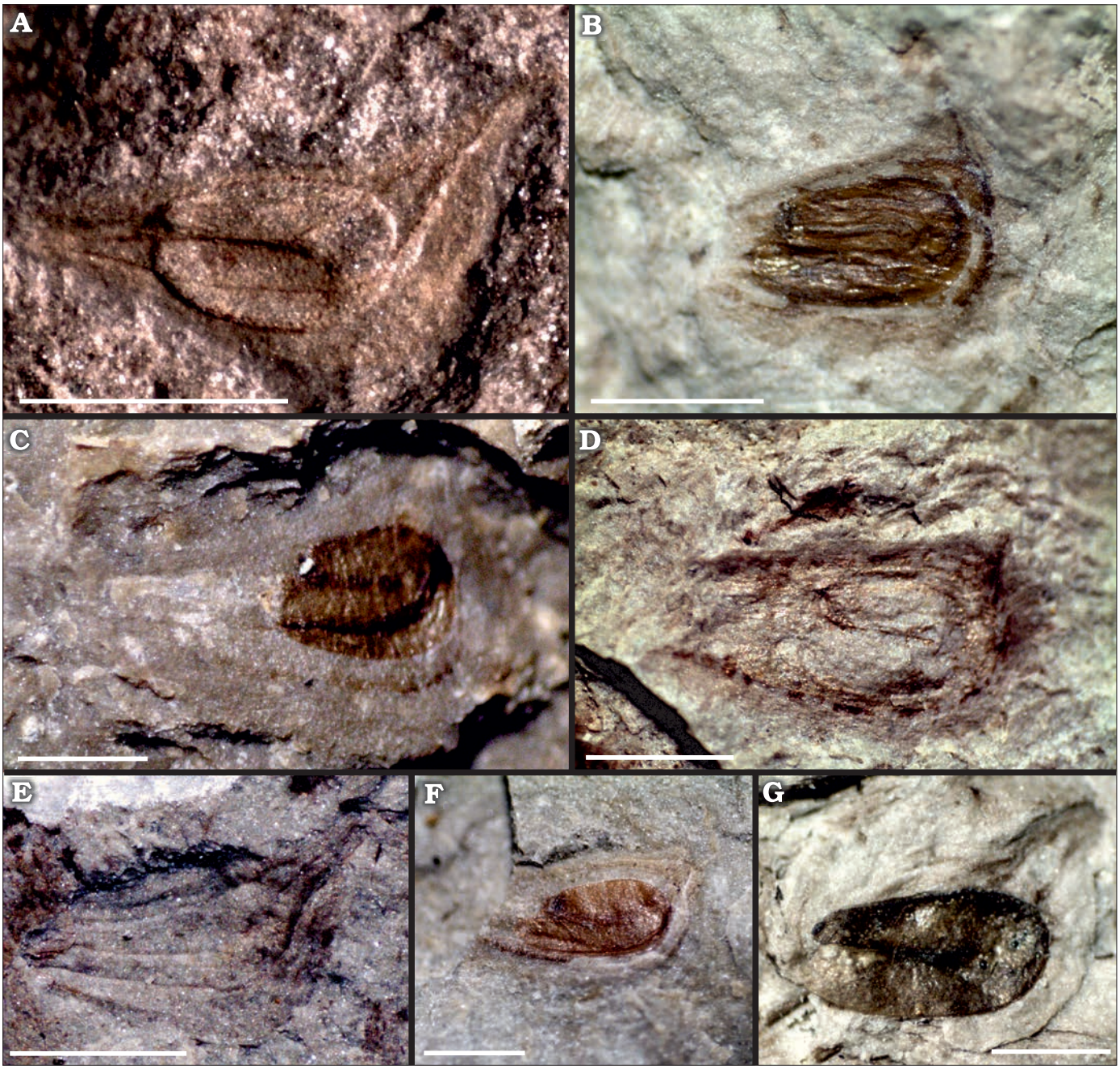

Fig. 4. Achenes of alismataceous plant *Sagittaria montevidensis* Chamisso and Schlectendal, 1827, from the Palo Pintado Formation, Quebrada El Estanque and Quebrada Salta localities, upper Miocene. **A**. Complete achene where the recurved seed and several veins are visible, CTES-PB 12911. **B**. Specimen showing the well-developed beak, almost in straight angle with the ventral face, CTES-PB 12916.**C**. Complete achene with organic remains, CTES-PB 12914. **D**. Fragment of achene where the beak and bottom are lacking, CTES-PB 12917. **E**. Complete fruit showing several veins, CTES-PB 12912. **F**. Incomplete achene where the bottom and beak are lacking, but the seed preserves some organic remains**,** CTES-PB 12913. **G**. Specimen showing the well-preserved seed inside the achene, CTES-PB 12915. Scale bars 1mm.

Description.—The studied material consists solely of fruits preserved as impressions from 1.75 mm (CTES-PB 12915) to 2.58 mm (CTES-PB 12917) in length and 0.75 mm (CTES-PB 12911) to 1.29 mm (CTES-PB 12916) in width. These fossils have a well-developed wing or keel on the dorsal face. All achenes bear an ascending beak ranging from 0.87 mm (CTES-PB 12914) to 1.40 mm (CTES-PB 12913, 12916). The angle formed by the beak and the ventral face ranges between 85° (CTES-PB 12916) and 153° (CTES-PB 12911). The curved seeds are preserved inside the achenes in most specimens. These seeds are 0.87 mm (CTES-PB 12914) to 1.40 mm (CTES-PB 12913, 12916) in length and 0.56 mm (CTES-PB 12911) to 0.85 mm (CTES-PB 12917) in width. Several specimens even preserve organic remains from the seeds (CTES-PB 12913–12916). All measurements are listed in Table 1.

Table 1. Characters and measurements (in mm) of all specimens analyzed in this work. "–", the structure was not observable; (f), the structure was fragmented.

CTES-PB	Length	Width	Angle	Beak	Seed-length	Seed-width
12911	2.12	0.75	152.8°	0.64	0.95	0.56
12912	2.00	1.01	135.8°	0.37	–	–
12913	1.86 (f)	1.07	123.1°	0.48	1.40	0.76
12914	1.84 (f)	0.97	132.5°	0.25 (f)	0.87	0.59
12915	1.75	0.96	140.0°	0.36	1.11	0.57
12916	1.97	1.29	84.8°	0.66	1.40	0.80
12917	2.58	1.20	142.1°	0.21	1.11	0.85

Remarks.—According to Keener (2005), the molecular data suggest *Sagittaria montevidensis* is most closely related to *S. intermedia* Micheli, 1881, and *S. calycina* (Engelmann, 1867) Bogin, 1955. Based on morphological similarities, Keener (2005) also suggests *Sagittaria sprucei* Micheli, 1881, as a close species. Fruits of these species are different from those of *S. montevidensis*. *S. calycina* (Fig. 5A) has achenes with broadly developed dorsal wings, the beak turned into a spine and the seed is slightly longer than *S. montevidensis* (Fig. 5N). The achenes in *S. intermedia* (Fig. 5G) have faces tuberculate and the beak is shorter (0.2 mm), while *S. montevidensis* has achenes tuberculate and the beak can reach 1 mm in length. The fruits of *S. sprucei* (Fig. 5U) can be two times longer (6.0 mm) than *S. montevidensis* (3.0 mm), and almost three times wider (4.0 mm in *S. sprucei* and 1.5 mm in *S. montevidensis*). Seeds in *S. sprucei* are slightly smaller (0.9 mm), the beak is two times shorter (0.3–0.5 mm) and the angle formed by the beak and the ventral face is almost horizontal (172°), while the seeds in *S. montevidensis* reach 2 mm, the beak up to 1 mm and the angle is 142°.

Five plesiomorphic species of *Sagittaria* are currently distributed in South America, *S. guayanensis* Kunth, 1816, *S. intermedia*, *S. montevidensis*, *S. planitiana* Agostini, 1970, and *S. rhombifolia* Chamisso, 1835 (Keener 2005; Chen et al. 2012). Three of them are reported from Argentina (*S. guayanensis*, *S. montevidensis*, and *S. rhombifolia*) (Rataj 1970). *S. guayanensis* (Fig. 5F) achenes have similar to those in *S. montevidensis*, but the first presents ribs bearing spiny ridges, both at the dorsal as the ventral faces, while the achenes of *S. montevidensis* have a smooth surface. In turn, *S. rhombifolia* (Fig. 5R) has ovobate achenes without ornaments (smooth surface), but these are from two to four times longer (5–8 mm in length) than achenes of *S. montevidensis*. Other species of *Sagittaria* also have some differences, like an absent or slightly developed beak, as observed in *S. longiloba* Engelmann, 1895 (Fig. 5L) and *S. planitiana* (Fig. 5O). Several species are considerably bigger than *S. montevidensis*, such as *S. lancifolia* Linnaeus, 1758 (Fig. 5I), *S. latifolia* Willdenow, 1805 (Fig. 5J), and *S. trifolia* Linnaeus, 1753 (Fig. 5X). Furthermore, *S. lancifolia* has fruits bearing conspicuous glands. *S. secundifolia* Kral, 1982 (Fig. 5T) presents robust and ornamented ribs. In addition, the beak in this species turned into a spine. More differences regarding measurements, development of beak and ornaments between *S. montevidensis* and other species of *Sagittaria* are listed in Table 2 and Fig. 5. Wang et al. (2010) reported another three species of *Sagittaria*, these are *S. natans*, *S. pymaea*, and *S. tengtsungensis*. The first is a synonym of *S. subulata* (Haynes and Holm-Nielsen 1994) (Fig. 5V), the remaining two were not illustrated in Fig. 5 because pictures or schemas of these species were not found.

Some species of *Echinodorus* (Alismataceae) have similar achenes to those in *Sagittaria*, but their fruits are mainly terete (cylindrical), rather than flat. The achenes of *Echinodorus berteroi* (Spreng, 1825) Fassett, 1955 and *E. paniculatus* Micheli, 1881, are similar in shape (Lehtonen 2009), although these are almost straight from the base to the beak, whereas in *Sagittaria montevidensis*, the beak and the ventral face form an angle that can even reach 90°. Moreover, the achenes of *E. berteroi* and *E. paniculatus* are proportionally bigger than the achenes of *Sagittaria montevidensis*, also they present well-developed ribs that in some cases are dichotomized (*E. paniculatus*), while *S. montevidensis* is not ribbed.

Stratigraphic and geographic range.—Miocene of Argentina and Recent from North and South America.

Discussion

The fossil record of Alismataceae.—The fossil fruits of *Sagittaria montevidensis* are the first Neogene report of Alismataceae from South America. In one previous work, pollen grains corresponding with Alismataceae were reported from Paso Otero locality (late Pleistocene–Holocene), in the Pampean region of Argentina (Gutiérrez et al. 2011). The specimens were dated between 9900–7700 BP, although the authors only mentioned the finding of Alismataceae pollen and do not provide descriptions or illustrations permitting the comparison with other palynological records.

After an analysis of the current distribution of its Recent species Chen (1989) suggested Late Cretaceous age for the origin of *Sagittaria*. Later Chen et al. (2012) interpreted late Eocene and the Miocene time of origination from DNA analysis. This suggestion is consistent with the oldest records of *Sagittaria* accepted by Haggard and Tiffney (1997) who rejected the age proposed by Chen (1989). Furthermore, Chen et al. (2012) suggested an African origin of *Sagittaria*

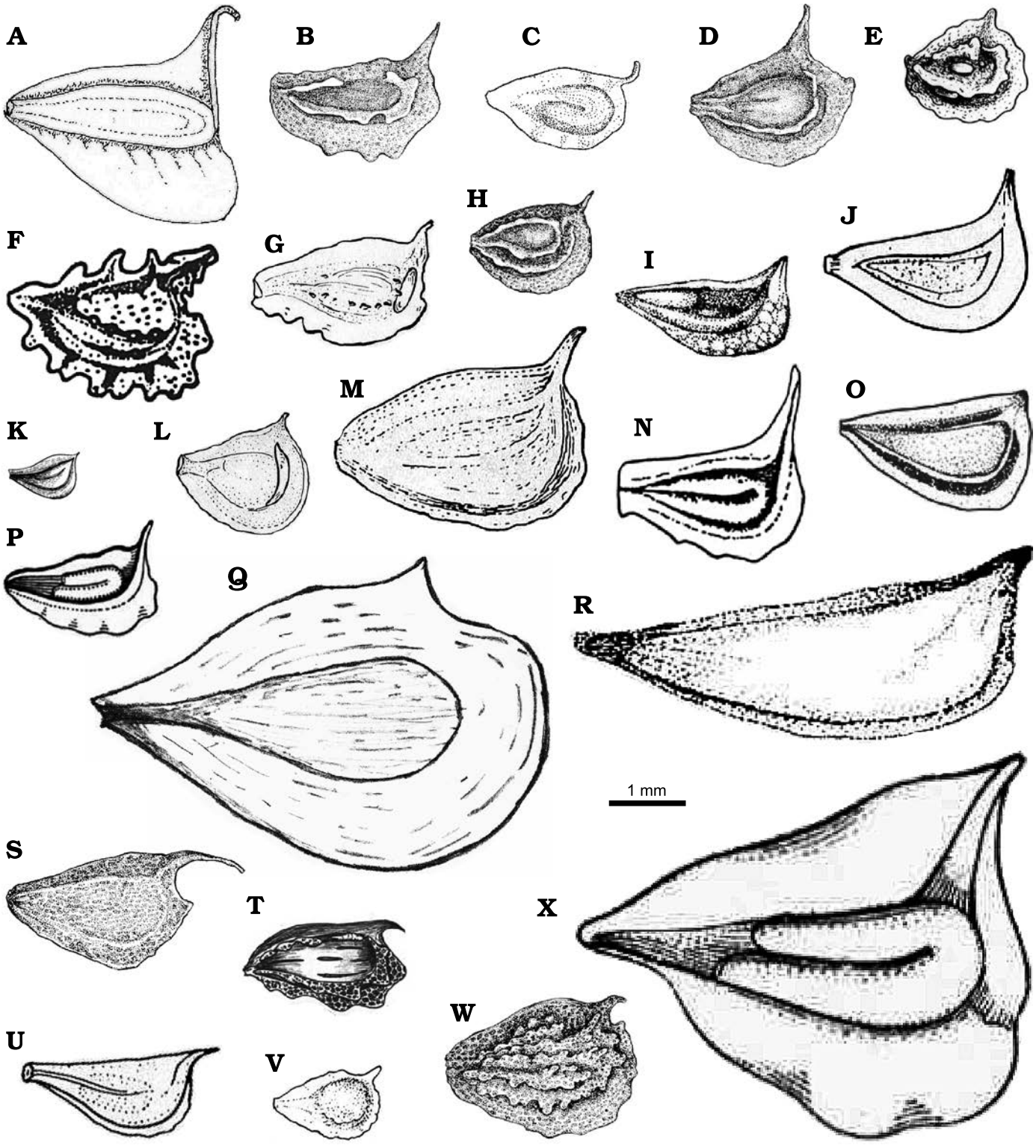

Fig. 5. Illustrations of species detailed in Table 2. **A**. *Sagittaria montevidensis* ssp. *calycina* (Ricketson 2018) (*S. calycina* following Keener 2005). **B**. *Sagittaria cristata* (Wooten 1973). **C**. *Sagittaria demersa* (Smith 1895). **D**. *Sagittaria fasciculata* (Wooten 1973). **E**. *Sagittaria graminea* ssp. *graminea* (Haynes and Holm-Nielsen 1994). **F**. *Sagittaria guayanensis* (Rataj 1970). **G**. *Sagittaria intermedia* (Haynes and Holm-Nielsen 1994). **H**. *Sagittaria isoetiformis* (Wooten 1973). **I**. *Sagittaria lancifolia* (Matias and Irgang 2006). **J**. *Sagittaria latifolia* (Haynes and Holm-Nielsen 1994). **K**. *Sagittaria lichuanensis* (Wang et al. 2010). **L**. *Sagittaria longiloba* (Haynes and Holm-Nielsen 1994). **M**. *Sagittaria macrophylla* (Haynes and Holm-Nielsen 1994). **N**. *Sagittaria montevidensis* ssp. *montevidensis* (Rataj 1978). **O**. *Sagittaria planitiana* (Matias and Irgang 2006). **P**. *Sagittaria platyphylla* (Den Hartog 1957). **Q**. *Sagittaria potamogetonifolia* (Wang et al. 2010). **R**. *Sagittaria rhombifolia* (Matias and Irgang 2006). **S**. *Sagittaria rigida* (Wooten 1973). **T**. *Sagittaria secundifolia* (Kral 1982). **U**. *Sagittaria sprucei* (Haynes and Holm-Nielsen 1994). **V**. *Sagittaria subulate* (Haynes and Holm-Nielsen 1994). **W**. *Sagittaria teres* (Wooten 1973). **X**. *Sagittaria sagittifolia* ssp. *S. leucopetala* (Den Hartog 1957) (*S. trifolia* following Lim 2015).

Table 2. Comparative chart (measurements in mm) of current *Sagittaria* fruits. Data obtained from: Smith (1895); Den Hartog (1957); Godfrey and Adams (1964); Rataj (1970, 1978); Wooten (1973); Kral (1982); Haynes and Holm-Nielsen (1994); Zepeda and Lot (1999); Matias and Irgang (2006); Moreira and Bove (2010); Wang et al. (2010); Matias and Sousa (2011); Lim (2015); Hall and Gil (2016); Canalli and Bove (2017); Ricketson (2018). *, authors differ in this character; –, the dimension could not to be established.

Species	Length	Width	Angle (in °)	Seed length	Seed width	Beak	Presence/development of keels and/or ornaments	Illustration on Fig. 5
S. calycina	2.6	1.9	118	2.4	0.7	0.9	dorsal wing broadly developed	A
S. cristata	2.1	1.2	120	1.4	0.5	0.6	crenate wings	B
S. demersa	1.5–2.0	1.0	135–178	1.0	0.6	1.1	without keel	C
S. fasciculata	2.1	1.3	116	1.0	0.6	0.6	dorsal wing broadly developed	D
S. graminea ssp. *graminea*	1.5–2.8	1.1–1.5	115	1.1	0.5	0.2	without keel; 1–2 conspicuous glands	E
S. guayanensis	1.5–2.7	1.2–2.0	155	1.7	1.0	0.2–0.5	keeled; margins echinate	F
S. intermedia	1.5–2.2	1.0–1.4	111	1.1	0.6	0.2	without keel, face tuberculate	G
S. isoetiformis	1.5	1.1	120	0.9	0.5	0.3	keeled; horizontal beak	H
S. lancifolia	1.2–2.5	0.7–1.1	139–145	0.6–1.6	0.1–0.5	0.3–0.7	keeled	I
S. latifolia	2.5–3.5	1.9–2.0	108–131	2.0	0.9	1.0–2.0	without keel	J
S. lichuanensis	0.8–1.0	0.4–0.6	130	0.6	0.3	0.1	narrowly winged	K
S. longiloba	1.2–2.5	0.8–1.6	148	1.0	0.7	0.1–0.6	keeled	L
S. macrophylla	3.1–3.5	1.8–2.4	122–132	1.8–1.9	0.9	0.6–1.2	without keel	M
S. montevidensis	2.0–3.0	1.0–1.5	142	1.1–2.0	0.69	0.3–1.0	without keel; smooth surface	N
S. planitiana	1.5–2.4	1.0–1.44	142–144	1.5	0.6	0.1–0.3	keeled*	O
S. platyphylla	1.2–2.2	0.8–1.3	118–158	0.8–1.4	0.4–0.7	0.3–0.6	without keel; 2-ribbed	P
S. potamogetonifolia	5.0–7.0	4.5–6.0	105	3.0	1.5	0.5	dorsal wing undulated	Q
S. rhombifolia	4.0–7.0	2.0–3.0	130–135	4.9	1.5	0.7–1.2	keeled	R
S. rigida	2.4	1.5	165	1.6	0.7	1.0	horizontal beak	S
S. secundifolia	2.1	1.1	172	1.5	0.6	0.3	beak turned in a spur; margins crested	T
S. sprucei	2.1–6.0	0.9–4.0	172	0.9	0.4	0.3–0.5	without keel	U
S. subulata	1.4–2.0	0.9–1.5	143	0.8	0.6	0.2–0.4	keeled, crenate wings	V
S. teres	2.4	1.7	173	–	–	0.4	keeled; horizontal beak; irregularly crenate dorsal wing	W
S. trifolia	3.0–5.0	1.5–3.0	150	1.5	0.6	0.5	dorsal wing broadly developed	X

and four potential dispersion routes during the Oligocene–Miocene: (i) the first route suggests that *Sagittaria* has migrated from tropical Africa to South America and later to North America; (ii) the second one proposes an initial dispersal to Europe, followed by dispersal to North America, and then to South America. The remaining routes hypothesize the arrival in (iii) Madagascar and (iv) Asia. Considering the great dispersal capacity of *Sagittaria,* including possible large distances by water in streams and rivers, both by asexual (tubers) as sexual reproduction (achenes) (Gordon 1996; Zhang et al. 2010), and since in the late Oligocene–late Miocene range, about 20 million years have elapsed, we consider that both routes (i) and (ii) would explain the presence of *Sagittaria montevidensis* in South America during the late Miocene. The first route seems more plausible, because besides of *Sagittaria montevidensis,* other four plesiomorphic species have a current South American distribution (*S. guayanensis*, *S. intermedia*, *S. planitiana*, and *S. rhombifolia*) (Keener 2005; Chen et al. 2012).

In addition to the South American occurrences reported herein, a large number of fossil records of Alismataceae from the Cretaceous and Cenozoic times have been reported in the Northern Hemisphere (Berry 1925; Teixeira 1948; Brown 1962; Doyle 1973; Muller 1981; Cevallos-Ferriz and Ramírez 1998; Retallack 2004). Before the year 2000, most of the authors agreed that the oldest remains of Alismataceae were the genera *Alisma* and *Caldesia*, from the Oligocene of Europe and early Miocene of the United States respectively (Daghlian 1981; Friis 1985; Haggard and Tiffney 1997). Recently, other authors proposed again that the Alismataceae have originated at the end of Mesozoic, most likely around the mid-Cretaceous (Chen et al. 2012; Smith 2013; Coiffard and Mohr 2018). Among the reports that undoubtedly correspond to Alismataceae, Riley and Stockey (2004) described the species *Cardstonia tolmanii* Riley and Stockey, 2004, from St. Mary River Formation (Campanian–Maastrichtian of Canada). Originally the species was included in Limnocharitaceae, but this family was later included into Alismataceae (APG III 2009; Chen et al. 2012). Furthermore, Smith (2013) suggested that *Haemantophyllum* Budantsev, 1983, a genus from Cretaceous of Russia (Golovneva 1997), correspond to the Alismataceae family. More recently, Coiffard and Mohr (2018) described an Alismataceae (Alismataceae gen. et sp. indet.), which

corresponds to an almost complete leaf from the Upper Cretaceous of Egypt and firstly assigned to *Echinodorus* cf. *cordifolius* by Kahlert et al. (2009).

The fossil record of *Sagittaria* in the late Miocene context.—The *Sagittaria* fossils studied here were recovered from late Miocene units ranging from approximately 10–5 Ma. According to Herbert et al. (2016) between 7–5.4 Ma, both hemispheres were affected by a drought, an increase in seasonality, and a restructuring of terrestrial plant and animal communities. These events were especially observed in the subtropical areas, but they were typically attributed to regional tectonic forces (Herbert et al. 2016). During the Neogene, the uplift of the Andes Mountains occurred in discrete periods, progressing from south to north and from west to east (Amarilla et al. 2015). The region experienced a deformation and compartmentalization of the basin, which extended during the Pliocene. These processes modified the environment, from a humid foreland to an elevated and hydrologically restricted semiarid intermontane basins (Pingel et al. 2016). The Andes Mountains became the sole barrier to atmospheric circulation in the Southern Hemisphere (Amarilla et al. 2015). However, the fossil assemblages and the sedimentological evidence from the Palo Pintado Formation are not consistent with dry environments. During the deposition of this formation, a warm climate with seasonal rainfall is observed without significant climatic changes. Bywater-Reyes et al. (2010) suggested relatively more humid conditions between 10 to 6 Ma, although with seasonal conditions (Galli et al. 2011; Anzótegui et al. 2019). Changes to more arid environments started about 5 Ma until reaching the current conditions to 1 Ma ago (Pingel et al. 2016). Other Neogene locations close to the studied sites, such as the Quebrada del Toro locality (Miocene–Pliocene; Salta Province), also reflect similar conditions, with the presence of plant remains associated with marshy environments (Robledo et al. 2020a). This evidence suggests that the changes to a drier environment in the Palo Pintado Formation would have been gradual.

The achenes of *Sagittaria montevidensis* were found in different sections of two outcrops of the Palo Pintado Formation (see Fig. 2). The Quebrada El Estanque locality yielded a smaller number of *Sagittaria* fruits but they were the most complete fossils. In turn, the Quebrada Salta locality yielded a greater number of *Sagittaria montevidensis* impressions, including both complete and incomplete fruits. In both localities, these fossils are related to the marsh and lacustrine environments and they would have developed under a warm and humid climate with dry seasonality suggested for the Palo Pintado Formation (Galli et al. 2011). These conditions are some of the characteristic environments where *Sagittaria* currently develops. The arrowheads like *Sagittaria montevidensis* are rooted aquatic plants that grow in freshwater and slow current wetlands (i.e., swamps and marshes), wet or flooded soils, alongside streams or in drainage channels (Costa and Forni-Martins 2003; Haynes and Les 2004; Lehtonen 2009, 2018). Their presence in the outcrops studied would suggest these types of environments during the Neogene in the study area. Additionally, Demetrio et al. (2014) suggested that this species could morphologically modify its corm as an adaptive response to environmental stress, as flood periods or dry seasons, both events proposed for Palo Pintado Formation. *Sagittaria montevidensis* coexisted with other aquatic or marsh plants (for example, *Cabomba*, *Salvinia*, *Azolla*, *Mayaca*, and *Equisetum*), previously recorded from sediments of the Palo Pintado Fm., attesting to the great diversity of aquatic plants preserved in these wetland deposits (Anzótegui et al. 2017, 2019).

Conclusions

The Miocene Alismataceae record introduced here is the first Neogene fossil belonging to this family in South America and the most well substantiated fossil record of *Sagittaria* found of the continent.

The finding of *Sagittaria* in these Neogene sediments supports the possibility of a migratory route from Africa to South America and thence to North America.

This record constitutes another evidence that the environment during the deposition of the Palo Pintado Formation was warm and humid, in the interval of 10–5 Ma. During the late Miocene these *Sagittaria* would have inhabited a fluvial paleoenvironment in a warm climate with seasonal rainfall and without significant climatic changes, very different from the current dry conditions of the place, where it is now part of the South American Arid Diagonal.

Acknowledgements

We would like to thank the reviewers Steven Manchester (Florida Museum of Natural History, Gainesville, USA) and Adam T. Halamski (Institute of Paleobiology, Polish Academy of Sciences, Warszawa, Poland) for insightful comments and suggestions. Samuli Lehtonen (Biodiversity Unit, University of Turku, Finland) for helping in the interpretation of the fossil structures. We thank Steven Manchester also for providing bibliography. This research received support from project PI 16F008 (Secretaría General de Ciencia y Técnica de la Universidad Nacional del Nordeste) to Lilia R. Mautino and PICT 2017-1010 to Claudia Galli.

References

Adair, R.J. Keener, B.R., Kwong, R.M., Sagliocco, J.L., and Flower, G.E. 2012. The Biology of Australian weeds. *Sagittaria platyphylla* (Engelmann) J.G. Smith and *Sagittaria calycina* Engelmann. *Plant Protection Quarterly* 27: 47–58.

Agostini, G. 1970. Notes on Alismataceae. *Phytologia* 20: 1–5.

Amarilla, L.D., Anton, A.M., Chiapella, J.O., Manifesto, M.M., Angulo, D.F., and Sosa, V. 2015. *Munroa argentina*, a grass of the South Amer-

ican Transition Zone, survived the Andean uplift, aridification and glaciations of the Quaternary. *PLoS ONE* 10 (6): e0128559.

Anzótegui, L.M. and Horn, M.Y. 2011. Megaflora de la Formación Palo Pintado (Mioceno Superior) Salta, Argentina. Parte II. *Revista Brasileira de Paleontologia* 14: 239–254.

Anzótegui, L.M., Horn, M.Y., Robledo, J.M., and Galli, C.I. 2015. Novedades paleoflorísticas en la Localidad Quebrada Salta, Formación Palo Pintado (Mioceno Tardío/Plioceno), Salta, Argentina. *In*: J. Bodnar and G. Márquez (eds.), *XVI Simposio Argentino de Paleobotánica y Palinología (Abstract Book)*, 40. Facultad de Ciencias Naturales y Museo (UNLP), La Plata.

Anzótegui, L.M., Mautino, L.R., Garralla, S.S., Herbst, R., Robledo, J.M., and Horn, M.Y. 2017. Paleovegetación cenozoica del Noroeste Argentino. *In:* C. Muruaga and P. Grosse (eds.), *Ciencias de la Tierra y Recursos Naturales del NOA, Relatorio del Congreso Geológico Argentino, No. 20*, 767–781. Asociación Geológica Argentina, Tucumán.

Anzótegui, L.M., Mautino, L.R., Horn, M.Y., Garralla, S.S., and Robledo, J.M., 2019. Paleovegetación del Mioceno tardío del Noroeste de Argentina. *Opera Lilloana* 52: 109–130.

APG III. 2009. An update of the Angiosperm Phylogeny Group classification for the orders and families of flowering plants. *Botanical Journal of the Linnean Society* 161: 105–121.

APG IV. 2016. An update of the Angiosperm Phylogeny Group classification for the orders and families of flowering plants. *Botanical Journal of the Linnean Society* 181: 1–20.

Barreda, V., Anzótegui, L.M., Prieto, A.R., Aceñolaza, P., Bianchi, M.M., Borromei, A.M., Brea, M., Caccavari, M., Cuadrado, G.A., Garralla, S.S., Grill, S.G., Guerstein, R., Lutz, A.I., Mancini, M.V., Mautino, L.R., Ottone, E.G., Quattrocchio, M., Romero, E.J., Zamaloa, M.C., and Zucol, A. 2007. Diversificación y cambios de las Angiospermas durante el Neógeno en Argentina. *Ameghiniana* 11: 173–191.

Bell, C.D., Soltis, D.E., and Soltis, P.S. 2010. The age and diversification of the angiosperms re-revisited. *American Journal of Botany* 97: 1296–1303.

Berchtold, F.G. von and Presl, J.S. 1820. *O Přirozenosti Rostlin*. 502 pp. K.W. Endersa, Prague.

Berry, E.W. 1925. The flora of the Ripley Formation. *US Geological Survey Professional Paper* 136: 1–94.

Bogin, C. 1955. Revision of the genus *Sagittaria* (Alismataceae). *Memoirs of the New York Botantical Garden* 9: 179–233.

Bona, P., Starck, D., Galli, C.I., Gasparini, Z., and Reguero, M. 2014. *Caiman* cf. *latirostris* (Alligatoridae, Caimaninae) in the late Miocene Palo Pintado Formation, Salta province, Argentina: Paleogeographic and Paleoenvironmental Considerations. *Ameghiniana* 51: 26–36.

Bona, P. and Barrios, F. 2015. The alligatoroidea of Argentina: An update of its fossil record. *Publicación Electrónica de la Asociación Paleontológica Argentina* 15: 143–158.

Brown, R.W. 1962. Paleocene flora of the Rocky Mountains and Great Plains. *US Geological Survey Professional Paper* 275: 1–119.

Budantsev, L.J. [Budancev, L.J.] 1983. *Istoriâ arktičeskoj flory epoki rannevo kainofita*. Nauka, Moskva.

Byng, J.W., Chase, M., Christenhusz, M., Fay, M.F., Judd, W.F., Mabberley, D., Sennikov, A., Soltis, D.E., Soltis, P.S., and Stevens, P. 2016. An update of the Angiosperm Phylogeny Group classification for the orders and families of flowering plants: APG IV. *Botanical Journal of the Linnean Society* 181: 1–20.

Bywater-Reyes, S., Carrapa, B., Clementz, M., Clementz, M., and Schoenbohm, L. 2010. Effect of late Cenozoic aridification on sedimentation in the Eastern Cordillera of north-west Argentina (Angastaco basin). *Geology* 38: 235–238.

Canalli, Y.M. and Bove, C.P. 2017. Flora of Rio de Janeiro: Alismataceae. *Rodriguésia* 68: 17–28.

Cerling, T.E., Harris, J.M., MacFadden, B.J., Leakey, M.G., Quade, J., Eisenmann, V., and Ehleringer, J.R. 1997. Global vegetation change through the Miocene/Pliocene boundary. *Nature* 389: 153–158.

Cevallos-Ferriz, S. and Ramírez, J.L. 1998. Las plantas con flores en el registro fósil. *Ciencias* 52: 46–57.

Chamisso, L.K.A. von 1835. Spicilegium Alismacearum. *Linnaea* 10: 219–220.

Chamisso, L.K.A. von and Schlechtendal, D.F.L. von. 1827. De plantis in expeditione speculatoria Romanzoffiana observatis. *Linnaea* 2: 145–233.

Chandler, M.E.J. 1963. *The Lower Tertiary Floras of Southern England. III. Flora of the Bournemouth Beds, the Boscombe and the Highcliff Sands*. 169 pp. British Museum (Natural History), London.

Chen, J.K., 1989. *Systematic and Evolutionary Botanical Studies on Chinese Sagittaria*. 141 pp. National Natural Science Foundation of China, Wuhan University Press, Wuhan.

Chen, L.-Y., Chen, J.-M., Gituru, R.W., Temam, T.D., and Wang, Q.-F. 2012. Generic phylogeny and historical biogeography of Alismataceae, inferred from multiple DNA sequences. *Molecular Phylogenetics and Evolution* 63: 407–416.

Coiffard, C. and Mohr, B.A.R. 2018. Cretaceous tropical Alismatales in Africa: diversity, climate and evolution. *Botanical Journal of the Linnean Society* 188: 117–131.

Coutand, I., Carrapa, B., Deeken, A., Schmitt, A.K., Sobel, E., and Strecker, M. 2006. Orogenic plateau formation and lateral growth of compressional basins and ranges: Insights from sandstone petrography and detrital apatite fission-track thermochronology in the Angastaco Basin, NW Argentina. *Basin Research* 18: 1–26.

Costa, J.I. and Forni-Martins, E.R. 2003. Karyology of some Brazilian species of Alismataceae. *Botanical Journal of the Linnean Society* 143: 159–164.

Cronquist, A. 1981. *An Integrated System of Classification of Flowering Plants*. 1262 pp. Columbia University Press, New York

Daghlian, C.P. 1981. A review of the fossil record of monocotyledons. *The Botanical Review* 47: 517–555.

Dahlgren, R.M.T. 1980. A revised system of classification of the angiosperms. *Botanical Journal of the Linnean Society* 80: 91–124.

Daudin, F.M. 1802. *Histoire Naturelle, Générale et Particulière des Reptiles, Vol. 2.* 452 pp. F. Dufart, Paris.

De Candolle, A.P. 1817. *Regni vegetabilis systema naturale, sive Ordines, Genera et Species Plantarum Secundum Methodi Naturalis Normas Digestarum et Descriptarum*. 564 pp. Treuttel et Würtz, Paris.

Demetrio, G.R., Barbosa, M.E.A., and Coelho, F.F. 2014. Water level-dependent morphological plasticity in *Sagittaria montevidensis* Cham. and Schl. (Alismataceae). *Brazilian Journal of Biology* 74: 199–206.

Den Hartog, C. 1957. Alismataceae. *In:* C.G.G.J. Van Steenis (ed.), *Flora Malesiana ser. 1, Vol. 5,* 317–334. Jakarta, Indonesia.

Díaz, J.I. and Malizzia, D.C. 1983. Estudio geológico y sedimentológico del Terciario Superior del valle Calchaquí (departamento de San Carlos, provincia de Salta). *Boletín Sedimentológico* 2: 8–28.

Doyle, J.A. 1973. Fossil evidence on early evolution of the monocotyledons. *Quarterly Review of Biology* 48: 399–413.

Engelmann, G. 1895. *Sagittaria longiloba. In*: J.G Smith (ed.), *A Revision of the North American Species of Sagittaria and Lophotocarpus, Vol. 16,* 16. Missouri Botanical Garden Press, Saint Louis.

Fassett, N.C. 1955. *Echinodorus* in the American tropics. *Rhodora* 57: 133–156.

Friis, E.M. 1985. Angiosperm fruits and seeds from the middle Miocene of Jutland (Denmark), Alismataceae. *Danske Videnskabernes Selskab, Copenhagen. Biologiske Skrifter* 24: 71–73.

Galli, C.I. and Reynolds, J. 2012. Evolución paleoambiental del Grupo Payogastilla (Eoceno–Plioceno) en el valle Calchaquí-Tonco, provincia de Salta, Argentina. *In*: R. Marquillas, C. Sanchez, and J. Salfity (eds.), Aportes Sedimentológicos a la Geología del Noroeste Argentino. *XIII Reunión Argentina de Sedimentología*, 67–80, Salta.

Galli, C.I., Alonso, R.N., and Coira, L.B. 2017. Integrated Stratigraphy of the Cenozoic Andean Foreland Basin (Northern Argentina), *In*: G. Aiello (ed.), *Seismic and Sequence Stratigraphy and Integrated Stratigraphy—New Insights and Contributions*, 129–156. IntechOpen, Budapest.

Galli, C.I., Anzótegui, L.M., Horn, M.Y., and Morton, L.S. 2011. Paleoambiente y paleocomunidades de la Formación Palo Pintado (Mioceno-Plioceno, Provincia de Salta, Argentina. *Revista Mexicana de Ciencias Geológicas* 28: 161–174.

Galli, C.I., Coira, L.B., Alonso, R.N., Matteini, M., and Hauser, N. 2014. Evolución tecto-sedimentaria del Grupo Payogastilla y su relación con el arco volcánico del Cenozoico, en los valles Calchaquí, Tonco y Amblayo, provincia de Salta, Argentina. *Acta Geológica Lilloana* 26: 30–52.

Galli, C.I., Ramirez, A., Barrientos, C., Reynolds, J., Viramonte, J.G., and Idleman, B. 2008. Estudio de proveniencia de los depósitos del Grupo Payogastilla (Mioceno Medio-Superior) aflorantes en el río Calchaquí, provincia de Salta, Argentina. *17° Congreso Geológico Argentino, Jujuy* 1: 353–354.

Godfrey, R.K. and Adams, P. 1964. The identity of *Sagittaria isoetiformis. SIDA, Contributions to Botany* 1: 269–273.

Golovneva, L.B. 1997. Morphology, systematics and distribution of the genus *Haemanthophyllum* in the Paleogene floras of the Northern Hemisphere. *Paleontological Journal* 31: 197–207.

Gordon, E. 1996. Tipo de dispersión, germinación y crecimiento de plántulas de *Sagittaria latifolia* (Alismataceae). *Fragmenta Floristica et Geobotanica* 41: 657–668.

Gutiérrez, M.A., Martínez, G.A., Luchsinger, H., Grill, S., Zucol, A.F., Hassan, G.S., Barros, M.P., Kaufmann, C.A., and Álvarez, M.C. 2011. Paleoenvironments in the Paso Otero locality during late Pleistocene–Holocene (Pampean region, Argentina): an interdisciplinary approach. *Quaternary International* 245: 37–47.

Haggard, K.K. and Tiffney, B. H. 1997. The flora of the early Miocene Brandon lignite, Vermont, USA. VIII. Caldesia (Alismataceae). *American Journal of Botany* 84: 239–252.

Hall, C.F. and Gil, A.S.B. 2016. Flora das cangas da Serra dos Carajás, Pará, Brasil: Alismataceae. *Rodriguésia* 67: 1195–1199.

Haynes, R.R. and Holm-Nielsen, L.B. 1994. The Alismataceae. *Flora Neotropica* 64: 1–112.

Haynes, R.R. and Les, D.H. 2004. Alismatales (water plantains). *In*: *Encyclopedia of Life Sciences*, 1–4. John Wiley & Sons Ltd, Chichester.

Herbst, R., Anzótegui, L.M., and Jalfin, G. 1987. Estratigrafía, paleoambientes y dos especies de Salvinia Adanson (Filicopsida) del Mioceno superior de Salta, Argentina. *Revista de la Facultad de Ciencias Exactas y Naturales y Agrimensura* 7: 15–42.

Herbert, T.D., Lawrence, K.T., Tzanova, A., Peterson, L.C., Caballero-Gill, R., and Kelly, C.S. 2016. Late Miocene global cooling and the rise of modern ecosystems. *Nature Geoscience* 9: 843–847.

Herbst, R., Anzótegui, L.M., Esteban, G., Mautino, L.R., Morton, S., and Nassif, N. 2000. Síntesis paleontológica del Mioceno de los valles Calchaquíes, noroeste argentino. *In:* F. Aceñolaza and R. Herbst (eds.), *El Neógeno de Argentina*, 263–288. Instituto Superior de Correlación Geológica, Serie Correlación Geológica N° 14, Consejo Nacional de Investigaciones Científicas y Técnicas Facultad de Ciencias Naturales e Instituto Miguel Lillo, Universidad Nacional de Tucumán, Argentina.

Hongn, F., and Seggiaro, R. 2001. Hoja Geológica 2566-III, Cachi (Escala 1:250 000). *Instituto de Geología y Recursos Minerales, Servicio Geológico Minero Argentino, Boletín* 248: 1–87.

Horn, M.Y., Galli, C.I., Mautino, L.R., and Anzótegui, L.M. 2011. Palinología y litofacies de la Formación Palo Pintado (Mioceno Superior) en las localidades Río Calchaquí y Quebrada El Estanque, Salta, Argentina. *Ameghiniana (Abstract book)* 48: R15.

Kahlert, E., Rüffle, L., and Gregor D.H.J. 2009. Die Oberkreide Flora (Campanian) von Baris (Ägypten) und ihre ökologische geographischen Beziehungen unter plattentektonischen Aspekten. *Documenta Naturae* 178: 1–71.

Keener, B.R. 2005. *Molecular Systematics and Revision of the Aquatic Monocot Genus* Sagittaria *(Alismataceae)*. 168 pp. Unpublished Ph.D. Thesis. The University of Alabama, Tuscaloosa.

Kral, R. 1982. A new phyllodial-leaved *Sagittaria* (Alismaceae) from Alabama. *Brittonia* 34: 12–17.

Kunth, C.S. 1816. Alismataceae. *In*: A. von Humboldt, A. Bonpland, and C.S. Kunth (eds.), *Nova genera et species plantarum, Vol. 4*, 250. Chez N. Maze Libraire, Paris.

Lehtonen, S. 2009. Systematics of the Alismataceae—a morphological evaluation. *Aquatic Botany* 91: 279–290.

Lehtonen, S. 2018. Alismataceae. *In:* L. Ramella (ed.), *Flora del Paraguay 49*, 1–48. Conservatoire et Jardin botaniques de la Ville de Genève, Geneva.

Lim, T.K. 2015. *Sagittaria trifolia*. *In:* T.K. Lim (ed.), *Edible Medicinal and Non Medicinal Plants*, 96–102. Springer, Dordrecht.

Linnaeus, C. 1753. *Species plantarum, exhibentes plantas rite cognitas ad genera relatas cum differentiis specificis, nominibus trivialibus, synonymis selectis, locis natalibus, secundum systema sexuale digestas. Tomus II*. 783 pp. Laurentii Salvius, Stokholm.

Linnaeus, C. 1758. *Systema naturæ per regna tria naturæ, secundum classes, ordines, genera, species, cum characteribus, differentiis, synonymis, locis. Tomus II. Editio decima, reformata*. 824 pp. Holmiæ, Stockholm.

Matias, L.Q. and Irgang, B.E. 2006. Taxonomy and distribution of *Sagittaria* (Alismataceae) in north-eastern Brazil. *Aquatic Botany* 84: 183–190.

Matias, L.Q. and Sousa, D.J.L. 2011. Alismataceae no estado do Ceará, Brasil. *Rodriguésia* 62: 887–900.

Micheli, M. 1881. Alismacaea. *In*: A.C.P De Candolle and A.P. De Candolle (eds.), *Monographiae phanerogamarum, Vol. 3,* 29–83. S.G. Masson, Paris.

Moreira, A.D.R. and Bove, C.P. 2010. Flórula do Parque Nacional da Restinga de Jurubatiba, Rio de Janeiro, Brasil: Alismataceae. *Arquivos do Museu Nacional* 68: 163–165.

Muller, J. 1981. Fossil pollen records of extant angiosperms. *The Botanical Review* 47: 1–142.

Osborne, C.P. 2008. Atmosphere, ecology and evolution: what drove the Miocene expansion of C_4 grasslands? *Journal of Ecology* 96: 35–45.

Pingel, H., Mulch, A., Alonso, R.N., Cottle, J., Scott, A., Jacob, P., Rohrmann, A., Schmitt, K., Stockli, D., and Strecker, M.R. 2016. Surface uplift and convective rainfall along the southern Central Andes (Angastaco Basin, NW Argentina). *Earth and Planetary Science Letters* 440: 33–42.

Quade, J., Cerling, T.E., and Bowman, J.R. 1989. Development of the Asian monsoon revealed by marked ecological shift during the latest Miocene in northern Pakistan. *Nature* 342: 163–166.

Rataj, K. 1970. Las Alismataceae de la República Argentina. *Darwiniana* 16: 9–39.

Rataj, K. 1972. Revision of the genus *Sagittaria* Part. II. *Annotations Zoologicae et Botanicae* 70: 1–61.

Rataj, K. 1978. Alismataceae of Brazil. *Acta Amazonica* 8: 5–53.

Retallack, G.J. 2004. Late Miocene climate and life on land in Oregon within a context of Neogene global change. *Palaeogeography, Palaeoclimatology, Palaeoecology* 214: 97–123.

Ricketson, J.M. 2018. Vascular plants of Arizona: Alismataceae. *Canotia* 14: 10–21.

Riley, M.G. and Stockey, R.A. 2004. *Cardostonia tolmanii* gen. et sp. nov. (Limnocharitaceae) from the Upper Cretaceous of Alberta, Canada. *International Journal of Plant Sciences* 165: 897–916.

Robledo, J.M., Anzótegui, L.M., Martínez, O.G., and Alonso, R.N. 2020a. Flora and insect trace fossils from the Mio-Pliocene Quebrada del Toro locality (Gobernador Solá, Salta, Argentina). *Journal of South American Earth Sciences* 100: 102544.

Robledo, J.M., Horn, M.Y., Galli, C.I., and Anzótegui, L.M. 2020b. Inferencias paleoclimáticas para el Mioceno tardío en la cuenca de Angastaco basadas en el análisis fisionómico foliar: Formación Palo Pintado, Salta, Argentina. *Andean Geology* 47: 418–429.

Rohrmann, A., Sachse, D., Mulch, A., Pingel, H., Tofelde, S., Alonso, R.N., and Strecker, M.R. 2016. Miocene orographic uplift forces rapid hydrological change in the southern central Andes. *Scientific Reports* 6: 35678.

Salfity, J. and Monaldi, C. 2006. Hoja Geológica 2566-IV, Metán, provincia de Salta. Servicio Geológico Minero Argentino, *Boletín Nº 352*, Buenos Aires.

Smith, J.G. 1895 A Revision of the North American Species of *Sagittaria* and *Lophotocarpus. Missouri Botanical Garden Annual Report* 1895: 27–64.

Smith, S.Y. 2013. The fossil record of noncommelinid monocots. *In:* P. Wilkin and S.J. Mayo (eds.), *Early Events in Monocot Evolution*, 29–59. Cambridge University Press, Cambridge.

Soltis, D.E., Soltis, P.S., Endress, P.K., and Chase, M.W. 2005. *Phylogeny and Evolution of Angiosperms*. 370 pp. Sinauer Associates, Sunderland.

Starck, D. and Anzótegui L.M. 2001. The late Miocene climatic change persistence of a climatic signal through the orogenic stratigraphic record in north-western of Argentina. *Journal of South American Earth Sciences* 14: 763–774.

Teixeira, C. 1948. *Flora Mesozoica Portuguesa. Parte 1*. 118 pp. Direção Geral da Minas e Serviços Geológicos de Portugal, Lisboa.

Ventenat, E.P. 1799. *Tableau du Règne Végétal, Selon de Méthode de Jussieu, Vol. 2.* 607 pp. J. Drisonnier, Paris.

Wang, Q.F., Haynes, R.R., and Hellquist, C.B. 2010. Alismataceae. *In*: Z.Y. Wu, P.H. Raven, and D.Y. Hong (eds.), *Flora of China (Acoraceae through Cyperaceae)*, 84–89. Science Press & Missouri Botanical Garden Press, Beijing & St. Louis.

Willdenow, C.L. 1805. *Species Plantarum*. *Vol. 4 (1)*. 629 pp. G.C. Nauk, Berlin.

Wooten, J.W. 1973. Taxonomy of seven species of *Sagittaria* from eastern North America. *Brittonia* 25: 64–74.

Zepeda, C. and Lot, A. 1999. Acuitlacpalli or *Sagittaria macrophylla* (Alismataceae): A Mexican endemic hydrophyte and a threatened food resource. *Economic Botany* 53: 221–223.

Zepeda, C. and Lot, A. 2005. Distribución y uso tradicional de *Sagittaria macrophylla* Zucc. y *S. latifolia* Willd. en el Estado de México. *CIENCIA ergo-sum, Revista Científica Multidisciplinaria de Prospectiva* 12: 282–290.

Zhang, Y.W., Huang, S.J., Zhao X.N., Liu F., and Zhao, J.M. 2010. New record of an invasive species, *Sagittaria graminea*, in Yalu river estuary wetland. *Journal of Wuhan Botanical Research* 28: 631–633.

Stable isotope analysis of middle Miocene mammals from the Siwalik sub-Group of Pakistan

MUHAMMAD TAHIR WASEEM, ABDUL MAJID KHAN, JAY QUADE, ANTHONY KRUPA, DAVID L. DETTMAN, AMTUR RAFEH, and RANA MANZOOR AHMAD

Waseem, M.T., Khan, A.M., Quade, J., Krupa, A., Dettman, D.L., Rafeh, A., and Ahmad, R.M. 2021. Stable isotope analysis of middle Miocene mammals from the Siwalik sub-Group of Pakistan. *Acta Palaeontologica Polonica* 66 (Supplement to 3): S123–S132.

Stable isotope analysis is pivotal for investigating the paleodiet and paleoecology of past mammals. In this paper, we analyzed thirty fossil enamel samples belonging to the families Suidae, Rhinocerotidae, and Deinotheriidae for $\delta^{13}C_{enamel}$ and $\delta^{18}O_{enamel}$ composition to investigate paleodiet and paleoecology of middle Miocene mammals of the Siwalik sub-Group of Pakistan. The three mammalian groups, when combined together, yielded an average $\delta^{13}C_{enamel}$ value of -12.2 ± 2‰, indicating a pure to nearly pure C_3 diet. Suids show slightly higher $\delta^{13}C_{enamel}$ values of -11.2 ± 1.4‰ when compared to rhinocerotids and deinotheres (-12.3 ± 0.8‰ and -12.5 ± 1.3‰, respectively), which could be explained by selective foraging on new leaf shoots or feeding from open spaces. Alternatively, the differences in $\delta^{13}C_{enamel}$ could be due to different digestive physiologies and different enamel-diet enrichment factors. Members of all three families showed significant differences in $\delta^{18}O_{enamel}$ values, where suids yielded higher $\delta^{18}O$ values of -8.2 ± 1.2‰ compared to rhinocerotids and deinotheres (-11.4 ± 1.8‰ and -10.4 ± 1.7‰, respectively). Based upon these results, we assume that these mammals inhabited subtropical forests similar that of mid-Miocene of the Siwalik Group, India and Nepal. The modern analogues of such vegetation system are present in East and South of Myanmar, Nepal, and Malaya where precipitation is enough to support evergreen C_3 forests. By contrast, today's floodplain environments in Pakistan are dominated by C_4 grasses, and C_3 vegetation is only present in non-floodplain settings.

Key words: Mammalia, paleoclimate, paleodiet, Miocene, Chinji Formation, Pakistan.

Muhammad Tahir Waseem [tahirmuhammad1213@gmail.com], Abdul Majid Khan [majid.zool@pu.edu.pk] (corresponding author), and Amtur Rafeh [amturrafeh@gmail.com], Department of Zoology, University of the Punjab, Lahore 54590, Pakistan.
Jay Quade [quadej@email.arizona.edu], Anthony Krupa [akrupa@email.arizona.edu], and David L. Dettman ([dettman@email.arizona.edu], Department of Geosciences, University of Arizona, Tucson AZ 85721, USA.
Rana Manzoor Ahmad [manzoor.zoology@uo.edu.pk], Department of Zoology, University of Okara, Punjab 56300, Pakistan.

Received 28 June 2020, accepted 23 October 2020, available online 24 May 2021.

Introduction

The temporal and spatial records of climate archived in thick Neogene and Quaternary continental deposits in northern Pakistan provide an exceptional opportunity to explore the patterns of evolution and adaptation of mammals over the time span of million years (Badgley et al. 2008; Morgan et al. 2009; Patnaik et al. 2019). Stable isotope (SI) analysis of carbon and oxygen of enamel from mammals, both expressed in the familiar delta (δ) notation in per mil (‰) according to V-PDB (Vienna Pee Dee Belemnite) standards, allow us to reconstruct the past diets ($\delta^{13}C_{diets}$) and paleoenvironmental meteoric water ($\delta^{18}O_{mw}$), which in turn reflect paleovegetation and paleoclimate during the Neogene and Quaternary (Quade et al. 1992, 1995a, b; Cerling et al. 1997a, 2015; White et al. 2009; Sanyal et al. 2005, 2010; Uno et al. 2011; Ben-David and Flaherty 2012; Khan et al. 2020; Waseem et al. 2020a). The Siwalik sub-Group of northern Pakistan contains a high-resolution fossil record spanning the Neogene time period (Quade et al. 1989; Barry et al. 2002, 2013; Dennell et al. 2006; Flynn et al. 2016; Fig. 1). Morgan et al. (1994), Uno et al. (2011), and Hynek et al. (2012) interpreted elevated $\delta^{13}C$ values in fossil herbivore enamel ($\delta^{13}C_{enamel}$) to reflect a component of C_4 vegetation in the mid-Miocene (~11–10 Ma) across several continents.

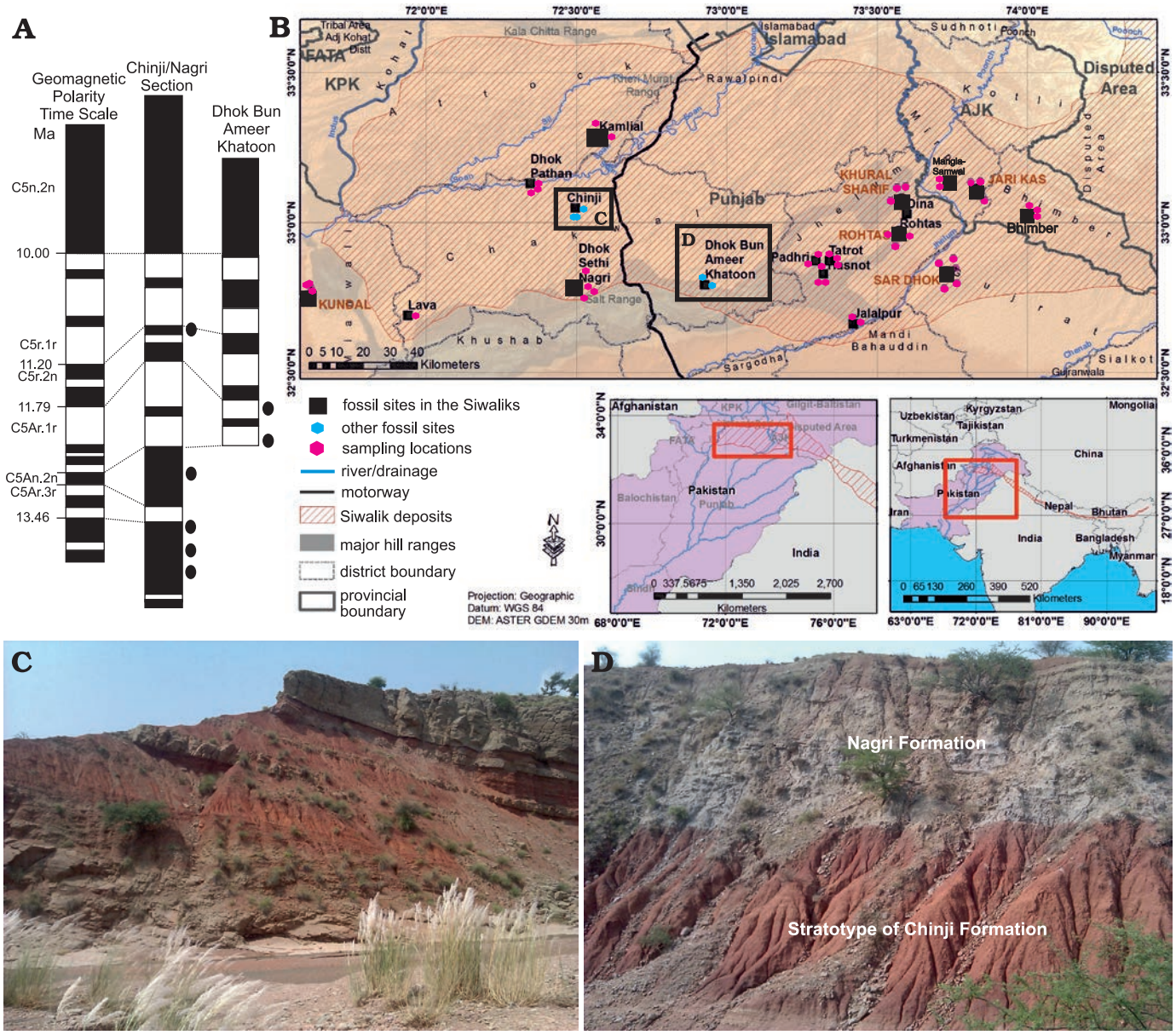

Fig. 1. Map of the Siwaliks indicating the middle Miocene localities from where fossil material for this study was recovered. **A**. Geomagnetic polarity time scale (Gradstein et al. 2012). **B**. Map of the Siwalik sub-Group of Pakistan along with the localities and studied area. **C**. Overview of Chinji-Nagri section. **D**. Overview of Dhok Bun Ameer Khatoon (DBAK) section.

However, the major C_4 radiation in the Siwalik sub-Group has been documented to occur after ~10 Ma (Barry et al. 1982, 2002; Quade et al. 1995a, b; Morgan et al. 2009). In this study, we explore the isotopic composition of enamel from three families of large herbivores to reconstruct paleoenvironments and check for evidence of C_4 dietary intake in the middle Miocene (14.2–11.2 Ma) of the Siwalik sub-Group of Pakistan. Enamel was selected for the analysis due to its high resistance to diagenesis and large crystal size and low porosity, which makes it the best material for paleodietary reconstruction in ancient ecosystems (Quade et al. 1992; Kohn et al. 1996, 2002; Kohn and Cerling 2002).

There are three metabolic pathways through which carbon is incorporated in the plants. Trees, nearly all shrubs, forbs, ferns, sedges, and most non-tropical or high altitude grasses utilize the C_3 pathway of photosynthesis in which $\delta^{13}C_{diet}$ ranges from -34 to -22‰ (Koch 1998; Pérez-Crespo et al. 2017), and average around -28.2 ± 6‰ under the present $\delta^{13}C_{CO2}$ = -8‰, or -6.7‰, pre-industrially (Kohn 2010). The C_4 pathway is found in most of the warm region-grasses and some sedges with a range of $\delta^{13}C_{diet}$ values from -14 to -10‰ (Cerling 1999). The abundance of C_3/C_4 vegetation in an ecosystem is governed by many factors, including the mean annual temperature (MAT), mean annual precipitation (MAP), and partial pressure of carbon dioxide in the atmosphere (pCO_2) (Kohn 2010; Waseem et al. 2020b). The comparatively cooler areas (MAT <25°C) with precipitation higher than 1–2 m/year show a dominance of C_3 vegetation while warmer areas (MAT >25°C) with drier conditions (MAP <1–2 m/year) show a dominance of C_4

grasses (Nelson 2007). Furthermore, the C_4 pathway can work efficiently under lower pCO_2 and lower humidity levels compared to C_3 pathway (Medrano and Flexas 2000; Bellasio et al. 2018) due to the fact that carbon is fixed twice in C_4 pathway as compared to C_3 pathway (Kohn and Cerling 2002). The $\delta^{13}C$ values of plants are governed by other factors such as low light intensity, saline soil, water availability, and local microhabitat conditions (Ehleringer et al. 1987; Codron et al. 2005; Bibi 2007).

These averages and ranges in $\delta^{13}C$ value for modern plants were ~1.3‰ higher during the middle Miocene in fossil C_3 and C_4 plants, due largely to the effect of fossil fuel burning in decreasing $\delta^{13}C_{CO2}$ of the atmosphere (see Tipple et al. 2010). Thus, we use the $\delta^{13}C_{CO2}$ (-5.2‰) as in Tipple et al. (2010) for pre-10 Ma time span. The third photosynthetic pathway, crassulacean acid metabolism (CAM), is found in succulent plants which are mostly present in deserts or epiphytic plants in closed forests (Passey et al. 2005; Andrade et al. 2007) and were probably negligible in the Siwaliks.

Upon feeding on plants, the carbon is incorporated in the herbivores tooth enamel during the period of tooth formation. When carbon isotopes are incorporated in the enamel of herbivores, $\delta^{13}C_{enamel}$ values are fractionated by an enrichment factor ($e_{enamel\text{-}diet}$):

$$e_{enamel\text{-}diet} = (a_{enamel\text{-}diet} - 1) \times 1000 \qquad (1)$$

where:

$$a_{enamel\text{-}diet} = (d_{enamel} + 1000)/(d_{diet} + 1000)$$

Thus, middle Miocene animals consuming C_3 vegetation outside of rainforests and deserts with $\delta^{13}C_{diet}$ values from -28.1 to -23.1‰ should show $\delta^{13}C_{enamel}$ values ranging from about -14 to -9‰, whereas middle Miocene animals feeding on C_4 vegetation should show $\delta^{13}C_{enamel}$ values ranging from ~-2 to ~+2‰. The values between ~-9 to ~-2‰ are considered to reflect mixed feeding on C_3/C_4 vegetation (MacFadden and Cerling 1996). In this study, we assume that $\delta^{13}C_{enamel}$ values ≤-16.1‰ denote browsing under closed-canopy forests, -16 to -14‰ for sub-canopy browsing, -14 to -12‰ for browsing in forests, and -12 to -8‰ for browsing in woodlands (Cerling and Harris 1999; Domingo et al. 2012). The $\delta^{13}C_{enamel}$ between -8 to -3‰ will be considered as mixed feeding on C_3/C_4 vegetation while values >-2‰ can be interpreted as grazing on dominantly C_4 grasses (Cerling et al. 1997a, b, 2004; Kohn 2010). However, $e_{enamel\text{-}diet}$ does not solely depend upon one factor. Tejada-Lara et al. (2018) argue that a single value of $e_{enamel\text{-}diet}$ of ~14.1‰ does not account for all the mammals from monkeys to elephants by overlooking the other metabolic and physiological effect on carbon fractionation. For example, different mammals show different $e_{enamel\text{-}diet}$ depending on body mass and digestive physiology (Tejada-Lara et al. 2018). Combining all factors, we assume an average $e_{enamel\text{-}diet}$ of ~+14.1‰ for large-bodied rhinocerotids and deinotheres and ~+13.1‰ for suids according to Codron et al. (2011) and Tejada-Lara et al. (2018).

Oxygen enters an animal's body in three main ways: (i) from drinking water, (ii) water derived from food, and (iii) inhalation, and leaves the body through sweat, exhalation, and urination (Sponheimer and Lee-Thorp 1999; Koch 2007; Sánchez 2005; Blumenthal et al. 2017, 2018). Of these sources, the majority of oxygen isotopes incorporated into enamel are from drinking water and diet, and $\delta^{18}O$ values of local meteoric water ($\delta^{18}O_{mw}$) are affected by environmental temperature, amount of precipitation, latitude, and altitude (Dansgaard 1964). The general trend of $\delta^{18}O_{enamel}$ values is set by the ecology as the animals living under closed habitat and in humid conditions (forests) tend to show lower $\delta^{18}O_{enamel}$ values compared to the animals living in open and arid (savannah or grasslands) areas (Feranec and MacFadden 2006). Levin et al. (2006) categorized the animals under two broad categories on the basis of their physiology and behavior. Evaporation sensitive (ES) taxa tend to obtain most of their water from their diet (leafy plants) and generally are ruminants ($\delta^{18}O$ values of their enamel is correlated to the evaporation of leaf water), whereas evaporation insensitive (EI) taxa are mostly non-ruminants that depend on surface water for their body water requirements ($\delta^{18}O_{enamel}$ is correlated to local drinking water sources). In this study, all the families sampled can be categorized as EI taxa on the basis of the physiology of the modern analogues, providing better insights into the $\delta^{18}O$ value of palaeo-precipitation (Levin et al. 2006; Blumenthal et al. 2017; Faith 2018).

The fossil fauna of Chinji Formation includes Rhinocerotidae, Suidae, Tragulidae, Bovidae, Giraffidae, Deinotheriidae, Gomphotheriidae, and other taxa including Hominidae, Rodentia, and Carnivora (Pilgrim 1937; Khan et al. 2013; Barry et al. 2013; Flynn et al. 2016). We focus here on the paleodiets, paleoenvironments, and niche partitioning among Rhinocerotidae, Suidae, and Deinotheriidae from the middle Miocene of northern Pakistan. We selected these three EI taxa over non-EI taxa as $\delta^{18}O_{enamel}$ value of EI taxa is correlated to their water source (Faith 2011, 2018). Furthermore, we selected one specialized browser (deinotheres), one taxon (i.e., *Hyotherium pilgrimi*) which disappeared from the Siwalik record during the late Miocene, and one taxon (rhinocerotid, *Chilotherium intermedium*) which shifted towards a C_4 diet during the late Miocene (Badgley et al. 2008; Morgan et al. 2009) to evaluate whether these taxa ate C_3 or C_4 plants during the middle Miocene time span in the Siwalik sub-Group of Pakistan.

The rhinocerotid, *Chilotherium intermedium*, was widespread in the Siwalik sub-Group of India and Pakistan, and existed up to the late Miocene (~7 Ma) in China. This species is characterized by low-crowned cheek teeth (brachydonty) with thin enamel folding and less complexity, indicating a diet composed of soft and less-gritty vegetation, preferably leaves of plants and trees (Khan 2009). *C. intermedium* was comparatively smaller (height 1.5 m and weight 1–2 tons) than modern black rhinos (*Diceros bicornis*) (height up to 1.8 m and weight up to 2.2 tons) (Decher 1999; Deng 2005).

Deinotherium pentapotamiae and *D. indicum* (Deinotheriidae) (body weight up to 11 tons and height up to 5 m, Larramendi 2016) was widespread in the Siwalik Group

and contemporaneous African sites for most of the middle Miocene, and it persisted as late as ~9 Ma in the Indian sub-continental region (Sarwar 1977). Two hooked shaped lower tusks were present in the species of *Deinotherium* with a flat skull, unlike other proboscideans, along with low-crowned teeth, indicating a browsing diet (Sarwar 1977; Shoshani and Tassy 2005).

Hyotherium pilgrimi (Suidae) was a species with bunodont (rounded cusps) and brachyodont cheek teeth which existed during the middle Miocene time span in the Siwaliks. It had a range of body weight from 150–200 kg and height up to 1.1 m (Sorkin 2008). The mesowear and morphological studies (low hypsodonty index of 1.1, simple bunodont dentition with thick enamel) show that this species browsed on leaves and fruits (Barry et al. 2002; Tariq 2010; Aslam 2018). In general, all the middle Miocene mammals of the Siwalik sub-Group of Pakistan show morphological characters indicating browsing diets in forests and woodland settings, like their Indian counterparts (Patnaik et al. 2019).

Institutional abbreviations.—EB, Environmental Biology Laboratory, Institute of Zoology, University of the Punjab, Lahore, Pakistan.

Other abbreviations.—CAM, crassulacean acid metabolism; EI, evaporation insensitive; ES, evaporation sensitive; MAP, mean annual precipitation; MAT, mean annual temperature; SI, stable isotopes; V-PDB, Vienna Pee Dee Belemnite.

Geological setting

The middle Miocene is represented by the Chinji Formation in the Siwalik sub-Group of Pakistan (Fig. 1), which spans 14.2–11.2 Ma (Barry et al. 2002). The thickness and near-continuous deposition of the strata have permitted the development of a robust chronostratigraphic framework for the Chinji Formation on the basis of paleomagnetic dating. The samples for this study were collected from the Chinji-Nagri and Dhok Bun Ameer Khatoon sections (Fig. 1). The Chinji-Nagri section (Fig. 1B, C) is present in Chakwal District, Punjab (32°39′N, 72°22′E), whereas the Dhok Bun Ameer Khatoon section (DBAK) (Fig. 1B, D) is located 50 km north of Chinji Village (32°47′N, 72°55′E). The boundary between Chinji and Nagri formations can be placed at 11.2 Ma (Fig. 1A), between magnetic zones C5r.3r and C5n.3n (Johnson et al. 1982, calibrated according to Gradstein et al. 2012). The lower boundary of the Chinji Formation with the underlying Kamlial Formation (Fig. 1A) can be placed between C5ACr and C5ADn at 14.2 Ma (Channell et al. 2013). Siltstone and sandstone deposited in an overall fluvial environment dominate the general lithology of the Siwalik sub-Group sediments. Most of the samples come from reddish to gray mudstone (Fig. 1C, D) marginal to large-river paleochannels. The ages are assigned as the mid points following Barry et al. (2002).

Material and methods

For SI analysis, thirty samples from three mammalian families were selected across the middle Miocene of the Siwalik sub-Group of Pakistan. The samples were identified to the species level and further processed for SI analysis. Statistical analysis was conducted using Statistical Package for Social Studies (SPSS) version 20.0.

For the extraction of enamel, a rotary dental drill with carbide burrs was used. Around 15–20 mg of enamel was extracted from each tooth (only molars and premolars were included). Enamel was extracted along one single transect from cervix to crown apex (longitudinal) from buccal surface of upper teeth and lingual surface of lower teeth.

Powdered enamel was further pre-treated with 10 ml of 2% NaOCl for one hour to remove organic matter and the solution was decanted and rinsed with distilled water three times. The samples were than treated with 10 ml of 0.1% acetic acid for 1 hour to remove exogenous carbonates and rinsed with water (Nelson 2007). Samples were then oven dried before isotope analysis (Koch et al. 1997).

$\delta^{18}O_{enamel}$ and $\delta^{13}C_{enamel}$ values were measured at the University of Arizona, USA, using an automated carbonate preparation device (KIEL-III) coupled to a gas-ratio mass spectrometer (Finnigan MAT 252). Powdered samples were reacted with dehydrated phosphoric acid under vacuum at 70°C. The isotope ratio measurement is calibrated based on repeated measurements of NBS-19 and NBS-18, and precision is 0.11‰ for $\delta^{18}O$ (V-PDB) and 0.08‰ for $\delta^{13}C$ (V-PDB).

Results

Stable Carbon Isotopes.—The average $\delta^{13}C_{enamel}$ across all the families was found to be -12.2 ± 2.2‰. The Suidae, Rhinocerotidae, and Deinotheriidae returned average values of $\delta^{13}C_{enamel}$ of -11.2 ± 1.4‰ (n = 10), -12.3 ± 0.8‰ (n = 10), and -12.5 ± 1.3‰ (n = 10), respectively (Table 1). Normality tests indicate that data were normally distributed. One-way ANOVA along with the post-hoc (Tukey's HSD) test show no significant differences in $\delta^{13}C$ values between Rhinocerotidae and Deinotheriidae ($p = 0.061$), whereas Suidae showed significant differences compared to Deinotheriidae ($p = 0.039$) and Rhinocerotidae ($p = 0.041$).

Stable Oxygen Isotopes.—The average $\delta^{18}O_{enamel}$ (V-PDB) across all the families was -9.9 ± 3‰, wherein Suidae, Rhinocerotidae, and Deinotheriidae yielded average values for $\delta^{18}O_{enamel}$ of -8.2 ± 1.2‰ (n = 10), -11.4 ± 1.8‰ (n = 10), and -10.4 ± 1.7‰ (n = 10), respectively (Table 1). The data were normally distributed. One-way ANOVA along with post-hoc test indicated that the $\delta^{18}O_{enamel}$ of suids is significantly different from the $\delta^{18}O_{enamel}$ of rhinos and deinotheres ($p = 0.041$) (Table 1, Fig. 2).

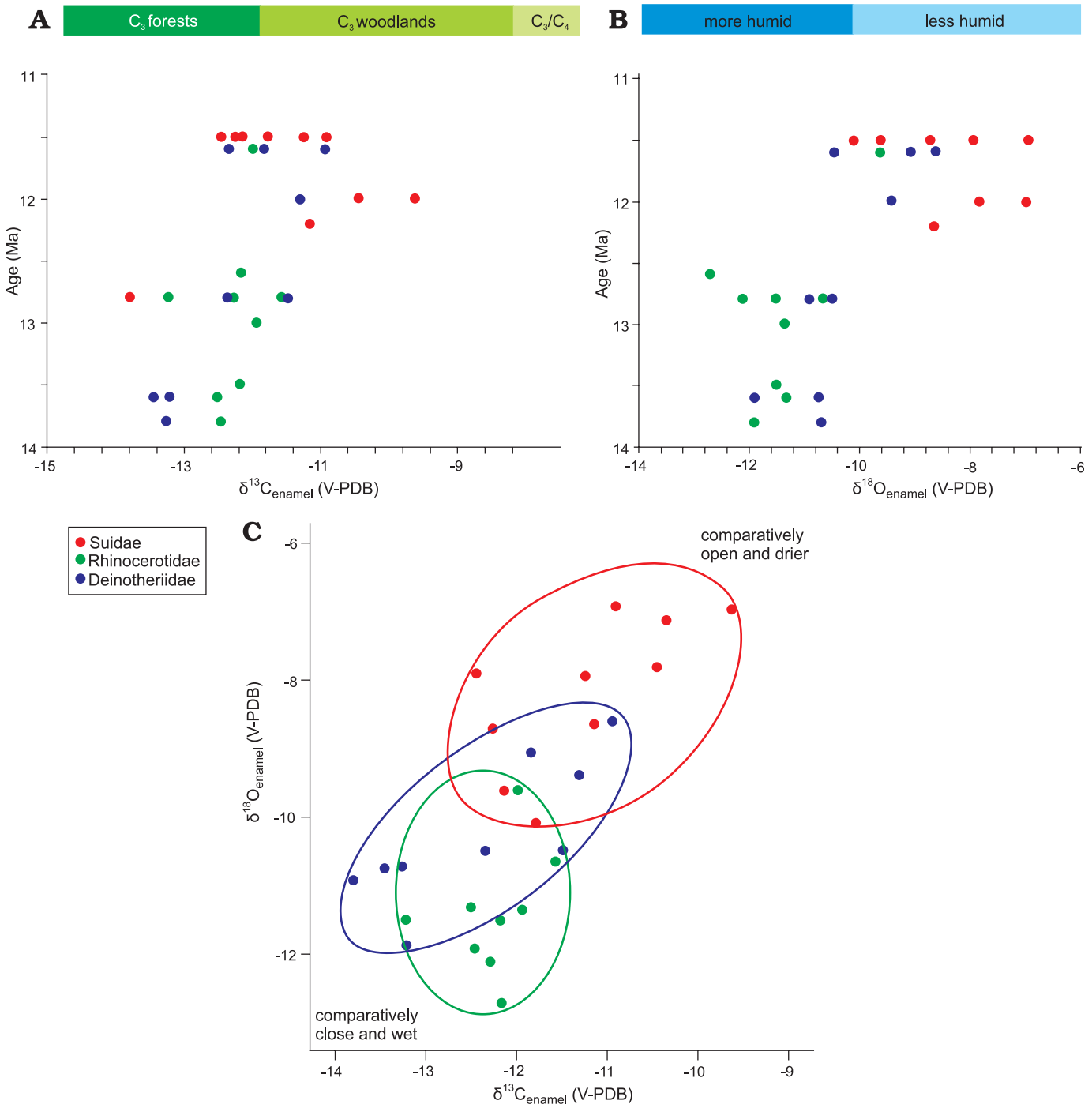

Fig. 2. $\delta^{13}C_{enamel}$ and $\delta^{18}O_{enamel}$ of all results on three herbivore families from the Chinji Formation. **A**. $\delta^{13}C_{enamel}$ values versus age (Ma) showing close and forest ecology of middle Miocene. **B**. $\delta^{18}O_{enamel}$ values versus age (Ma) indicating the moisture conditions in middle Miocene. **C**. The niche partitioning in $\delta^{18}O_{enamel}$ versus $\delta^{13}C_{enamel}$ space among the suids, rhinocerotids, and deinotheres.

Discussion

The average $\delta^{13}C_{enamel}$ value of middle Miocene mammals (-12.2 ± 2‰) in our data overall indicates a diet composed of C_3 vegetation, which was likely present in the form of forests and woodlands (Kohn and Cerling 2002; Kohn 2010). Patnaik et al. (2019) report the range of $\delta^{13}C_{enamel}$ for large herbivores from -13.9 to -11.6‰ for middle Miocene Siwalik sub-Group of India, which matches our results. The lowest $\delta^{13}C_{enamel}$ value in our results (-13.9‰) was recorded at ~13 Ma interval, whereas the highest value (-9.6‰) was recorded at ~12 Ma (Fig. 2, Table 1). This shows that the lower Chinji Formation was dominated by C_3 vegetation, likely present in the form of forestland, whereas the upper Chinji was dominated by C_3 open woodlands (Kohn and Cerling 2002; Kohn 2010). Thus, vegetation and habitat appear to have changed towards more

Table 1. $\delta^{13}C_{enamel}$ and $\delta^{18}O_{enamel}$ values for thirty enamel samples of fossil mammals from the middle Miocene Siwaliks of Pakistan. The ages of the samples have been calibrated according to Gradstein et al. (2012). Abbreviations: l, left; M/m, upper/lower molar; PM, upper premolar; r, right; V-PDB, Vienna Pee Dee Belemnite.

Sample ID	Family	Species	Horizon	Type of tooth	Age (Ma)	$\delta^{13}C_{enamel}$ V-PDB (‰)	$\delta^{18}O_{enamel}$ V-PDB (‰)
EB 470	Suidae	*Hyotherium pilgrimi*	upper Chinji	lM2	12.0	-10.3	-7.1
EB 471	Suidae	*Hyotherium pilgrimi*	upper Chinji	lM2	12.2	-9.6	-7.0
EB 472	Suidae	*Hyotherium pilgrimi*	upper Chinji	rP3	11.5	-11.1	-8.6
EB 473	Suidae	*Hyotherium pilgrimi*	upper Chinji	rm3	11.5	-12.1	-9.6
EB 474	Suidae	*Hyotherium pilgrimi*	upper Chinji	rm2	12	-12.25	-8.7
EB 475	Suidae	*Hyotherium pilgrimi*	upper Chinji	rM2	11.5	-11.8	-10.1
EB 476	Suidae	*Hyotherium pilgrimi*	upper Chinji	rM2	11.5	-10.4	-7.8
EB 477	Suidae	*Hyotherium pilgrimi*	upper Chinji	rM2	11.5	-12.45	-7.9
EB 478	Suidae	*Hyotherium pilgrimi*	upper Chinji	lM3	12.0	-11.2	-7.9
EB 479	Suidae	*Hyotherium pilgrimi*	upper Chinji	lM3	12.0	-10.9	-6.9
EB 480	Rhinocerotidae	*Chilotherium intermedium*	lower Chinji	lm2	13.6	-12.5	-11.3
EB 481	Rhinocerotidae	*Chilotherium intermedium*	lower Chinji	lM3	13.6	-12.2	-11.5
EB 482	Rhinocerotidae	*Chilotherium intermedium*	lower Chinji	lM3	12.6	-12.2	-12.7
EB 483	Rhinocerotidae	*Chilotherium intermedium*	upper Chinji	P4	11.6	-12.0	-9.6
EB 484	Rhinocerotidae	*Chilotherium intermedium*	lower Chinji	lM3	13.6	-12.5	-11.3
EB 485	Rhinocerotidae	*Chilotherium intermedium*	lower Chinji	rm2	13.8	-12.45	-11.9
EB 486	Rhinocerotidae	*Chilotherium intermedium*	lower Chinji	rM2	13.0	-11.9	-11.3
EB 487	Rhinocerotidae	*Chilotherium intermedium*	lower Chinji	lM2	12.8	-13.2	-11.5
EB 488	Rhinocerotidae	*Chilotherium intermedium*	lower Chinji	lM2	12.8	-11.6	-10.65
EB 489	Rhinocerotidae	*Chilotherium intermedium*	lower Chinji	rm3	12.8	-12.3	-12.1
EB 490	Deinotheriidae	*Deinotherium pentapotamiae*	upper Chinji	M2	11.6	-11.8	-9.1
EB 491	Deinotheriidae	*Deinotherium pentapotamiae*	upper Chinji	M3	11.6	-12.3	-10.45
EB 492	Deinotheriidae	*Deinotherium indicum*	lower Chinji	lm1	12.8	-13.8	-10.9
EB 493	Deinotheriidae	*Deinotherium indicum*	lower Chinji	lm2	12.8	-11.5	-10.5
EB 494	Deinotheriidae	*Deinotherium indicum*	lower Chinji	rM3	13.6	-13.2	-11.9
EB 495	Deinotheriidae	*Deinotherium indicum*	lower Chinji	rm3	13.6	-13.4	-10.7
EB 496	Deinotheriidae	*Deinotherium pentapotamiae*	upper Chinji	lm3	12.0	-11.3	-9.4
EB 497	Deinotheriidae	*Deinotherium pentapotamiae*	upper Chinji	lm3	11.6	-10.9	-8.6
EB 498	Deinotheriidae	*Deinotherium indicum*	lower Chinji	lm3	13.8	-13.25	-10.7
EB 499	Deinotheriidae	*Deinotherium pentapotamiae*	lower Chinji	lm3	13	-12.3	-10.5

open ecological settings in the upper Chinji Formation. The shift to open woodland is also apparent in the suid $\delta^{13}C_{enamel}$ results, which return an estimate for suid diet of -22.7‰, assuming $e_{enamel\text{-}diet}$ = +13.1‰. (Kohn 2010; Cerling et al. 2015; Table 1). Moreover, the possibility of consumption of C_3 grasses cannot be ruled out as extant suids in eastern Africa also consume C_3 grasses but show a low-crowned dental morphology (Harris and Cerling 2002; Souron 2017).

These findings are supported by evidence presented in Quade and Cerling (1995), who reported $\delta^{13}C_{paleosol\ carbonate}$ values from Kamlial and Chinji formations ranging from -12.9 to -9.5‰, indicating a forestland and woodland environment. Further afield, Quade et al. (1995b) from Pasalar, Turkey, and Uno et al. (2016) from eastern Africa report the $\delta^{13}C$ values from paleosol and ungulate enamel, respectively. Both studies report a dominance of C_3 vegetation with very little or no C_4 vegetation during the middle Miocene time span.

The higher $\delta^{13}C_{enamel}$ values in suids compared to rhinocerotids and deinotheres indicate that this family preferred more open areas for their feeding or browsed on a leafy vegetation. Tariq (2010) reports a frugivorous component to diets in suids on the basis of mesowear analysis. The mesowear analysis coupled with the morphological features of suid teeth (bunodont teeth with thick enamel) is in agreement with the hypothesis, based upon our $\delta^{13}C_{enamel}$ data, that suids of middle Miocene utilized C_3 plants in open habitats, including fruits, as their dietary resource and inhabited relatively more open areas (Tariq 2010; Aslam 2018; Waseem et al. 2020b).

On the basis of average $\delta^{13}C_{enamel}$ and $\delta^{18}O_{enamel}$ values, we may hypothesize that middle Miocene climate was sub-humid and animals drank from shaded water holes or rivers (Sanyal et al. 2010; Tada et al. 2016). If we use the equation for MAP calculation on the basis of $\delta^{13}C_{diet}$ following Kohn (2010), we can say that in middle Miocene of the Siwalik sub-Group of Pakistan MAP was lower than ~700 mm/year (see Kohn 2010: fig. 3). The average value of $\delta^{18}O_{enamel}$ (-9.9 ± 3‰) of all non-ruminant taxa is low, indicating sub-humid conditions (Fig. 2B) during the middle Miocene time span in the Siwalik sub-Group of Pakistan,

Fig. 3. Reconstruction of the middle Miocene ecology of the Siwaliks and relative habitat partitioning among three mammalian families based on the stable isotope data of carbon and oxygen. Deinotheres (**A**), rhinocerotids (**B**), and suids (**C**).

which is consistent with Indian contemporaneous sites (Patnaik et al. 2019). The low $\delta^{18}O_{enamel}$ values also probably indicate that in the middle Miocene, animals drank from relatively unevaporated water holes or rivers.

The $\delta^{18}O_{enamel}$ and $\delta^{13}C_{enamel}$ values increase gradually from ~14 Ma to ~11 Ma (Fig. 2A, B), culminating in more open environments supporting a woodland or perhaps minor C_4 vegetation (0–18% cover). However, the *Hyotherium pilgrimi* samples show higher $\delta^{13}C_{enamel}$ values in our data which may also imply that this response may be species specific. Even if we consider the values as species specific, the open ecology towards the end of middle Miocene is still supported as we consider that the studied suid species occupied more open areas similar to the late Miocene suids. However, suids in the late Miocene showed feeding in both open and closed environments (Nelson 2005, 2007).

Niche partitioning among middle Miocene mammals

The studied middle Miocene mammals show some degree of niche partitioning (Fig. 3). The deinotheres and rhinocerotids from middle Miocene of Indian Siwaliks show an average $\delta^{13}C_{enamel}$ values of -12.5‰ and -12.8‰, respectively, very close to the ranges in our results for these taxa (Patnaik et al. 2019), pointing to overall similar ecological and dietary preferences. The suids (average $\delta^{13}C_{enamel}$ = -11.2 ± 1.4‰) inhabited a woodland/forestland setting where they fed on C_3 vegetation consisting of plants, including fruits. They may have drunk from less shaded water holes as represented by their elevated $\delta^{18}O_{enamel}$ values (-8.1‰) compared to the other middle Miocene taxa (Fig. 2B, C). The rhinocerotids and deinotheres show similarly low ($p > 0.05$) $\delta^{13}C$ values (-12.2‰ and -12.4‰, respectively), indicating that both families inhabited a forestland setting and browsed from understory vegetation (Fig. 2A, C), as reported by Patnaik et al. (2019) for contemporaneous Indian sites. However, the $\delta^{18}O_{enamel}$ values significantly differ between these two families (-11.3 ± 1.8‰ and -10.4 ± 1.7‰; Fig. 2B). Heissig (1972, 2003) reports that middle Miocene rhinocerotids of Pakistan preferred a habitat close to water bodies and Biasatti et al. (2018) report the same behavior for middle Miocene rhinocerotids of China. Thus, we may assume that middle Miocene rhinocerotids lived in habitats close to water, resulting in the lowest $\delta^{18}O_{enamel}$ values among all the middle Miocene taxa analyzed in this study. Deinotheres preferred a forested habitat where they had access to water but they did not live

very close to the water bodies like rhinocerotids as indicated by the $\delta^{18}O_{enamel}$ values (Fig. 3).

Conclusions

We analyzed thirty specimens belonging to three families of middle Miocene Siwalik sub-Group of Pakistan. On the basis of our results, we conclude that these middle Miocene species inhabited dense forests and woodlands where they fed on the C_3 vegetation and drank from shaded water resources like ponds or rivers which were frequently refilled by precipitation (Fig. 3). We did not find clear evidence of significant C_4 vegetation in their diet. The $\delta^{18}O_{enamel}$ results reveal that the environment was more humid at ~14 Ma and became less humid towards the upper Chinji Formation (12–11.2 Ma). In general, the middle Miocene Siwaliks of Pakistan were dominated by forests and woodlands with precipitation supporting a more evergreen ecology as in the middle Miocene of eastern Africa, India, and Nepal and present-day vegetation of Myanmar (Quade et al. 1995a, b; Uno et al. 2016).

Acknowledgements

The authors are thankful to Antoine Souron (University of Bordeaux, France) and anonymous reviewers for their constructive commentary and very helpful comments which enhanced the quality of the manuscript. This work has been supported by the Higher Education Commission indigenous fellowship to MTW for Ph.D. studies vide pin no. 315-28107-2BS3-243. We also acknowledge the support in sample analysis from Desert Laboratory, University of Arizona, Tucson, USA.

References

Andrade, J.L., De La Barrera, E., Reyes-García, C., Ricalde, M.F., Vargas-Soto, G., and Cervera, C.J. 2007. El metabolismo ácido de las crasuláceas: diversidad, fisiología ambiental y productividad. *Boletín de la Sociedad Botánica de México* 87: 37–50.

Aslam, S. 2018. *Dental and Cranial Morphological Studies Based on New Collection of Neogene Suids from the Siwalik Hills of Pakistan*. 206 pp. Unpublished Ph.D. Thesis, University of the Punjab, Lahore.

Badgley, C., Barry, J.C., Morgan, M.E., Nelson, S.V., Behrensmeyer, A.K., Cerling, T.E., and Pilbeam, D. 2008. Ecological changes in Miocene mammalian record show impact of prolonged climatic forcing. *Proceeding of National Academy of Science USA* 105: 12145–12149.

Barry, J.C., Behrensmeyer, A.K., Badgley, C.E., Flynn, L.J., Peltonen, H., Cheema, I.U., Pilbeam, D., Lindsay, E.H., Raza, S.M., Rajpar, A.R., and Morgan, M.E. 2013. The Neogene Siwaliks of the Potwar Plateau, Pakistan. *In*: X. Wang, L.J. Flynn, and M. Fortelius (eds.), *Fossil Mammals of Asia: Neogene Biostratigraphy and Chronology*, 373–399. Columbia University Press, New York.

Barry, J.C., Lindsay, E.H., and Jacobs, L.L. 1982. A biostratigraphic zonation of the middle and upper Siwaliks of the Potwar Plateau of Northern Pakistan. *Palaeogeography, Palaeoclimatology, Palaeoecology* 37: 95–130.

Barry, J.C., Morgan, M., Flynn, L.J., Pilbeam, D., Behrensmeyer, A.K., Raza, S.M., Khan, I., Badgely, C., Hicks, J., and Kelley, J. 2002. Faunal and environmental change in the L=late Miocene Siwaliks of Northern Pakistan. *Palaeobiology* 28:1–72.

Bellasio, C., Quirk, J., and Beerling, D.J. 2018. Stomatal and non-stomatal limitations in savanna tress and C_4 grasses grown at low, ambient and high atmospheric CO_2. *Plant Science* 274: 181–192.

Ben-David, M. and Flaherty, E.A. 2012. Stable isotopes in mammalian research: a beginner's guide. *Journal of Mammalogy* 93: 312–328.

Biasatti, D., Yang, W., and Deng, T. 2018. Paleoecology of Cenozoic rhinos from northwest China: a stable isotope perspective. *Vertebrata PalAsiatica* 56: 45–68.

Bibi, F. 2007. Dietary niche partitioning among fossil bovids in late Miocene C_3 habitats: consilience of functional morphology and stable isotope analysis. *Palaeogeography, Palaeoclimatology, Palaeoecology* 253: 529–538.

Blumenthal, S.A., Levin, N.E., Brown, F.H., Brugal, J.P., Chritz, K.L., and Cerling, T.E. 2018. Diet and evaporation sensitivity in African ungulates: A comment on Faith (2018). *Palaeogeography, Palaeoclimatology, Palaeoecology* 506: 250–251.

Blumenthal, S.A., Levin, N.E., Brown, F.H., Brugal, J.-P., Chritz, K.L., Harris, J.M., Jehle, G.E. and Cerling, T.E. 2017. Aridity and hominin environments. *Proceedings of the National Academy Sciences* 114: 7331–7336.

Cerling, T.E. 1999. Paleorecords of C_4 plants and ecosystems. *In*: R.F. Sage and R.K. Monson (eds.), *C_4 Plant Biology*, 445–469. Academic Press, London.

Cerling, T.E. and Harris, J.M. 1999. Carbon isotope fractionation between diet and bioapatite in ungulate mammals and implications for ecological and paleoecological studies. *Oecologia* 120: 347–363.

Cerling, T.E., Andanje, S.A., Blumenthal, S.A., Brown, F.H., Chritz, K.L., Harris, J.M., Hart, J., Kirera, F., Kaleme, P., Leakey, L., Meave, L., Levin, N.E., Manthi, F., Passey, B.H., and Uno, K.T. 2015. Dietary changes of large herbivores in the Turkana Basin, Kenya from 4 to 1 Ma. *Proceeding of National Academy of Science USA* 112: 11467–11472.

Cerling, T.E., Harris, J.M., Ambrose, S.H., Leakey, M.G., and Solounias, N. 1997a. Dietary and environmental reconstruction with stable isotope analyses of herbivore tooth enamel from the Miocene locality of Fort Ternan, Kenya. *Journal of Human Evolution* 33: 635–650.

Cerling, T.E., Harris, J.M., MacFadden, B.J., Leakey, M.G., Quade, J., Eisenmann, V., and Ehleringer, J.R. 1997b. Global vegetation change through the Miocene–Pliocene boundary. *Nature* 389:153–158.

Cerling, T.E., Hart, J.A., and Hart, T.B. 2004. Stable isotope ecology in the Ituri Forest. *Oecologia* 138: 5–12.

Channell, J.E.T., Ohneiser, C., Yamamoto, Y., and Kesler, M.S. 2013. Oligocene–Miocene magnetic stratigraphy carried by biogenic magnetite at sites U1334 and U1335 (equatorial Pacific Ocean). *Geochemistry, Geophysics, Geoecosystem* 14: 265–282.

Codron, J., Codron, D., Lee-Throp, J.A., Sponheimer, M., Bond, W.J., de Ruiter, D. and Grant, R. 2005. Taxonomic, anatomical, and spatiotemporal variations in the stable carbon and nitrogen isotopic compositions of plants from African savanna. *Journal of Archaeological Science* 32: 1757–1772.

Codron, D., Hull, J., Brink, J S., Codron, J., Ward, D., and Clauss, M. 2011. Effect of competition on niche dynamics of syntopic grazing ungulates: contrasting the predictions of habitat selection models using stable isotope analysis. *Evolutionary Ecology Research* 13 (3): 217–235.

Dansgaard, W. 1964. Stable isotopes in precipitation. *Tellus* 16: 436–468.

Decher, J. 1999. Book review: "The Kingdon Field Guide to African Mammals" by J. Kingdom. *Journal of Mammalogy* 80 (2): 692–693.

Deng, T. 2005. New discovery of *Iranotherium morgani* (Perissodactyla, Rhinocerotidae) from the late Miocene of the Linxia Basin in Gansu, China, and its sexual dimorphism. *Journal of Vertebrate Paleontology* 25: 442–450.

Dennell, R.W., Coard, R., and Turner, A. 2006. The biostratigraphy and magnetic polarity zonation of the Pabbi Hills, northern Pakistan: an Upper Siwalik (Pinjor Stage) upper Pliocene–Lower Pleistocene fluvial sequence. *Palaeogeography, Palaeoclimatology, Palaeoecology* 234: 168–185.

Domingo, L., Prado, J.L., and Alberdi, M.T. 2012. The effect of paleoeco-

logy and paleobiogeography on stable isotopes of Quaternary mammals from South America. *Quaternary Science Reviews 55*: 103–113.

Ehleringer, J.R., Lin, Z.F., Field, C.D., Sun, G.L., and You, L.Y. 1987. Leaf isotope ratios of plants from a subtropical monsoon forest. *Oecologia* 72: 109–114.

Faith, J.T. 2011. Late Quaternary dietary shifts of the Cape grysbok (*Raphicerus melanotis*) in Southern Africa. *Quaternary Research* 75: 159–165.

Faith, J.T. 2018. Paleodietary change and its implications for aridity indices derived from $\delta^{18}O$ of herbivore tooth enamel. *Palaeogeography, Palaeoclimatology, Palaeoecology* 490: 571–578.

Feranec, R.S. and MacFadden, B.J. 2006. Isotopic discrimination of resource partitioning among ungulates in C_3-dominated communities from the Miocene of Florida and California. *Paleobiology* 32: 191–205.

Flynn, L.J., Pilbeam, D., Barry, J.C., Morgan, M.E., and Raza, S.M. 2016. Siwalik synopsis: A long stratigraphic sequence for the later Cenozoic of South Asia. *Comptes Rendus Palevol* 15: 877–887.

Gradstein, F.M., Ogg, J.G., and Hilgen, F.J. 2012. On the Geologic Time Scale. *Newsletters on Stratigraphy* 45: 171–188.

Harris, J.M. and Cerling, T.E. 2002. Dietary adaptations of extant and Neogene African suids. *Journal of Zoology* 256: 45–54.

Heissig, K. 1972. Paläontologische und geologische Untersuchungen im Tertiär von Pakistan, 5. Rhinocerotidae (Mamm.) aus den unteren und mittleren Siwalik-Schichten. *Bayerische Akademie der Wissenschaften Mathematisch Naturwissenschaftliche Klasse, Abhandlungen, Neue Folge* 152: 1–112.

Heissig, K. 2003. *Change and Continuity in Rhinoceros Faunas of Western Eurasia from the Middle to the Upper Miocene*. 89 pp. EEDEN, Stará Lesná.

Hynek, S.A., Passey, B.H., Prado, J.L., Brown, F.H., Cerling, T.E., and Quade, J. 2012. Small mammal carbon isotope ecology across the Miocene–Pliocene boundary, northwestern Argentina. *Earth and Planetary Science Letters* 321–322: 177–188.

Johnson, N.M., Opdyke, N.D., Johnson, G.D., Lindsay, E.H., and Tahirkheli, R.A.K. 1982. Magnetic polarity stratigraphy and ages of Siwalik group rocks of the Potwar Plateau, Pakistan. *Palaeogeography, Palaeoclimatology, Palaeoecology* 37: 17–42.

Khan, A.M. 2009. *Taxonomy and Distribution of Rhinoceroses from the Siwalik Hills of Pakistan*. 182 pp. Unpublished Ph.D. Thesis, University of the Punjab, Lahore.

Khan, M.A., Batool, A., Nayyer, A.Q., and Akhtar, M. 2013. *Gazella lydekkeri* (Cetartiodactyla: Ruminantia: Bovidae) from the Middle Siwaliks of Hasnot (late Miocene), Pakistan. *Pakistan Journal of Zoology* 45: 981–988.

Khan, A.M., Iqbal, A., Waseem, M.T., Ahmad, R.M., and Ali, Z. 2020. Palaeodietary and palaeoclimatic interpretations for herbivore fauna from late Pliocene to early Pleistocene Siwaliks of Pakistan. *Journal of Animal and Plant Sciences* 30: 355–363.

Koch, P.L. 1998. Isotopic reconstruction of past continental environments. *Annual Review of Earth and Planetary Science* 26: 573–613.

Koch, P.L. 2007. Isotopic study of the biology of modern and fossil vertebrates. *In*: R.H. Michener and K. Lajtha (eds.), *Stable Isotopes in Ecology and Environmental Science*, 99–154. Blackwell Publishing, Boston.

Kohn, M.J. 2010. Carbon isotope compositions of terrestrial C3 plants as indicators of (paleo)ecology and (paleo)climate. *Proceedings of the National Academy Sciences* 107: 19691–19695.

Kohn, M.J. and Cerling, T.E. 2002. Stable Isotope Compositions of Biological Apatite. *In*: M.J. Kohn, J. Rakovan, and J.M. Hughes (eds.), Phosphates—Geochemical, Geobiological, and Materials Importance. *Reviews in Mineralogy and Geochemistry* 48: 455–488.

Kohn, M.J., Schoeninger, M.J., and Valley, J.W. 1996. Herbivore tooth oxygen isotope compositions: effects of diet and physiology. *Geochimica et Cosmochimica Acta* 60: 3889–3896.

Koch, P.L., Tuross, N., and Fogel, M.L. 1997. The effects of sample treatment and diagenesis on the isotopic integrity of carbonate in biogenic hydroxylapatite. *Journal of Archaeological Science* 24: 417–429.

Larramendi, A. 2016. Shoulder height, body mass, and shape of proboscideans. *Acta Palaeontologica Polonica* 61: 537–574.

Levin, N.E., Cerling, T.E., Passey, B.H., Harris, J.M., and Ehleringer, J.R. 2006. A stable isotope aridity index for terrestrial environments. *Proceedings of the National Academy Sciences* 103: 11201–11205.

MacFadden, B.J. and Cerling, T.E. 1996. Mammalian herbivore communities, ancient feeding ecology, and carbon isotopes: a 10 million-year sequence from the Neogene of Florida. *Journal of Vertebrate Paleontology* 16:103–115

MacFadden, B.J. and Higgins, P. 2004. Ancient ecology of 15-million-year old browsing mammals within C_3 plant communities from Panama. *Oecologia* 140: 169–182.

Medrano, H. and Flexas, J. 2000. Fotorrespiración y mecanismos de concentración del dióxido de carbono. *In*: J. Azcón-Bieto and M. Talón (eds.), *Fundamentos de Fisiología Vegetal*, 187–201. McGraw-Hill Interamericana, Madrid.

Morgan, M.E., Behrensmeyer, A.K., Badgley, C., Barry, J.C., Nelson, S., and Pilbeam, D. 2009. Lateral trends in carbon isotope ratios reveal a Miocene vegetation gradient in the Siwaliks of Pakistan. *Geology* 37: 103–106.

Morgan, M.E., Kingston, J.D., and Marino, B.D. 1994. Carbon isotopic evidence for the emergence of C4 plants in the Neogene from Pakistan and Kenya. *Nature* 367: 162–165.

Nelson, S.V. 2005. Paleoseasonality inferred from equid teeth and intra-tooth isotopic variability. *Palaeogeography, Palaeoclimatology, Palaeoecology* 222: 122–144.

Nelson, S.V. 2007. Isotopic reconstructions of habitat change surrounding the extinction of *Sivapithecus*, a Miocene hominoid, in the Siwalik Group of Pakistan. *Palaeogeography, Palaeoclimatology, Palaeoecology* 243: 204–222.

Patnaik, R., Singh, N.P., Paul, D., and Sukumar, R. 2019. Dietary and habitat shifts in relation to climate of Neogene–Quaternary and associated mammals of Indian Subcontinent. *Quaternary Science Reviews* 224: 105968.

Passey, B.H., Robinson, T.F., Ayliffe, L.K., Cerling, T.E., Sponheimer, M., Dearing, M.D., Roeder, B.L., and Ehleringer, J.R. 2005. Carbon isotope fractionation between diet, breath CO_2, and bioapatite in different mammals. *Journal of Archaeological Science* 32: 1459–1470.

Pérez-Crespo, V.A., Carranza y Castañeda, O., Arroyo-Cabrales, J., Morales-Puente, P., Cienfuegos-Alvarado, E., and Otero, F.J. 2017. Diet and habitat of unique individuals of *Dinohippus mexicanus* and *Neohipparion eurystile* (Equidae) from the late Hemphillian (Hh3) of Guanajuato and Jalisco, central Mexico: stable studies isotopes. *Revista Mexicana de Ciencias Geológicas* 34: 38–44.

Pilgrim, G.E. 1937. Siwalik antelopes and oxen in the American Museum of Natural History. *Bulletin of American Museum of Natural History* 72: 729–874.

Quade, J. and Cerling, T.E. 1995. Expansion of C_4 grasses in the late Miocene of northern Pakistan: Evidence from stable isotopes in paleosols. *Palaeogeography, Palaeoclimatology, Palaeoecology* 115: 91–116.

Quade, J., Cater, J.M.L., Adam, J., and Harrison, T.M. 1995a. Late Miocene environmental change in Nepal and the northern Indian subcontinent: Stable isotopic evidence from paleosols. *GSA Bulletin* 107: 1381–1397.

Quade, J., Cerling, T.E., and Bowman, J.R. 1989. Development of Asian monsoon revealed by marked ecological shift during the latest Miocene in northern Pakistan. *Nature* 342: 163–166.

Quade, J., Cerling, T.E., Andrews, P., and Alpagut, B. 1995b. Paleodietary reconstruction of Miocene faunas from Paşalar, Turkey, using stable carbon and oxygen isotopes of fossil tooth enamel. *Journal of Human Evolution* 28: 373.

Quade, J., Cerling, T.E., Barry, J., Morgan. M.M., Pilbeam, D.R., Chivas. A.R., Lee-Thorp, J.A., and Van der Merwe, N.J. 1992. A 16 Ma record of paleodiet using carbon and oxygen isotopes in fossil teeth from Pakistan. *Chemical Geology* 94:182–192.

Sánchez, B. 2005. Reconstrucción del ambiente de mamíferos extintos a

partir del análisis isotópico de los restos esqueléticos. *In*: P. Alcorno, R. Redondo, and J. Toledo (eds.), *Nuevas técnicas metodológicas aplicadas al estudio de los sistemas ambientales: los isótopos estables*, 49–64. Universidad Autónoma de Madrid, Madrid.

Sanyal, P., Bhattacharya, S.K., Kumar, R., Ghosh, S.K., and Sangode S.J. 2005. Palaeovegetational reconstruction in Late Miocene: a case study based on early diagenetic carbonate cement from the Indian Siwalik. *Palaeogeography, Palaeoclimatology, Palaeoecology* 228: 245–259.

Sanyal, P., Sarkar, A., Bhattacharya, S.K., Kumar, R., Ghosh, S.K., and Agarwal, S. 2010. Intensification of monsoon, microclimate, and asynchronous C_4 appearance: isotopic evidence from the Indian Siwalik sediments. *Palaeogeography, Palaeoclimatology, Palaeoecology* 296: 165–173.

Sarwar, M. 1977. Taxonomy and distribution of the Siwalik Proboscidea. *Bulletin Department of Zoology University of the Punjab Lahore* 10: 1–172.

Shoshani, J. and Tassy, P. 2005. Advances in proboscidean taxonomy & classification, anatomy & physiology, and ecology & behavior. *Quaternary International* 126–128: 5–20.

Sorkin, B. 2008. A biomechanical constraint on body mass in terrestrial mammalian predators. *Lethaia* 41: 333–347.

Souron, A. 2017. Diet and ecology of extant and fossil wild pigs. *In*: M. Melletti and E. Meijaard (eds.), *Ecology, Conservation and Management of Wild Pigs and Peccaries*, 29–38. Cambridge University Press, Cambridge.

Sponheimer, M. and Lee-Thorp, J. A. 1999. Oxygen isotopes in enamel carbonate and their ecological significance. *Journal of Archaeological Science* 26: 723–728.

Tada, R., Zheng, H., and Clift, P.D. 2016. Evolution and variability of the Asian monsoon and its potential linkage with uplift of the Himalaya and Tibetan Plateau. *Progress in Earth and Planetary Science* 3: 4.

Tariq, M. 2010. *Palaeoenvironmental Study of Pakistan Siwaliks*, 78–122. Unpublished Ph.D. Thesis, Government College University, Lahore.

Tejada-Lara, J.V., MacFadden, B.J., Bermudez, L., Rojas, G., Salas-Gismondi, R., and Flynn, J.J. 2018. Body mass predicts isotope enrichment in herbivorous mammals. *Proceedings of the Royal Society B* 285 (1881), 20181020.

Tipple, B.J., Meyers, S.R., and Pagani, M. 2010. Carbon isotope ratio of Cenozoic CO_2: a comparative evaluation of available geochemical proxies. *Paleoceanography* 25: PA3202.

Uno, K.T., Cerling, T.E., Harris, J.M., Kunimatsu, Y., Leakey, M.G., and Nakatsukasa, M. 2011. Late Miocene to Pliocene carbon isotope record of differential diet change among East African herbivores. *Proceedings of National Academy of Science* 18: 1–6.

Uno, K.T., Polissar, P.J., Jackson, K.E., and de Menocal, P. 2016. Neogene biomarker record of vegetation change in Africa. *Proceedings of National Academy of Science* 113: 6355–6363.

Waseem, M.T., Khan, A.M., Ghaffar, A., Iqbal, A., and Ahmad, R.M. 2020a. Palaeodietary and palaeoclimatic reconstruction for late Miocene hipparionines from the Siwaliks of Pakistan. *Pakistan Journal of Zoology* [published online, https://dx.doi.org/10.17582/journal.pjz/20180314070354].

Waseem, M.T., Khan, A.M., Quade, J., Krupa, A., and Dettman, D.L. 2020b. Stable isotope analysis of middle Miocene faunal communities from the Siwaliks (Pakistan). *In*: E. Vlachos, D. Crespo, C. Martinez-Perez, H.G. Ferron, J.L. Herraiz, A. Gamonal, F.A.M. Arnal, F. Gasco, and P. Citton (eds.), *2nd Palaeontological Virtual Congress*, 199.

White, T.D., Ambrose, S.H., Suwa, G., Su, D.F., DeGusta, D., Bernor, R.L., Boisserie, J.-R., Brunet, M., Delson, E., Frost, S., Garcia, N., Giaourtsakis, I.X., Haile-Selassie, Y., Howell, F.C., Lehmann, T., Likius, A., Pehlevan, C., Saegusa, H., Semprebon, G., Teaford, M., and Vrba, E. 2009. Macrovertebrate paleontology and the Pliocene habitat of *Ardipithecus ramidus*. *Science* 326: 67–93.

Instructions for authors—abridged version

ACTA PALAEONTOLOGICA POLONICA accepts papers of moderate length. Longer manuscripts should be directed to the monographic series PALAEONTOLOGIA POLONICA. Submissions may be in the form of articles (usually 4000–10 000 words, the maximum length being set at 120 double-spaced manuscript pages, including illustrations, or up to 30,000 words), brief reports (usually 2000–3000 words, ca. 12 double-spaced pages including illustrations), discussions (1000–1500 words, ca. 6 double-spaced pages), or paper/book reviews (500–1500 words, ca. 3 double-spaced pages). The journal publishes in English (consistently with either American or British spelling).

Submission

Acta Palaeontologica Polonica uses a web-based submission and review system at http://www.app.pan.pl/esubmission.html.

Cover letter

The cover letter should provide the background for the problem or question your research answers. The corresponding author must give written assurance that neither the submitted material nor portions thereof have been published previously or are under consideration for publication elsewhere.

Manuscript

Title.—A title should be informative but as brief as possible. Do not use terms or names that may not be known to most readers, for instance those introduced in the paper for the first time. Avoid abbreviated words, names of high rank systematic or stratigraphic units given in parentheses, and authorities and dates.

Abstract.—A concise abstract of 100–300 words should summarize methods, results, and conclusions of the study rather than describing its contents.

Introduction.—The Introduction should be concise and intelligible to a professional paleontologist or geologist, and preferably to an educated lay reader. Provide the minimum background information and do not engage in a literature review.

Material and methods.—In accordance with the recommendations of the International Codes of Zoological and Botanical Nomenclature (ICZN, ICBN), all illustrated and described fossils should be deposited in an appropriate public institution.

Results.—Present your results in a logical sequence in the text, tables, and illustrations, emphasize or summarize only important observations. In papers dealing with taxonomy, ensure that diagnoses distinguish the taxa in question from all morphologically similar taxa.

Discussion.—The discussion should focus on the interpretation and significance of the findings. State the implications of the findings and their limitations, including possibilities for future research.

Acknowledgements.—Acknowledge contributions that do not justify authorship, technical help, and financial support.

References.—For examples of exact formatting of references, consult the bibliographies in recent APP papers.

Figures, tables, and supplementary material.—Illustrations can be printed at two-column width (183 mm) or one-column width (89 mm), and should be designed accordingly. First sentence of the figure caption should summarize the main information presented in the figure. Figure captions of taxonomic papers should include authority name(s), date, age, and locality of the illustrated taxa. A detailed instruction describing how the figures should be prepared is available at https://e-system.app.pan.pl/app/journal/for_authors/#id4

Use appendices for longer tables or listings such as specimens examined and locality information. Authors are welcome to submit animations, movie files, sound files or any additional information for Supplementary Online Material.

Paper acceptance

Accepted papers are published online in the Forthcoming papers section. After acceptance by APP, we recommend that authors of papers concerning animal fossils register nomenclatural acts, including the erection of new taxa at all ranks and acts of synonymy, with Zoobank, at http://zoobank.org/, and cross-reference the codes in their APP paper.

For details see information for authors available at our web site: https://e-system.app.pan.pl/app/journal/for_authors/

ACTA PALAEONTOLOGICA POLONICA

Instytut Paleobiologii PAN
ul. Twarda 51/55
00-818 Warszawa, Poland

fax: (+48 22) 620 62 25
e-mail: app@twarda.pan.pl

Supplement to Vol. 66 No. 3 **2021**

Contents

ACTA PALAEONTOLOGICA POLONICA is indexed in AGRO Poznań, Biological Abstracts, BIOSIS Previews, Current Contents/Physical, Chemical, and Earth Sciences, Geological Abstracts, GeoRef, Index Copernicus, Petroleum Abstracts, VINITI RAN, Science Citation Index Expanded, SciSearch, Scopus, Zoological Record. Contents of current issues available at http://app.pan.pl and through digital repositories and portals: Web of Science, EBSCO, AGRO Poznań, and Polona.

ONLINE ACCESS: http://app.pan.pl APP-ALERT: http://app.pan.pl/appalert.html